Risk Predictive Collision Avoidance System for Intersection Right Turn: System Development and Validation

A dissertation of Doctor degree

(Mechanical Engineering)
in Tokyo University of Agriculture and Technology

2021

by

Yohei Fujinami

Student ID No. 17833009

Supervisor

Professor Pongsathorn Raksincharoensak

Department of Mechanical Systems Engineering

Faculty of Engineering

Tokyo University of Agriculture and Technology

Abstract

Reducing traffic accidents has been one of the most imperative topics for automobile industries for long decades. According to the statistics on traffic accidents in Japan, most fatal traffic accidents have occurred in the cities. The city driving requires the driver to correctly predict the risk not only on the visible hazards but also on the possibilities such as a sudden lane change or a darting-out from the blind spot. We call these possibilities the potential risks. It is known that skilled drivers can drive the city safely and comfortably by predicting the potential risks and handling the vehicle properly to reduce the risks. We define these driving skills as risk predictive driving. This risk predictive driving is imperative factors to diminish the traffic accident in the city area.

The latest development of the Advanced Driver Assistance Systems (ADAS) could enhance the comfortability and traffic safety of automobiles. In the aspect of comfortability, a lot of research have made on driving assistance for no-risk conditions such as highway driving. In terms of safety as well, plenty of studies on emergency functions such as emergency braking, emergency steering, and stability controls. However, although risk predictive driving scenarios are the meaningful aspect to diminish the traffic accident in city driving, many of those studies on ADAS did not undertake the risk predictive driving scenarios.

One of the essences of developing the risk predictive driver assistance systems is to be consistent in terms of the “safety” and the “driver acceptance” at the same time. Because once the system becomes too conservative for safety, the driver may not accept the driver assistance system. Usually, the “safety” and the “driver acceptance” are in the trade-off relationships.

Our research project addressed the risk predictive scenario in the intersection right-turn and developed an advanced driver assistance system that predicts the risk of the darting-out from a blind spot. Our proposal ADAS enables the vehicle to decelerate to a safe speed when there’s the risk for a darting-out object while making a right-turn at the intersection. In addition to that, this paper proposes a methodology on the vehicle trajectory prediction for the driver assistance system. This method realizes to predict the smooth and high accuracy intersection turning trajectories in the real-time calculation rate. To evaluate the effectiveness of the risk predictive driver assistance systems, the evaluations of the “safety” and the “driver acceptance” are indispensable. This paper presents a methodology to evaluate both the safety and the driver acceptance from the full-vehicle simulations and the driver subjected experiments.

Contents

Nomenclatures

2. Risk Predictive Driver Assistance System for Intersection Right-Turn

P_{gas}	Driver gas pedal input.
P_{brake}	Driver brake pedal input.
δ_{sw}	Steering wheel input.
θ_{cross}	Crossing angle of the intersection.
$X_{intersec}$	Intersection position.
$Y_{intersec}$	Intersection position.
x_{obj}	Sensor perceived position of darting-out object.
y_{obj}	Sensor perceived position of darting-out object.
v_{obj}	Sensor perceived speed of darting-out object.
ψ_{obj}	Sensor perceived yaw angle of darting-out object.
x_{occ}	Sensor perceived position of occluding vehicle.
y_{occ}	Sensor perceived position of occluding vehicle.
v_{ego}	Ego vehicle speed.
a_{ego}	Ego vehicle acceleration.
ψ_{ego}	Ego vehicle yaw angle.
x_{traj}	Predicted trajectory.
y_{traj}	Predicted trajectory.
B_{PBS}	Brake command from PBS.
B_{EBS}	Brake command from EBS.
$B_{command}$	Brake command to brake actuator of vehicle.
D_{vir_occ}	Offset distance from the left-front corner of the occluding vehicle.
x_{traj}	Trajectory of ego vehicle at the sensor position.
y_{traj}	Trajectory of ego vehicle at the sensor position.
L_{sensor}	Length from rear-axle to sensor position of ego vehicle.
ψ_{ego}	Yaw angle of ego vehicle.
x_{occ}	Occluding vehicle position.
y_{occ}	Occluding vehicle position.
θ_{vir}	Relative angle from ego vehicle to direction angle of the entering road of the intersection.
d_{vir}	Darting-out distance of virtual darting-out object.
v_{vir}	Velocity of virtual darting-out object.
t_{vir}	Time to conflict of virtual darting-out object after detected by ego vehicle.
t_{vir_d}	Critical time to conflict of virtual darting-out object.
d_{stop}	Distance to stop vehicle by emergency braking.
d_{cp_PBS}	Distance from ego vehicle position to conflict point.
d_{PBS}	Distance to control by PBS.
D_{safe}	Safety margin.
v_{safe}	Safe speed.

a_{EBS}	Representative acceleration of emergency braking.
τ	Latency of the system.
J_1	The first jerk of the speed profile.
J_2	The second jerk of the speed profile.
a_0	Initial acceleration of the speed profile.
a_f	Final acceleration of the speed profile.
v_0	Initial velocity of the speed profile.
v_f	Final velocity of the speed profile.
a_{target}	Target acceleration of PBS.
v_{target}	Target velocity of PBS.
t_{pre}	Prediction time.

3. Right-Turn Trajectory Prediction Method with Triclothoidal Curve

R	Turning radius.
δ_f	Ego vehicle front steering angle.
l_{wb}	Ego vehicle wheelbase.
ψ	Tangent angle of curve.
κ	Curvature of curve.
ψ_0	Initial tangent angle of curve.
κ_0	Initial curvature of curve.
ψ_f	Terminal tangent angle of curve.
κ_f	Terminal curvature of curve.
L	Curve length.
θ_{cross}	Crossing angle of the intersection.
l_{in}	Distance from the driving center lane to the right-side edge of the entering road.
l_{out}	Distance from the driving center lane to the right-side edge of the escaping road.
d_{pre}	Terminal point distance parameter.
X_f	Terminal point position of predicted trajectory.
Y_f	Terminal point position of predicted trajectory.
$\hat{d}_{pre}$	Estimated terminal point distance parameter.

4. Collision Avoidance Ability Evaluation with Full-Vehicle Simulation

R_{turn}	Turning radius.
R_1	Turning radius at the left-front corner of ego vehicle.
R_2	Turning radius at the right-front corner of ego vehicle.
L_{wb}	Ego vehicle wheelbase.
L_{rax}	Length from front-tip to rear-axle of ego vehicle.
W_{ego}	Ego vehicle width.
x_{obj}	Sensor perceived position of darting-out object.
y_{obj}	Sensor perceived position of darting-out object.
v_{obj}	Sensor perceived speed of darting-out object.
ψ_{obj}	Sensor perceived yaw angle of darting-out object.

x_{cp1} Predicted conflict point position at the left-front corner of ego vehicle.
y_{cp1} Predicted conflict point position at the left-front corner of ego vehicle.
x_{cp2} Predicted conflict point position at the right-front corner of ego vehicle.
y_{cp2} Predicted conflict point position at the right-front corner of ego vehicle.
d_{EBS} Distance to stop by EBS.
d_{cp_EBS} Distance from ego vehicle current position to the conflict point.
D_{safe_EBS} Safety margin.
τ_{EBS} Latency of the system.
B_{EBS} Braking command of EBS.
θ_{cross} Crossing angle of the intersection.
l_{in} Distance from the driving center lane to the right-side edge of the entering road.
l_{out} Distance from the driving center lane to the right-side edge of the escaping road.
d_{pre} Terminal point distance parameter.
X_{occ} Occluding vehicle position.
Y_{occ} Occluding vehicle position.
$X_{intersec}$ Intersection position.
$Y_{intersec}$ Intersection position.
X_{occ_offset} Offset condition of occluding vehicle.
X_{obj_offset} Offset condition of darting-out object.

5. Driver Acceptance Evaluation of Advanced Driver Assistance System

P_{gas} Driver gas pedal input.
P_{brake} Driver brake pedal input.
δ_{sw} Steering wheel input.
v_{ego} Ego vehicle speed.
a_{ego} Ego vehicle acceleration.
ψ_{ego} Ego vehicle yaw angle.
x_{traj} Predicted trajectory.
y_{traj} Predicted trajectory.
B_{PBS} Brake command from PBS.
J_1 The first jerk of the speed profile.
J_2 The second jerk of the speed profile.
a_0 Initial acceleration of the speed profile.

6. Generalization of Advanced Driver Assistance System for Risk Predictive Driving in Urban Areas

D_{vir_occ} Offset from the corner position of the occluding object to trajectory.
v_{vir} Darting-out velocity.
θ_{vir} Darting-out direction.
θ_{cross} Trajectory direction at the terminal point.
d_{pre} Distance parameter to define the positions of the terminal point.
κ_f Trajectory curvature at the terminal point.

1. Introduction

This chapter introduces this paper. First, Section 1.1 describes the background and motivation. Next, Section 1.2 explains the developed Advanced Driver Assistance Systems (ADAS) to reduce the traffic accident. Then, Section 1.3 describes the problem statement. Section 1.4 presents the objectives of this paper. And finally, Section 1.5 describes the thesis structure.

1.1 Background and Motivation

WHO reported that approximately 1.35 million people are killed in road traffic accidents every year in this world [1]. Besides, in 2016, road traffic injuries placed 8th of the leading cause of death in the world. To make matters worse, it was forecasted that road traffic injuries to be 5th place of the leading cause of death in 2030 [2]. Thus, road traffic accidents have been regarded as a public health issue [3]. Therefore, reducing road traffic accidents has been one of the most imperative topics for automobile industries for long decades.

Focusing on the Japanese road traffic situation, Fig. 1.1.1 shows the number of road traffic accidents, injuries, and fatalities from 1989 to 2019 [4]. Both the number of accidents and deaths are monotonically decreasing in recent years. These recessions were accomplished by the improvement of the road structure, improvement in driving behaviors, development of passive and active safety technologies on automobiles, and so on [5]-[7]. However, despite the number of road traffic accidents involving motor vehicles have decreased year by year, yet 381237 cases have occurred,461775 people have injured, and 3215 people have died in road traffic accidents in 2019 [4]. In Europe as well, while the number of fatalities by road traffic accidents tends to decrease in recent years as shown in Fig. 1.1.2 [8][9], and reported 22800 people died in road traffic accidents in 2019 [10].

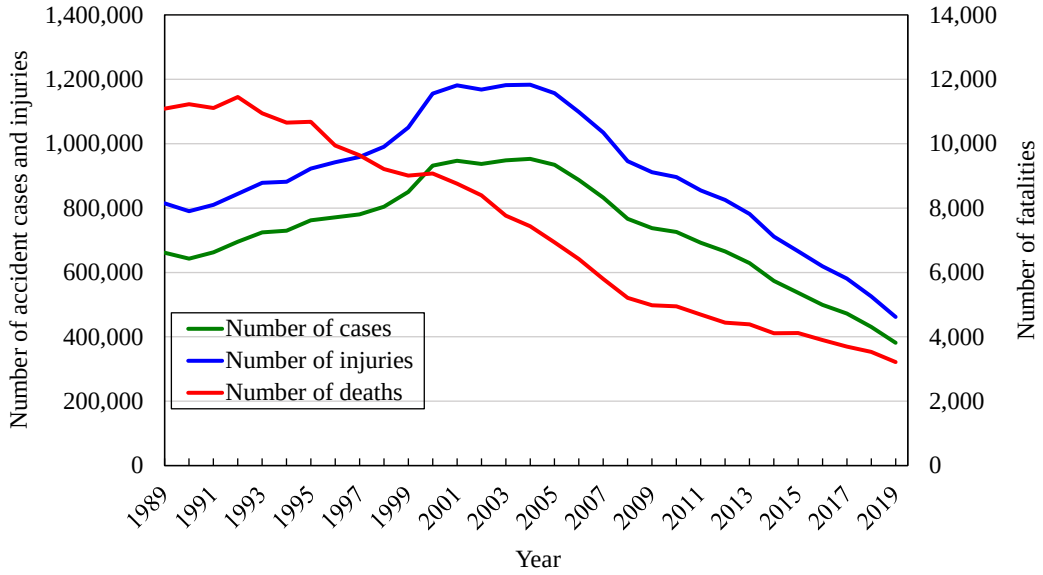

Fig. 1.1.1 The number of road traffic accident cases, injuries, and fatalities from 1989 to 2019 in Japan.

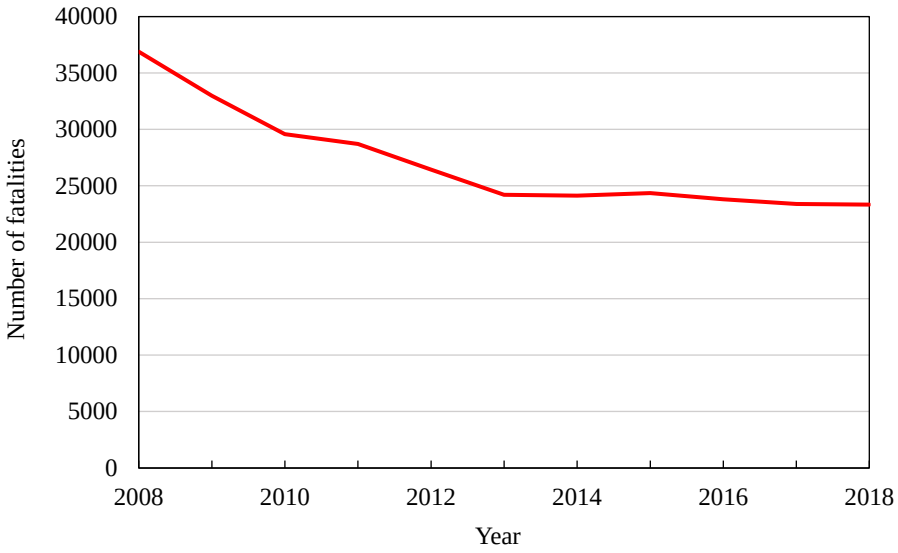

Fig. 1.1.2 The number of traffic fatalities in the EU (28 countries) from 2008 to 2018.

Plenty of projects objected to reduce or vanish the fatalities or heavy injuries by traffic accidents. As local objectives and strategies to reduce the fatalities, Table 1.1.1 shows recent numbers of the traffic fatalities and national targets of deaths by 2020 in Japan, Korea, United States, Italy, United Kingdom, Germany, France, Spain, and Sweden [4][9][11]-[22]. As a representative international project, Vision Zero provided a philosophy of road safety to achieve no fatality and heavy injury by traffic accidents. The target of Vision Zero is not to accomplish the particular target but to guide the road safety vision to strategy to enhance road traffic safety. This vision does not define a certain date to achieve the goal, however, Vision Zero defines the two basic ethical rules to accomplish the vision:

"Life and health can never be exchanged for other benefits within the society."

"Whenever someone is killed or seriously injured, necessary steps must be taken to avoid a similar event."

Sweden first adopted Vision Zero in October 1997. After that, Vision Zero has been adopted and supported by many countries until now [23][24].

Table 1.1.1 Recent numbers of traffic fatalities by countries and national targets by 2020.

Country	2016	2017	2018	Target fatalities by 2020	Unit
Japan	3904	3694	3532	3000	Fatalities
Korea	4294	4185	3781	3071	Fatalities
United States	1.19	1.17	1.13	1.01	Fatalities per 100 million vehicle miles traveled
Italy	3283	3378	3334	2057	Fatalities
United Kingdom	1860	1856	1839	NA	Fatalities
Germany	3206	3180	3275	2189	Fatalities
France	3471	3444	3246	1996	Fatalities
Spain	1810	1830	1806	1239	Fatalities
Sweden	270	253	324	220	Fatalities

Focusing on the location of road traffic accidents in Japan, as shown in Fig. 1.1.3, 97.0% of the fatalities had died on non-motorway roads in 2018 [16]. On the other hand, the accidents in motorways, though the driveling speed is much higher, the number of traffic accidents was not dominating and suppressed around 3.0%. And 58.5% of the fatalities were on urban roads. Therefore, in Japan, more than half of the traffic accidents have occurred on urban roads [16]. Zooming out to the other countries, Fig. 1.1.4 shows the repartition charts of traffic accident fatalities by road type in Japan, Korea, United States, Italy, United Kingdom, Germany, France, Spain, and Sweden [12]-[21]. The mutual point thorough all countries in the figure was that the ratios at urban and rural roads were overwhelming the ratios at motorways. And the pie chart indicates that the percentages of fatalities on urban roads accounted for non-negligible numbers in most countries. Especially in Japan, the percentages of deaths on urban roads were notably higher compared to the countries in the figure. Thus, improving road safety at non-motorway roads such as rural and urban roads is one of the prioritized topics to reduce the number of traffic accidents involving automobiles.

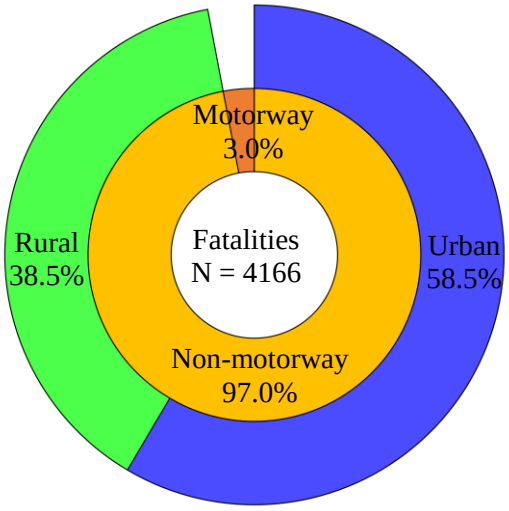

Fig. 1.1.3 Breakdown of road traffic accidents fatalities by locations.

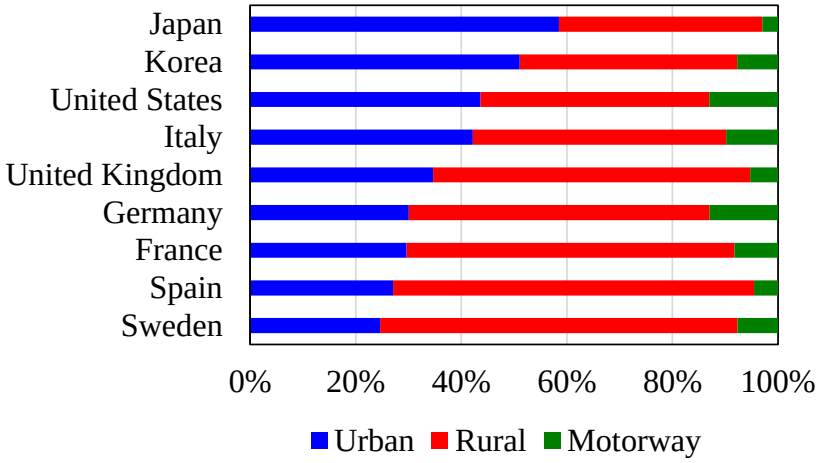

Fig. 1.1.4 The repartition charts of traffic accident fatalities by road type by countries in 2018 (The fatalities of the United States and the United Kingdom are from the data in 2017).

Focusing on more detail about the location of traffic accidents in Japan, more than 45% of the fatal accidents were intersection related accidents as indicated in Fig. 1.1.5 [25]. Besides, the statistical data regarding fatal intersection accidents in Fig. 1.1.6 shows that although the number of fatal intersection accidents has been decreasing, the percentages of fatal intersection accidents have not been decreasing for long years [25]. Likewise, in the United States, approximately 30% of vehicles involved in fatal road traffic accidents in 2017 were intersection related accidents [26]. According to those statistical facts, driving through the intersections is one of the riskiest scenarios while driving non-motorway roads and the improvement of traffic safety at the intersection can play a large role in diminishing road traffic accidents. Especially in Japan, the percentage of traffic accidents on urban roads and at intersections were higher. Therefore, the countermeasures at the intersection will be efficient in reducing road traffic accidents.

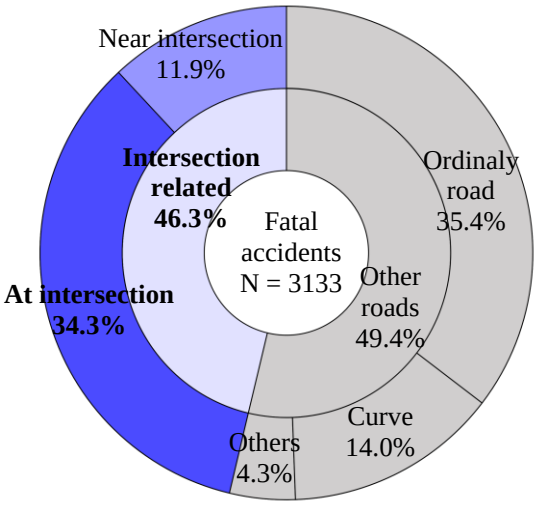

Fig. 1.1.5 Breakdown of the road traffic accidents fatalities by road types.

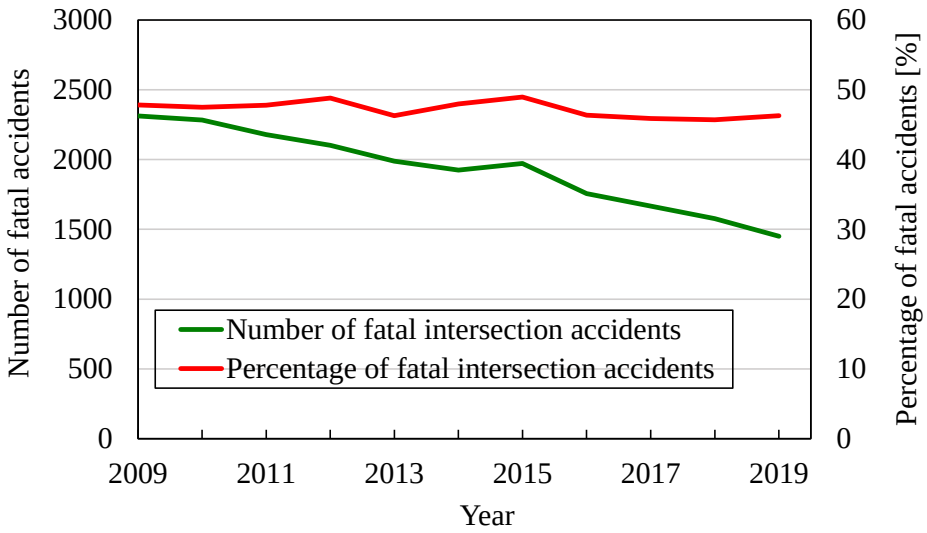

Fig. 1.1.6 The number and component percentage of fatal intersection accidents.

The main reason for the dangerousness of driving intersections is its difficulties in driving through an intersection. Even if there is a traffic signal to control the traffic, when the vehicle makes turnings, the drivers must be aware of oncoming traffic, crossing bicycles, crossing pedestrians, and other possible risks.

Besides, both cyclists and pedestrians may cross the road from the right and left sides, and these complex situations make drivers misunderstand the risk and lead to accidents [27]-[29]. Those factors make intersection driving more difficult compare to other driving scenarios. Fig. 1.1.7 lists the ten most occurred collision cases at signalized intersections in Japan [29]. The case numbers in the subfigures show the accident cases in Japan from 2008 to 2010.

1.	A rear-end collision with a car 23915 cases 7.48%		6.	A left-turn collision with a bicycle 14360 cases 4.49%	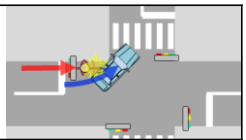
2.	A collision with an oncoming car in right-turn maneuver 22507 cases 7.04%	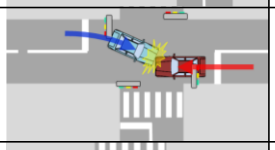	7.	A right-turn collision with a bicycle coming from right 13860 cases 4.34%	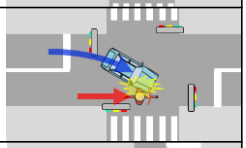
3.	A collision with an oncoming motorcycle in right-turn maneuver 19374 cases 6.06%	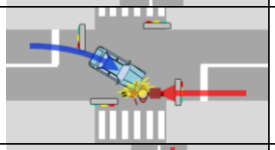	8.	A left-turn collision with a motorcycle 12331 cases 3.86%	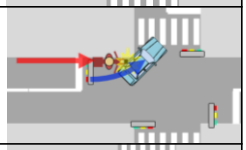
4.	A collision with a car from left side 18743 cases 5.78%	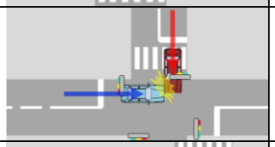	9.	A right-turn collision with a bicycle coming from left 11738 cases 3.67%	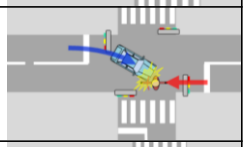
5.	A collision with a car from right side 15426 cases 4.83%	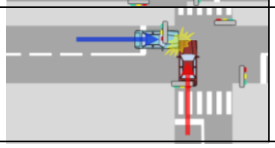	10.	A right-turn collision with a pedestrian coming from right 10042 cases 3.14%	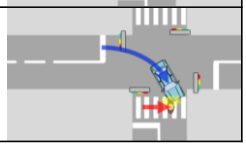

Fig. 1.1.7 The list of 10 most occurred collision cases at signalized intersections in Japan from 2008 to 2010.

The figure explains that the accidents at the intersection contain the various types of accidents. Focusing on the right-turn cases, 5 out of 10 cases (2, 3, 7, 9, and 10) are accidents while making right turns. As mentioned, particularly right-turns (or left-turns in right-hand traffic) require drivers to handle many complex tasks, skills, and enough concentration. And lack of those factors led to fatal accidents. Thus, to challenge to improve intersection safety, this paper focuses on improving traffic safety at intersection right-turn employing the Advanced Driver Assistance System.

1.2 Development of Advanced Driver Assistance System for Road Traffic Safety

Nowadays, to improve comfort and safety, Advanced Driver Assistance Systems (ADAS) became widespread in the automobile market. ADAS are vehicle onboard intelligent systems that encourage the driver appropriately by actively controlling the vehicle [30]. In this study, the ADAS defines its position as Automated Level 1 or 2 in the definitions of SAE J3016 Levels of Driving Automation referred from Fig. 1.2.1 [31]. The ADAS in this context is expected to reduce the burdens on driving, suppress human errors, recover from unstable vehicle stability, mitigate collision damage, and avoid a collision. In 2018, the number of vehicles equipped with ADAS or autonomous driving systems was reaching 23 million vehicles, and this was 24.3% growth from the previous year [32].

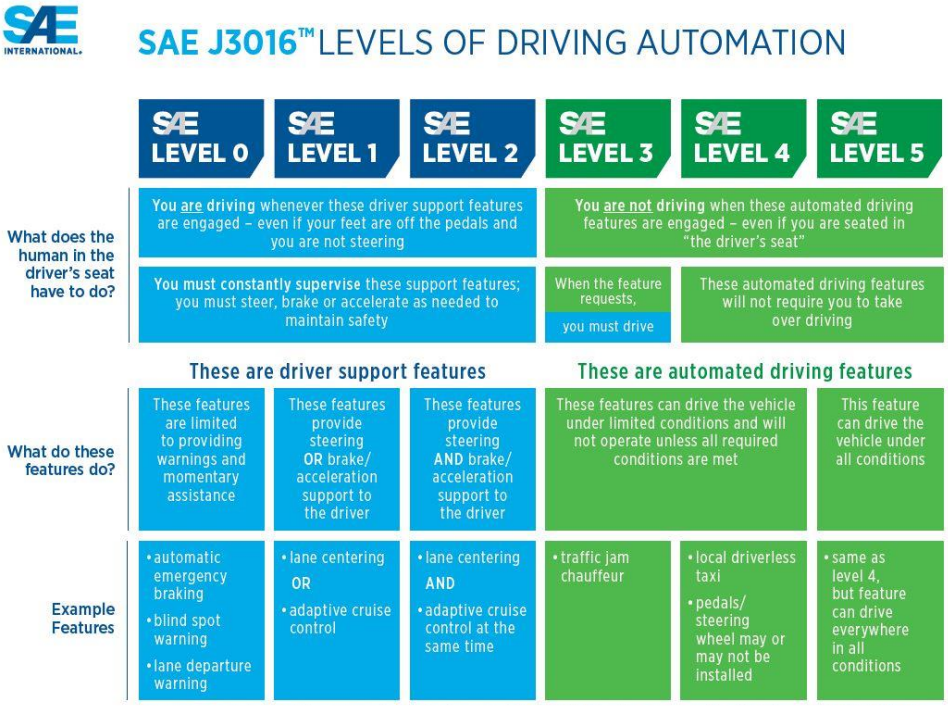

Fig. 1.2.1 SAE J3016 Levels of Driving Automation [30].

At the same time as the market growth, the safety performances of the ADAS have been actively evaluated by organizations through vehicle testing. The European New Car Assessment Program (Euro NCAP) is a good example of the safety evaluation program. Euro NCAP introduced the evaluation tests for the Autonomous Emergency Braking System to the rear-end car-to-car collision from 2013. Thereafter, Euro NCAP tested the collision avoidance system for pedestrian crossing accidents [33][34]. Since 2018, the Euro NCAP has tested the performances of ADAS at critical scenarios in highway driving. The tests evaluated the cut-in and cut-out scenario while Adaptive Cruise Control (ACC) was engaged. To provide details, the cut-in scenario is a scenario where a slower vehicle in the adjacent lane merges into the lane just in front of the test vehicle. The cut-out scenario is a scenario where a preceding vehicle suddenly leaves the lane to avoid a stopping vehicle ahead. Other tests evaluated the steering support functions in obstacle avoidance scenario and lane centering function. The former test measures the driver's steering effort to avoid an obstacle on the road. Latter test measures the lane centering performance of the ADAS in the S-bend test with different speeds [35]. Currently, as of November 2020, as a part of Safety Assist (SA) and Vulnerable Road User (VRU) Protection, Euro NCAP also evaluated the driver assistance system for intersection turnings [117][118]. In the assessments, the vehicle under test makes a turning at the intersection. The SA evaluates the collision avoidance performance between the car coming from the opposite direction, and the VRU Protection evaluates the collision avoidance performance between the pedestrian crossing from the opposite direction [117][118].

Table 1.2.1 shows the examples of the well-known commercialized driver assistance system that directly controls the vehicle, and the table describes the intervention contents, target situations, and target road types of the system.

Table 1.2.1 Well-known commercialized driver assistance systems.

Commercialized ADAS	Intervention (major method)	Situation	Road type
Adaptive Cruise Control (ACC)	Gas and brake	Normal driving	Highway
Lane Keeping Assistance System (LKAS)	Steer	Normal driving	Highway
Electric Stability Control (ESC)	Brake	Emergency	Highway
Lane Departure Prevention (LDP)	Steer	Emergency	Highway
Anti-lock Braking System (ABS)	Brake	Emergency	Highway Urban road
Autonomous Emergency Braking System (AEBS)	Brake	Emergency	Highway Urban road
Emergency Steering Function (ESF)	Steer, brake	Emergency	Highway Urban road
Intersection Turn Assistant	Brake	Emergency	Urban road
Automated Parking	Gas, brake, and steer	Normal driving (parking)	Urban road (Parking)

ACC is a system that controls the cruising speed distance of the preceding vehicle by acceleration and braking. LKAS is a system that controls the vehicle to keep in the center of the lane by steering control. ESC is a system that prevents the vehicle from being dynamically unstable. This system engages braking assistance to the individual wheel to stabilize the vehicle when it goes to the oversteer or understeer. LDP is a system that brings back the vehicle in the lane by strong steering intervention when the vehicle departs the lane unintendedly. AEBS is a system to avoid collisions with the object ahead with emergency braking. ESF is a collision avoidance system with steering intervention. This system engages when the collision cannot be avoided only by the AEBS. However, the activation conditions are strict, and the system cannot engage the ESF when the sensor system cannot find out enough space for steering maneuvers. Intersection Turn Assist is an emergency braking function for intersection turnings. This system is sometimes handled as a partial function of AEBS, but the biggest difference is required sensor specifications. AEBS requires long-distance perception. On the other hand, the Intersection Turn Assist requires short-range but wide field-of-view perception sensors. Therefore, the vehicle equips Intersection Turn Assist mounts environment perception sensors in addition to the sensor for AEBS. Automated Parking is a driver assistance system that helps the driver park the vehicle. The system controls the steering wheel to the target parking position. Some systems also operate acceleration, braking, and shifting. Therefore, the vehicle parks to the parking position fully controlled by the ADAS.

As shown in Table 1.2.1, most of the ADAS can divide into two types: a system for normal driving and emergency situation. The ADAS for normal driving usually do not consider the risk for the collision but the comfortability. And those systems are recommended to use on highways. On the other hand, the ADAS for emergency situations only intervene after the collision risk or risk for unstable states became apparent. Therefore, the systems do not consider the comfort. Hence, when we design an ADAS for urban roads, the driver assistance system for normal driving is not very appropriate because those assistances do not consider the collision risks in the urban area.

An important principle for safe driving in the urban area is to predict the possible risks surrounding the driving vehicle, for example, a risk that a pedestrian darts out from a blind spot, a risk that a bicycle crosses a lane, and a risk that a vehicle suddenly cuts in from another lane or parking space. Researchers pointed out that skilled drivers could avoid collision risks by correctly predicting the possibilities before the possibilities become imminent or unavoidable risks [36][37]. We call these possibilities potential risks. It is known that skilled drivers can drive the city safely and comfortably by predicting the potential risks and handling the vehicle properly to reduce the risks [36][37]. Defining this driving skill as "a risk predictive driving", we presume that risk predictive driving is imperative factors to diminish the traffic accident on urban roads.

Return to the story about the existing emergency functions in Table 1.2.1, those ADAS could only intervene in the emergency situation. Therefore, the systems cannot apply assistance to the potential risks, but only after actualized (detected) the risk. Thus, even many vehicles currently equip both the ADAS for normal driving and emergency situation, when the drivers do not understand and deal with the potential risks correctly, it is hard to avoid the collision in the risk predictive scenarios.

To solve these problems on the existing ADAS, the target of the ADAS for risk predictive scenarios defines as to control the vehicle to a safer state by predicting the potential risks in urban roads before the vehicle getting into the emergency situation. Thus, the ADAS for risk predictive driving locates intermediate between the ADAS for normal driving and emergency situation as represented in Fig. 1.2.2.

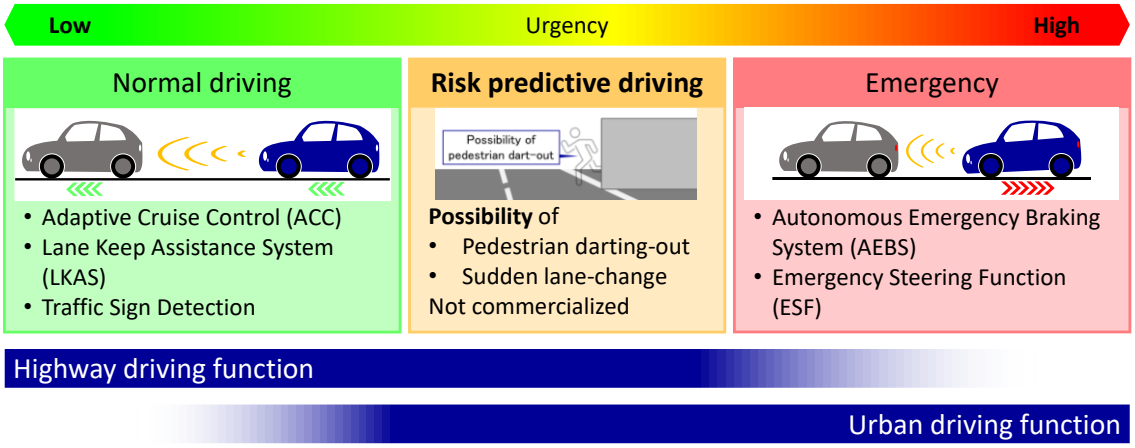

Fig. 1.2.2 The position of the ADAS for risk predictive driving.

Extensive research has objected to develop ADAS from the aspect of road traffic safety to reduce the number of accidents at intersections, especially when a vehicle makes a right-turn. Focusing on the urban driving and intersection right-turn (or left-turn in right-hand traffic) scenario, the following subsections present previous research and developments regarding the ADAS for emergency functions and risk predictive driving. Fig. 1.2.3 presents the map of the research and developments about safety on intersection right turnings.

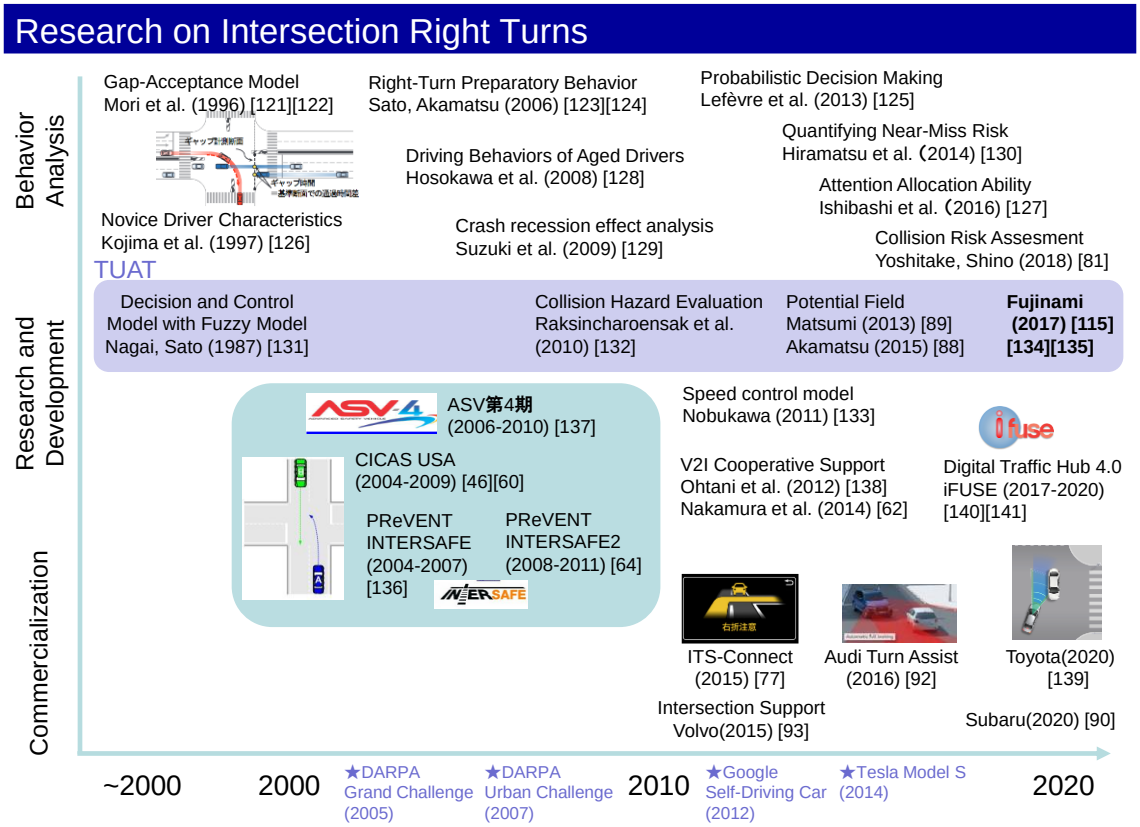

Fig. 1.2.3 Research and developments on intersection right turns.

1.2.1 Related Research on ADAS for Intersection Turnings with Vehicle-to-Vehicle and Vehicle-to-Infrastructure Communications

Research on ADAS that use Vehicle-to-Everything (V2X) communication was expected to reduce the number of accidents at intersections. V2X technology mainly contains four communication categories: Vehicle-to-Vehicle (V2V), Vehicle-to-Infrastructure (V2I), Vehicle-to-Pedestrian (V2P), and Vehicle-to-Network (V2N) as shown in Fig. 1.2.4 [38]. Those communication technologies are expected to play an influential role in the risk predictive driving situation because the communication enables to obtain the information of the surrounding objects even in blind spot [39][40].

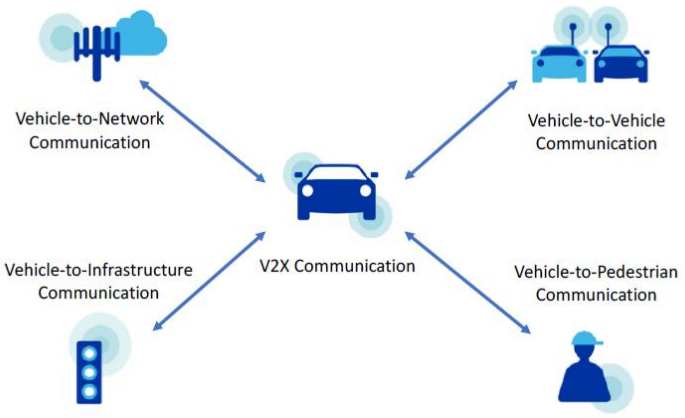

Fig. 1.2.4 Contents of the V2X communications [38].

V2V communications enable communication between vehicles and vehicles. By equipping the communication devices to the vehicles, this technology can inform the existence of the vehicle or other objects in blind spot [41]-[46], to improve the smoothness and safety of the ACC [47]-[51], and to obtain traffic information ahead such as traffic congestion, weather, the crash site and so on [52]-[54].

V2I communications are the technology that enables us to communicate with the vehicles and infrastructures. A lot of research focuses on intersection safety and proposed systems to alert or avoid collisions with other road users detected by the sensors on traffic signals or road structures [55]-[62][137][138]. In Japan, the National Police Agency promoted a project to develop an infrastructure cooperated driver assistance system using optical beacons. This driver assistance system is called Driver Safety Support System (DSSS) [63]. As an international research project to develop and demonstrate a cooperative intersection Safety system, European Commission led a project InterSafe-2 [64][65]. V2I and/or V2V communication has been also used for a highly automated driving function to localize the vehicle position [66][67].

The security, accuracy, speed, capacity, and privacy of the communication also trends topics through the V2V and V2I communications [68][69]. Considering those tasks, several standards have been established for V2V and V2I communication. Recently, DSRC (Dedicated Short-Range Communications) and C-V2X (Cellular-Vehicle-to-Everything) are known as the standardized communication standards for Intelligent Transportation Systems (ITS).

DSRC is a telecommunication technology especially used for V2V or V2I communications. In the US, DSRC was standardized as IEEE 802.11p in 2010 by allocating 75MHz in the 5.9Hz band [70]. This standard is also known as WAVE (Wireless Access in Vehicular Environments). In Europe, the communication technology called DSRC was standardized in European Standards EN 12253 to use the 5.8 GHz band for Automatic dynamic debiting systems and automatic access control systems in 2004 [71]. And Japan as well, DSRC was standardized in ARIB STD-T75 by the Association of Radio Industries and Businesses (ARIB) in 2001 by allocating 80MHz in the 5.8 GHz [72]. In Japan, an electric toll collection system ETC2.0 adopted DSRC and providing wide service not only for payment method but also for providing maximum 1000km range traffic information, camera images of the traffic ahead, and audio information [73].

C-V2X is a communication standard using cellular networks. The Third Generation Partnership Project (3GPP) has developed C-V2X from 2016 and aiming to use LTE and 5G cellular networks for ITS functions [74][75]. The C-V2X possesses two communication modes: Direct mode and Network mode. The Direct mode is based on LTE Direct and enables device-to-device communication. Therefore, the Direct mode makes C-V2X possible to implement the V2V, V2I, and Vehicle-to-Pedestrian (V2P) in high-speed communication. This concept also enables to relay the information via device-to-device communication that helps to reach the cellular network. The Network mode is used for the Vehicle-to-Network (V2N) communication. This service access the network to obtain and provide traffic information to the network that enables them to obtain traffic information and cloud services [74][76].

As functions using commercialized communication technology, Toyota and Honda adopted the DSSS V2I communication using the optical beacon.

DSSS from Toyota is a partial function of the ITS Connect function. In the DSSS from Toyota ITS Connect, the transmitters on traffic lights provide information about the existence of an oncoming vehicle and crossing pedestrian detected by sensors on the traffic signals to the waiting vehicle to make a right-turn. When the driver of the vehicle tried to make a right-turn in a dangerous situation, the system alerts

the driver with graphic information and sounds. Fig. 1.2.5 shows the conceptual diagram of the DSSS from Toyota ITS Connect [77]. The left figure in Fig. 1.2.5 shows the detection of the blinded vehicle behind the bus, and the intersection unit transmits the vehicle information to the ego vehicle (blue vehicle). When the driver of the ego vehicle steps on the gas pedal, the onboard system alert with a pictogram as shown in the right figure.

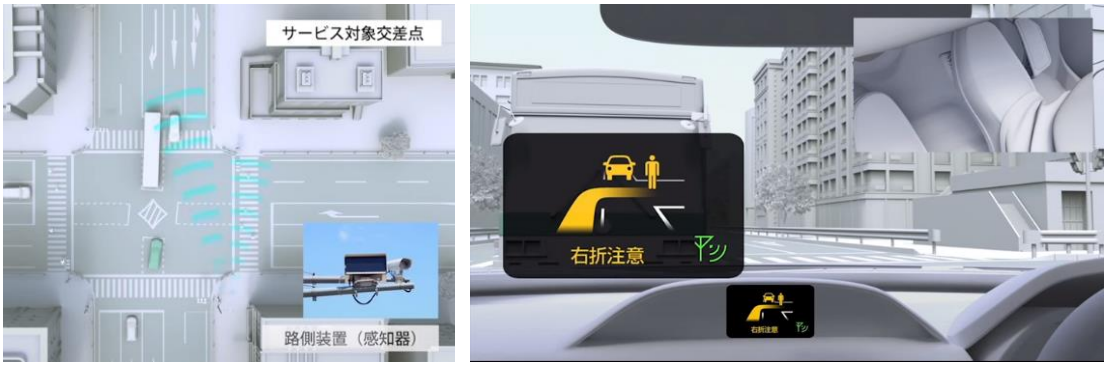

Fig. 1.2.5 DSSS function of Toyota ITS Connect [77].

Honda DSSS also uses traffic information. The vehicle receives the signal from the traffic signal and informs the driver appropriate speed to drive to the next intersection to prevent from stopping at the red light [78].

Regarding the V2V communication function, Toyota has developed a driver assistance system using the V2V communication called Connected Vehicles Support Systems (CVSS) as a partial function of the ITS Connect. The CVSS can communicate with the vehicle that also equips the CVSS and enhance the smoothness of the ACC function. Currently, the CVSS also covers the collision warning function. This function assists the driving in two situations as shown in Fig. 1.2.6. The first situation is when the vehicle stops at the entrance of the intersection, and a vehicle is oncoming from the left or right of the crossing road as shown in the left figure of Fig. 1.2.6. When the driver releases the brake pedal and tries to go into the intersection, the system alerts the existence of the oncoming object with graphic information and sound. The second situation is when the vehicle waiting for a right-turn in the intersection with blinking the turning indicator, and an oncoming vehicle is existing as shown in the right figure of Fig. 1.2.6. The CVSS activates when the driver releases the brake pedal and try to make the right-turn and informs the driver about the existence of the oncoming vehicle by graphical information and sound [77].

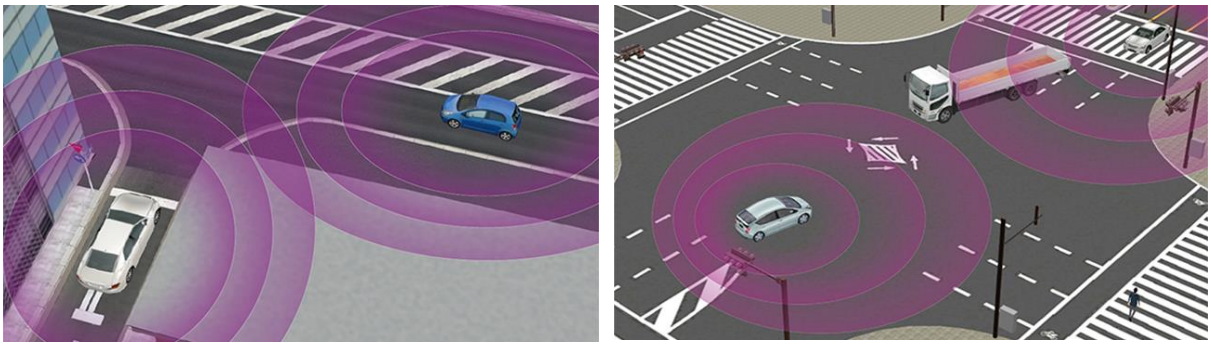

Fig. 1.2.6 CVSS function of Toyota ITS Connect [77].

The communication technologies are expected to change road safety drastically because the information covers a very wide range even it is out of the vehicle onboard sensor range. However, to accomplish the communication, both a sender and a receiver are required on the traffic. Therefore, it may take several years to widely deploy the facilities and functions to entire cars and urban roads. Currently, only 33 intersections applied DSSS in Tokyo Metropolitan (October 2020) [77]. Also, the problems in maintaining the infrastructure were lying on V2I communication technologies. National Police Agency of Japan expressed quitting the DSSS service by March 2027 because of the difficulties in its maintenance [79].

1.2.2 Related Research on ADAS for Intersection Turnings without Depending on Communication Technologies

With other challenges to avoid collisions while turning right at intersections, ADAS or other risk prediction methods have been proposed without depending on the communication technologies. The focuses of the research cover various topics including decision making, risk prediction, risk assessment, trajectory prediction, human-machine interface (HMI), vehicle control, and effectiveness evaluation [80]-[84][121]-[135].

As research project aims to develop an intelligent vehicle with ADAS especially focusing on city driving, “Autonomous Driving Intelligence System to Enhance Safe and Secured Traffic Society for Elderly Drivers” of Strategic Promotion of Innovation Research and Development Program (S-Innovation) has undertaken to assist the elderly driver to safely handle the risk predictive scenarios such as passing through unsignalized intersection scenario and overtaking parking vehicle scenario [85]-[87].

Our research team also have worked on the ADAS for intersection right-turn without depending on the communication. Fig. 1.2.7 shows the use-case scenarios of the intersection right-turn safety functions.

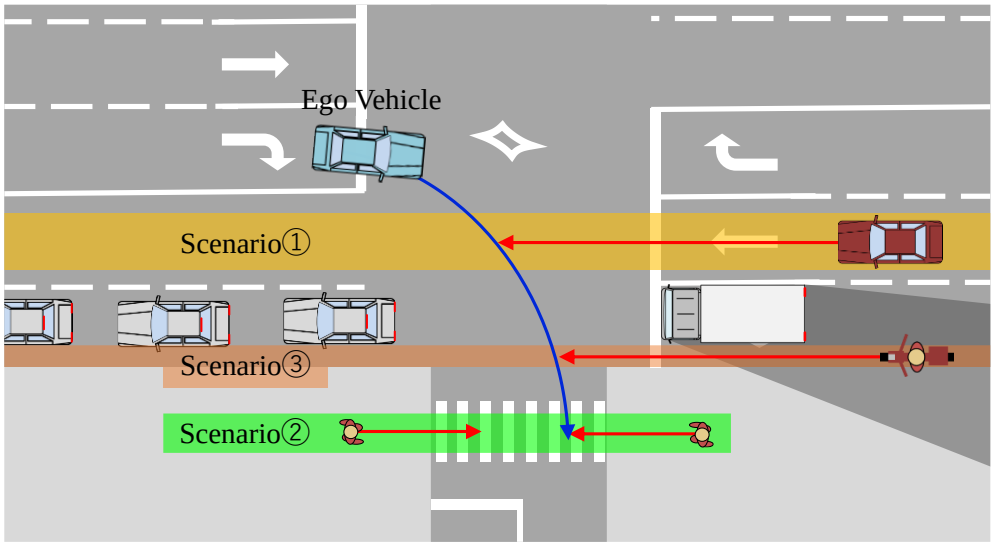

Fig. 1.2.7 Use case scenarios of the intersection right-turn safety functions where our research team has focused.

The scenario ① in the figure is a scenario where an oncoming vehicle approaches the intersection when the ego vehicle makes a right-turn at the intersection. The research proposed a deceleration system and a collision avoidance system to avoid oncoming vehicles for intersection right-turn [88]. This system

applies brake assistance to decelerate the vehicle as skilled drivers' driving before entering the intersection. This research also covers the effective evaluation using the vehicle-in-the-loop simulation as seen in Fig. 1.2.8 [88].

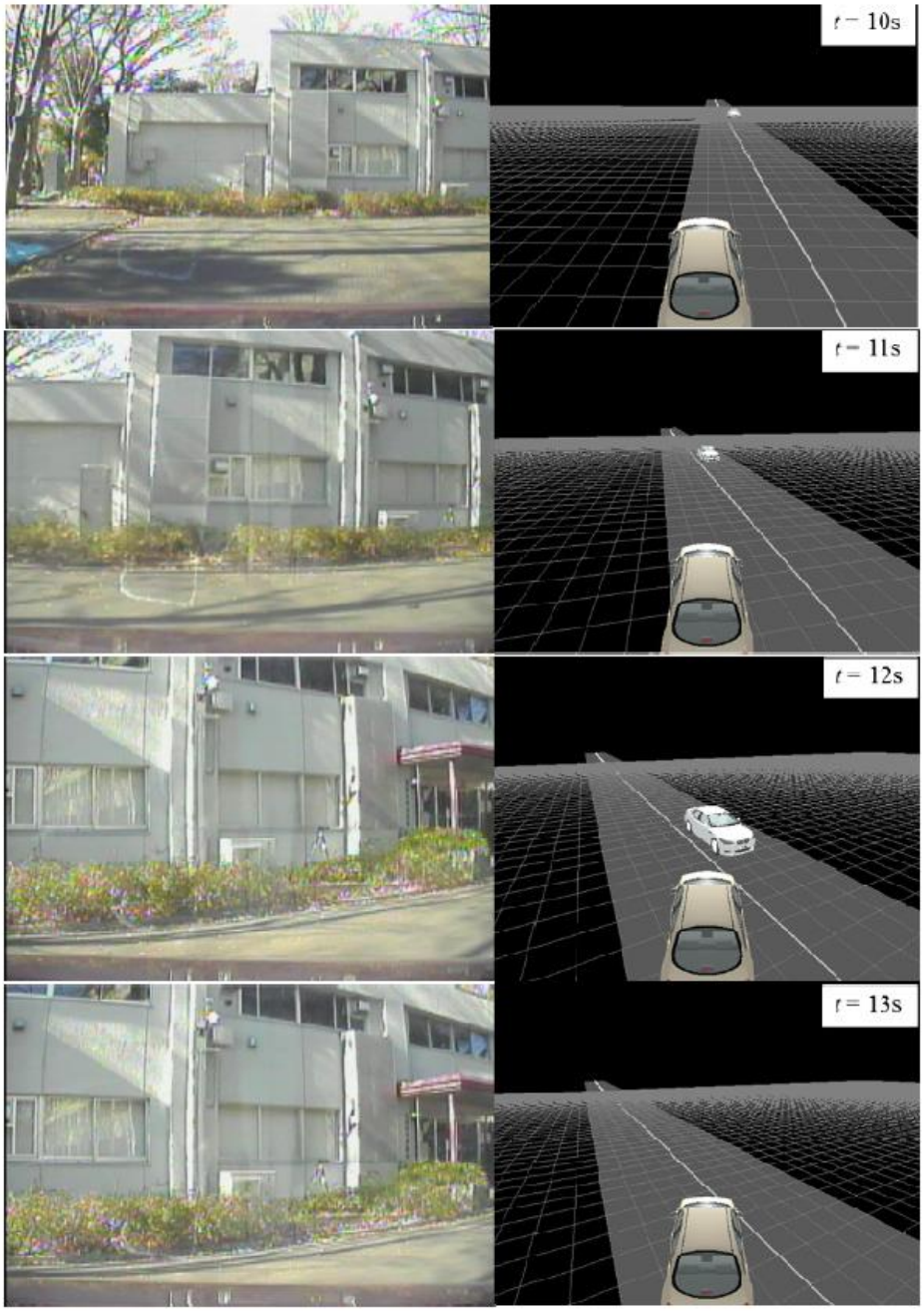

Fig. 1.2.8 Vehicle-in-the-loop simulation using the real test vehicle. Figures on the right show the virtual target to avoid, and figures on the left show the footages of the onboard camera on the test vehicle [88].

The scenario ② is a scenario where a pedestrian starts to cross the crosswalk from the blind spot when the ego vehicle makes a right-turn at the intersection. This research focused on the crosswalk at the intersection right-turn and proposed a "driver intelligent" model to turn the intersection safely. The concept of the system is to control the vehicle by predicting the potential risk for the pedestrian crossing [89]. The testing scenario is shown in Fig. 1.2.9.

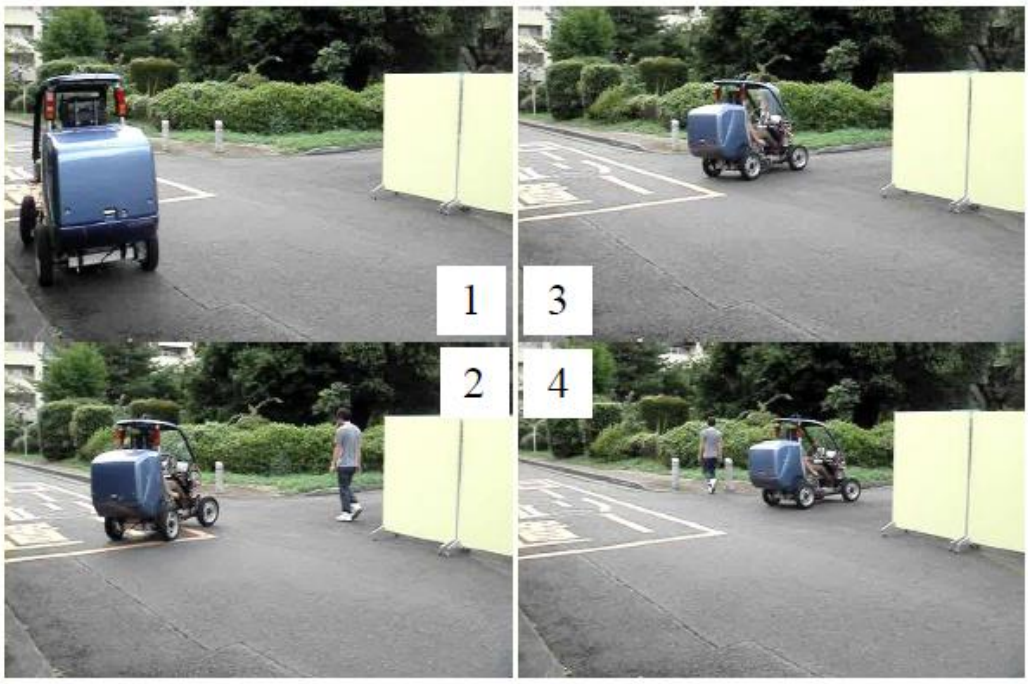

Fig. 1.2.9 Snapshots of the experiment during the right-turn maneuver [89].

The scenario ③ is a scenario where this paper focuses. A driving scenario where the ego vehicle makes an intersection right-turn with a blind spot in the oncoming lane, and a motorcycle or bicycle darts out from the blind when the ego vehicle makes a right-turn at the intersection [134][135]. In this scenario, if the driver of the vehicle does not predict the risk correctly, it is hard to avoid the collision even if the vehicle equipped the conventional emergency braking systems. This paper focuses on this risk predictive scenario and developed an ADAS. The details of the target scenario are explained in Section 2.1 in Chapter 2.

As a result of vigorous research and development on intersection safety, recently ADAS for intersection turnings are commercialized to passenger vehicles. Subaru released an ADAS that included the intersection right-turn collision avoidance New Generation EyeSight in 2019. Fig. 1.2.8 shows the overview of the right-turn collision avoidance. New Generation EyeSight equipped stereo cameras and four-millimeter wave radars and that enabled us to sense 360 degrees around the vehicle. New Generation EyeSight adopted the assistance for several intersection emergency cases such as head-on collisions at the blinded intersection, left-turn collisions with vulnerable road users, and right-turn collisions with oncoming cars or vulnerable road users [90][91]. Other manufacturers also developed ADAS for intersection right-turn (left-turn for right-hand traffic) collision avoidance systems. Audi developed Audi Turn Assist to avoid the intersection turning collision [92]. Volvo as well, developed a function called Intersection Support to avoid collisions at intersection right-turn [93][94].

The Euro NCAP extended the assessment for AEBS to a crossing and turning intersection scenarios. The testing currently includes collisions with a car and a pedestrian [117][118]. In the future, the collisions with a bicycle and a motorcycle will be included for the intersection turning scenarios [34].

1.3 Problem Statement

Plenty of research and developments of the ADAS at the intersection have been conducted and

revealed the effectiveness and tasks to achieve the goals. The ADAS using V2V or V2I communication technologies have great potential to improve road traffic safety however has difficulties in the deployment [95][96]. Especially, V2I usually requires cooperation with local governments to deploy the roadside units such as sensors and transmitters therefore it may take more time and cost for deployment and maintenance. On the other hand, the ADAS without depending on communication technologies can be deployed quickly, however, perceiving objects from onboard sensors has limitations on their detecting performance. Therefore, to avoid accidents in the complex urban area, ADAS are favored to predict the risk as early as possible. Especially in the darting-out scenario from blind spots, it is quite hard to control the vehicle to avoid a collision after detecting the avoidance object. Therefore, the ADAS requires predicting the potential risk in an earlier phase and in high accuracy with long-term risk prediction before "detecting the darting-out object".

The driver acceptance of the ADAS is also an indispensable discussion while designing the ADAS [97]. Because if the driver acceptance is bothering for the driver, the acceptance will be lower, and the driver may turn off the system. To design the ADAS acceptable for the drivers, the intervention of the system should not be too conservative and should be convincing assistance for the drivers.

One of the essences of developing the risk predictive driver assistance systems is to be consistent with the "safety" and the "driver acceptance" at the same time. Because once the system becomes too conservative for safety, the driver may not accept the system. Usually, the "safety" and the "driver acceptance" are in the trade-off relationship. Thus, the main question of this research is how to obtain enough safety performance to avoid the collision before detecting the darting-out object, and simultaneously, how to let the driver accept the ADAS.

Also, another topic raised that how we can prove the proposed system is "safe" and/or "accepted" by the driver. Currently, the Euro NCAP assesses the active safety functions for the intersection turning by using a real test vehicle at the real test track, however, conditions are limited. For example, in the assessment of Car-to-Car Front turn-across-path test, only the combinations of three test vehicle speeds combined with three target vehicle speeds are available, and the collision position when no braking action is fixed only to the center of the test vehicle [117]. In addition, to evaluate the performances in the risk predictive scenario, more conditions such as the position of occluding object may be required. In terms of developing the ADAS for risk predictive scenarios, because of the time and cost efficiency, evaluating the collision avoidance performance with the real test vehicle by comprehensively changing the conditions is not the best idea. To sum up, three questions addressed in this thesis as follows:

- How can the system define and predict the darting-out risk quantitatively before detecting the darting-out?
- How can the system be consistent with both "safety" and "driver acceptance" simultaneously?
- How can the "safety" and "driver acceptance" of the ADAS be proved by the simulation?

1.4 Research Objective

To solve the problems above and accomplish an ADAS for the risk predictive driving scenario at intersection right-turn, the research objectives of this paper are to develop an ADAS by explainable risk prediction without depending on the V2V/V2I communication facilities but with onboard sensors.

As explained in Subsection 1.2.2, this research focused on the scenario where the ego vehicle makes an intersection right-turn with a blind spot in the oncoming lane, and a motorcycle or bicycle darts out from the blind when the ego vehicle makes a right-turn at the intersection. To design a risk predictive driver assistance system for the target scenario, the following requirements must be fulfilled.

- Driver's manual steering.
- High driver acceptance.
- Moderate braking assistance to minimize the potential risk.
- Starting intervention before detecting the avoidance object.
- Long-term risk prediction before the ego vehicle driving into the intersection.

In this research, the goal of the intervention is to decelerate the vehicle to a certain speed called "safe speed" by brake assistance with minimizing the conflict between the system and driver. To actualize this control, the system controls the vehicle with minimal assistance only by moderate braking, thus, the driver has control to steer the vehicle. However, when the driver steers manually, the driver input makes it difficult to predict the vehicle motion for long-distance. To actualize the long-term prediction and start the brake intervention before the vehicle starting the intersection turning, this project covers not only proposing the algorithm of the risk prediction but also proposes a curve generation method that enables to predict long-distance intersection turning trajectory with high accuracy from the ego vehicle current motion and intersection geometry.

Besides, this study aims to evaluate the ADAS from the aspects of effectiveness for collision avoidance and driver acceptance. This paper aims to evaluate both aspects under the rapid prototyping concepts such as full-vehicle simulations and driver-in-the-loop simulations. The full-vehicle simulations enable us to conduct the collision avoidance simulations at high speed under various possible darting-out conditions. The driver-in-the-loop simulations enable us to realize the realistic driving conditions with subject drivers. The subject drivers can safely experience the functions of ADAS and risky darting-out. Therefore, the acceptance evaluation process can be done easily and short time without influenced by actual environmental conditions such as the weather and time.

1.5 Thesis Structure

This paper proposes a risk predictive Advanced Driver Assistance System for intersection right-turn with a blind spot. This paper has six chapters, and the following contents are described. Chapter 1 introduced the overview of the backgrounds, social demand, related research and products, tasks of the current technology, and objectives of the research. Chapter 2 presents the concept and core algorithms of the proposed driver assistance system. In Chapter 3, to predict the smooth and accurate trajectory of the ego vehicle motion, a curve generation method using the Triclothoidal curve is proposed, and the comparative trajectory prediction experiments on real city traffic are presented in the later sections. Chapter 4 evaluates the effectiveness of "safety" of the proposed ADAS under various conditions of darting-out patterns and intersection shapes. This chapter also mentions the simulation setup, emergency

braking function which used in the simulations, and a parameter estimation method to predict the Triclothoidal trajectory. In Chapter 5, subject driver experiments to evaluate the “driver acceptance” are presented as follows: First, the results and tasks of demonstrational experiments with the real test vehicle in the test track are described. Second, the driver acceptance evaluation experiments with driver-in-the-loop simulations. This section contains the simulation equipment, the acceptance evaluation method, and the results of the acceptance evaluation experiments. In order to enhance the driver assistance system to adopt to the various kinds of risk predictive scenarios in real urban driving scenes, generalization of the proposed driver assistance system is described. Besides providing several scenarios that requires the risk prediction, demonstrations on the generalized driver assistance system that prevents from traffic accidents have done through the full-vehicle simulations. In the last chapter, Chapter 7 concludes the paper and mentions the outlook of this project.

This page is intentionally left blank.

2. Risk Predictive Driver Assistance System for Intersection Right-Turn

As an aim to reduce the fatality at road traffic accidents, we propose an Advanced Driver Assistance System (ADAS) for intersection right-turn with risk predictive brake assistance. This chapter presents the major subsystem of the proposed ADAS, the Proactive Braking System (PBS). The following sections explain the overview and algorithm of the PBS. Firstly, Section 2.1 defines the target scenario that the proposed driver assistance system engages the brake assistance. Secondly, Section 2.2 describes the concept and structure of the proposed ADAS. Thirdly, Section 2.3 explains details about the algorithm of the PBS. And finally, Section 2.4 concludes the chapter.

2.1 Definitions of Target Scenario

Though there are plenty of risk predictive scenarios in real city driving, this research focuses on the intersection right-turn scenario. We chose the scenario for the following reasons. Firstly, traffic accidents at intersection right-turn accounted for the high percentages in city driving. Secondly, the past research did not focus on the risk predictive driver assistance system in the intersection turning scenario. And finally, intersection turning especially right-turning requires skills and concentration on driving, therefore the scenario naturally requires driver assistance.

As a risk predictive scenario in the intersection right-turn scenario, we selected the scenario when oncoming traffic is occluding the space next to the oncoming traffic while the ego vehicle making the right-turn. In this scenario, a car, a motorcycle, a bicycle, or a pedestrian may dart out from the blind spot. Fig. 2.1.1 shows the representative darting-out scenario during making a right-turn. The screen images in the figure are the screenshots from Near-miss Incident Data Base (NIDB) that is owned by TUAT Smart Mobility Research Center. NIDB records the driving data before and after the near-miss incident. The database contains recorded data from a video camera, an accelerometer, a GPS module, and several input terminals to record forward-facing video and changes in running speed, acceleration, brake signals, turn indicators, and location. The strong acceleration triggers the recording when the acceleration is larger than 0.45 G and record the data 5s before and 10s after the trigger [98][99].

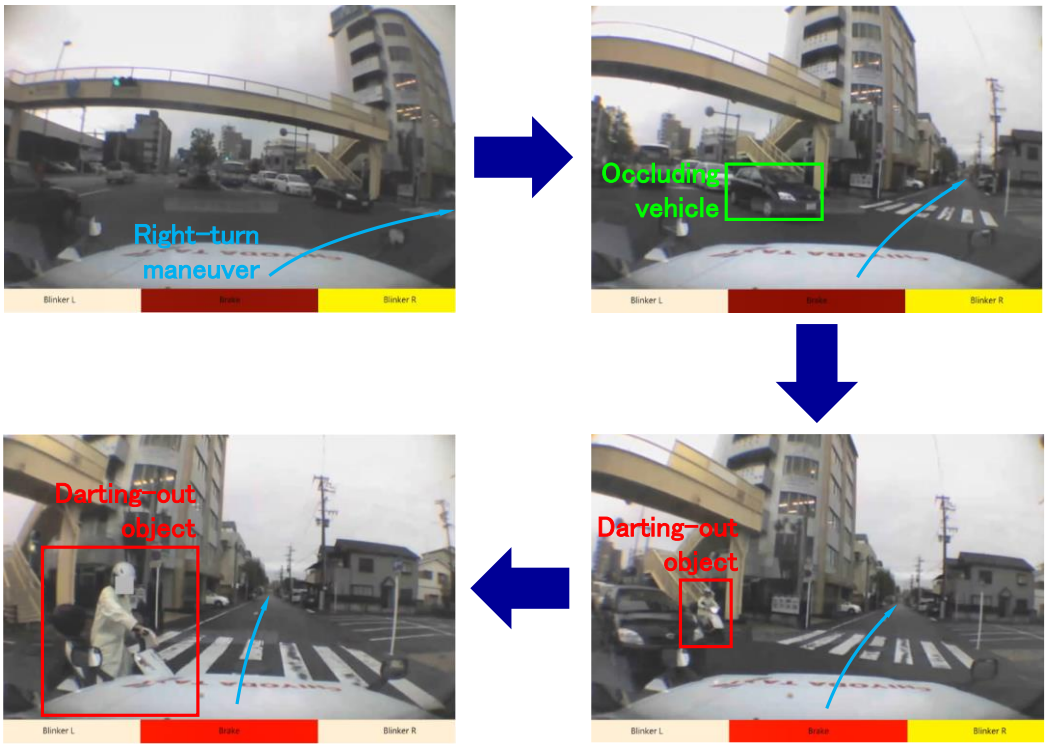

Fig. 2.1.1 The scenario that an object darts out from the blind spot [98][99].

This risk predictive scenario tends to occur when the following situations are existing in the intersection: (a) when the oncoming traffic is congested and the oncoming vehicle at the entrance of the intersection is stopping and yielding the way for right-turning vehicles, (b) when an oncoming vehicle is waiting to make a right-turn and stopping in the intersection, and (c) when the oncoming road has multiple lanes and a vehicle on the closer lane is somehow stopping but the traffic on the farther lane is flowing. Fig. 2.1.2 shows the representative risk predictive scenarios in the intersection right-turns from (a) to (c). The mutual factors of the situations are the existence of the stopping oncoming traffic at the entrance of the intersection (in front of the ego vehicle) and a space behind the occluding vehicle.

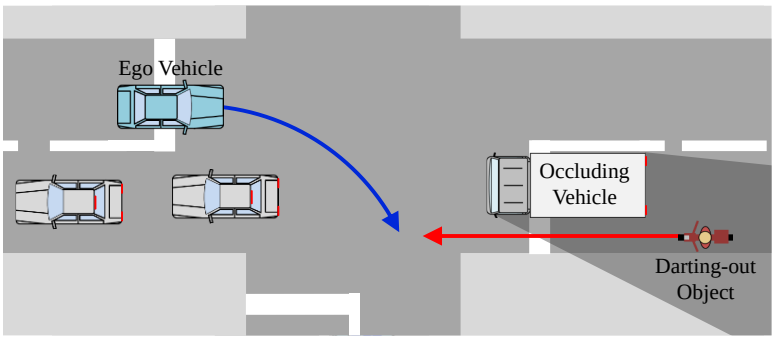

(a) When the oncoming traffic is congested and the oncoming vehicle at the entrance of the intersection is stopping and yielding the way for right-turning vehicles.

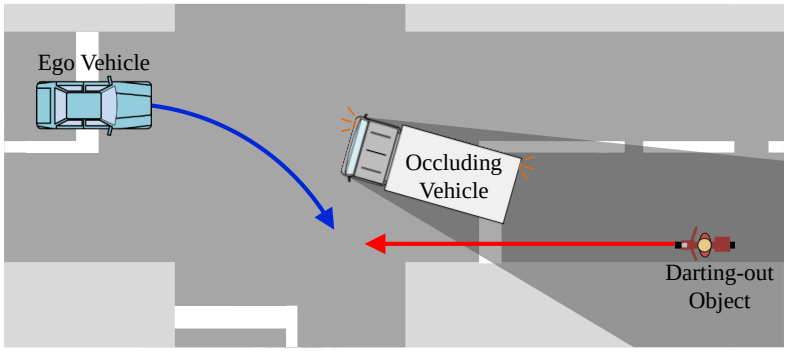

(b) When an oncoming vehicle is waiting to make a right-turn and stopping in the intersection.

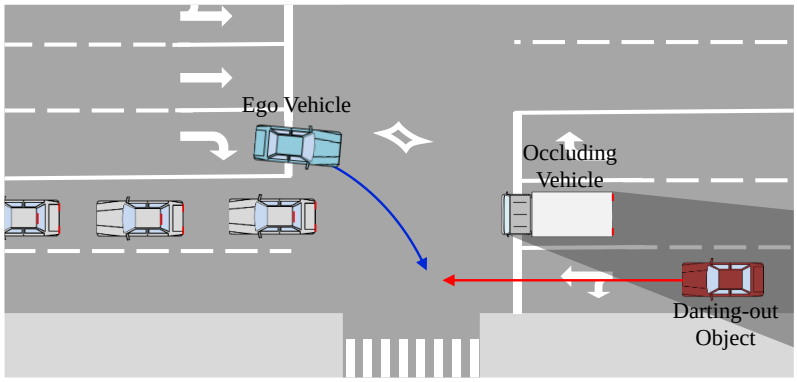

(c) When the oncoming road has multiple lanes and a vehicle on the closer lane is somehow stopping but the traffic on the farther lane is flowing.

Fig. 2.1.2 Representative example situations of the target scenario.

To know the occurrence of the cases above, we analyzed the NIDB. The database had recorded 1759 cases of near-miss incidents and accidents between the right turning vehicle and going straight vehicles (criteria: middle-risk near-miss incidents, high-risk near-miss incidents, accidents, intersections, right-turn vehicles, straight going vehicles, 4-wheelers, motorcycles, and bicycles). Form those cases, 454 cases (26%) were the cases with the darting-out object from the blind spot, and 7 cases were the accident cases. Considering the percentages of the accidents between the right turning vehicle and going straight vehicles accounted for the high ratio according to Fig. 1.1.7, it is presumed that the driver assistance at the introduced target scenario will be effective to improve the safety at the intersection turning scenario.

2.2 Concept of Proactive Braking System (PBS)

We propose a risk predictive driver assistance system, the Proactive Braking System (PBS), to minimize the potential risk in the target scenario in the intersection right-turn. The PBS applies the brake assistance to minimize the potential risk that enables to prepare the possible emergency situation of darting-out. This section introduces the concept and the system structure of the proposed PBS.

2.2.1 Concept

To design the risk predictive driver assistance system PBS, this study puts the emphasis to be consistent in terms of the "safety" and the "driver assistance". The main concept of the risk predictive driver assistance system is to minimize the potential risk with minimal driver assistance. Thus, in this study, the PBS applies only for brake assistance and leaves steering control for the driver. In other words, the driver can flexibly take any kind of right-turn maneuver and the system applies for moderate brake assistance regarding the predicted right-turn trajectory.

The target of the deceleration by the driver assistance system is to decelerate the vehicle to the speed that can stop the vehicle by emergency braking before colliding into the darting-out object. We define that speed as the "safe speed". Fig. 2.2.1 explains the concept of the deceleration of the PBS.

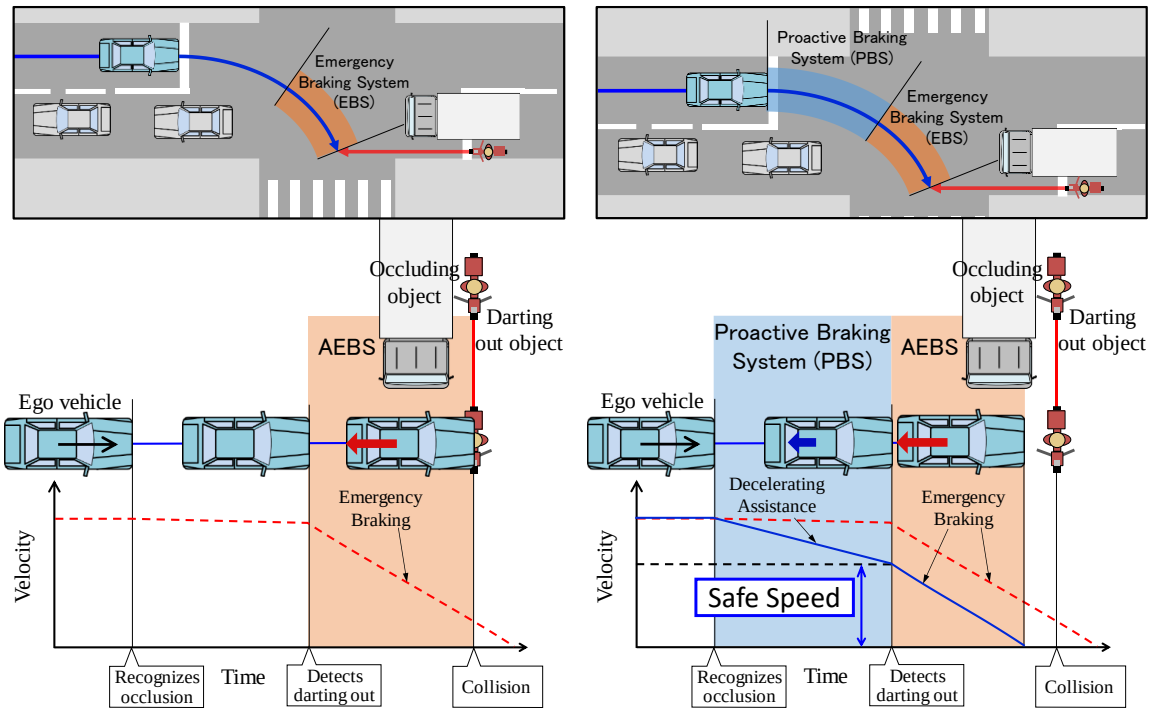

(a) The case with only AEBS. (b) The case with PBS and AEBS.

Fig. 2.2.1 The concept of the Proactive Braking System.

Focusing on the case without PBS, when the driver does not decelerate the vehicle enough in the right-turn scenario with the potential risk, the driver or AEBS cannot stop the vehicle before colliding into the darting-out object if there actually has a darting-out object from the blind spot. On the other hand, with equipping PBS, when the system detects the driver's intention to make a right turn and the existence of the occluding vehicle, the system applies moderate brake assistance to decelerate to the safe speed whether the

darting-out object detected or not. Therefore, if there has a darting-out, the vehicle can stop before colliding with the object. If there is no object darting out, the system completes the assistance, and the vehicle can pass through the intersection.

2.2.2 System Structure

The schematic structure of the whole driver assistance system is shown in Fig. 2.2.2.

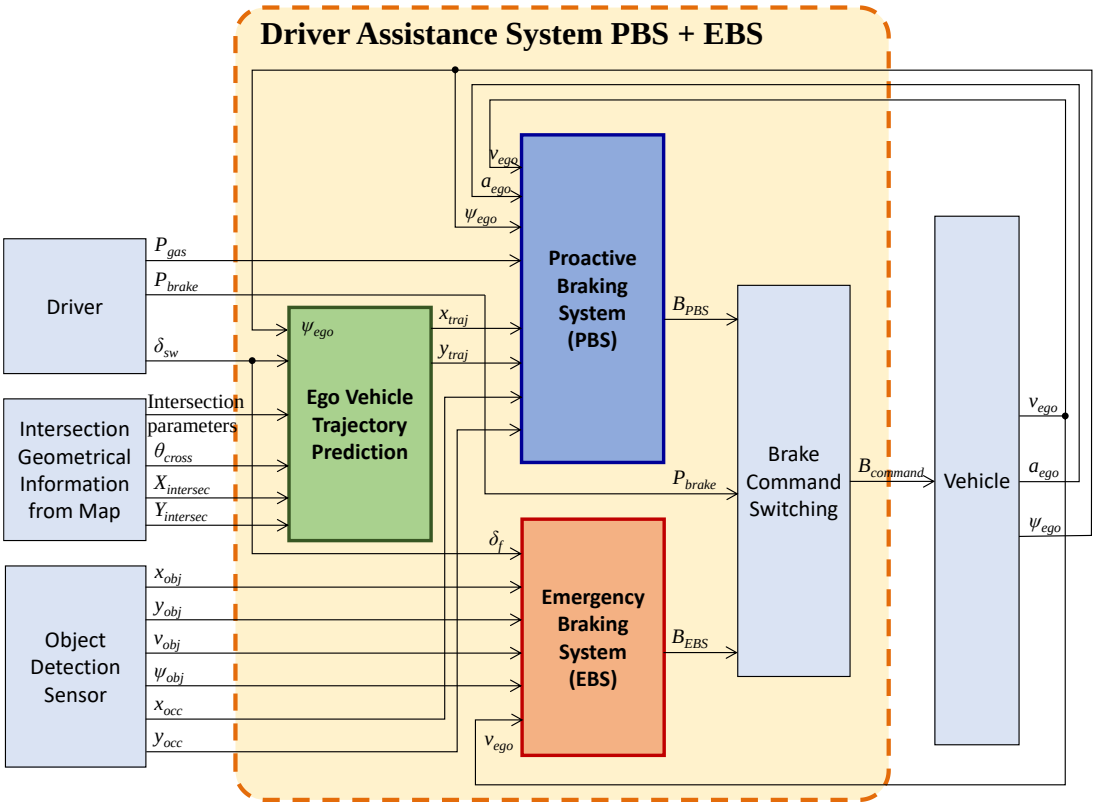

Variables

- Driver
  - P_{gas} Gas pedal input.
  - P_{brake} Brake pedal input.
  - δ_{sw} Steering wheel input.
- Intersection geometrical information from map
  - θ_{cross} Crossing angle of the intersection.
  - $X_{intersec}$ Intersection position.
  - $Y_{intersec}$ Intersection position.
- Object detection sensor
  - x_{obj} Perceived position of darting-out object.
  - y_{obj} Perceived position of darting-out object.
  - v_{obj} Perceived speed of darting-out object.
  - ψ_{obj} Perceived yaw angle of darting-out object.
  - x_{occ} Perceived position of occluding vehicle.
  - y_{occ} Perceived position of occluding vehicle.
- Vehicle
  - v_{ego} Ego vehicle speed.
  - a_{ego} Ego vehicle acceleration.
  - ψ_{ego} Ego vehicle yaw angle.
- Trajectory prediction.
  - x_{traj} Predicted trajectory.
  - y_{traj} Predicted trajectory.
- Brake command
  - B_{PBS} Brake command from PBS.
  - B_{EBS} Brake command from EBS.
  - $B_{command}$ Brake command to brake actuator of vehicle.

Fig. 2.2.2 The system structure of the proposed driver assistance system.

The orange area in the figure shows the proposed driver assistance system. The onboard sensor perceiving the surrounding object and the map including intersection information is required to activate the driver assistance system. The map requires to contain information about the intersection sizes, the crossing angle, and the absolute positions. Receiving the input data from the driver, the map, the onboard sensor,

and the vehicle, the driver assistance system output the brake command of the vehicle. The whole driver assistance system involves three subsystems and a switching function. The first subsystem of three subsystems is the Ego Vehicle Trajectory Prediction. This subsystem predicts the trajectory of the ego vehicle to predict the conflict point between the ego vehicle and the virtual darting-out object. The virtual darting-out object is presented in the next subsection. The trajectory prediction method in the subsystem used a unique method that can generate a smooth trajectory to reach an arbitrary point with an arbitrary direction without discontinuity in the curvature. The details about the trajectory prediction are introduced in Chapter 3. The second subsystem is the proposed Proactive Braking System (PBS). Receiving the predicted trajectory from the previous subsystem and the sensor data about the occluding vehicle, the system calculates the safe speed. The brake command to control the vehicle is decided from the feedforward and feedback control regarding the velocity and the acceleration. The last subsystem is the Emergency Braking System (EBS). This is the system that imitates the function of commercial AEBS for intersection turning. The system calculates the target acceleration to avoid the collision when the collision with the oncoming vehicle is imminent. This subsystem is an optional function, and this subsystem supposes to be replaceable with other collision avoidance functions. This study focuses only on the risk predictive driving assistance system however, the PBS actually can enhance the collision avoidance performance only when the system was integrated with emergency braking by the AEBS or the driver. Therefore, this paper also describes the design of the EBS in Chapter 4, but the design of the EBS itself is not the focus of the research.

In addition, we provided that the design of this system is not dependent on the V2V or V2I communication, however, the principle of the system does not reject the communication technologies. The advantage of the proposing system is that the system can be operated in every intersection without the communication facility, but the proposed system potentially can improve its performance by the information via V2V/V2I communications. For example, if the roadside unit or other vehicle sensor did not detect the darting-out object, the PBS does not need to engage the brake assistance even when the oncoming vehicle stops and makes the blind spot. In another case, when the existence of the darting-out object is provided via communication, the PBS flexibly can change the safe speed by changing the parameter of the system. Besides, by obtaining the information of traffic signal via communication, the system can avoid excessive brake assistance when the right-turn vehicles are protected by a traffic signal.

2.3 Risk Prediction Algorithm of Proactive Braking System (PBS)

The main question in designing the driver assistance system is how to fulfill both requirements about “safety” and “driver acceptance”. To solve this question, applying the concept of “safe speed” in the PBS, this section presents the design of the PBS including how to calculate the “safe speed” and the deceleration algorithms to actualize the comfortable deceleration.

When the ego vehicle heading to an intersection, the followings trigger to activate the PBS: the driver intends to make a right turn at the intersection with the turning indicator, the onboard sensor is detecting an occluding vehicle on the oncoming lane, and there is enough space behind the occluding vehicle where an object can dart out. The flowchart to activate the PBS is diagramed in Fig. 2.3.1. When the PBS was triggered, the algorithms in the following subsections calculates the safe speed and target acceleration and controls the vehicle.

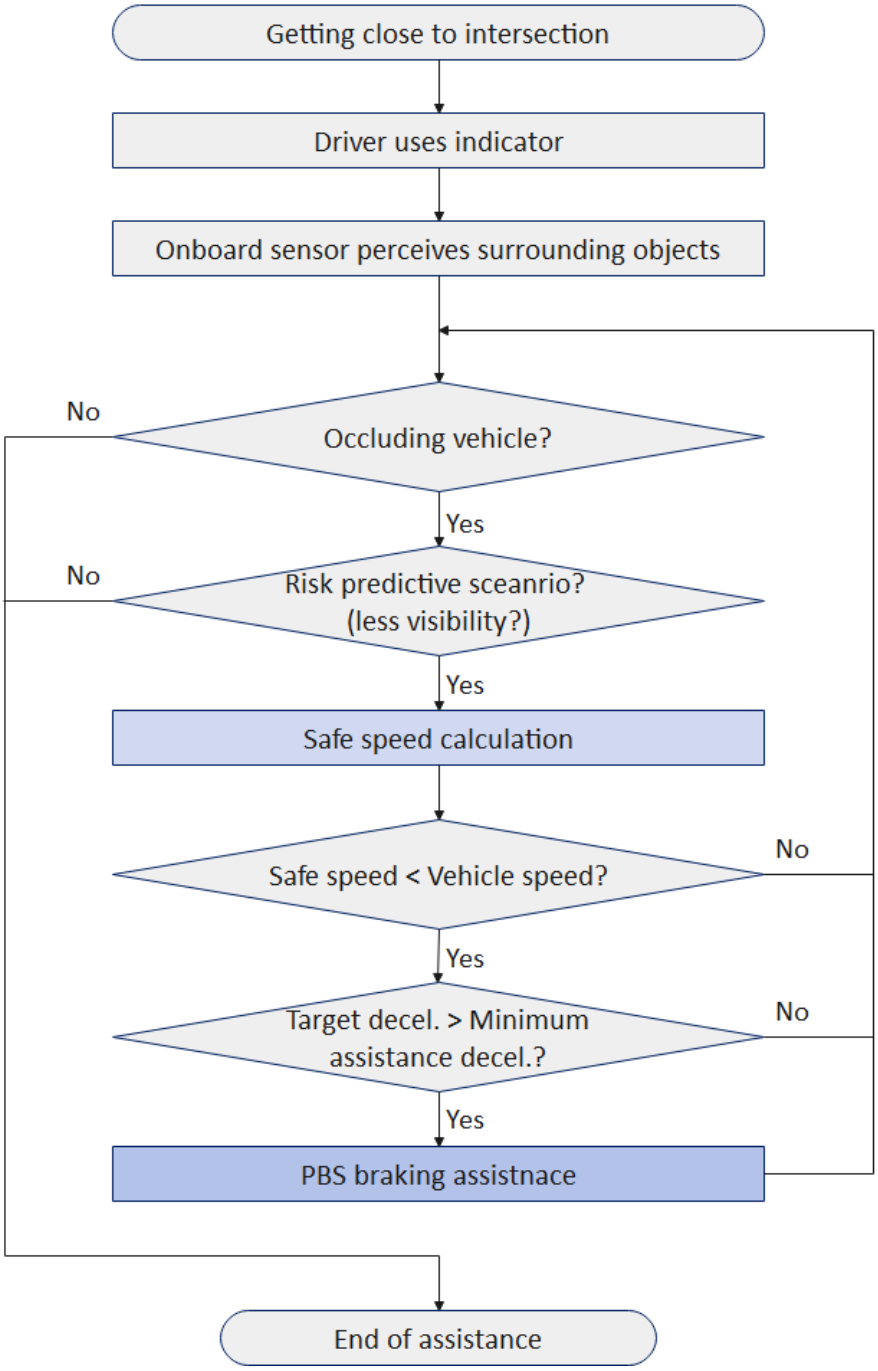

Fig. 2.3.1 Flowchart of the PBS activation.

2.3.1 Virtual Darting-Out Object

To predict and calculate the safe speed to avoid the actual darting-out object from the blind spot, a virtual darting-out object is assumed to dart-out from the blind spot. The virtual darting-out object defines to dart out in parallel to the direction of the entering road of the intersection. Here, Fig. 2.3.1 schematically explains the definitions of the virtual darting-out object.

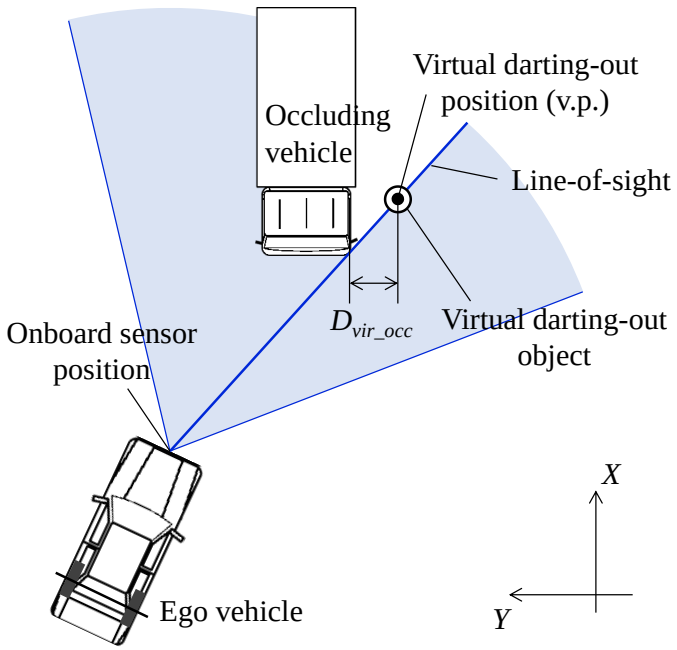

Fig. 2.3.1 The virtual darting-out object.

The trajectory of the virtual darting-out object defines as a straight trajectory that has offset with distance D_{vir_occ} from the left-front corner of the occluding vehicle. The darting-out position of the virtual darting-out object defines as a point, indicated as v.p. in the figure, on the trajectory of the virtual darting-out object. This v.p. is dependent on the line-of-sight from the onboard sensor of the ego vehicle. To say more specifically, the position of the v.p. is the crossing point between the darting-out trajectory and the line-of-sight from the onboard sensor. Therefore, the v.p. differs its position by the position of the ego vehicle, because when the car moves, the sensor itself moves as well.

2.3.2 Conflict Point Prediction

The conflict point (c.p.) can be predicted from the defined trajectory of the virtual darting-out object and the predicted trajectory of the ego vehicle. The prediction method of the ego vehicle trajectory is presented in Chapter 3. This study assumes that the dimensions of the vehicle and the front steering angle geometrically defines the trajectory of the vehicle. Therefore, presuming that the trajectory always meets at right angles at the center point of the rear-axle of the ego vehicle. On the other hand, to implement the predicted curve for the Proactive Braking System, the trajectory at the sensor position must be predicted to know the future position of the darting-out position of the virtual darting-out object v.p. Regarding that the trajectory at the center point of rear-axle can be discretely predicted as $\left(x_{traj0}(k), y_{traj0}(k)\right)$ $(k=1,2,3,\cdots,N)$, the following equation derives the trajectory at sensor position of the vehicle $\left(x_{traj}(k), y_{traj}(k)\right)$:

$$\begin{cases} x_{traj}(k) = L_{sensor}\cos\left(\psi_{ego}(k)\right) + x_{traj0}(k) \\ y_{traj}(k) = L_{sensor}\sin\left(\psi_{ego}(k)\right) + y_{traj0}(k) \end{cases} \quad (k=1,2,3,\cdots,N), \tag{2.3.1}$$

where L_{sensor} is the length from rear-axle to sensor position of the vehicle, $\psi_{ego}(k)$ is the relative yaw angle from the current ego vehicle yaw angle. This relative angle $\psi_{ego}(k)$ is determined as the tangential angle at $\left(x_{traj0}(k), y_{traj0}(k)\right)$.

In this section, the predicted trajectory of the ego vehicle indicates the trajectory at the sensor position of the vehicle.

The derivation of the trajectory of the virtual darting-out object is as follows. The distance from the left-front tip of the occluding vehicle to the virtual darting-out trajectory D_{vir_occ} defines the trajectory of the virtual darting-out trajectory as shown in Fig. 2.3.2 and the following equation:

$$\left(x - x_{occ}\right)\tan\theta_{vir} - \left(y - y_{occ}\right) - \frac{D_{vir\_occ}}{\cos\theta_{vir}} = 0, \tag{2.3.2}$$

where (x_{occ}, y_{occ}) are the position of the left-front corner of the occlusion vehicle, and θ_{vir} is the relative angle from the ego yaw angle to the direction angle of the entering road of the intersection.

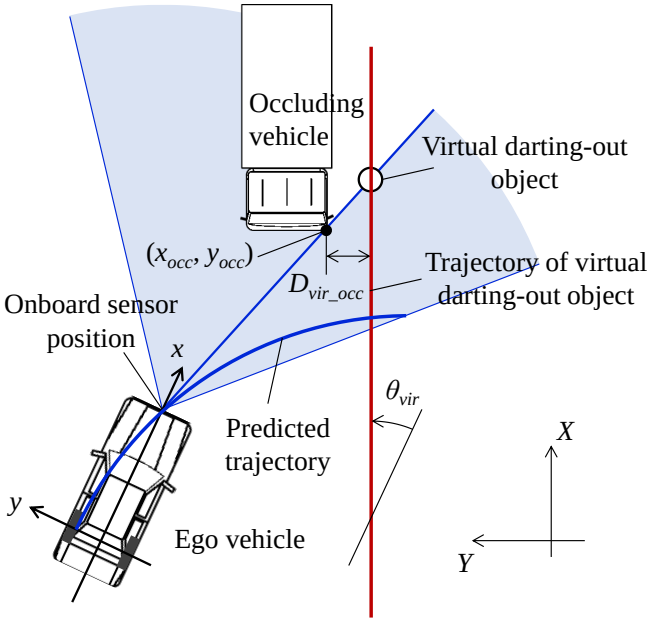

Fig. 2.3.2 The definition of the virtual darting-out trajectory.

From the definition, the position of the v.p. at the current state can be calculated from the crossing point between the line-of-sight of the sensor and the darting-out trajectory defined in (2.3.2). The position of c.p. looks up the closest point to the darting out trajectory (2.3.2) from the point list of the discrete ego vehicle trajectory $\left(x_{traj}(k), y_{traj}(k)\right)$ in (2.3.1). From above, the positions of the v.p. and the c.p. can derive the distance from the v.p. to c.p. d_{vir}. By giving the darting-out speed v_{vir} and time-to-collision (TTC) from the v.p. to c.p. t_{vir}, the distance d_{vir} from v.p. to c.p. can be derived as $d_{vir} = v_{vir} t_{vir}$.

By the way, in the design of the deceleration function, we have to consider two factors, “safety” and “acceptance.” In terms of “safety”, all darting-out cases can be avoided by the ADAS, then the system must consider every possible risk. However, this means the car will stop by the system and will not be able to pass over the predicted c.p. Therefore, we have to give a constraint to the algorithm to secure the “acceptance.”

In this study, we gave a constraint that the system assists only when the TTC of the virtual darting-out object t_{vir} is smaller than a certain value t_{vir_d}. By giving this constraint, the system completes the assistance when the ego vehicle has enough visibility behind the occluding vehicle. In this study, TTC t_{vir_d} was fixed to 2.0 s to take enough time for the darting-out object to avoid the turning ego vehicle. Thus, the position

of the ego vehicle when the TTC of the virtual object becomes t_{vir_d} defines as the detecting point (d.p.). The schematic of the geometrical relationship between the ego vehicle, the occluding vehicle, and the d.p. is shown in Fig. 2.3.3. The target of the PBS is to complete the deceleration assistance to the safe speed until the ego vehicle reaching the d.p. Then, the system can guarantee the safety of the function when the TTC of the virtual darting-out object is less than t_{vir_d}.

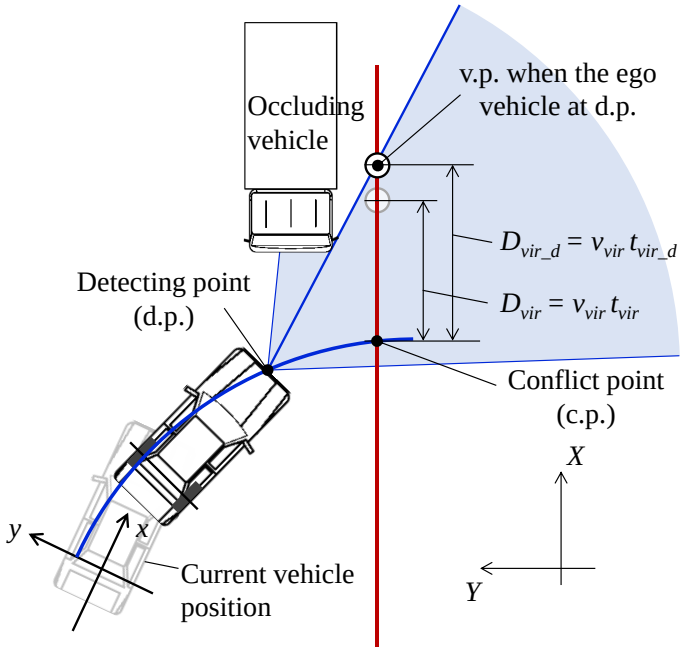

Fig. 2.3.3 The definitions of the TTC of the virtual darting-out object and the detecting point d.p.

2.3.3 Safe Speed Calculation

The definition of the safe speed in this study is the speed that can be stopped by the emergency braking before reaching the c.p. Besides, as mentioned in the previous subsection, the system needs to complete the assistance before reaching the d.p. Since the distances from the ego vehicle position to c.p. and d.p. are geometrically derived from the relationship as shown in Fig. 2.3.4, the distance to stop d_{stop} is given by the following equation:

$$d_{stop} = d_{cp\_PBS} - d_{PBS} - D_{safe}, \tag{2.3.3}$$

where d_{PBS} is the distance of the PBS control section that is equivalent to the distance from the ego vehicle to the c.p., D_{safe} is the safety margin, and d_{cp_PBS} is the distance from the ego vehicle to the c.p.

To stop the vehicle in the distance d_{stop} by the emergency braking from the safe speed, the following equation defines the safe speed v_{safe}.

$$v_{safe} = a_{EBS}\tau + \sqrt{a_{EBS}^2\tau^2 - 2a_{EBS}d_{stop}}, \tag{2.3.4}$$

where a_{EBS} is the expected acceleration of the emergency braking and τ is the latency of the braking system.

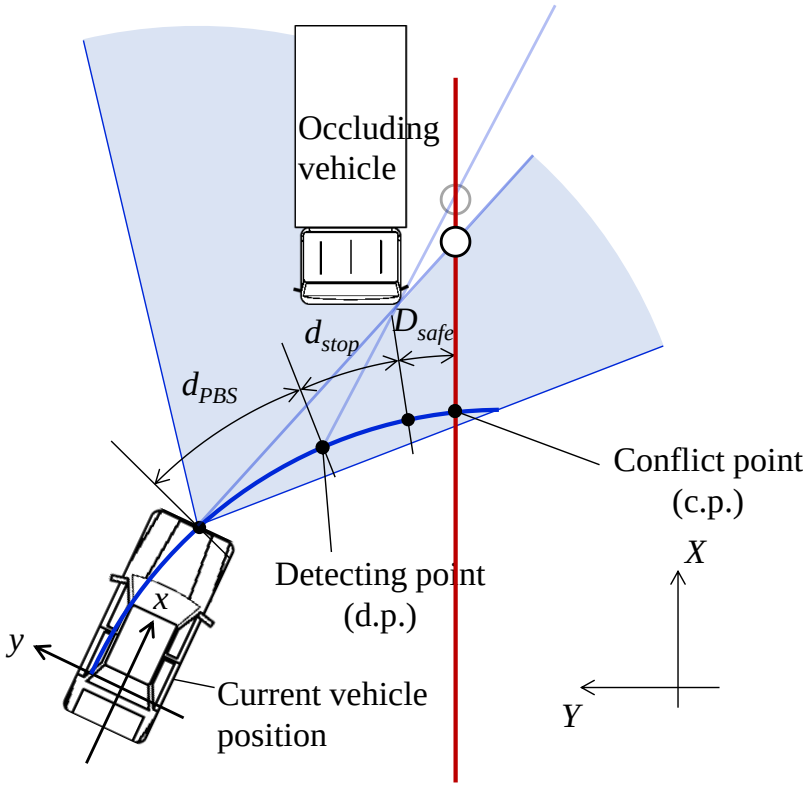

Fig. 2.3.4 The definitions of the distances for the PBS and the emergency braking.

2.3.4 Deceleration Speed Planning of PBS

As an aim of the design concept, deceleration planning of the system is indispensable to secure the acceptance of the driver assistance system. In this study, to make the deceleration as comfortable and less plaguey assistance, we discussed speed profiles to decelerate to the safe speed.

This method provides a smooth speed profile to decelerate from initial velocity to terminal velocity. This profile consists of two constant jerks and switches the jerk in the half time of the control time. This profile requires generating the smooth speed profile without discontinuities in the acceleration and fulfill conditions about the acceleration, the velocity, and the position at the initial and the terminal position. Fig. 2.3.5 provides an example speed profile with this method. Wherein, J_1 is the jerk in the first half of the control time, J_2 is the jerk in the second half of the control time, a_0 and a_f are the initial and terminal acceleration, v_0 and v_f are the initial and terminal velocity, x_2 is the distance from initial to the terminal point position, t_1 is the first half of the control time, and t_2 is the total time of the control time. As the boundary conditions of the speed profile, the following parameters must be defined: initial acceleration, initial velocity, terminal acceleration, terminal velocity, and distance from initial to the terminal position. The current acceleration and velocity of the ego vehicle give the initial acceleration and velocity. The length of the control section by PBS d_{PBS} provides the distance from the initial to the terminal position. The terminal velocity defines as the safe speed. Giving the terminal acceleration as 0. The two jerks J_1 and J_2 are determined from the provided boundary conditions and the speed profile can be obtained.

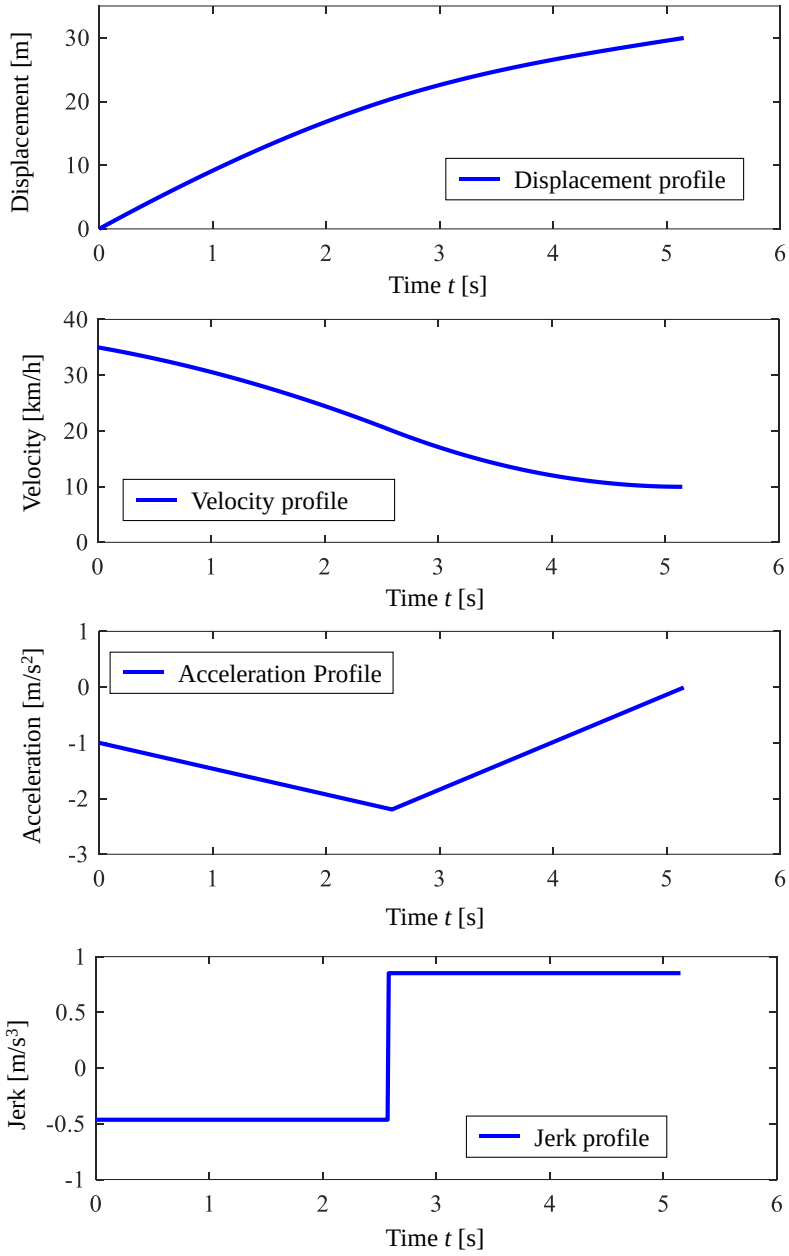

Fig. 2.3.5 The speed profile consists of two constant jerks.

The followings describe how to derive the jerks J_1 and J_2 to fulfill the requirements. The following equations represent the displacement trajectory generated by the speed profile at time t from the defined boundary conditions.

$$\begin{cases} x(t) = v_0 t + \frac{1}{2} a_0 t^2 + \frac{1}{6} J_1 t^3 & (0 \le t \le t_1) \\ x(t) = x_1 + v_1 (t - t_1) + \frac{1}{2} a_1 (t - t_1)^2 + \frac{1}{6} J_2 (t - t_1)^3 & (t_1 < t \le t_2), \end{cases} \tag{2.3.5}$$

where x_1, v_1, a_1 are the displacement, the velocity, and the acceleration at the time t_1 respectively.

From the upper equation of (2.3.5),

$$\begin{cases} x_1 = v_0 t_1 + \frac{1}{2} a_0 t_1^2 + \frac{1}{6} J_1 t_1^3 \\ v_1 = v_0 + a_0 t_1 + \frac{1}{2} J_1 t_1^2 \\ a_1 = a_0 + J_1 t_1. \end{cases} \tag{2.3.6}$$

Regarding the total control time t_2 as $t_2 = 2t_1$, from the lower equation of (2.3.5), the displacement, the velocity, and the acceleration at t_1 and t_2 are described as follows:

$$\begin{cases} x(t_2) = d_{PBS} = x_1 + v_1 t_1 + \frac{1}{2} a_1 t_1^2 + \frac{1}{6} J_2 t_1^3 \\ \dot{x}(t_2) = v_{safe} = v_1 + a_1 t_1 + \frac{1}{2} J_2 t_1^2 \\ \ddot{x}(t_2) = 0 = a_1 + J_2 t_1, \end{cases} \tag{2.3.7}$$

therefore,

$$\begin{cases} a_1 = -J_2 t_1 \\ v_1 = v_{safe} + \frac{1}{2} J_2 t_1^2 \\ x_1 = d_{PBS} - v_{safe} t_1 - \frac{1}{6} J_2 t_1^3. \end{cases} \tag{2.3.8}$$

From (2.3.6) and (2.3.8),

$$v_0 t_1 + \frac{1}{2} a_0 t_1^2 + \frac{1}{6} J_1 t_1^3 = d_{PBS} - v_{safe} t_1 - \frac{1}{6} J_2 t_1^3, \tag{2.3.9}$$

$$v_0 + a_0 t_1 + \frac{1}{2} J_1 t_1^2 = v_{safe} + \frac{1}{2} J_2 t_1^2, \tag{2.3.10}$$

$$a_0 + J_1 t_1 = -J_2 t_1. \tag{2.3.11}$$

When $a_0 \neq 0$, from (2.3.11),

$$t_1 = -\frac{a_0}{J_1 + J_2}. \tag{2.3.12}$$

Introducing $X = J_1 + J_2$ and substituting (2.3.12) into (2.3.10), the following equation can be obtained:

$$\begin{aligned} &\left(v_0 - v_{safe}\right)\left(J_1 + J_2\right)^2 - \frac{1}{2} a_0^2 \left(J_1 + 3J_2\right) = 0 \\ &\Leftrightarrow \left(v_0 - v_{safe}\right) X^2 - \frac{1}{2} a_0^2 \left(X + 2J_2\right). \end{aligned} \tag{2.3.13}$$

From (2.3.13), the second jerk J_2 is

$$J_2 = \frac{v_0 - v_{safe}}{a_0^2} X^2 - \frac{1}{2} X. \tag{2.3.14}$$

From $X = J_1 + J_2$ and (2.3.14), the first jerk J_1 is

$$J_1 = X - J_2 = -\frac{v_0 - v_{safe}}{a_0^2} X^2 + \frac{3}{2} X. \tag{2.3.15}$$

By substituting (2.3.12) into (2.3.9), the following equation can be obtained.

$$\begin{aligned} & d_{PBS}\left(J_1 + J_2\right)^2 + a_0\left(v_0 + v_{safe}\right)\left(J_1 + J_2\right) - \frac{1}{3}a_0^3 = 0 \\ & \Leftrightarrow J_1 + J_2 = X = -\frac{a_0}{2d_{PBS}}\left\{\left(v_0 + v_{safe}\right) \pm \sqrt{\left(v_0 + v_{safe}\right)^2 + \frac{4}{3}a_0 d_{PBS}}\right\}, \end{aligned} \tag{2.3.16}$$

when $\left(v_0 + v_{safe}\right)^2 + 4a_0 d_{PBS}/3 < 0$, the root of X does not exist. In this case, the initial acceleration is handled as

$$a_0 = -\frac{3\left(v_0 + v_{safe}\right)^2}{4d_{PBS}}. \tag{2.3.17}$$

Besides, when $\left(v_0 + v_{safe}\right)^2 + 4a_0 d_{PBS}/3 = 0$, X has a double root. Therefore, in the cases $\left(v_0 + v_{safe}\right)^2 + 4a_0 d_{PBS}/3 \le 0$, $X = J_1 + J_2$ is calculated as

$$X = -\frac{a_0}{2d_{PBS}}\left(v_0 + v_{safe}\right). \tag{2.3.18}$$

When $\left(v_0 + v_{safe}\right)^2 + 4a_0 d_{PBS}/3 > 0$, X has two roots as described in (2.3.16). To select the appropriate root for the speed profile of the proposed driver assistance system, the problem is discussed from three cases: (i) $a_0 > 0$, (ii) $a_0 = 0$, and (iii) $a_0 < 0$.

(i) When $a_0 > 0$, the range of X is $X < 0$ since $J_1 t_1 + J_2(t_2 - t_1) = -a_0 \Leftrightarrow X t_1 = -a_0$. Therefore,

$$X = -\frac{a_0}{2d_{PBS}}\left\{\left(v_0 + v_{safe}\right) \pm \sqrt{\left(v_0 + v_{safe}\right)^2 + \frac{4}{3}a_0 d_{PBS}}\right\} > 0. \tag{2.3.19}$$

Considering $a_0 > 0$, the condition that fulfills the inequality is

$$\left(v_0 + v_{safe}\right) + \sqrt{\left(v_0 + v_{safe}\right)^2 + \frac{4}{3}a_0 d_{PBS}} > 0. \tag{2.3.20}$$

Therefore, the root of (2.3.16) at $a_0 > 0$ is

$$X = -\frac{a_0}{2d_{PBS}}\left\{\left(v_0 + v_{safe}\right) + \sqrt{\left(v_0 + v_{safe}\right)^2 + \frac{4}{3}a_0 d_{PBS}}\right\}. \tag{2.3.21}$$

Substitute (2.3.21) into (2.3.15) and (2.3.14), the jerks J_1 and J_2 can be obtained respectively.

(ii) When $a_0 = 0$, since $X = 0$, the relationship between two jerks is $J_1 = -J_2$. Substituting $J_1 = -J_2$ into (2.3.10), the time t_1 can be expressed as

$$t_1 = \sqrt{\frac{v_{safe} - v_0}{J_1}}. \tag{2.3.22}$$

Substituting (2.3.22) into (2.3.9) and considering $J_1 = -J_2$ and $a_0 = 0$, the first jerk J_1 can be obtained as follows:

$$v_0 t_1 + \frac{1}{2} a_0 t_1^2 + \frac{1}{6} J_1 t_1^3 = d_{PBS} - v_{safe} t_1 - \frac{1}{6} J_2 t_1^3$$
$$\Leftrightarrow v_0 \sqrt{\frac{v_{safe} - v_0}{J_1}} = d_{PBS} - v_{safe} \sqrt{\frac{v_{safe} - v_0}{J_1}} \tag{2.3.23}$$
$$\Leftrightarrow J_1 = -\frac{\left(v_0 + v_{safe}\right)\left(v_0^2 - v_{safe}^2\right)}{d_{PBS}^2}.$$

Therefore,

$$J_2 = \frac{\left(v_0 + v_{safe}\right)\left(v_0^2 - v_{safe}^2\right)}{d_{PBS}^2}. \tag{2.3.24}$$

(iii) When $a_0 < 0$, the range of X is $X > 0$ since $J_1 t_1 + J_2(t_2 - t_1) = -a_0 \Leftrightarrow X t_1 = -a_0$. While this speed profile is for braking function, to make it consistent, the speed profile would not increase the velocity at the section $t_1 < t < t_2$. Thus, the velocity at the section would be higher than the safe speed v_{safe}. Therefore, the second jerk J_2 would also be higher than 0. From this preference, in this study, the solution is decided as

$$X = -\frac{a_0}{2 d_{PBS}} \left\{ \left(v_0 + v_{safe}\right) + \sqrt{\left(v_0 + v_{safe}\right)^2 + \frac{4}{3} a_0 d_{PBS}} \right\}. \tag{2.3.25}$$

Substitute (2.3.25) into (2.3.15) and (2.3.14), the jerks J_1 and J_2 can be obtained respectively.

2.3.5 Deceleration Control Algorithm

To complete the deceleration to the safe speed by reaching the distance d_{PBS} with smooth acceleration, the target velocity and the target acceleration are defined from the deceleration speed profile. Introducing a prediction time t_{pre}, the target velocity and acceleration are determined in the following equations:

$$\begin{cases} v_{target} = \dot{x}\left(t_{pre}\right) = v_0 + a_0 t_{pre} + \frac{1}{2} J_1 t_{pre}^2 & \left(0 \le t_{pre} \le t_1\right) \\ v_{target} = \dot{x}\left(t_{pre}\right) = v_1 + a_1\left(t_{pre} - t_1\right) + \frac{1}{2} J_2 \left(t_{pre} - t_1\right)^2 & \left(t_1 < t_{pre} \le t_2\right) \\ v_{target} = \dot{x}\left(t_{pre}\right) = v_{safe} & \left(t_2 < t_{pre}\right), \end{cases} \tag{2.3.26}$$

$$\begin{cases} a_{target} = \ddot{x}\left(t_{pre}\right) = a_0 + J_1 t_{pre} & \left(0 \le t_{pre} \le t_1\right) \\ a_{target} = \ddot{x}\left(t_{pre}\right) = a_1 + J_2\left(t_{pre} - t_1\right) & \left(t_1 < t_{pre} \le t_2\right) \\ a_{target} = \ddot{x}\left(t_{pre}\right) = 0 & \left(t_2 < t_{pre}\right). \end{cases} \tag{2.3.27}$$

Fig. 2.3.6 shows the block diagram of the deceleration function of the PBS. The normalized brake command of the PBS B_{PBS} to control the vehicle is calculated with the following equation.

$$B_{PBS0} = -K_{ff} a_{target} - K_a \left\{ a_{target} - \ddot{x}(0) \right\} - K_v \left\{ v_{target} - \dot{x}(0) \right\}, \tag{2.3.28}$$

where $\ddot{x}(0)$ is the current vehicle acceleration, $\dot{x}(0)$ is the current vehicle velocity, K_{ff} is a feedforward gain, and K_a and K_v are feedback gains.

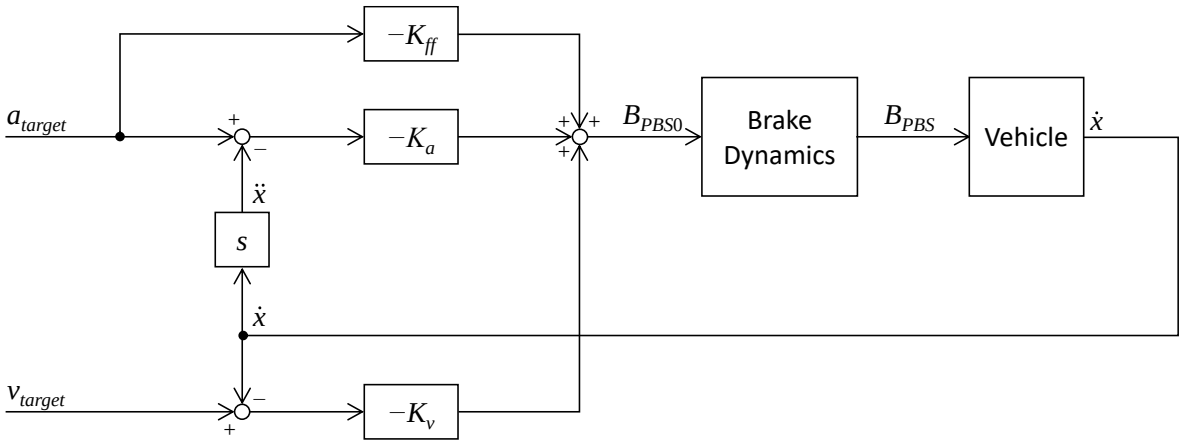

Fig. 2.3.6 The block diagram of the deceleration function of PBS.

In order to avoid the excessive assistance of the PBS, when the brake command B_{PBS0} exceeds the limit B_{PBS_max}, the brake command B_{PBS} saturates to the B_{PBS_max}, and when the ego velocity is below the safe speed v_{safe}, the PBS turned off the brake assistance.

$$\begin{cases} B_{PBS} = B_{PBS\_max} & \left(B_{PBS\_max} \le B_{PBS0}\right) \\ B_{PBS} = B_{PBS0} & \left(0 \le B_{PBS\_max} < B_{PBS0}\right) \\ B_{PBS} = 0 & \left(\dot{x}(0) < v_{safe}\right). \end{cases} \tag{2.3.29}$$

2.4 Conclusion

Defining the target scenario as an intersection right-turn scenario when the blind spot is existing on the oncoming lane, we proposed a risk predictive driver assistance system to enhance the collision avoidance performance system. The proposed system Proactive Braking System (PBS) calculates the safe speed by considering the geometrical relationships and physical limitations. This chapter also proposed a smooth deceleration speed profile to obtain the driver-acceptable braking assistant. The effectiveness evaluation regarding “safety” of the proposed PBS is described in Chapter 4, and the effectiveness evaluation regarding “driver acceptance” of the proposed PBS is described in Chapter 5.

3. Right-Turn Trajectory Prediction Method with Triclothoidal Curve

Turning trajectory prediction is an indispensable topic for the Advanced Driver Assistance System (ADAS) for turning. In this section, a brand-new method that predicts the turning trajectory in high accuracy compared to the conventional methods. Here in this chapter, we propose the trajectory method and explain the derivation of the curve and evaluate the accuracy of the prediction. In Section 3.1, as an introduction, background of the trajectory prediction for ADAS, and conventional curve generation methods are presented. Section 3.2 explains the derivation of the proposed curve generation method, the Triclothoidal curve. Section 3.3 evaluates the effectiveness and accuracy of the proposal curve generation method as the intersection turning trajectory prediction through the data acquisition experiments and comparative evaluations. Section 3.4 presents a parameter estimation method that relatively defines the terminal position of the Triclothoidal trajectory. Lastly, Section 3.5 concludes the chapter.

3.1 Trajectory Prediction Methods

For ADAS at intersection turning, an imperative point is to predict a vehicle's trajectory correctly and assess the risk for collision accurately while turning at the intersection. In the following text, we briefly review previous studies that have correctly predicted the trajectory of the vehicle.

Some researchers took the approach of planning the intersection turning path for automated vehicles by generating the target path from digital maps [100][101]. However, for most driver assistance systems, especially for systems in urban areas, including intersection turnings, drivers were required to hold the steering wheel even during the assistance. Hence, the design of the ADAS requires the driver's input such as dynamic steering wheel motion. Thus, the trajectory prediction method that uses digital maps only is not suitable for ADAS for turning at intersections.

Other studies for the trajectory prediction proposed methods that stochastically predicted the future trajectory from the observed previous motion of the ego vehicle [82][102]-[104]. However, stochastic prediction makes risk assessment and decision-making a more complex problem. Besides, there are no big advantages to use stochastic methods for turning at intersections because the destination of the ego vehicle during turning is usually obvious and definitive. Thus, our proposal intends to provide a trajectory that is adaptive to the driver's input rather than the prediction method from digital maps. Further, our proposed method is more accurate in the prediction than those by the stochastic methods.

To enhance the accuracy of trajectory prediction, a smooth trajectory must be generated by considering both the driver's input and the vehicle's current state. However, the smoother the trajectory becomes, the calculation costs incurred to generate a curve becomes higher. On the other hand, trajectory predictions for ADAS require real-time calculation ability, and therefore, a higher calculation cost is not acceptable. Our main concern is balancing the smoothness and calculation cost of the curve while developing the trajectory prediction method. The following subsections introduce the conventional methods to generate the smooth trajectory with a very low calculation cost.

As a traditional method to generate a smooth trajectory with a very low calculation cost, a circular arc is one of the simplest and the most well-known ways to predict the turning trajectory. The circular arc requires determining the initial point position, the direction, and the turning radius. The current position and azimuth of the ego vehicle determine the initial point position and the direction. To draw the

intersection turning trajectory with the circular arc, a constant and a variable radius are frequently used as the circular arc trajectory.

3.1.1 Circular Arc with Constant Radius

The circular arc with the constant radius determines simply by giving a turning radius as a constant value. The size of the turning radius is defined from the size of the intersection. An example shape of the circular arc is indicated in Fig. 3.1.1. The superiorities of this method are its simplicity and the very low calculation cost. On the other hand, the prediction accuracy of the trajectory is not very high because in most cases, the drivers do not turn with the constant radius. In addition to this, the trajectory with constant radius cannot predict trajectory from the far distance, therefore the collision point prediction in the driver assistance system unable to predict properly in the early phase of the assistance.

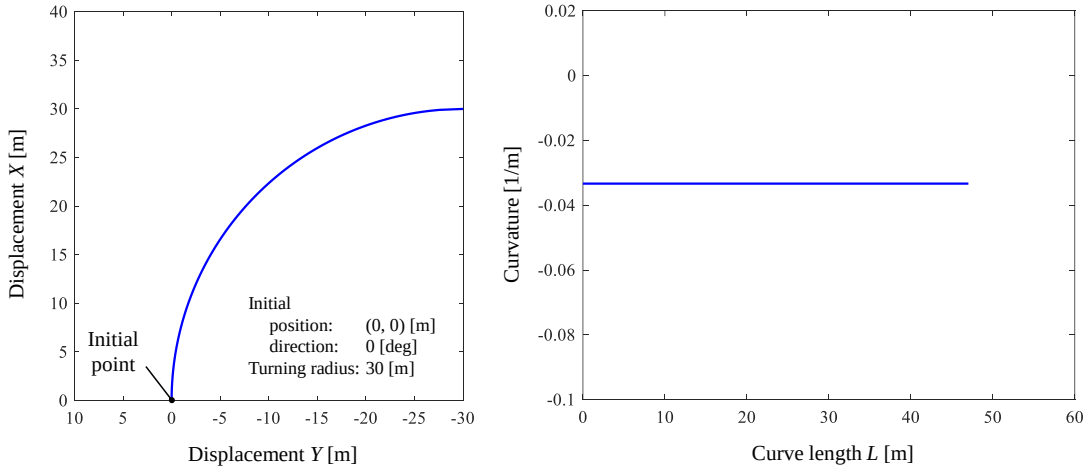

Fig. 3.1.1 An example shape of the circular arc.

3.1.2 Circular Arc Considering Steering Angle

The circular arc is determined from the turning radius calculated from the current steering angle of the ego vehicle. The turning radius R is simply defined from the following equation.

$$R = \frac{l_{wb}}{\tan\left(\left|\delta_f\right|\right)}, \tag{3.1.1}$$

where l_{wb} is the wheelbase of the ego vehicle and δ_f is the steering angle at the front wheels of the ego vehicle.

The superiorities of the curve are not only about the simplicity and the calculation cost but also this method does not require any of the intersection information. Therefore, this method can predict the turning trajectories in any turning include non-intersection turnings such as the case when driving into parking lots. On the other hand, because the trajectory dependent on the steering angle, the method can predict the collision point correctly after the vehicle started turning, therefore, before starting to turn, the accuracy of the prediction is extremely low.

3.1.3 Biarc Curve

Combining two arcs (Biarc) is one way for obtaining enough degrees of freedom to satisfy both the position and the azimuth at the endpoint. An example shape of the Biarc curve is indicated in Fig. 3.1.2. Kimia et al. showed that such a Biarc can be generated in a straightforward manner (i.e., there is no need to conduct an iterative calculation to obtain the curve) by determining the initial and terminal position and direction [105]. For the intersection trajectory prediction, by giving only the position and the direction of the intersection exit, the trajectory can be obtained with very few calculation costs. A disadvantage of the curve is that the turning radius or curvature cannot give as the parameter. Therefore, there always has a gap between the predicted curvature and the actual curvature of the ego vehicle. In addition to this, there is a discontinuity in the curvature in the middle of the curve. Thus, for example, if the vehicle traces the trajectory very precisely, the motion of the steering wheel will be harsh and discontinuous.

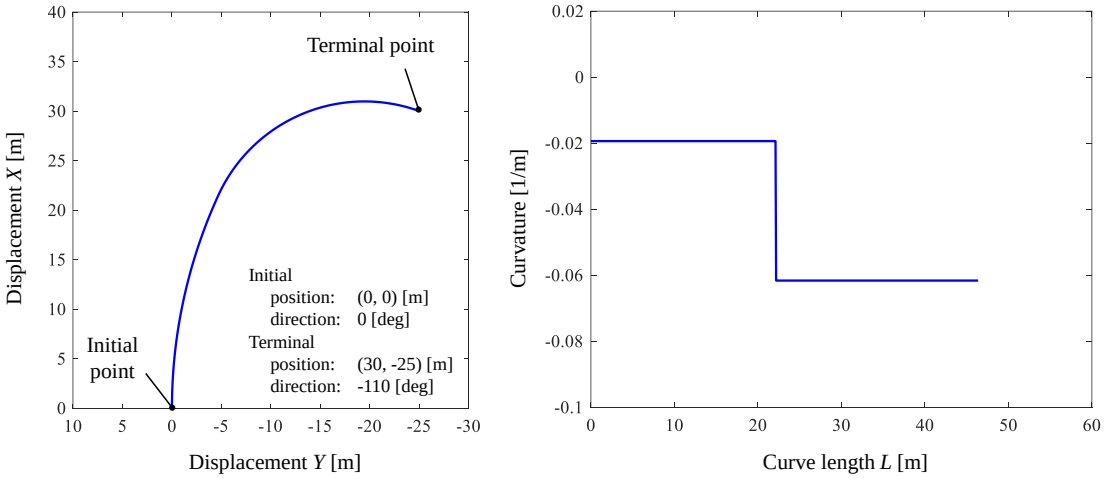

Fig. 3.1.2 An example shape of the Biarc curve.

3.1.4 Single Clothoidal Curve

The clothoidal curve is another candidate of the path that can specify both the position and the azimuth at the endpoint. Furthermore, the linearly changing curvature, which is a feature of the clothoidal, has an advantage in terms of comfort driving [106], and hence, it is expected to be closer to the actual route. An example shape of the clothoidal curve is indicated in Fig. 3.1.3. Bertolazzi and Frego proposed a method to obtain the clothoidal curve easily [107], and therefore, we can implement it in the ADAS. By using Bertolazzi's method, a curve can be obtained by solving a nonlinear equation of one variable. This is a sufficiently small calculation even if real-time calculations are assumed. For the trajectory prediction for intersection turning, the most essential part of using the clothoidal curve is its smoothness. This shape is closer to the trajectory when a driver rotates the steering wheel with constant angler velocity while the vehicle goes with constant speed. Even this method can predict the real vehicle motion, because of the limitation in the degree of the freedom, this method cannot define the initial curvature. Hence, the method always cannot consider the current steering angle of the vehicle.

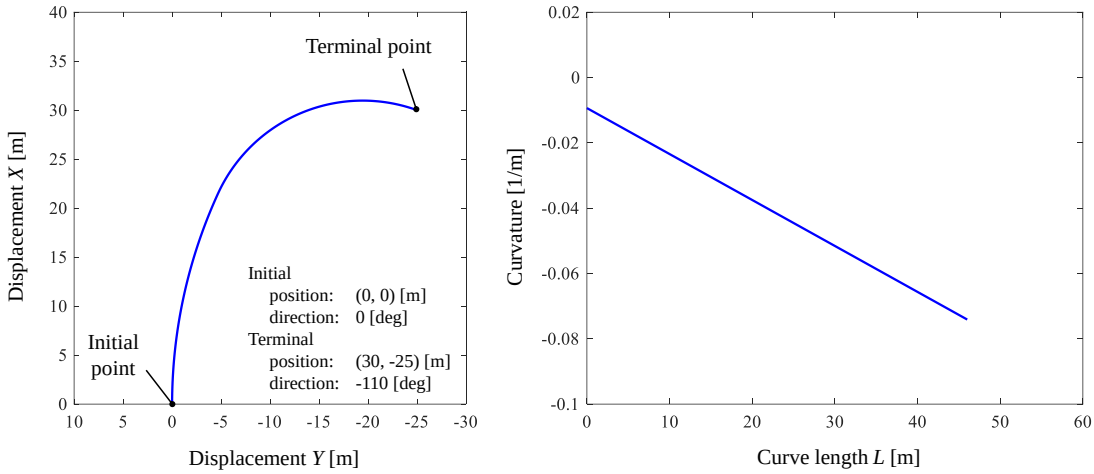

Fig. 3.1.3 An example shape of the clothoidal curve.

3.2 Curve Generation Algorithms of Triclothoidal Curve

To generate a more probable predicted route, it is preferable to consider not only the current vehicle direction but also the amount of steering. This means that the curvature at the initial position should be specifiable. However, the above four methods cannot specify the curvature at the initial point. This is due to a lack of degrees of freedom in the curve. Therefore, Arita et al. proposed a method to obtain the required degrees of freedom by combining three clothoidal curves (Triclothoidal curve) and also proposed a method to determine such a curve easily [120]. This method can generate the predicted route by solving simultaneous equations with at most two variables. The cost of this calculation is reasonable when compared to the case of the clothoidal curve. An example shape of the Triclothoidal curve is indicated in Fig. 3.2.1. Following the Triclothoidal generation method, we extend the generation method to the intersection turning trajectory prediction of automobiles. The following sections propose the intersection turning trajectory prediction method with the Triclothoidal curve.

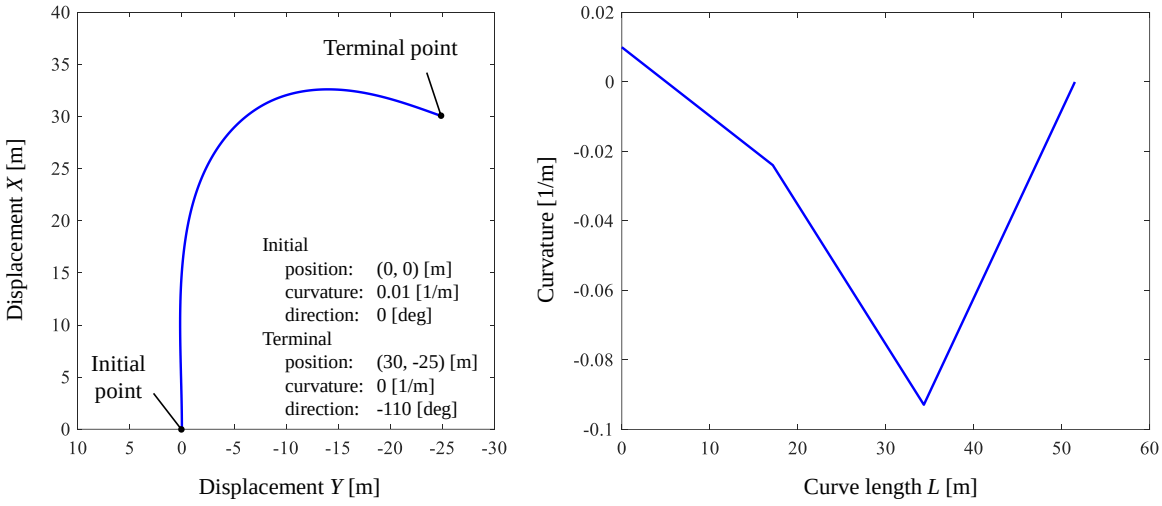

Fig. 3.2.1 An example shape of the Triclothoidal curve.

3.2.1 Problem Formulation for Triclothoidal Curve

Without loss of generality, we can define the coordinate and state as shown in Fig. 3.2.2. x, y, s, ψ, κ are positions of the path, the length, tangent angle, and curvature, respectively. Subscripts 0 and f represent initial and terminal points with states that are normalized by using the direct distance between these points.

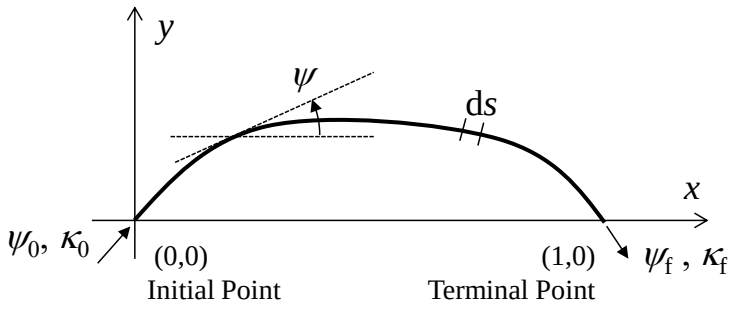

Fig. 3.2.2 Definitions of the coordinate and states [120].

Assuming that s is the independent variable, we have the differential equations of the states as follows:

$$\frac{dx}{ds}=\cos\psi,\frac{dy}{ds}=\sin\psi,\frac{d\psi}{ds}=\kappa,\frac{d\kappa}{ds}=\kappa', \tag{3.2.1}$$

where, κ' is the change rate of the curvature, and it is constant in one clothoidal curve.

3.2.2 Method to Obtain Triclothoidal Curve

The proposed Triclothoidal curve is as shown in Fig. 3.2.3. It must be noted that the states of a point on the Triclothoidal curve whose distance is s from the initial point is represented by $\left(x(s),y(s),\psi(s),\kappa(s)\right)$. The curvature rates of the clothoidal curves that are components of the Triclothoidal curve are $\kappa_1',\kappa_2',\kappa_3'$. Subscripts ij on variables x_{ij},y_{ij},ψ_{ij} and κ_{ij} show the states at the connecting point of the ith and jth clothoidal curves. It is assumed that each clothoidal curve has the same length and that the length of the Triclothoidal curve is L.

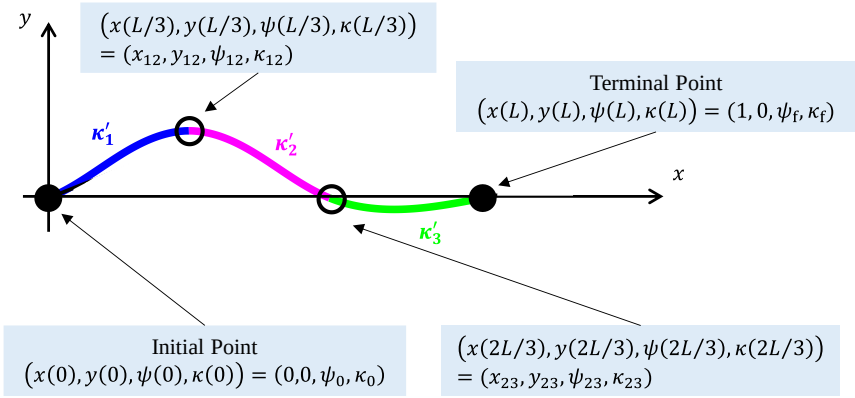

Fig. 3.2.3 Schematic explanation of Triclothoidal curve [120].

Integrating (3.2.1) from the initial point, the states at the terminal point can be obtained by the following equations:

$$x(L)=\int_0^{\frac{L}{3}}\cos\left(\frac{1}{2}\kappa_1' s^2+\kappa_0 s+\psi_0\right)ds+\int_0^{\frac{L}{3}}\cos\left(\frac{1}{2}\kappa_2' s^2+\kappa_{12} s+\psi_{12}\right)ds + \int_0^{\frac{L}{3}}\cos\left(\frac{1}{2}\kappa_3' s^2+\kappa_{23} s+\psi_{23}\right)ds, \tag{3.2.2}$$

$$y(L)=\int_0^{\frac{L}{3}}\sin\left(\frac{1}{2}\kappa_1' s^2+\kappa_0 s+\psi_0\right)ds+\int_0^{\frac{L}{3}}\sin\left(\frac{1}{2}\kappa_2' s^2+\kappa_{12} s+\psi_{12}\right)ds + \int_0^{\frac{L}{3}}\sin\left(\frac{1}{2}\kappa_3' s^2+\kappa_{23} s+\psi_{23}\right)ds, \tag{3.2.3}$$

$$\psi(L)=\psi_0+\kappa_0 L+\left(\frac{5}{2}\kappa_1'+\frac{3}{2}\kappa_2'+\frac{1}{2}\kappa_3'\right)\left(\frac{L}{3}\right)^2, \tag{3.2.4}$$

$$\kappa(L)=\kappa_0+\left(\kappa_1'+\kappa_2'+\kappa_3'\right)\frac{L}{3}, \tag{3.2.5}$$

where the states at the connecting points are

$$\psi_{12}=\frac{1}{2}\kappa_1'\left(\frac{L}{3}\right)^2+\kappa_0\frac{L}{3}+\psi_0, \tag{3.2.6}$$

$$\kappa_{12}=\kappa_1'\frac{L}{3}+\kappa_0, \tag{3.2.7}$$

$$\psi_{23}=\frac{1}{2}\kappa_2'\left(\frac{L}{3}\right)^2+\frac{3}{2}\kappa_1'\left(\frac{L}{3}\right)^2+\frac{2}{3}L\kappa_0+\psi_0, \tag{3.2.8}$$

$$\kappa_{23}=\kappa_2'\frac{L}{3}+\kappa_1'\frac{L}{3}+\kappa_0. \tag{3.2.9}$$

We must determine the four variables $\kappa_1', \kappa_2', \kappa_3'$, and L so that the values of (3.2.2) to (3.2.5) match the terminal values provided by the boundary conditions of the curve generation problem or the intersection layout. Note that considering the definition of coordinates, x, y positions at the initial and terminal points are always $(0,0)$ and $(0,1)$ respectively; hence, the boundary conditions that we can set arbitrarily are ψ_0, ψ_f, κ_0, and κ_f. In other words, if we determine the tangent angles and curvatures of the curve both at the initial and terminal points, the Triclothoidal curve is uniquely defined. The relationships between these arbitrarily definable boundary conditions and intersection layouts are discussed in the next section.

The following are problem reductions where four unknown variables are determined by solving nonlinear equations with at most two variables.

Introducing the new variables $A_i=\kappa_i'(L/3)^2, i=1,2,3$ and substituting them into (3.2.4) and (3.2.5), A_3, and L can be derived with the functions of A_1 and A_2 as shown in (3.2.10) and (3.2.11).

$$A_3=\frac{1}{1+\Delta\kappa/6\kappa_0}\left\{\frac{\Delta\kappa}{3\kappa_0}\left(-\frac{5}{2}A_1-\frac{3}{2}A_2+\Delta\psi\right)-A_1-A_2\right\} \tag{3.2.10}$$

$$L=\frac{1}{\kappa_0}\left(-\frac{5}{2}A_1-\frac{3}{2}A_2+\Delta\psi\right) - \frac{1}{2\kappa_0\left(1+\Delta\kappa/6\kappa_0\right)}\left\{\frac{\Delta\kappa}{3\kappa_0}\left(-\frac{5}{2}A_1-\frac{3}{2}A_2+\Delta\psi\right)-A_1-A_2\right\}. \tag{3.2.11}$$

where $\Delta\psi=\psi_f-\psi_0, \Delta\kappa=\kappa_f-\kappa_0$.

In the case where $\Delta\kappa = 0, \kappa_0 \neq 0$, (3.2.10) and (3.2.11) are

$$A_3 = -A_1 - A_2, \tag{3.2.12}$$

$$L = \frac{1}{\kappa_0}\left(-2A_1 - A_2 + \Delta\psi\right). \tag{3.2.13}$$

In the case where $\Delta\kappa \neq 0, \kappa_0 = 0$, these are

$$A_3 = -5A_1 - 3A_2 + 2\Delta\psi, \tag{3.2.14}$$

$$L = \frac{3}{\Delta\kappa}\left(-4A_1 - 2A_2 + 2\Delta\psi\right). \tag{3.2.15}$$

In addition to these, in the case of $\Delta\kappa = 0, \kappa_0 = 0$, L can be eliminated from (3.2.4) and (3.2.5) as

$$A_2 = -2A_1 + \Delta\psi, \tag{3.2.16}$$

$$A_3 = A_1 - \Delta\psi. \tag{3.2.17}$$

Applying variable transformation $\tau = \left(3/L\right)s$ in (3.2.2) and (3.2.3), we can obtain the following equations:

$$\begin{aligned}\frac{L}{3} &= \int_0^1 \cos\left(\frac{1}{2}A_1\tau^2 + \frac{1}{3}\kappa_0 L\tau + \psi_0\right)d\tau \\ &+ \int_0^1 \cos\left\{\frac{1}{2}A_2\tau^2 + \left(A_1 + \frac{1}{3}\kappa_0 L\right)\tau + \frac{1}{2}A_1 + \frac{1}{3}\kappa_0 L + \psi_0\right\}d\tau \\ &+ \int_0^1 \cos\left\{\frac{1}{2}A_3\tau^2 + \left(A_1 + A_2 + \frac{1}{3}\kappa_0 L\right)\tau + \frac{1}{2}A_2 + \frac{3}{2}A_1 + \frac{2}{3}\kappa_0 L + \psi_0\right\}d\tau,\end{aligned} \tag{3.2.18}$$

$$\begin{aligned}0 &= \int_0^1 \sin\left(\frac{1}{2}A_1\tau^2 + \frac{1}{3}\kappa_0 L\tau + \psi_0\right)d\tau \\ &+ \int_0^1 \sin\left\{\frac{1}{2}A_2\tau^2 + \left(A_1 + \frac{1}{3}\kappa_0 L\right)\tau + \frac{1}{2}A_1 + \frac{1}{3}\kappa_0 L + \psi_0\right\}d\tau \\ &+ \int_0^1 \sin\left\{\frac{1}{2}A_3\tau^2 + \left(A_1 + A_2 + \frac{1}{3}\kappa_0 L\right)\tau + \frac{1}{2}A_2 + \frac{3}{2}A_1 + \frac{2}{3}\kappa_0 L + \psi_0\right\}d\tau.\end{aligned} \tag{3.2.19}$$

By substituting (3.2.10) to (3.2.15) into the above (3.2.16) to (3.2.17), the remaining unknown variables reduce to two, namely A_1 and A_2. Moreover, in the case of $\Delta\kappa = 0, \kappa_0 = 0$, by substituting (3.2.16) and (3.2.17) into (3.2.19), A_1 becomes the only one unknown variable.

These unknown variables can be obtained by solving the above-defined equations or simultaneous equations with one or two variables. The remaining unknown variables of the Triclothoidal curve are determined by (3.2.10) and (3.2.11).

Although iterative calculations are required to solve the simultaneous equations, we can provide reasonable initial assumptions. If we assume that $L \approx 1$ and $\sin\left(\psi\left(s\right)\right) \approx \psi\left(s\right)$, and substituting it into (3.2.19), the initial guesses for iterative calculations are the following:

$$\begin{aligned}A_{1guess} = \frac{1}{108\kappa_0\left(1 + \Delta\kappa/6\kappa_0\right)}&\left(-108\kappa_0\Delta\psi - 54\kappa_0^2 + 3\kappa_0\Delta\kappa\right. \\ &\left.-18\Delta\kappa\Delta\psi + 2\Delta\kappa^2 - 324\kappa_0\psi_0 - 54\Delta\kappa\psi_0\right),\end{aligned} \tag{3.2.20}$$

$$A_{2guess} = -2A_{1guess} + \Delta\psi - \kappa_0 - \frac{1}{6}\Delta\kappa, \tag{3.2.21}$$

where subscript *guess* represents the initial guesses for iterative calculations.

In the case of $\Delta\kappa = 0, \kappa_0 = 0$, the initial guess of A_1 is

$$A_{1guess} = -\Delta\psi - 3\psi_0. \tag{3.2.22}$$

An additional remark on this calculation is that these initial guesses are derived based on the assumption that the path is a straight line. Therefore, the accuracy of the initial guesses becomes degraded when the intersection layout configuration contains large curvature of the radius. However, the degradation does not affect the iteration process for the determination of unknown variables.

3.3 Experimental Comparative Evaluation Between Turning Trajectory Prediction Methods

To evaluate the trajectory prediction accuracy and the smoothness of the proposed Triclothoidal curve, this section compares the five trajectory prediction methods presented in the previous sections. We prepared an experiment vehicle and conducted data acquisition experiments at the intersections in the real city traffic. In this section, subsection 3.5.1 introduces the evaluation process and the goal of the evaluation. Subsection 3.5.2 describes the experiment vehicle. In subsection 3.5.3, the definitions of each parameter and coordinate for the Triclothoidal curve trajectory generation for ADAS for the intersection right-turn.

3.3.1 Evaluation Process and Goal

The evaluation goal of the experiment is to prove the trajectory accuracy of the proposed method Triclothoidal curve by using the driving data in a real city driving experiment. The prediction accuracies of the predicted trajectories by five curve generation methods are compared from the actual driving path of the experiment vehicle. Besides, the curve shapes and features of each trajectory prediction method in the real traffic are also explained from the recorded data and predicted trajectories.

3.3.2 Experiment Vehicle and Data Acquisition Experiment

An experiment vehicle to acquire the intersection turning driving data is prepared for the experiments. The experiment vehicle equipped additional sensors as follows and in the Table 3.3.1: a LiDAR, two GNSS antennae, and an inertia measurement unit (IMU). The onboard laptop pc stored the time series data during the acquisition. Fig. 3.3.1 shows the external view of the experiment vehicle.

Reference
Velodyne LiDAR: https://velodynelidar.com/products/hdl-32e/
OxTS: https://www.oxts.com/gnss-receiver/

Fig. 3.3.1 The overview of the experiment vehicle [108][109].

Table 3.3.1 The additional sensors on the experiment vehicle.

Sensor name	Measurement value	Product name	Manufacturer	Number
LiDAR	Range	HDL-32E	Velodyne Lidar	1
GNSS antenna	GNSS position	RT3102	OxTS	2
IMU	9-DoF orientation			1

The additional sensors and internal sensors acquired the following data: the accelerations, the azimuth, the GNSS positions, the point cloud data of the surrounding environment, the steering wheel angle, the vehicle speed, and the yaw rate.

In each acquisition experiment, three onboard operators operated the experiment. The first operator drove the experiment vehicle. The second operator supported the safety experiment. And the last operator started and stopped the data acquisition at the recording sections.

The experiments were conducted at 31 intersections in Koganei city and Musashino city, Tokyo, Japan. Fig. 3.3.2 shows the locations of the target intersections and Table 3.3.2 shows the list of the characteristic parameters of the target intersections. Those target intersections were selected from the aspect of the variety of the size and the crossing angle of the intersection. The characteristic parameters of the intersection were defined from three values l_{in}, l_{out}, and θ_{cross}. Here, as shown in Fig. 3.3.3, the distance from the central part of the driving lane to the right-side edge of the entering road was defined as l_{in}, and the distance from the driving center lane to the right-side edge of the escaping road was defined as l_{out}, and the crossing angle of the entering road and the escaping road was defined as θ_{cross}. The size of the intersections and the angles of turning right were measured by using Google Earth Pro. Those parameters are handled to estimate the parameter to implement the curve generation method to the driver assistance system. The details about the implementation are mentioned in Section 3.4.

Reference:
Geospatial Information Authority of Japan (地理院地図Vector)
https://maps.gsi.go.jp/vector

Fig. 3.3.2 The location of the target intersections [110].

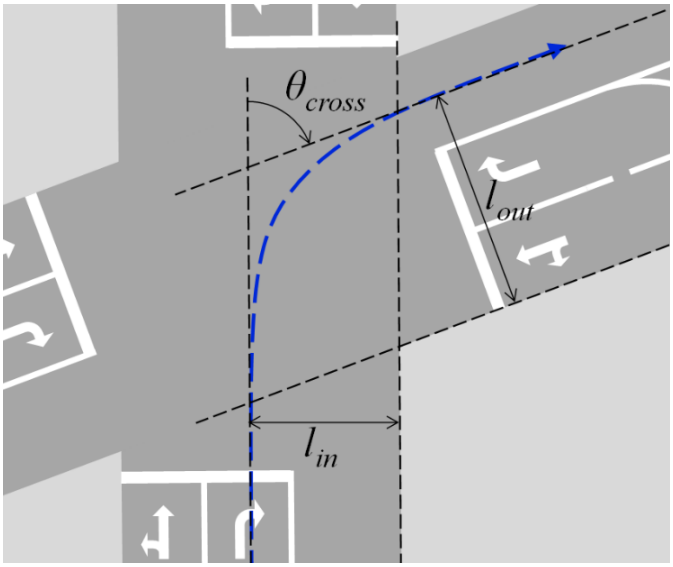

Fig. 3.3.3 Definitions of intersection shape-related parameters.

Table 3.3.2 The parameters for the target intersections.

Intersection ID	Crossing angle	Size parameters	
	θ_{cross}	l_{in}	l_{out}
1-1	−87.7	2.90	8.88
1-2	−53.7	4.30	18.30
1-3	−112.9	5.65	14.90
1-4	−76.8	12.90	9.27
1-5	−109.0	5.10	7.04
1-6	−85.9	4.19	4.00
1-7	−105.3	4.86	2.10
1-8	−92.2	3.10	6.68
1-9	−112.5	5.92	7.70
1-10	−75.0	4.10	7.68
1-11	−107.0	4.99	8.00
1-12	−76.4	3.85	4.78
1-13	−102.8	5.81	5.86
1-14	−93.4	4.57	12.30
1-15	−91.7	7.92	4.82
1-16	−92.0	4.73	4.00
1-17	−100.5	8.18	6.10
1-18	−98.4	3.84	7.10
1-19	−82.3	3.99	4.40
1-20	−89.3	4.47	7.21
1-21	−97.8	4.61	1.59
1-22	−91.1	4.19	9.41
1-23	−97.7	3.93	4.74
1-24	−107.4	4.59	3.63
1-25	−91.8	7.69	4.21
1-26	−83.3	5.84	7.75
1-27	−83.4	6.00	6.64
1-28	−96.0	4.34	8.33
1-29	−91.7	4.65	6.92
1-30	−95.9	4.66	4.18
1-31	−92.2	4.19	5.67

3.3.3 Definition of Parameters and Coordinates for Triclothoidal Trajectory Generation at Intersection

As one of the most important reasons to use the Triclothoidal curve for trajectory prediction for ADAS at intersection turning, the curve can be generated simply by providing positions, angles, and curvatures of the initial and terminal points. This section explains the definitions of parameters and coordinates to apply the Triclothoidal curve generation introduced in the previous section into trajectory prediction at intersection turning. To apply the Triclothoidal curve to the trajectory prediction, at first, the initial and terminal points for intersection turning are defined. As shown in Fig. 3.3.4, the initial point is defined as the center of the rear wheel axle of the ego vehicle, and the terminal point is defined as a point on the central part of the escaping road of the intersection. When the escaping road has multiple lanes, the terminal point is defined as the central part of those lanes. Here, introducing a vehicle coordinate system (X, Y), an origin of the coordinates is defined as a center of the rear wheel axle of the ego vehicle.

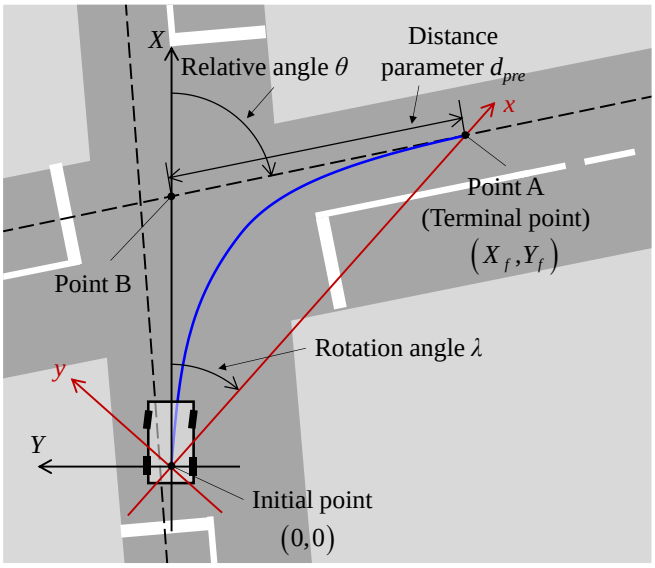

Fig. 3.3.4 Parameter definitions for Triclothoidal curve generation.

In this coordinate system, the following boundary conditions are defined to generate the Triclothoidal curve. The positions at the initial point for the Triclothoidal curve generation are defined as (0, 0), and the initial direction of the curve is defined as the ego vehicle's longitudinal direction. Therefore, the initial angle of the curve on the coordinate system is always 0. The initial curvature can be geometrically derived as $\tan\delta_f / l_{wb}$.

To define the conditions at the terminal point of the curve, and to adapt to the various sizes of the intersection, the terminal point is defined as an adjustable point on the lane center of the escaping road (point A in Fig. 3.3.4).

The positions at the terminal point (X_f, Y_f) can be adjusted by a distance parameter d_{pre}. This parameter d_{pre} is defined as the distance from point B to the terminal position. Point B is a crossing point of the ego vehicle's longitudinal centerline and the lane center of the escaping road. The distance parameter d_{pre} is an important parameter to control the accuracy of the predicted trajectory. The method to decide the parameter d_{pre} is described in Section 4.4, Chapter 4. The terminal direction of the curve is equal to the relative angle θ from the ego vehicle's driving direction to the direction of the escaping road of the intersection. In this study, we regard the shape of the escaping road as a straight road, and therefore, the curvature at the terminal point is defined as 0.

Then, to generate the Triclothoidal curve as the trajectory, the boundary conditions defined on the coordinate system (X, Y) must be redefined on the coordinate system (x, y) that was explained in Section II. The coordinates (x, y) are rotated with the rotation angle λ, and the distances in the coordinates are normalized by the direct distance between the initial point and terminal point. By applying this coordinate transformation, the conditions at initial and terminal points to generate the Triclothoidal curve $\left(x(s), y(s), \psi(s), \kappa(s)\right)$ can be expressed as follows:

$$\left(x(0), y(0), \psi(0), \kappa(0)\right) = \left(0, 0, -\lambda, \frac{\tan\delta_f}{l_{wb}}\sqrt{X_f^2 + Y_f^2}\right), \tag{3.3.1}$$

$$\left(x(L), y(L), \psi(L), \kappa(L)\right) = (1, 0, \theta - \lambda, 0), \tag{3.3.2}$$

where the angle λ is $\arctan\left(Y_f / X_f\right)$.

To sum up, the Triclothoidal trajectory for the intersection turning can be predicted by simply giving the following values: the lane center positions along the escaping road, the relative angle from the ego vehicle's driving direction to the direction of the escaping road θ, steering angle, and the distance parameter d_{pre}.

3.3.4 Simulation Result and Evaluation

From the acquired data, the driving paths of the experiment vehicle could be obtained. These driving paths were used as references to evaluate the prediction performances of the trajectory prediction methods.

An example of making a right turn at the intersection (ID 1-3) from the data acquisition experiments is shown in Fig. 3.3.5. This figure contains four subfigures: (a) shows a bird's-eye view of the intersection; (b) shows point cloud data and the observed driver's path in the experiment; (c) and (d) show the recorded results of observed velocity and steering wheel angle in the experiment, respectively. On the point cloud data in (b), a white line indicates the path that the experiment vehicle took. White boxes on the point cloud data indicate the positions of the ego vehicle. The boxes are plotted every 5 m on the right turning maneuver. The distance values by the white boxes show the travel distances of the vehicle at each box.

Image: Google

(a) Bird's-eye view.

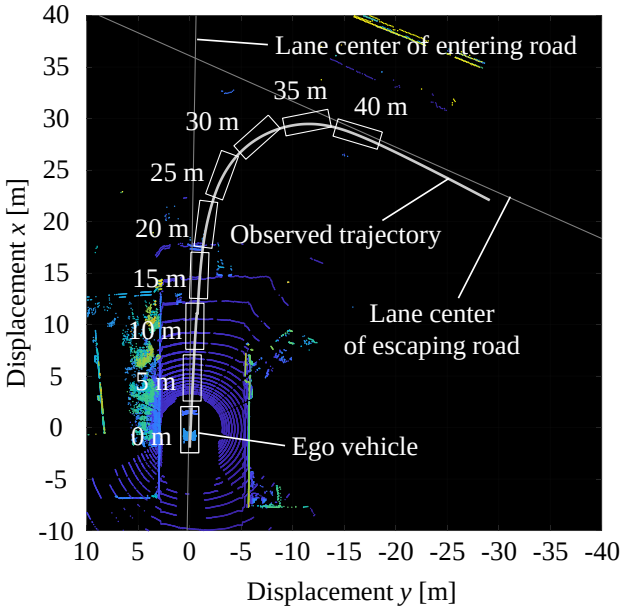

(b) Observed driver's trajectory

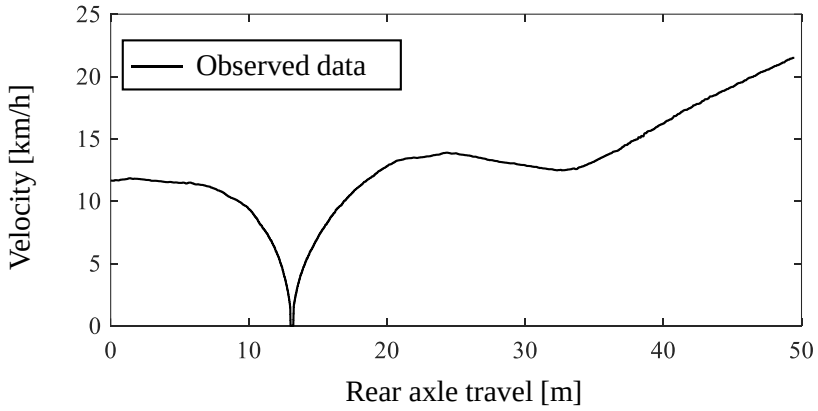

(c) Observed velocity of the experiment vehicle.

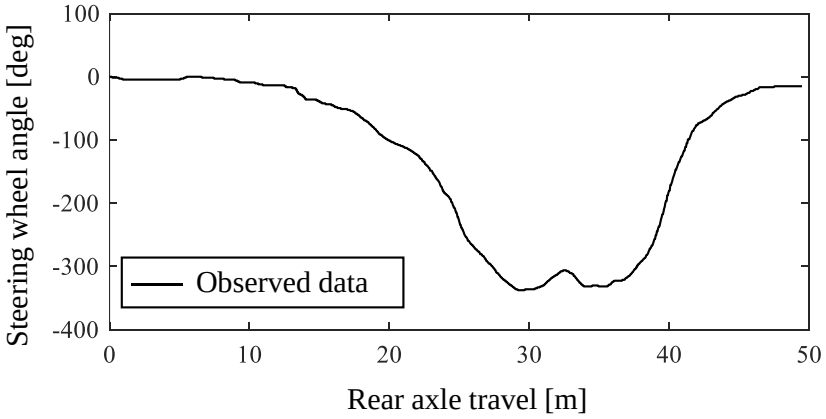

(d) Observed steering wheel angle of the experiment vehicle.

Fig. 3.3.5 An example case of the recorded data from the intersection right-turning experiments at the intersection ID 1-3.

From the acquired driving data, the prediction performance was evaluated as follows. First, from the point cloud data, the position of the escaping road and the relative angle from the ego vehicle to the escaping road θ were derived. Second, from the recorded vehicle data, given trajectory prediction parameters and intersection information, geometrical trajectories of each method including the proposed Triclothoidal curve were sequentially calculated in every time frame. Finally, comparing the recorded actual path of the ego vehicle and predicted trajectories, the effectiveness of the prediction performance of each prediction method was evaluated.

Fig. 3.3.6 shows the point clouds data from turning right at the intersection, the observed trajectory, and the predicted trajectories from each trajectory prediction method: (a) a circular arc with a constant radius, (b) a circular arc considering the steering angle, (c) Biarc curve, (d) a clothoidal curve, and (e) Triclothoidal curve. In Fig. 3.3.6, a white broken line indicates the path that the experiment vehicle took. White boxes on the point cloud data indicate the positions of the ego vehicle. The boxes are plotted every 5 m of the turning right maneuver. Green lines indicate the predicted trajectories. Green lines are also plotted every 5 m of the turning right maneuver. Fig. 3.3.7 shows the comparison of the curvatures of the observed driving data and predicted trajectories on each trajectory prediction method. A black, bold solid line shows the curvature from the observed data and the colored fine solid lines show the curvature of the predicted trajectories. The predicted curvatures are plotted every 5 m of the turning right maneuver. The colors of the predicted trajectories are corresponding to the positions of the vehicle. The left-side tip of each colored line is corresponding to each position of the vehicle that was shown in Fig. 3.3.6 as white boxes. Note that in the experiments, the parameters such as turning radius for (a) the circular arc with a constant radius, and distance parameters d_{pre} to define the terminal point positions for (c) Biarc, (d) clothoidal curve, and (e) the Triclothoidal curve were exploratorily optimized by minimizing the prediction error between the predicted trajectory and actual driving path from the experiment data.

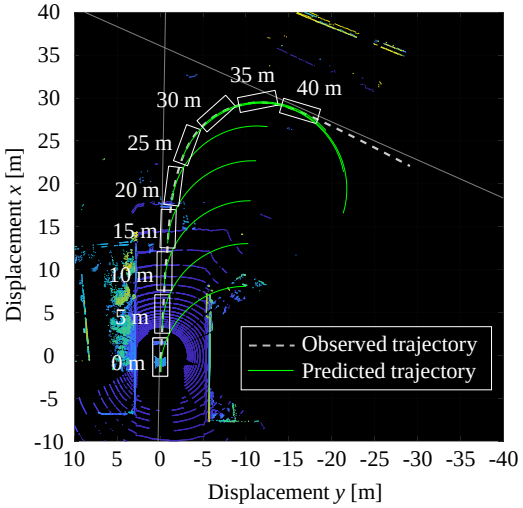

(a) Circular arc with a constant radius.

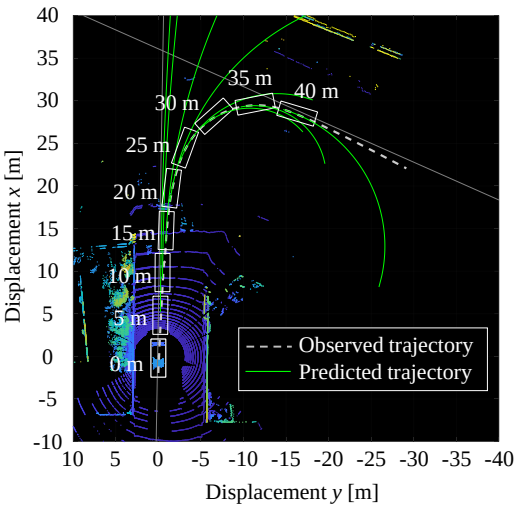

(b) Circular arc considering steering angle.

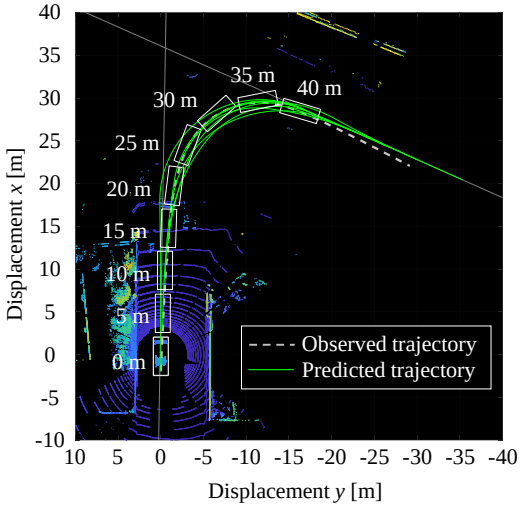

(c) Biarc curve.

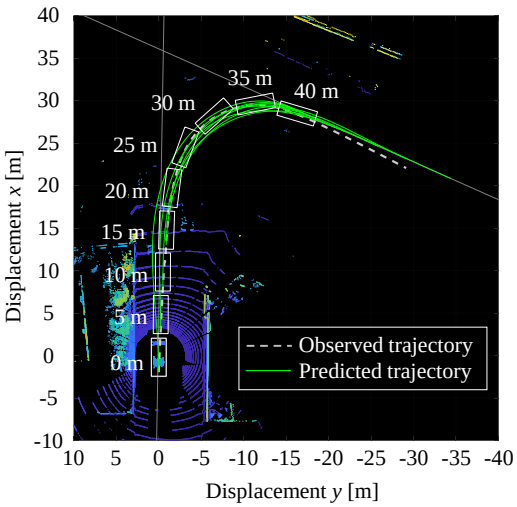

(d) Clothoidal curve.

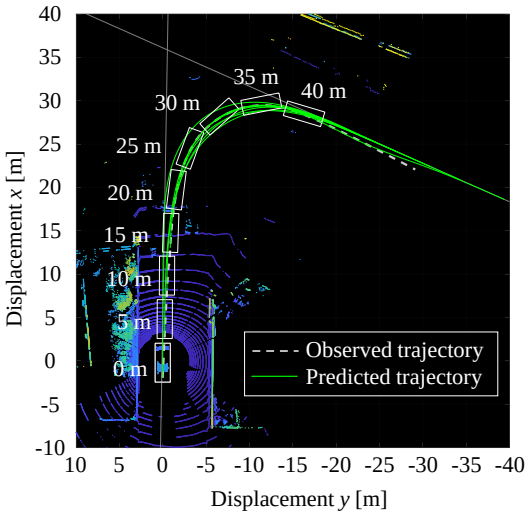

(e) Triclothoidal curve.

Fig. 3.3.6 An example of the trajectory prediction in a real intersection by each trajectory prediction method. (Intersection ID 1-3)

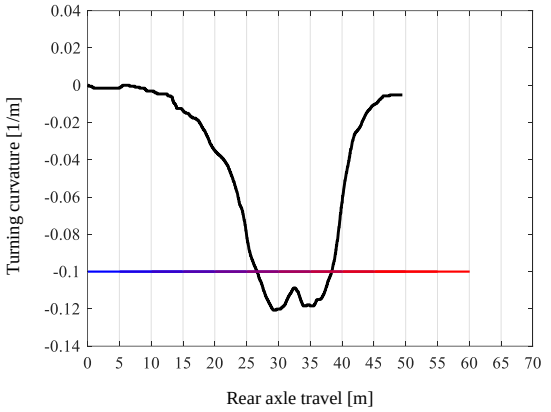

(a) Circular arc with a constant radius.

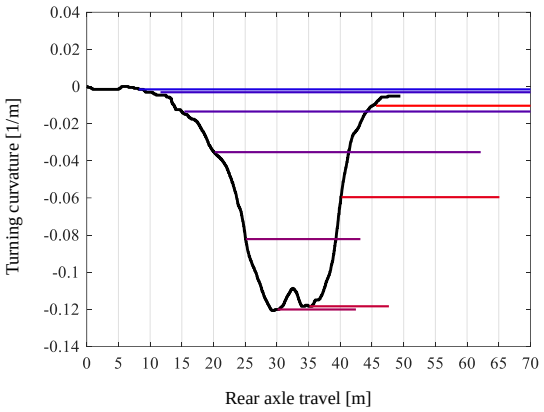

(b) Circular arc considering steering angle.

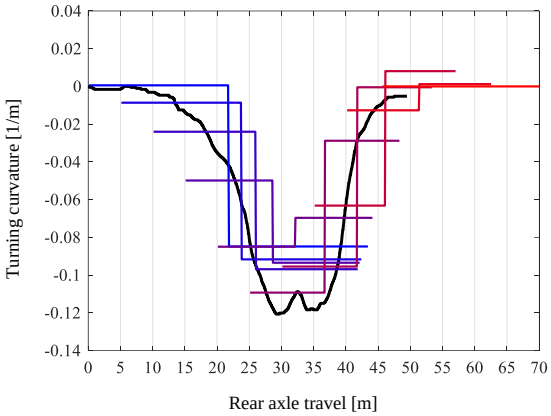

(c) Biarc curve.

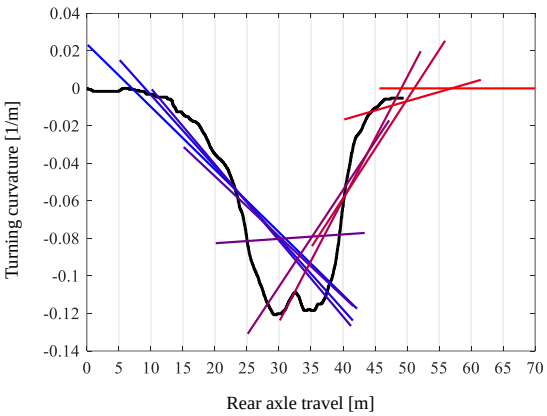

(d) Clothoidal curve.

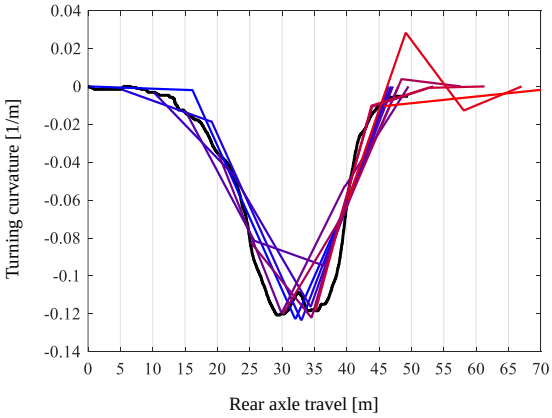

(e) Triclothoidal curve.

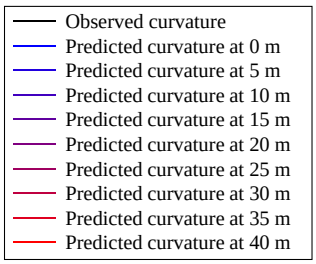

Fig. 3.3.7 Curvatures of observed data and each trajectory prediction method in the experiment. (Intersection ID 1-3)

From Fig. 3.3.6 and Fig. 3.3.7, while the methods using circular arc trajectories (a) and (b) were not required to define the position of the terminal point, prediction accuracy was lower especially before entering the intersection. And the deviations of curvature between observed data and prediction were large. Prediction accuracy of the (c) Biarc curve, (d) clothoidal curve, and (e) Triclothoidal curve were higher, however, the (c) Biarc curve and (d) clothoidal curve swelled out to the left at the beginning of the

prediction because the predicted curvature of those curves were positive values at the beginning. On the other hand, because (e) the Triclothoidal curve considers the current steering angle of the vehicle, this method could predict the curvature as negative values so that the predicted trajectory does not swell out to the left. Also, the Triclothoidal curve could predict the curvature of the driver's intersection right-turn accurately.

Fig. 3.3.8 shows the comparison of the absolute prediction error between the trajectory prediction methods (c) Biarc curve, (d) clothoidal curve, and (e) Triclothoidal curve from the driving experiments at 31 urban intersections in Tokyo. In the evaluation, prediction curves were generated every 5 m of the ego vehicle travel, and errors between the predicted trajectory and the observed actual path were calculated every 1 m step. The absolute errors were the measured deviations in the normal direction from the actual driving path of the ego vehicle and the errors were used only before and while the vehicle passing through the intersection. Therefore, the prediction errors after turning right were not considered. From the result, more than 70% of the prediction by the Triclothoidal curve had less than 0.3 m of absolute error. Comparing to the other prediction methods, the Triclothoidal curve was overwhelming the accuracy. Therefore, the Triclothoidal trajectory prediction had a strong advantage over the trajectory prediction at the intersection right-turn.

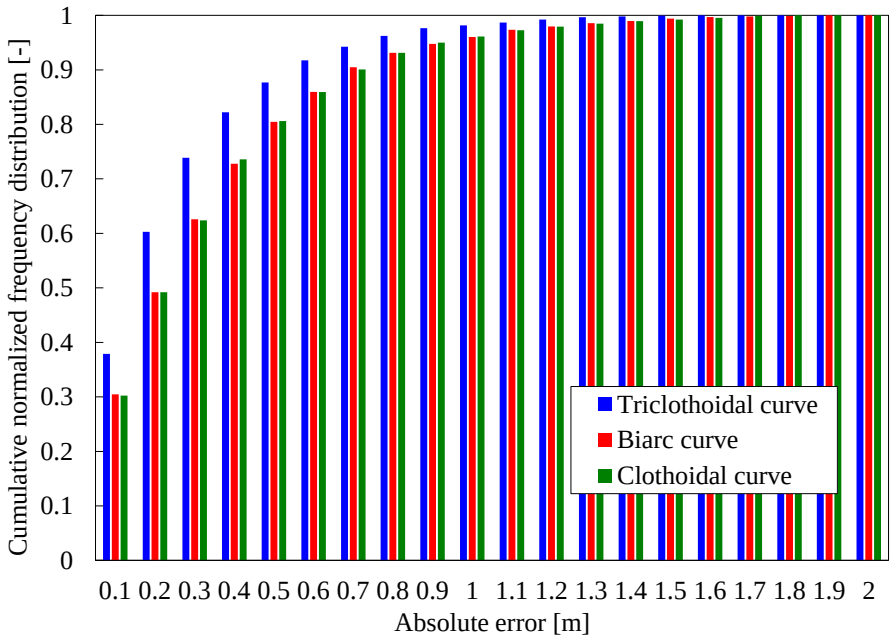

Fig. 3.3.8 The comparison of the accuracy of trajectory prediction methods.

3.4 Parameter Estimation for Trajectory Prediction

To implement the Triclothoidal curve generation method into the proposed driver assistance system, the Proactive Braking System (PBS), the position of the terminal position of the curve must be defined. To enable the consistent trajectory prediction in every kind of intersection, we defined the terminal point as a movable point on the lane center of the escaping road. This section presents the way to fix the movable point to a certain point that respectively defined from the intersection geometry. This section consists of two subsections, and the first subsection explains the definitions of the parameter estimation equation. The second subsection evaluates the estimation performance of the derived equation.

3.4.1 Parameter Estimation Equation

In this research, the terminal point was defined as mentioned in Section 3.3. The position of the terminal point was decided as a point on the central part of the lane of the escaping road of the intersection with the distance d_{pre} from Point B. From this definition, the accuracy of the trajectory prediction is highly dependent on the distance parameter d_{pre}. To predict the turning trajectory in high accuracy, the distance d_{pre} has to be estimated before generating the turning trajectory. We hypothesized that there is a correlation between the distance parameter d_{pre} and the shape of the intersections.

The correlations between the parameters were estimated by linear regression $\hat{d}_{pre} = ax + b$ by using the results from data acquisition experiments at 31 intersections. Some assumptions for variables x were prepared as listed in Table 3.4.1. Where, the parameters l_{in}, l_{out}, and θ_{cross} can be referred to from Table 3.2.2. The definitions of the parameters are mentioned in subsection 3.2.2. From the experiments at 31 intersections, the parameters d_{pre} at each experiment case were calculated from the acquired driving data by optimizing the predicted trajectory to minimize the error from the recorded actual driving path. From the assumptions x and calculated d_{pre}, coefficients a, b, and correlation coefficient in $\hat{d}_{pre} = ax + b$ were decided by the linear regression as shown in Table 3.4.1.

Table 3.4.1 Correlation equation between optimal distance parameter and intersection geometry related parameter.

x	a	b	Correlation coefficient
l_{in}	1.01	11.6	0.472
l_{out}	0.755	12.0	0.591
$\sin(\theta_{cross})$	-55.9	71.8	-0.489
$l_{in} + l_{out}$	0.812	7.45	0.735
$l_{in} \cdot l_{out}$	0.139	12.3	0.733
$(l_{in} \cdot l_{out})\sin(\theta_{cross})$	0.146	12.2	0.714
$(l_{in} + l_{out})/\sin(\theta_{cross})$	0.687	8.68	0.731
$(l_{in} \cdot l_{out})/\sin(\theta_{cross})$	0.129	12.5	0.743

From the table, $x = l_{in} + l_{out}$ and $x = l_{in} \cdot l_{out}$ had a slightly strong linear correlation between d_{pre} and x. $x = l_{in} \cdot l_{out} \cdot \sin(|\theta_{cross}|)$ is an area of parallelogram consists of l_{in} and l_{out} however because correlation by $\sin(|\theta_{cross}|)$ had a negative correlation, the correlation coefficient by $x = l_{in} \cdot l_{out} \cdot \sin(|\theta_{cross}|)$ became lower than the coefficient by $x = l_{in} \cdot l_{out}$. In contrast, the correlation coefficient of $x = l_{in} \cdot l_{out}/\sin(|\theta_{cross}|)$ was the highest in the assumptions, and there was a slightly strong linear correlation between d_{pre} and x. A scatter plot of the correlation between d_{pre} and $x = l_{in} \cdot l_{out}/\sin(|\theta_{cross}|)$ was shown in Fig. 3.4.1. In this study, choosing $x = l_{in} \cdot l_{out}/\sin(|\theta_{cross}|)$, an equation to estimate a distance parameter $\hat{d}_{pre}$ was defined as

$$\hat{d}_{pre} = 0.129 l_{in} \cdot l_{out}/\sin(|\theta_{cross}|) + 12.5. \quad (3.4.1)$$

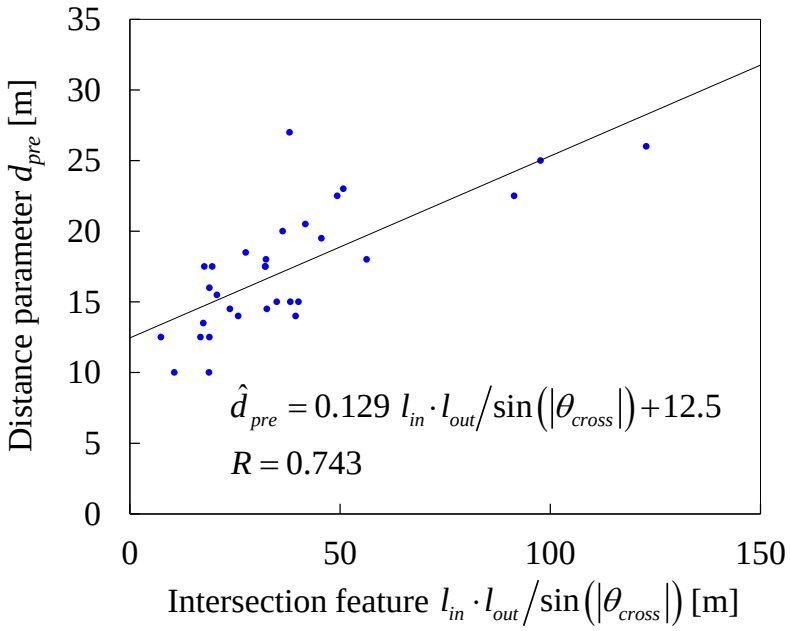

Fig. 3.4.1 Parameter estimation for the Triclothoidal curve.

3.4.2 Performance Evaluation with Estimated Parameter

By using the derived equation in (3.4.1), the parameter $\hat{d}_{pre}$ for the trajectory prediction can be estimated with given information about the shape of the intersections. To evaluate the accuracy of the trajectory prediction, additional intersection right-turn experiments were conducted in the other three intersections in Tokyo. Fig. 3.4.2 shows the locations of the intersection and Fig. 3.4.3 shows the bird's-eye view of the intersections. The specification and estimated parameter $\hat{d}_{pre}$ of the three intersections were shown in Table 3.4.2.

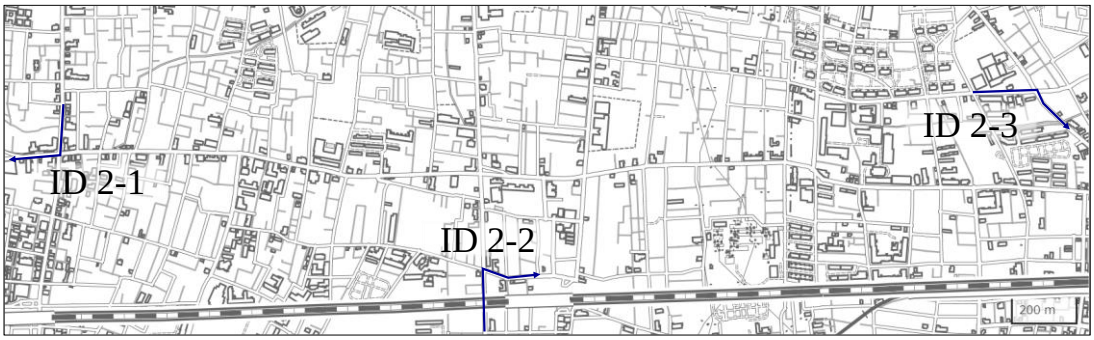

Fig. 3.4.2 Locations of the intersections [110].

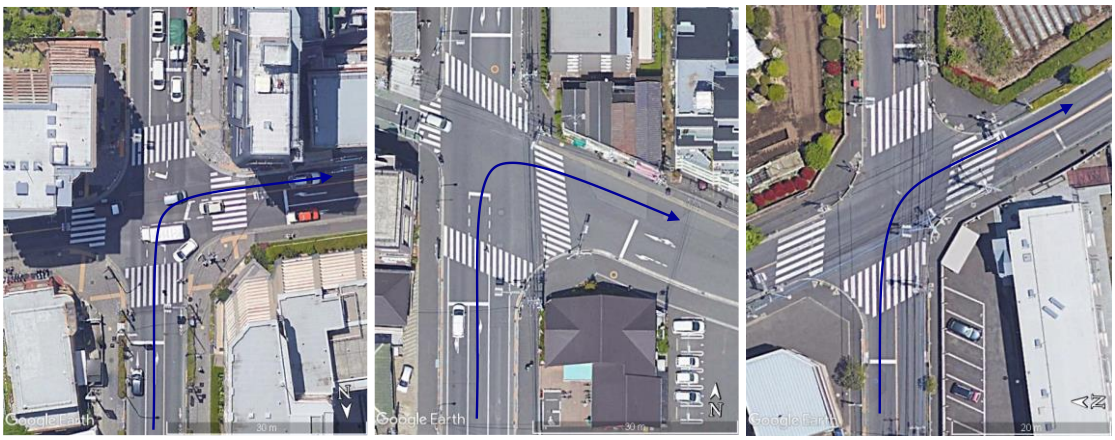

(a) Intersection ID 2-1. (b) Intersection ID 2-2. (c) Intersection ID 2-3.

Fig. 3.4.3 Bird's-eye views of the target intersections. (Image: Google)

Table 3.4.2 Specifications of target intersections and estimated parameters.

Intersection ID	θ_{cross} [deg]	l_{in} [m]	l_{out} [m]	$\hat{d}_{pre}$ [m]
2-1	−87.3	4.23	6.53	16.0
2-2	−113.0	5.60	8.74	19.3
2-3	−66.7	5.96	4.61	16.3

Fig. 3.4.4, Fig. 3.4.5, and Fig. 3.4.6 show the experiment results of intersection ID 2-1, 2-2, and 2-3, respectively by using the estimated parameter $\hat{d}_{pre}$, and Fig. 3.4.7 shows the box plot of the absolute prediction error between the predicted trajectories and the actual driving paths. In the subfigure (b) and (c) in Fig. 3.4.4 to Fig. 3.4.6, P.v. in the legends stands for predicted value. Absolute errors refer to the deviation of the predicted vehicle rear axle trajectory in the curvilinear normal direction concerning the measured driving path. The trajectory predictions were calculated at 20 Hz. The absolute prediction errors in Fig. 3.4.4, Fig. 3.4.5, Fig. 3.4.6, and Fig. 3.4.7 refer to the deviation of the predicted vehicle rear axle trajectory in the curvilinear normal direction concerning the measured driving path. These errors were measured every at 0.5 m interval of each predicted trajectory. To evaluate trajectory prediction errors only around the intersections, in Fig. 3.4.7, the evaluated section was limited to the displacement $y \geq -25$ [m].

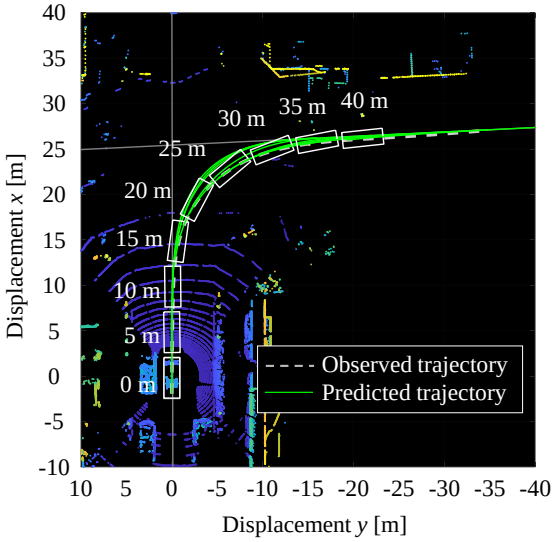

(a) Point cloud data and predicted trajectories.

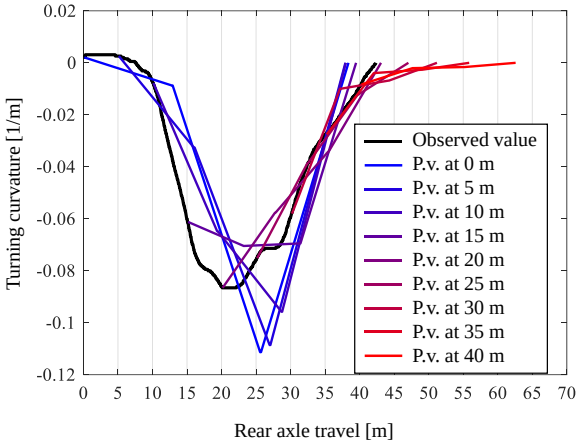

(b) Observed curvature and predicted curvatures.

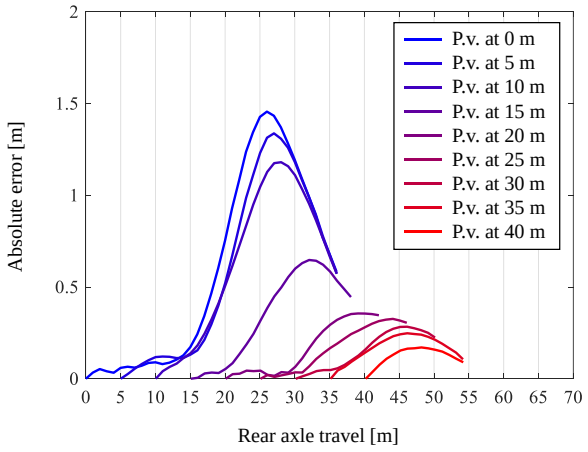

(c) Absolute prediction errors.

Fig. 3.4.4 Prediction results with estimated distance parameter from the experiment at intersection ID 2-1.

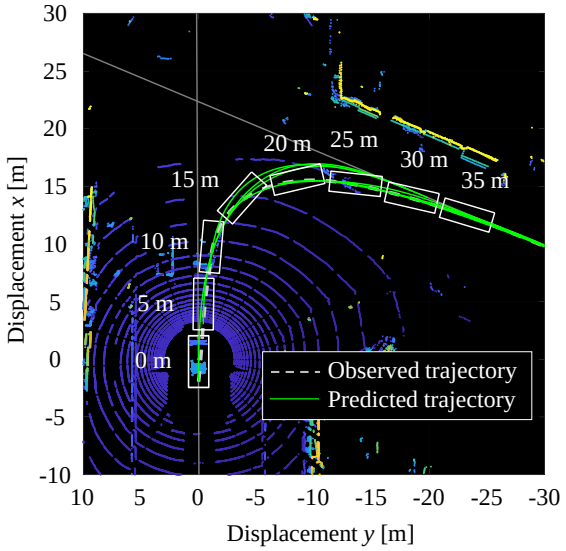

(a) Point cloud data and predicted trajectories.

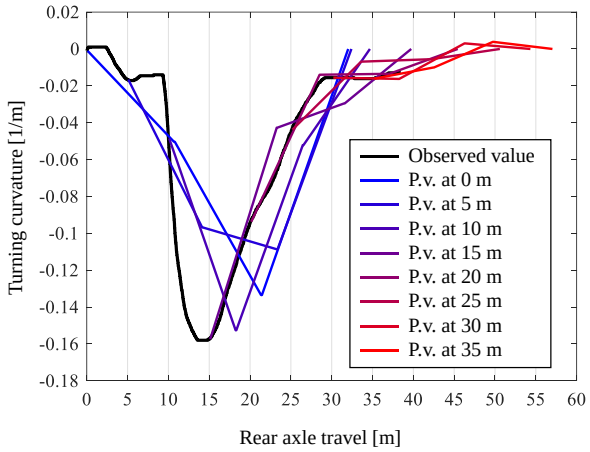

(b) Observed curvature and predicted curvatures.

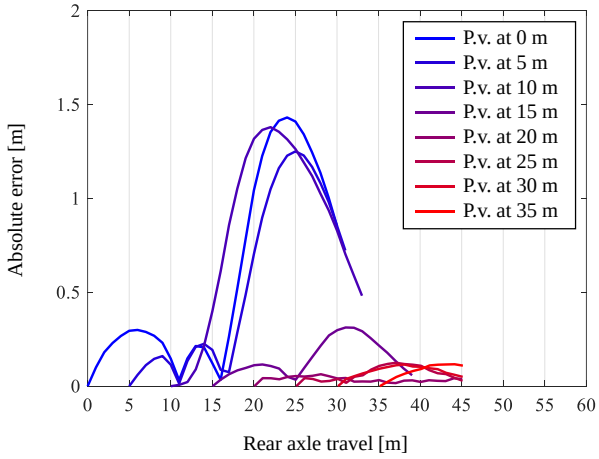

(c) Absolute prediction errors.

Fig. 3.4.5 Prediction results with estimated distance parameter from the experiment at intersection ID 2-2.

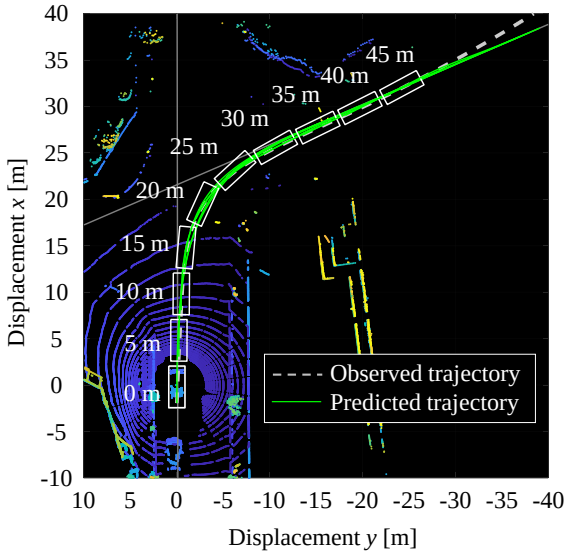

(a) Point cloud data and predicted trajectories.

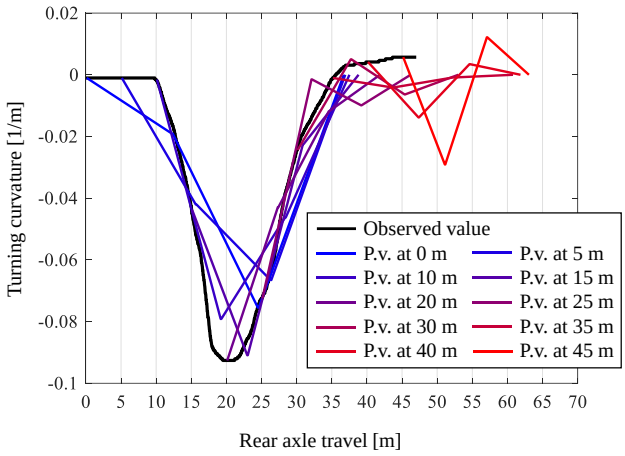

(b) Observed curvature and predicted curvatures.

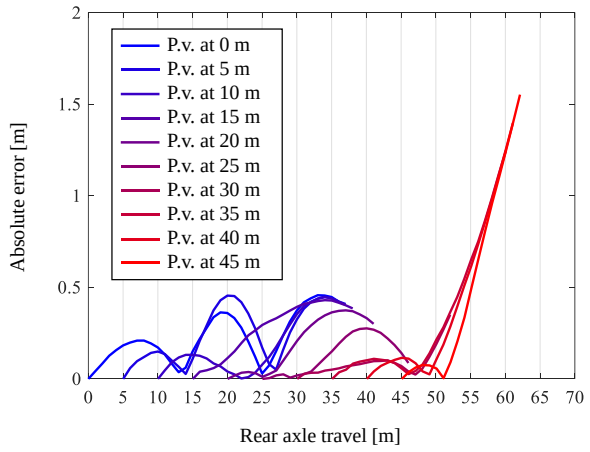

(c) Absolute prediction errors.

Fig. 3.4.6 Prediction results with estimated distance parameter from the experiment at intersection ID 2-3.

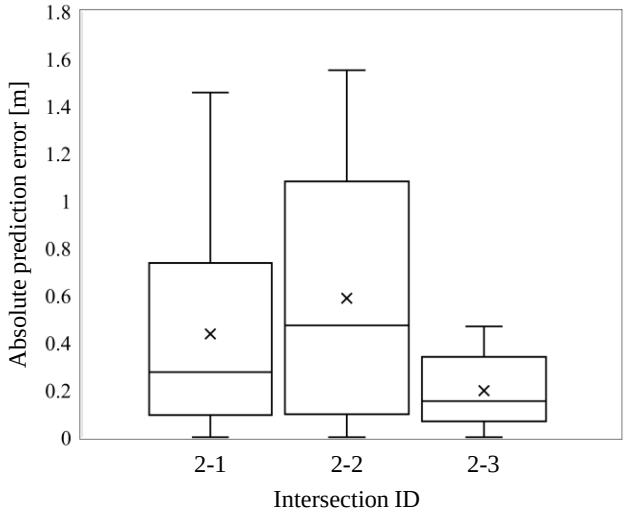

Fig. 3.4.7 The box plot of the absolute prediction errors in each target intersection.

From Fig. 3.4.4, Fig. 3.4.5, and Fig. 3.4.6, the trajectory predictions with the estimated parameters could predict the right turning trajectory overall, and the method could predict the vehicle trajectory before the vehicle drove into the intersection. The graphs that show absolute prediction errors indicate that the errors were suppressed under 1.6 m in all cases. After the turning started, the prediction errors became suppressed to around 0.5 m. In the result of the intersection ID 2-3, some absolute errors became larger at the end of the predictions; however, these errors were from the displacement after the vehicle completed the turning, therefore these errors were out of the evaluation.

Moreover, in most predictions, prediction errors at prediction positions that were shorter than 15 m ahead of the vehicle position were very low at around 0.5 m. Thus, also for driver assistance systems that require short-range trajectory prediction such as emergency braking or steering assistance, the results showed that the proposed method could effectively predict the future positions of the ego vehicle.

From Fig. 3.4.7, 75% of absolute errors in all cases were less than 1.2 m, and especially in the intersection ID 2-3, 75% of prediction errors were less than 0.4 m. Besides, 50% of absolute errors in all cases were less than 0.5 m. These results indicate that the proposed method had high prediction precision and accuracy. However, there was a variance in prediction errors by the intersection shapes. To improve the accuracy of the prediction, more intersection turning data may be needed to tune the parameter estimation equation (3.4.1).

3.5 Conclusion

This chapter proposed a trajectory prediction method using a Triclothoidal curve. Triclothoidal curve can generate the curve between two points considering the initial and terminal directions and curvatures without discontinuity in the curvature. From the analysis with data acquisition experiment in the real city traffic, the accuracy of the Triclothoidal trajectory was higher than the conventional trajectory prediction methods. This chapter also mentioned the parameter estimation method that enables consistent trajectory prediction in every kind of intersection.

This page is intentionally left blank.

4. Collision Avoidance Ability Evaluation with Full-Vehicle Simulation

Because we cannot test every possible collision case with the real test vehicle, proving “safety” is a difficult task in the development of collision avoidance function. In this chapter, we attempt to evaluate the “safety” performance of the proposed Proactive Braking System (PBS) from the iterative full-vehicle simulations in the comprehensively reconstructed possible risk predictive scenario and collision scenario. This chapter contains the following sections. First, Section 4.1 describes the evaluation process and goal of the full-vehicle simulation. Next, Section 4.2 describes the simulation software we used for the full-vehicle simulation. In Section 4.3, an emergency braking function, Emergency Braking System (EBS) is introduced for the full-vehicle simulation. Section 4.4 evaluates the collision avoidance performance by comparing the results of iterative full-vehicle simulations by EBS and PBS+EBS. And the last section of this chapter, Section 4.5, concludes the chapter.

4.1 Evaluation Process and Goal

The goal of this evaluation is to prove the proposed PBS is effective to reduce the collision at the target scenario from the iterative full-vehicle simulations. The collision avoidance is evaluated with the system combining PBS and emergency braking function. Therefore, the effectiveness of the PBS is evaluated by comparing the collision avoidance results at PBS+EBS and EBS. In addition, the collision avoidance performance is evaluated iteratively by changing the following conditions of the scenario, intersection shape, position of the occluding vehicle, darting-out speed, and darting-out timing.

4.2 Simulation Software

To evaluate the collision avoidance performance safely and repeatability, we used virtual vehicles in the full-vehicle simulations. As to prepare the virtual environments, we used a simulation software called IPG CarMaker. Fig. 4.2.1 shows the image of virtual test driving with IPG CarMaker.

IPG CarMaker enables us to build virtual test scenarios including the surrounding environment. The models in CarMaker including full-vehicle models, a driver model, sensor models, traffic models, road models, and environment models are real-time capable. Besides, CarMaker enables us to conduct the extended simulation and development process such as model-in-the-loop, software-in-the-loop, hardware-in-the-loop, and vehicle-in-the-loop by integrating with other development tools [119].

Fig. 4.2.1 The image of virtual test driving with IPG CarMaker [119].

The vehicle models can simulate the realistic vehicle motion not only from the nonlinear mechanical dynamics of the multibody vehicle model, but also from the dynamic models including aerodynamics, non-linear powertrain characteristics, and frictions of mechanical systems. And those characteristics can be easily and flexibly tuned from the configurations. Also, CarMaker provides a wide variety of pre-defined models for vehicles that are actually in the market.

The road models in CarMaker can design realistic virtual test tracks easily and quickly. The configuration of the road models can construct straight roads, curves, slopes, multi-lane roads, bumps, intersections, roundabouts, and highway ramps. In addition, additive visual objects make the scenario more realistic and understandable. The additive visual objects including lane markings, road paintings, traffic signals, road signs, streetlights, buildings, houses, trees, bushes, static vehicles, and so on.

The driver model, IPG Driver, is an adaptive driver model with artificial intelligence. Lateral motion and longitudinal motion can be configured individually. The longitudinal motion follows the configured target speed, and adaptively slows down the vehicle regarding the surrounding traffic, road curvature, traffic lights, and stop signs. The lateral motion follows the lane but realistically by taking the smooth steering maneuver into the corner. Besides, the driver model can be configured by tuning the driver parameter such as maximum lateral and longitudinal acceleration, corner-cutting coefficient, headway distance time, etc. Also, the driver model adapts to different vehicles, road characteristics, road signs, and road users due to automatic learning function [119].

In addition, IPG CarMaker offers an open integration and test platform. In this thesis, we developed the whole driver assistance system on MATLAB and Simulink. IPG CarMaker also offers a development platform for Simulink (CarMaker for Simulink), therefore, we implied the whole system into CarMaker for Simulink and whole simulations were conducted on CarMaker for Simulink.

4.3 Emergency Braking System (EBS)

To compare the collision avoidance performance, the experiment vehicle equipped an emergency braking system (EBS) to mitigate the collision impact. The EBS was installed in all conditions of the

simulation. The system applied when the collision with the darting-out object is imminent, the system calculates the appropriate target acceleration to avoid or mitigate the collision impact. The followings describe the methodology to calculate the target acceleration.

When the object sensor perceives the darting-out object, the system predicts the motion of the detected object. From the perceived velocity and direction of the object, the motion of the darting-out object is predicted as a straight trajectory. Assuming the trajectory of the ego vehicle is predicted as circular arc as shown in Fig. 4.3.1. As shown in the figure, the center point of the rear axle of the ego vehicle defines the origin of the coordinate, and the direction of the x-axis is the longitudinal direction of the ego vehicle.

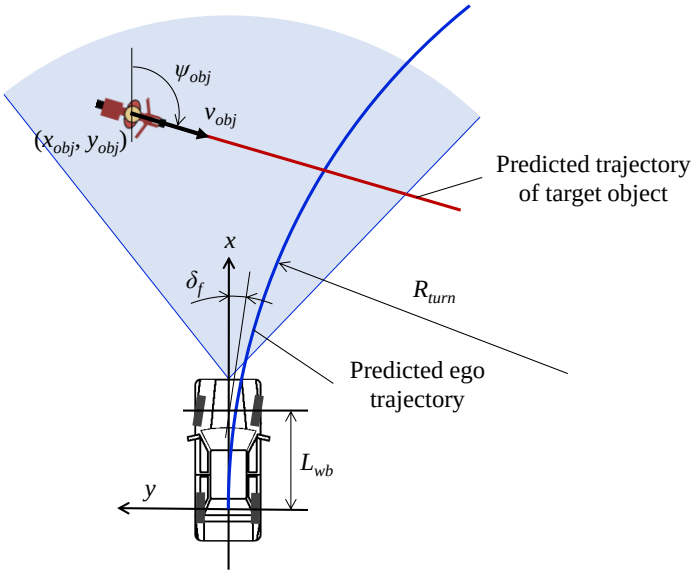

Fig. 4.3.1 The circular arc ego trajectory and straight trajectory of the target vehicle.

Considering the width and the length of the ego vehicle, the front-left and front-right corner of the ego vehicle draw the trajectories as Fig. 4.3.2 and the following equations:

$$x^2 + \left(y - R_{turn}\right)^2 = R_1^2, \tag{4.3.1}$$

$$x^2 + \left(y - R_{turn}\right)^2 = R_2^2. \tag{4.3.2}$$

where R_1 is the radius of the trajectory of the left-front corner of the ego vehicle, R_2 is the radius of the trajectory of the right-front corner of the ego vehicle, and R_{turn} is the turning radius at the center point of the rear axle and can be calculated from the wheelbase L_{wb} and the steering angle δ_f as $R_{turn} = L_{wb} / \tan\delta_f$. Notice that when the steering angle δ_f is lower than 0, the radiuses R_{turn}, R_1, and R_2 take the negative numbers.

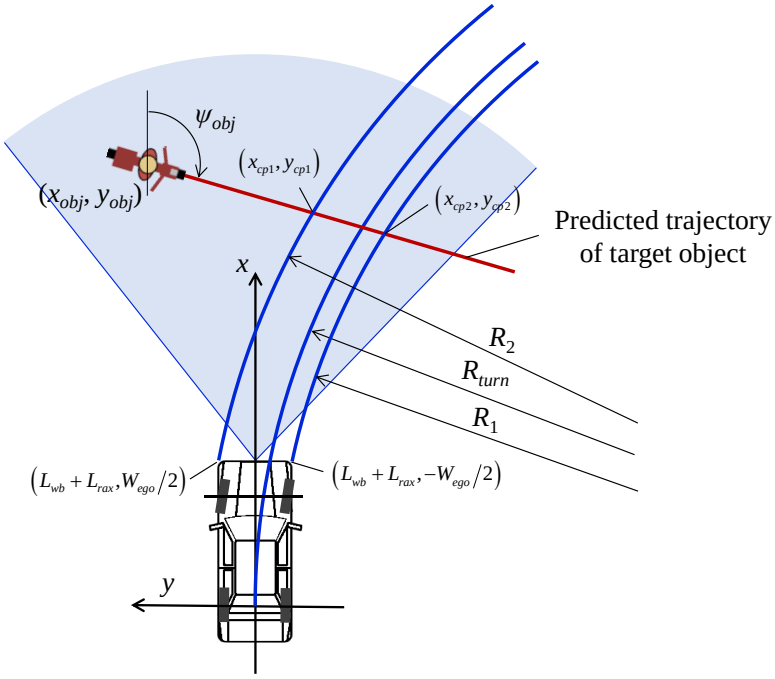

Fig. 4.3.2 Definitions of the parameters for the target acceleration calculation on the EBS.

The trajectories at the front-left and the front-right corner are geometrically defined from the size of the vehicle. When the vehicle trajectory is the circular arc, the trajectories at the corners also take the circular arc trajectories. The following equations calculate the radius at the corners R_1 and R_2.

$$R_1 = \text{sign}\left(R_{turn}\right)\sqrt{L_{rax}^2 + \left(\frac{W_{ego}}{2} - R_{turn}\right)^2}, \tag{4.3.3}$$

$$R_2 = \text{sign}\left(R_{turn}\right)\sqrt{L_{rax}^2 + \left(\frac{W_{ego}}{2} + R_{turn}\right)^2}, \tag{4.3.4}$$

where L_{rax} is the length from the front-tip to the rear-axle of the ego vehicle, W_{ego} is the width of the ego vehicle.

The trajectory of the darting-out object defines as

$$y = \left(x - x_{obj}\right)\tan\psi_{obj} + y_{obj}, \tag{4.3.5}$$

where (x_{obj}, y_{obj}) are the positions of the darting-out object, and ψ_{obj} is the relative angle between the darting-out object and the ego vehicle.

From (4.3.1), (4.3.2), and (4.3.5), the conflict point of left-front corner of the vehicle (x_{cp1}, y_{cp1}) can be derived from the following equations:

$$
\begin{aligned}
&\begin{cases} x_{cp1}^2 + \left(y_{cp1} - R_{turn}\right)^2 = R_1^2 \\ y_{cp1} = \left(x_{cp1} - x_{obj}\right)\tan\psi_{obj} + y_{obj} \end{cases} \\
&\Rightarrow x_{cp1}^2 + \left\{\left(x_{cp1} - x_{obj}\right)\tan\psi_{obj} + y_{obj} - R_{turn}\right\}^2 = R_1^2 \\
&\Leftrightarrow x_{cp1}^2 + \left\{\left(x_{cp1} - x_{obj}\right)A + B\right\}^2 = R_1^2 \quad \left(\because A = \tan\psi_{obj}, B = y_{obj} - R_{turn}\right) \\
&\Leftrightarrow \left(1 + A^2\right)x_{cp1}^2 - 2A\left(Ax_{obj} - B\right)x_{cp1} + \left(Ax_{obj} - B\right)^2 - R_1^2 = 0 \\
&\Leftrightarrow \left(1 + A^2\right)x_{cp1}^2 - 2ACx_{cp1} + C^2 - R_1^2 = 0 \quad \left(\because C = Ax_{obj} - B\right) \\
&\therefore x_{cp1} = \frac{AC \pm \sqrt{A^2C^2 - \left(1 + A^2\right)\left(C^2 - R_1^2\right)}}{1 + A^2}.
\end{aligned}
\tag{4.3.6}
$$

Therefore, the conflict point (x_{cp1}, y_{cp1}) is

$$
\begin{aligned}
&x_{cp1} = \frac{AC + \sqrt{A^2C^2 - \left(1 + A^2\right)\left(C^2 - R_1^2\right)}}{1 + A^2} \\
&y_{cp1} = \left(x_{cp1} - x_{obj}\right)\tan\psi_{obj} + y_{obj} \\
&\left(\because A = \tan\psi_{obj}, B = y_{obj} - R_{turn}, C = Ax_{obj} - B\right).
\end{aligned}
\tag{4.3.7}
$$

From the same derivation, the conflict point of the right-front corner of the vehicle (x_{cp2}, y_{cp2}) is expressed as

$$
\begin{aligned}
&x_{cp2} = \frac{AC + \sqrt{A^2C^2 - \left(1 + A^2\right)\left(C^2 - R_2^2\right)}}{1 + A^2} \\
&y_{cp2} = \left(x_{cp2} - x_{obj}\right)\tan\psi_{obj} + y_{obj} \\
&\left(\because A = \tan\psi_{obj}, B = y_{obj} - R_{turn}, C = Ax_{obj} - B\right).
\end{aligned}
\tag{4.3.8}
$$

Since the trajectory is a circular arc, the curve lengths from the left-front corner and the right-front corner to the conflict point d_{cp1} and d_{cp2} are calculated as

$$
d_{cp1} = 2\left|R_1\right|\arcsin\left(\frac{\sqrt{\left(x_{cp1} - L_{rax}\right)^2 + \left(y_{cp1} - W_{ego}/2\right)^2}}{2\left|R_1\right|}\right), \tag{4.3.9}
$$

$$
d_{cp2} = 2\left|R_2\right|\arcsin\left(\frac{\sqrt{\left(x_{cp2} - L_{rax}\right)^2 + \left(y_{cp2} + W_{ego}/2\right)^2}}{2\left|R_2\right|}\right). \tag{4.3.10}
$$

As conditions to trigger the activation of the emergency braking, we considered the time-to-collision (TTC) of both the ego vehicle and the darting-out object. From (4.3.9) and (4.3.10), the TTC at left-front and the right-front corner t_{tc1} and t_{tc2} are calculated as

$$
t_{tc1} = \frac{d_{cp1}}{v_0}, \tag{4.3.11}
$$

$$
t_{tc2} = \frac{d_{cp2}}{v_0}. \tag{4.3.12}
$$

where v0 is the current velocity of the ego vehicle.

Then, the TTC of the darting-out object to reach each conflict point are

$$t_{tc\_obj1} = \frac{\sqrt{\left(x_{obj} - x_{cp1}\right)^2 + \left(y_{obj} - y_{cp1}\right)^2}}{v_{obj}}, \tag{4.3.13}$$

$$t_{tc\_obj2} = \frac{\sqrt{\left(x_{obj} - x_{cp2}\right)^2 + \left(y_{obj} - y_{cp2}\right)^2}}{v_{obj}}, \tag{4.3.14}$$

where v_{obj} is the velocity of the darting-out object.

The system applies the emergency brake when the times t_{tc1} and t_{tc2} fulfill the condition $t_{tc1} \le 2 \cup t_{tc2} \le 2$. Under this condition, to apply the emergency brake only when the conflict is imminent, the following condition must be fulfilled: $t_{tc1} - t_{tc\_obj1} > -0.5 \cap t_{tc2} - t_{tc\_obj2} < 0.5$.

To design the collision avoidance function, the conflict at the most dangerous condition must be avoided. Thus, comparing the curve lengths at the left-front and the front-right corner, choose the shortest curve length as the distance to conflict d_{cp_EBS}.

$$\begin{cases} d_{cp\_EBS} = d_{cp1} & \left(d_{cp1} \le d_{cp2}\right) \\ d_{cp\_EBS} = d_{cp2} & \left(d_{cp1} > d_{cp2}\right). \end{cases} \tag{4.3.15}$$

By considering the safety margin D_{safe_EBS} to avoid the conflict, the length of the control section of the EBS can be expressed as

$$d_{EBS} = d_{cp\_EBS} - D_{safe\_EBS}. \tag{4.3.16}$$

Hence, to stop the vehicle within the length of the control section d_{EBS}, the target acceleration is

$$a_{EBS} = \frac{v_0^2}{2\left(\tau_{EBS} v_0 - d_{EBS}\right)}, \tag{4.3.17}$$

where τ_{EBS} is the latency of the system.

The normalized brake command to the vehicle B_{EBS} is controlled by the feedforward controller. Considering the exception, the brake command B_{EBS} is dealt as

$$\begin{cases} B_{EBS} = 0 & \left(B_{EBS} < B_{EBS\_min}\right) \\ B_{EBS} = -K_{EBS} a_{EBS} & \left(B_{EBS\_min} \le B_{EBS} \le B_{EBS\_max}\right) \\ B_{EBS} = B_{EBS\_max} & \left(B_{EBS\_max} \le B_{EBS}\right) \\ B_{EBS} = B_{EBS\_max} & \left(a_{EBS} > 0 \Leftrightarrow \tau_{EBS} v_0 - d_{EBS} > 0\right). \end{cases} \tag{4.3.18}$$

when $\tau_{EBS} v_0 - d_{EBS} > 0$, even the system cannot activate the emergency braking function, EBS outputs the maximum braking command.

In the simulations, we set the sensor model which recognizes the object later than τ_{EBS} after detecting the object. The latency τ_{EBS} was roughly defined by referring to the results of the Multi-Object Tracking and Segmentation (MOTS) Evaluation [142].

4.4 Collision Avoidance Ability Evaluation with Full-Vehicle Simulation

In this section, the collision avoidance performance between the vehicle equips only EBS and PBS+EBS are compared from the full-vehicle simulations. This section contains five subsections: Subsection 4.4.1 describes the intersections that were prepared for the simulations. Subsection 4.4.2 describes the experiment vehicle. Subsection 4.4.3 explains the collision avoidance performance of the EBS in nominal conditions without occluding vehicles. Subsection 4.4.4 describes detailed simulation conditions of the iterative full-vehicle simulation. Subsection 4.4.5 evaluates the effectiveness regarding the "safety" of the proposed PBS by comparing the results between EBS and PBS+EBS.

4.4.1 Target Scenario

Simulation scenarios were prepared on the IPG CarMaker. Three crossing angles of the intersection were prepared, namely 60 degrees, 90 degrees, and 120 degrees. The bird's-eye views of the intersections are shown from Fig. 4.4.1 to Fig. 4.4.3. Table 4.4.1 shows each specification of the three intersections.

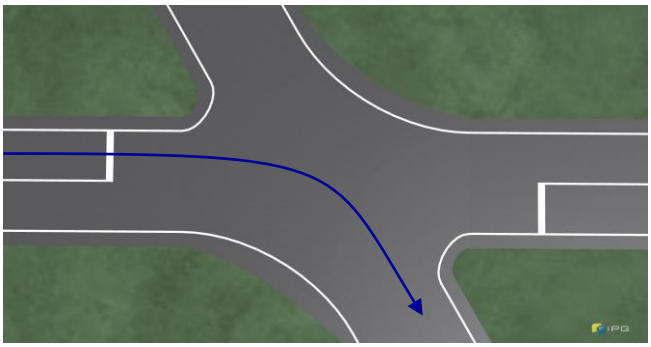

Fig. 4.4.1 The bird's-eye view of the intersection S60.

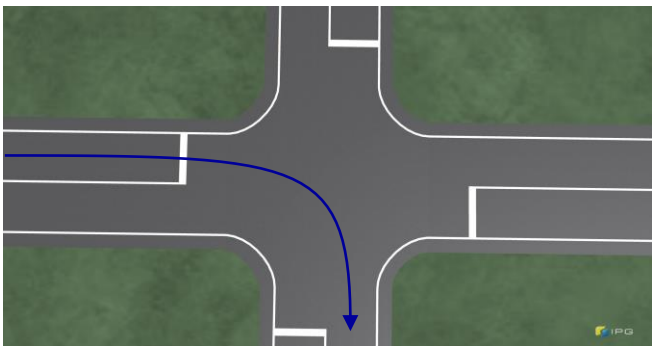

Fig. 4.4.2 The bird's-eye view of the intersection S90.

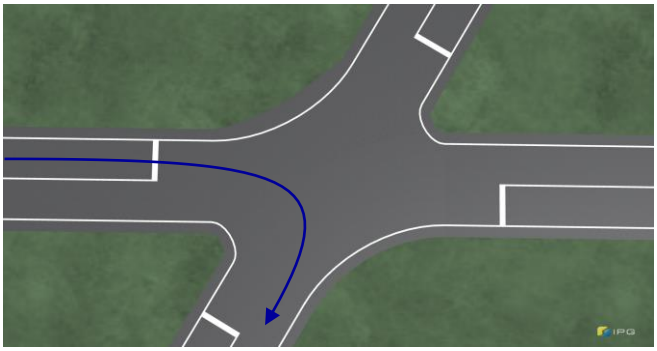

Fig. 4.4.3 The bird's-eye view of the intersection S120.

Table 4.4.1 Specification of the intersections in the simulations.

Intersection ID	θ_{cross} [deg]	l_{in} [m]	l_{out} [m]
S60	-60	5.25	5.25
S90	-90	5.25	5.25
S120	-120	5.25	5.25

In these intersections, an occluding vehicle was prepared on the oncoming lane and the vehicle is stopping at the entrance of the intersections (for example, because of the traffic congestion, the oncoming vehicle is yielding and making space for a right-turning vehicle.) The following equation and Fig. 4.4.4 define the initial condition of the occluding vehicle position:

$$\left(X_{occ}, Y_{occ}\right) = \left(X_{intersec} + X_{base} + X_{occ\_offset}, Y_{intersec} - Y_{base}\right), \tag{4.4.1}$$

where (X_{occ}, Y_{occ}) are the position of the right-front corner of the occlusion vehicle, ($X_{intersec}$, $Y_{intersec}$) are the position of the center point of the intersection, X_{base} and Y_{base} are the base offsets regarding the shape of the intersection, and X_{occ_offset} is the position offset of the occluding vehicle.

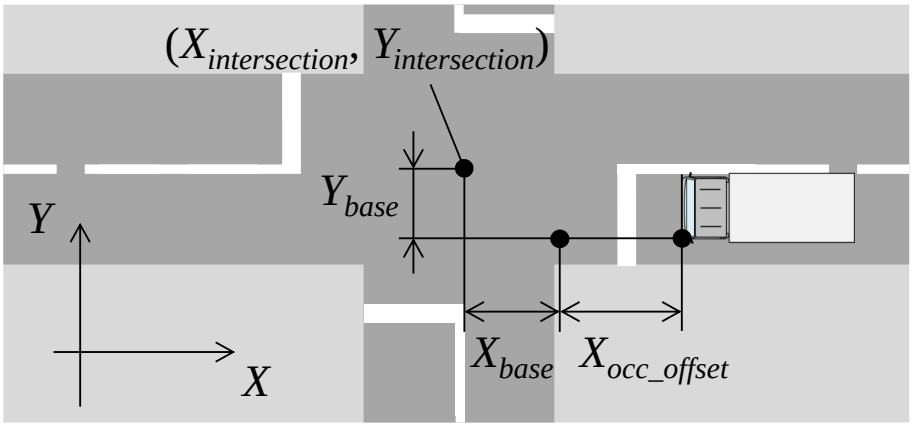

Fig. 4.4.4 Definitions of the initial position conditions of the occluding vehicle.

In this study, the center point of the intersection ($X_{intersec}$, $Y_{intersec}$) defines the origin of the target scenario, therefore, ($X_{intersec}$, $Y_{intersec}$) = (0, 0). The values of the base offsets X_{base}, Y_{base}, and the position offset X_{occ_offset} for the evaluation examples are described in Subsection 4.4.3.

4.4.2 Experiment Vehicle

A predefined vehicle (Honda Fit) in IPG CarMaker was used for the vehicle model of the simulation. The dimensions of the vehicle are shown in Fig. 4.4.5. The vehicle equipped an onboard object detection sensor on the font-tip center of the vehicle. The dimensions of the vehicle, the mounted position, and the specifications of the sensor are shown in Table 4.4.2. This sensor can perceive the position, relative velocity, and relative heading angle of the occluding vehicle on the oncoming lane and the darting-out object.

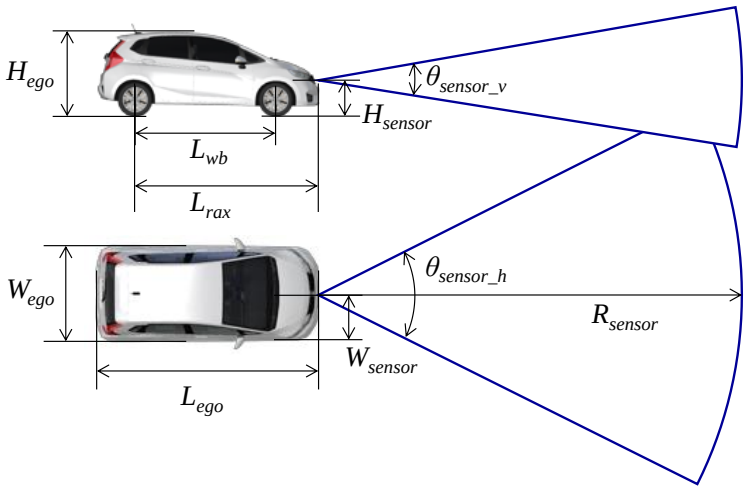

Fig. 4.4.5 The definition of vehicle dimensions and sensor positions.

Table 4.4.2 The parameters of simulation vehicle and onboard sensor.

Description		Variable	Value	Unit
Ego vehicle	Length	L_{ego}	3.995	m
	Width	W_{ego}	1.695	m
	Height	H_{ego}	1.290	m
	Wheelbase	L_{wb}	2.530	m
	Distance from front-tip to rear-axle	L_{rax}	3.395	m
Sensor position	Lateral position	W_{sensor}	$W_{ego}/2 = 0.848$	m
	Vertical position	H_{sensor}	0.6	m
	Horizontal FoV	θ_{sensor_h}	150.0	deg
	Vertical FoV	θ_{sensor_v}	10.0	deg
	Detection range	R_{range}	150.0	m

4.4.3 Simulation Result and Performance Evaluation of EBS

To evaluate the collision avoidance performance, full-vehicle simulations were conducted on the IPG CarMaker. In the evaluation simulations, the ego vehicle drove the three types of intersections and made right-turns at the intersections. The three types of intersection consist of three crossing angles: 60 degrees, 90 degrees, and 120 degrees. Every intersection crossed with two straight roads and the roads had two lanes as shown in Fig. 4.4.1 to Fig. 4.4.3.

In the simulation, the ego vehicle releases at the starting point with the initial velocity. Then the vehicle rolls without operating any pedals. The driver model steers the vehicle and makes a right-turn at the intersection regarding a path following control dubbed IPG Driver. Hence, during the simulations, the driver in the simulations does not attempt to avoid the collision avoidance target object, and only EBS works to avoid the target object. The time historical vehicle motion at the intersections when there is no darting-out object are shown in the figures from Fig. 4.4.6 to Fig. 4.4.8.

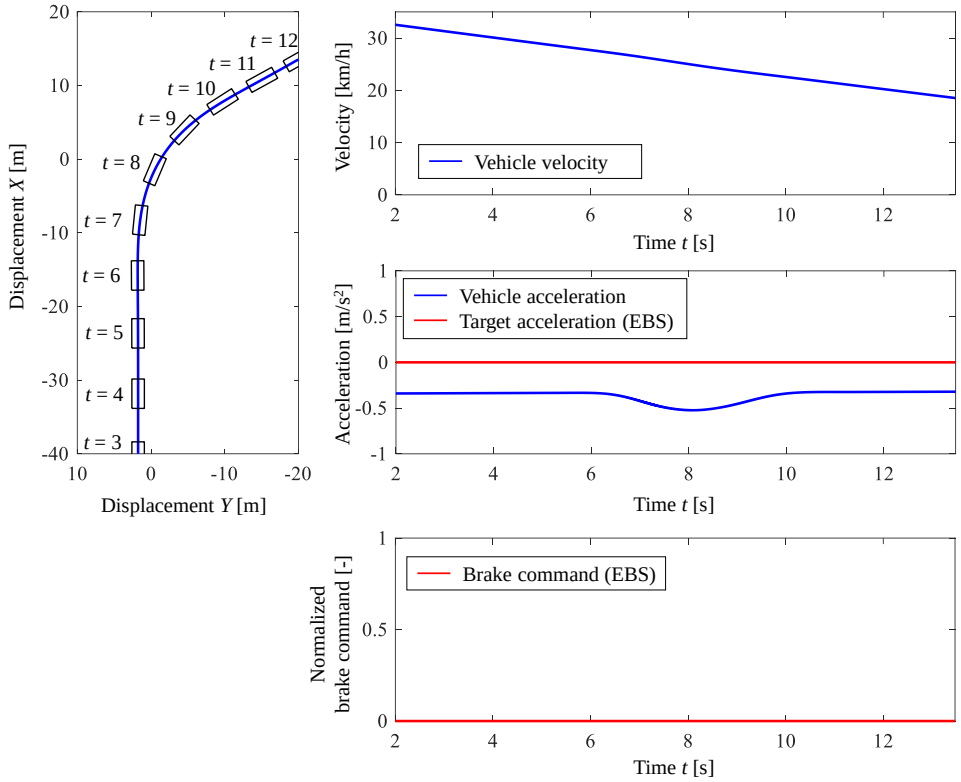

Fig. 4.4.6 The time historical vehicle motion at the intersection S60 when there is no darting-out object.

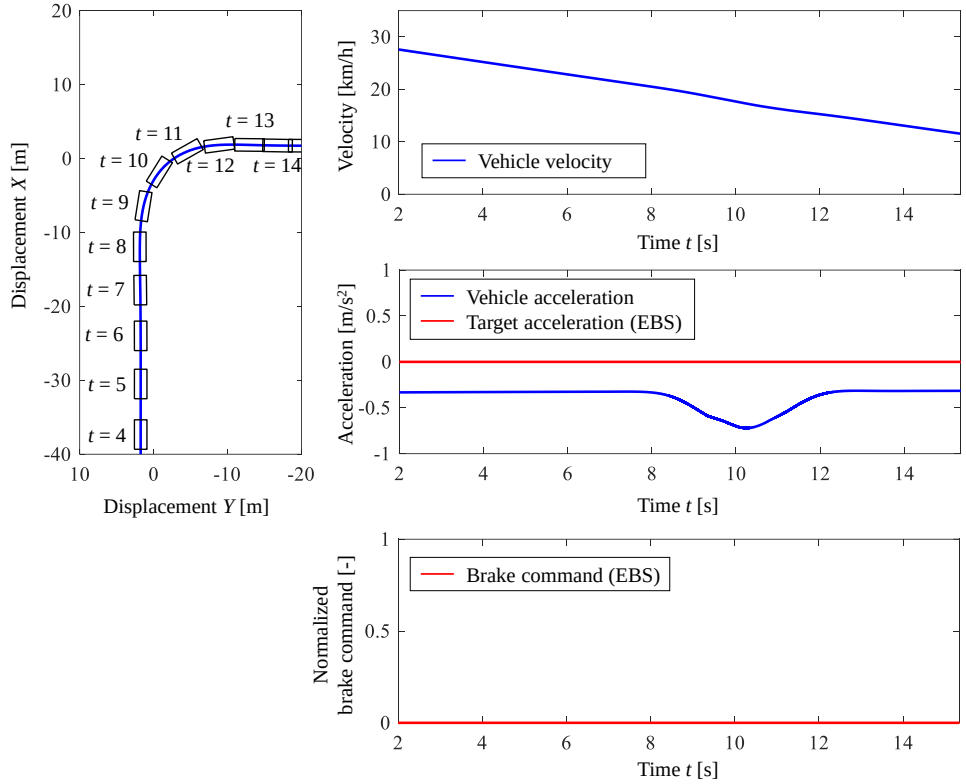

Fig. 4.4.7 The time historical vehicle motion at the intersection S90 when there is no darting-out object.

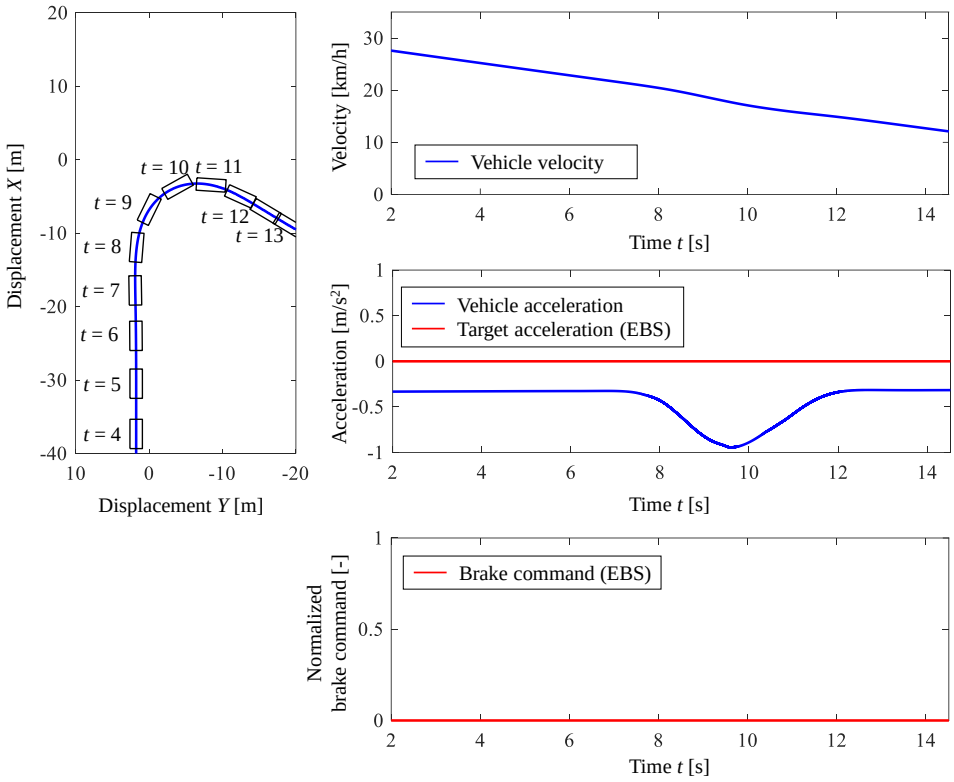

Fig. 4.4.8 The time historical vehicle motion at the intersection S120 when there is no darting-out object.

A motorcycle was set on the simulations as the avoidance target object of the EBS. The target object drove straight in the oncoming lane with keeping the driving speed. The target object has no lateral motion. To consider the various conflict timing, multiple initial positions of the target object are prepared. Defining the position of the target object when the front-center point of the ego vehicle without EBS collides into the center point of the target object as the standard conflict condition (X_{obj_offset} = 0 [m]), we prepared the offset conditions of the conflict position X_{obj_offset} from -10m to 10m as shown in Fig. 4.4.9. The following tables from Table 4.4.3 to Table 4.4.5 show the parameters of the EBS, the darting-out object, and the darting-out conditions respectively.

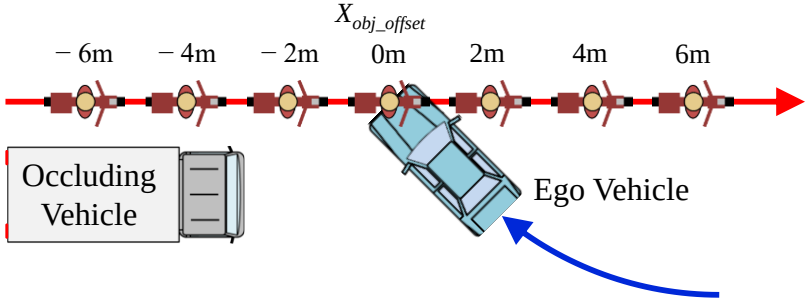

Fig. 4.4.9 The offset conditions of the conflict position

Table 4.4.3 Parameters of the EBS in the simulations.

Description	Variable	Value	Unit
Safety margin	D_{safe_EBS}	0.5	m
Latency of EBS	τ_{EBS}	0.3	s
Control gain	K_{EBS}	0.1	s^2/m
Maximum brake command	B_{EBS_max}	1.0	-
Minimum brake command	B_{EBS_min}	0.5	-

Table 4.4.4 Parameters of the darting-out object.

Description	Variable	Value	Unit
Vehicle length	L_{obj}	2.1	m
Vehicle width	W_{obj}	0.6	m

Table 4.4.5 Darting-out conditions.

Description	Variable	Value	Unit
Conflict position	X_{obj_offset}	−10, −8, −6, −4, −2, 0, 2, 4, 6, 8, 10	m
Darting-out speed	v_{obj}	20, 30, 40	km/h
Intersection crossing angle	θ_{cross}	−60, −90, −120	deg

To evaluate the collision avoidance performance of the EBS in terms of the various darting-out cases, the simulations conducted under all combinations of conflict position and darting-out speed are described in Table 4.4.5.

From Fig. 4.4.10 to Fig. 4.4.12 show the time historical results of the conditions where the offset position of the target X_{obj_offset} was 0 m, and the speed of the target object v_{obj} was 30 km/h. The figures are corresponding to each intersection crossing angle θ_{cross} = −60, −90, −120 [deg]. The first graph in each figure shows the velocity of the ego vehicle. The second graph shows the acceleration of the ego vehicle and the target acceleration. The third graph shows the TTC of the ego vehicle and the target object.

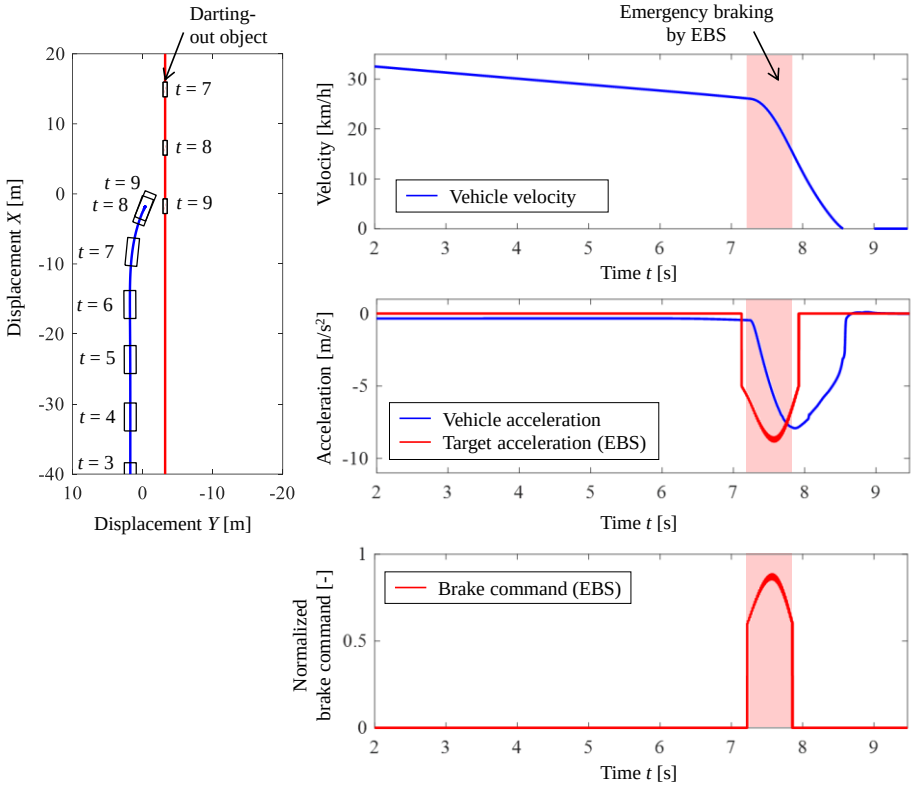

Fig. 4.4.10 Simulation results of the EBS at the intersection with the crossing angle $\theta_{cross} = -60$ [deg].

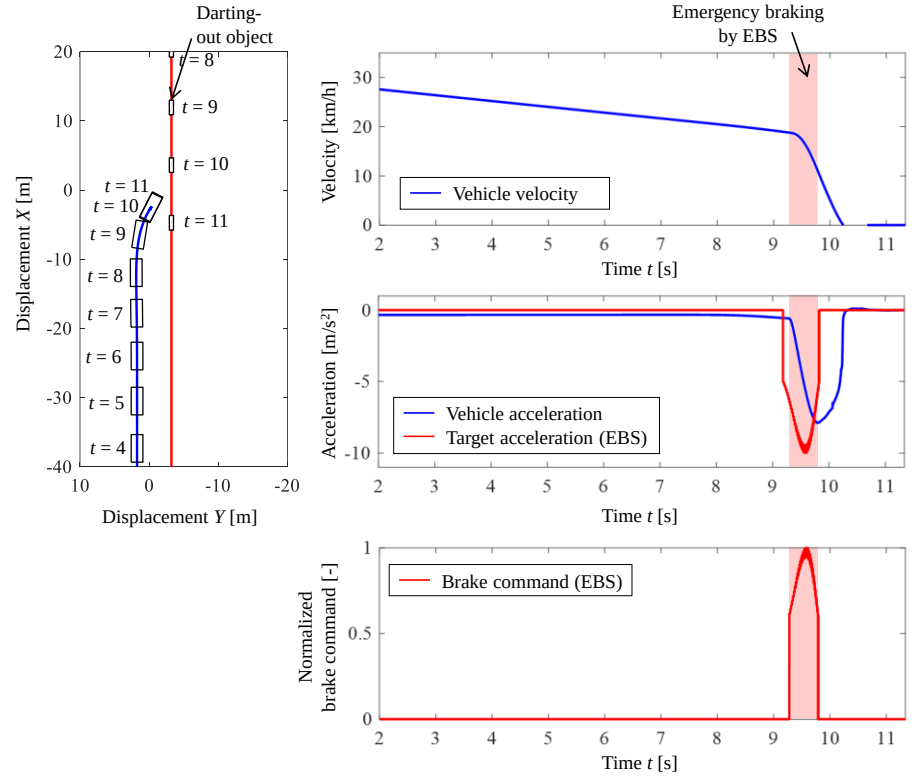

Fig. 4.4.11 Simulation results of the EBS at the intersection with the crossing angle $\theta_{cross} = -90$ [deg].

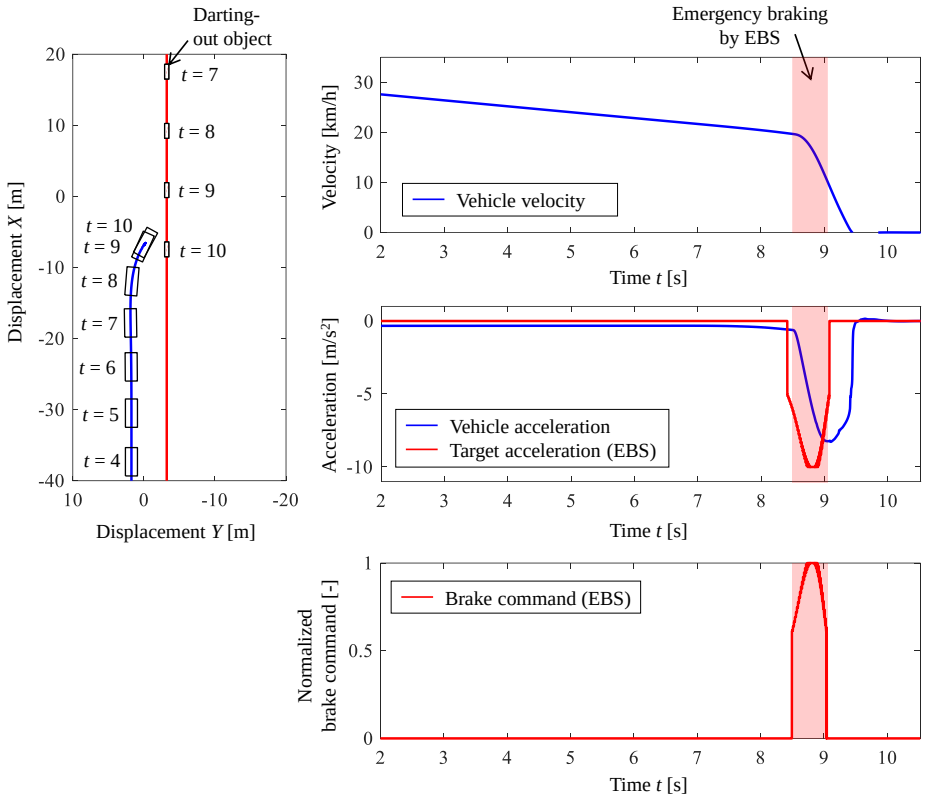

Fig. 4.4.12 Simulation results of the EBS at the intersection with the crossing angle $\theta_{cross} = -120$ [deg].

From the results in those conditions, the EBS could decelerate and stop the vehicle before collided with the object independently to the crossing angles. The target accelerations show that the system could operate only when in an emergency situation.

From Fig. 4.4.13 to Fig. 4.4.15 show the collision avoidance results at each condition regarding the intersection crossing angles, the driving speed of the target object, and the offset position of the target object. In the figures, the x-axis shows the offset position of the target object X_{obj_offset}, the y-axis shows the driving speed of the target object v_{obj}, and the gray cells with bold boxes show the collided conditions and white cells show the conditions that could avoid the collision. From the figures, the collision was avoided by EBS in most cases.

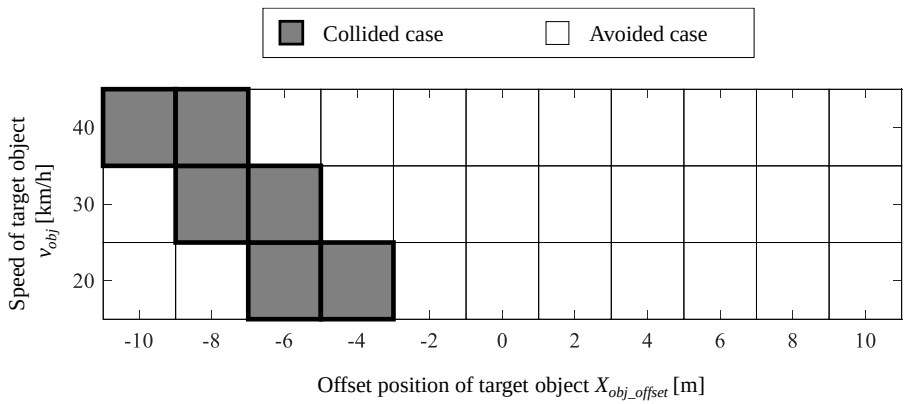

Fig. 4.4.13 The collision avoidance results under various conditions at the intersection with the crossing angle $\theta_{cross} = -60$ [deg].

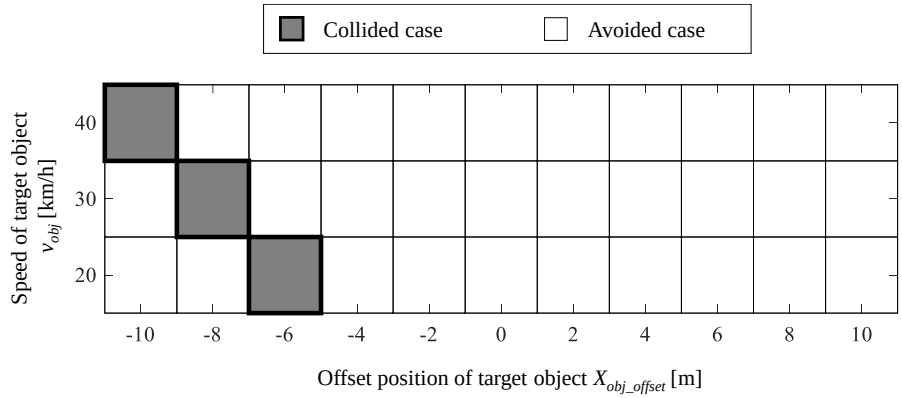

Fig. 4.4.14 The collision avoidance results under various conditions at the intersection with the crossing angle $\theta_{cross} = -90$ [deg].

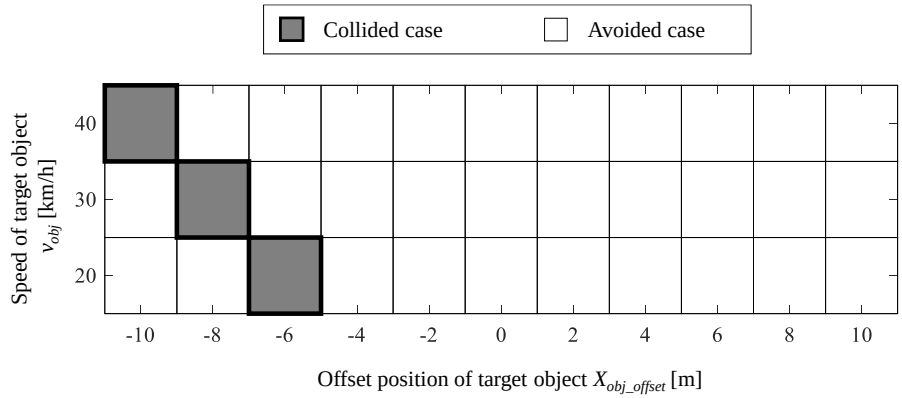

Fig. 4.4.15 The collision avoidance results under various conditions at the intersection with the crossing angle $\theta_{cross} = -120$ [deg].

The figures from Fig. 4.4.16 to Fig. 4.4.18 show the collision velocity of the ego vehicle. The grayed cells are the collided conditions and the red numbers in the cells indicate the collision velocity in km/h.

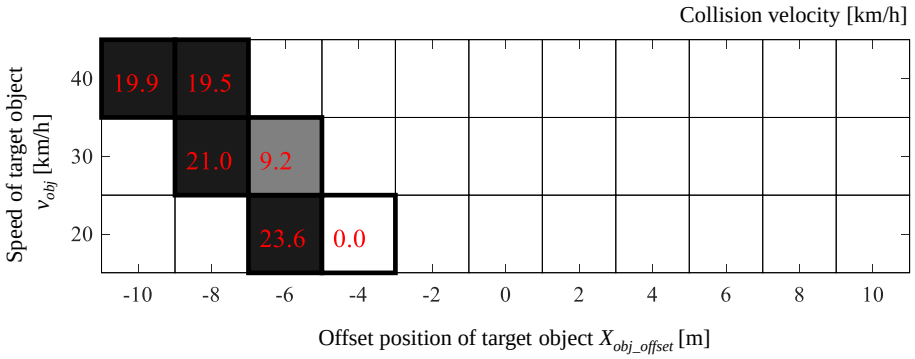

Fig. 4.4.16 The collision velocities at the intersection with the crossing angle $\theta_{cross} = -60$ [deg].

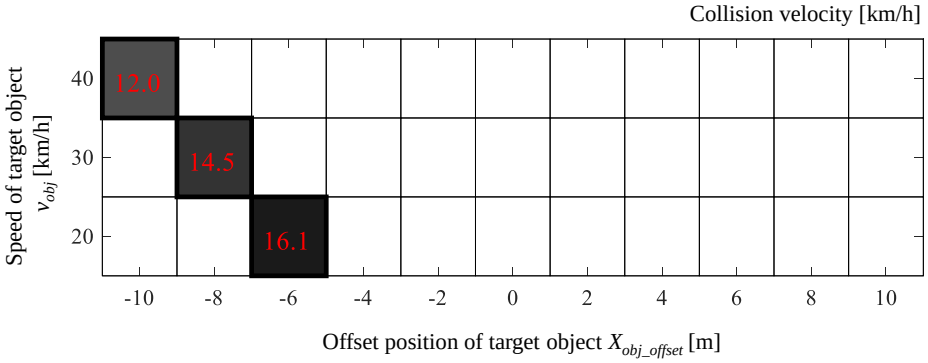

Fig. 4.4.17 The collision velocities at the intersection with the crossing angle θ_{cross} = −90 [deg].

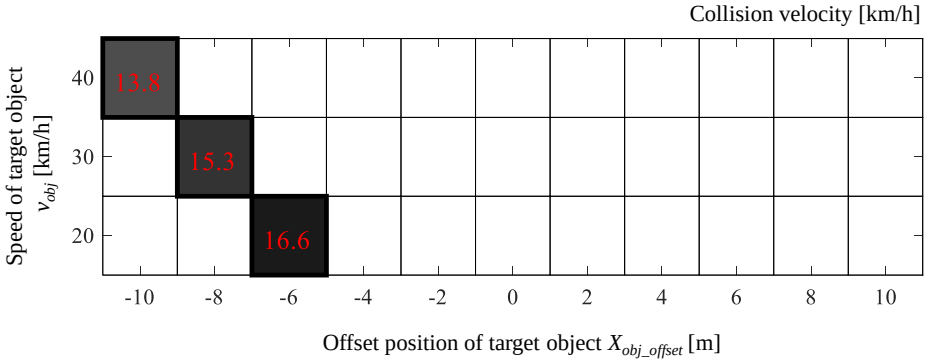

Fig. 4.4.18 The collision velocities at the intersection with the crossing angle θ_{cross} = −120 [deg].

In several conditions, the collision velocities reached about 20 km/h. However, all of the collided cases in the simulations were the cases when the ego vehicle already reached the conflict point before the EBS applies. Therefore, the target object collided into the left side of the ego vehicle. In those cases, it's impossible to avoid the collision only by braking when the object drives steadily in motion.

Nevertheless, in the real condition, the motorcycles also can take collision avoidance maneuvers if they have enough TTC. Therefore, in this paper, when the TTC of the target object had more than 2 seconds when the ego vehicle first time detected the object, the conditions were not counted as collided cases. Basically, this means we do not consider the situation when the target object has enough time to avoid the collision. From Fig. 4.4.19 to Fig. 4.4.21 show the simulation results of the collision velocity of the ego vehicle when the cases that the TTC of the target object has more than 2 seconds were eliminated.

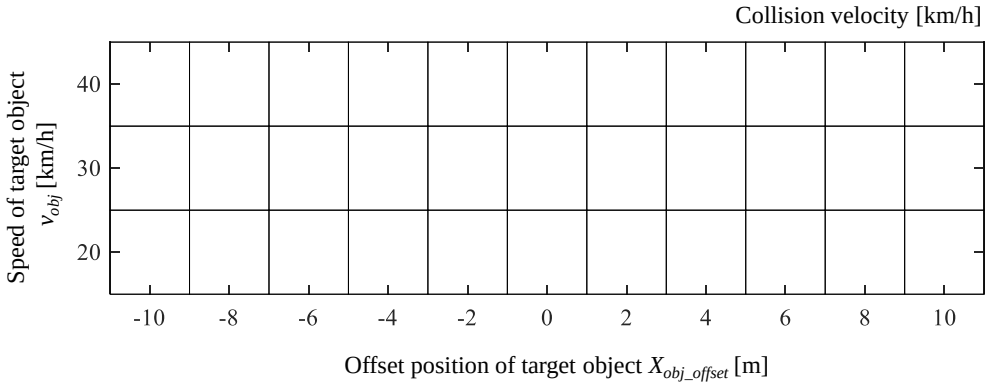

Fig. 4.4.19 The collision velocities that eliminated the cases when the TTC of the target object was larger than 2 seconds. (θ_{cross} = −60 [deg]).

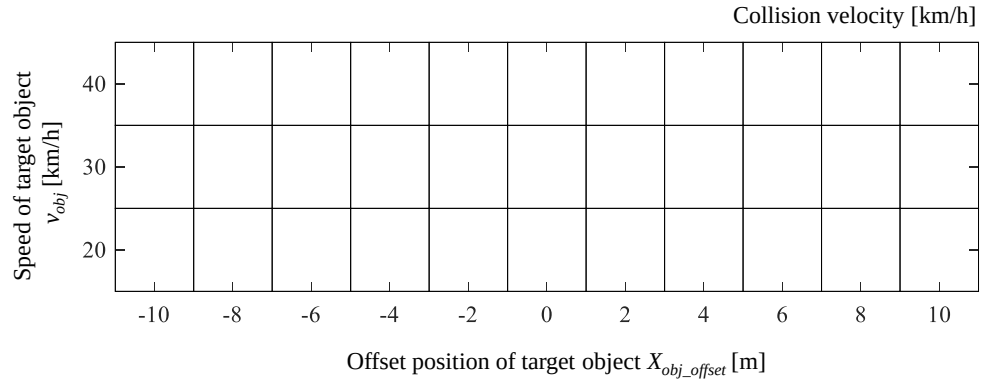

Fig. 4.4.20 The collision velocities that eliminated the cases when the TTC of the target object was larger than 2 seconds. (θ_{cross} = −90 [deg]).

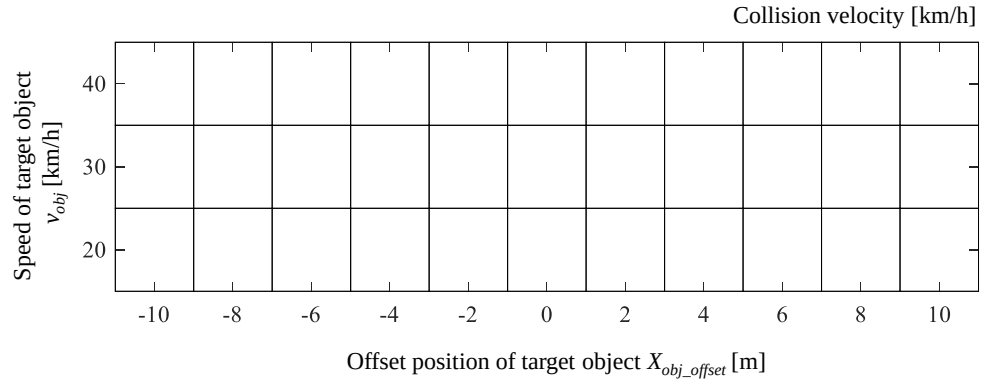

Fig. 4.4.21 The collision velocities that eliminated the cases when the TTC of the target object was larger than 2 seconds. (θ_{cross} = −120 [deg]).

From the figures, the collisions were safely avoided with EBS in all conditions. From these results, the EBS has enough performance for the collision avoidance function in the intersection right-turn scenario. Thus, the performance evaluation simulation of the proposed ADAS adopts the EBS as the emergency braking function.

4.4.4 Simulation Condition

The simulation parameters of the three target intersections, occluding vehicle, PBS, and darting-out conditions are shown in the tables from Table 4.4.6 to Table 4.4.9 respectively. Provided that the parameters of the ego vehicle, onboard sensor, darting-out object, EBS, and parameter estimation equation are referred from the corresponding sections in this chapter. To compare the effectiveness for the collision avoidance performance by only EBS and PBS+EBS in terms of the various darting-out cases, the simulations conducted under the all combination of conflict position, occluding position, and darting-out speed described in Table 4.4.9.

Table 4.4.6 Specification of the intersections in the simulations.

Intersection ID	θ_{cross} [deg]	l_{in} [m]	l_{out} [m]	$\hat{d}_{pre}$ [m]
S60	−60	5.25	5.25	16.6
S90	−90	5.25	5.25	16.1
S120	−120	5.25	5.25	16.6

Table 4.4.7 Parameters of the occluding vehicle.

Description		Variable	Value	Unit
Vehicle length		L_{occ}	7.0	m
Vehicle width		W_{occ}	2.0	m
Base offset	S60	X_{base}	11.95	m
		Y_{base}	2.22	m
	S90	X_{base}	9.95	m
		Y_{base}	2.22	m
	S120	X_{base}	6.95	m
		Y_{base}	2.22	m

Table 4.4.8 Parameters of the PBS in the simulations.

Description	Variable	Value	Unit
Standard time to collision for PBS	t_{vir_d}	2.0	s
Distance from occluding vehicle to virtual darting-out object	D_{vir_occ}	1.0	m
Darting-out velocity of virtual darting-out object	v_{vir}	36	km/h
Expected emergency braking acceleration	a_{EBS}	−8.0	m/s^2
Safety margin	D_{safe}	1.0	m
Latency of PBS	τ	0.5	s
Control gain	K_{ff}	0.06	s^2/m
	K_v	0.05	s/m
	K_a	0.05	s^2/m
Maximum brake command	B_{PBS_max}	0.5	-
Minimum assistance velocity	v_{PBS_min}	3.6	km/h
Prediction time on speed profile	t_{pre}	0.3	s

Table 4.4.9 Darting-out conditions.

Description	Variable	Value	Unit
Conflict position	X_{obj_offset}	−10, −8, −6, −4, −2, 0, 2, 4, 6, 8, 10	m
Occluding vehicle position	X_{occ_offset}	0, 1, 2, 3, 4, 5, 6, 7, 8, 9, 10, 11, 12	m
Darting-out speed	v_{obj}	20, 30, 40	km/h
Intersection crossing angle	θ_{cross}	−60, −90, −120	deg

4.4.5 Simulation Result and Performance Evaluation of Comparative Simulation between PBS+EBS and EBS

First, to see the behavior of the ego vehicle when only PBS applied for the braking assistance, 6 cases of the simulations were conducted without the darting-out object. From Fig. 4.4.22 to Fig. 4.4.27 show the outline of the deceleration by PBS in the situation without the darting-out object. Fig. 4.4.22 to Fig. 4.4.24 show the simulation results when the positions of the occlusion vehicle were set to X_{occ_offset} = 6 [m]. Each figure corresponds to the intersection crossing angles θ_{cross} = −60, −90, −120 [deg]. The rest of the figures Fig. 4.4.25 to Fig. 4.4.27 show the simulation results when the positions of the occlusion vehicle were set to X_{occ_offset} = 2 [m]. In each figure, the subfigure on the left shows the trajectory of the ego vehicle, the subfigure on the right-top shows the time historic result of the ego vehicle velocity, the subfigure on the right-middle shows the time historic result of the ego vehicle acceleration and the subfigure on the right-bottom shows the time historic result of the normalized brake command.

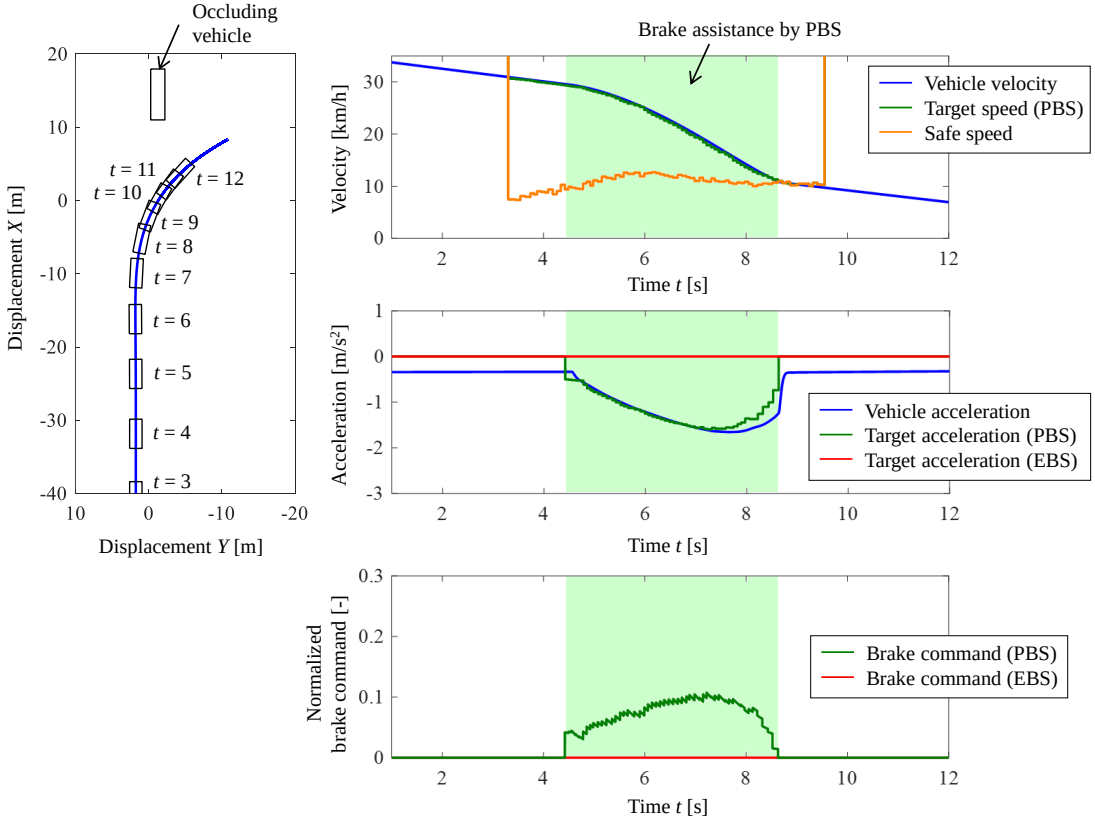

Fig. 4.4.22 Simulation results of the PBS without darting-out at the intersection with the crossing angle θ_{cross} = −60 [deg] and the position of occluding vehicle X_{occ_offset} = 6 [m].

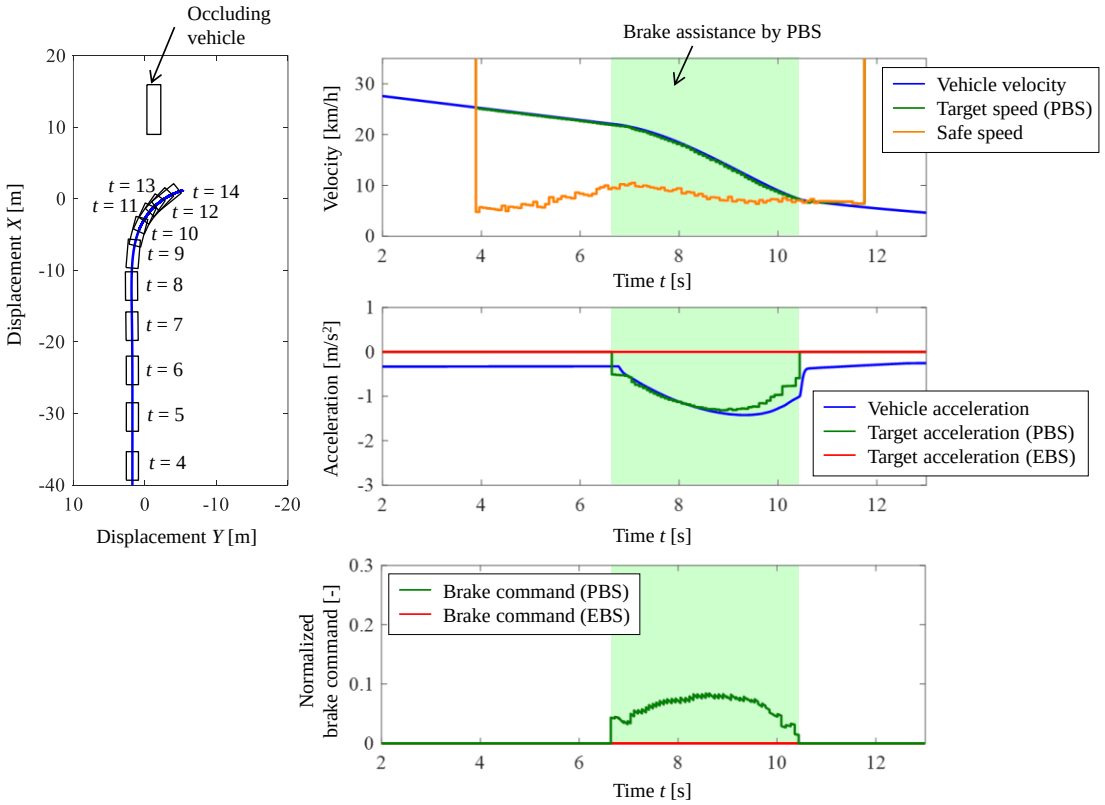

Fig. 4.4.23 Simulation results of the PBS without darting-out at the intersection with the crossing angle θ_{cross} = −90 [deg] and the position of occluding vehicle X_{occ_offset} = 6 [m].

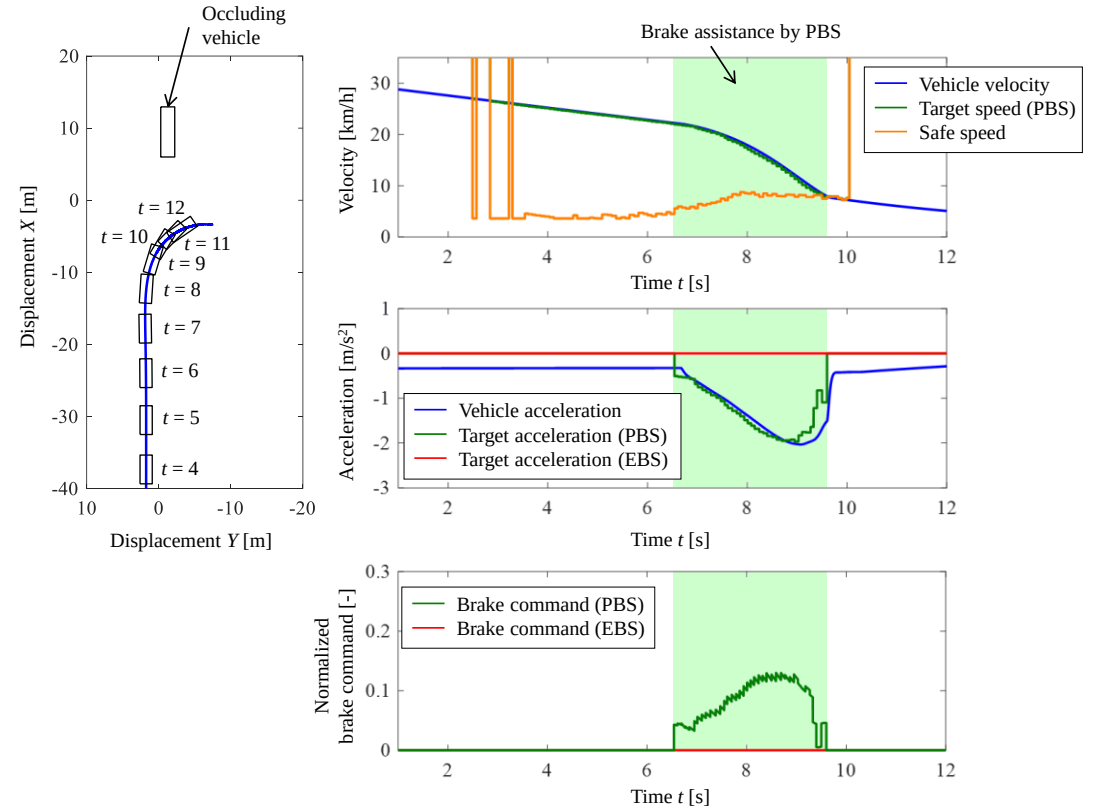

Fig. 4.4.24 Simulation results of the PBS without darting-out at the intersection with the crossing angle θ_{cross} = −120 [deg] and the position of occluding vehicle X_{occ_offset} = 6 [m].

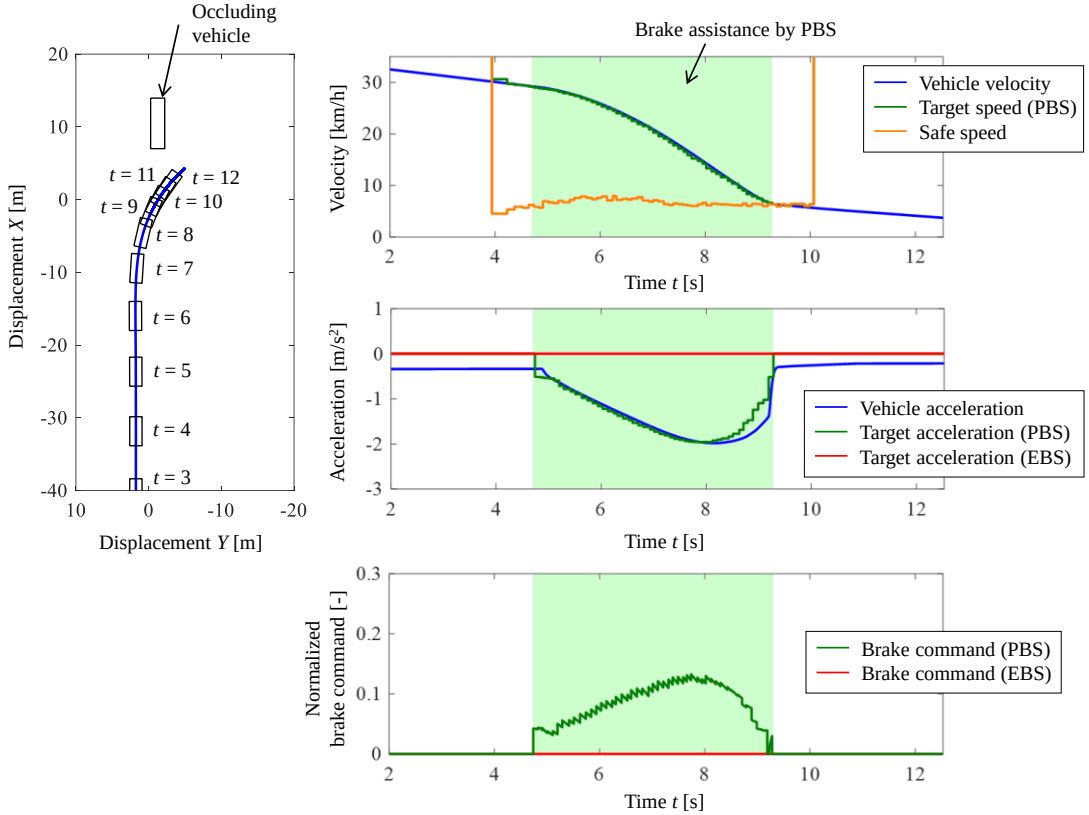

Fig. 4.4.25 Simulation results of the PBS without darting-out at the intersection with the crossing angle θ_{cross} = −60 [deg] and the position of occluding vehicle X_{occ_offset} = 2 [m].

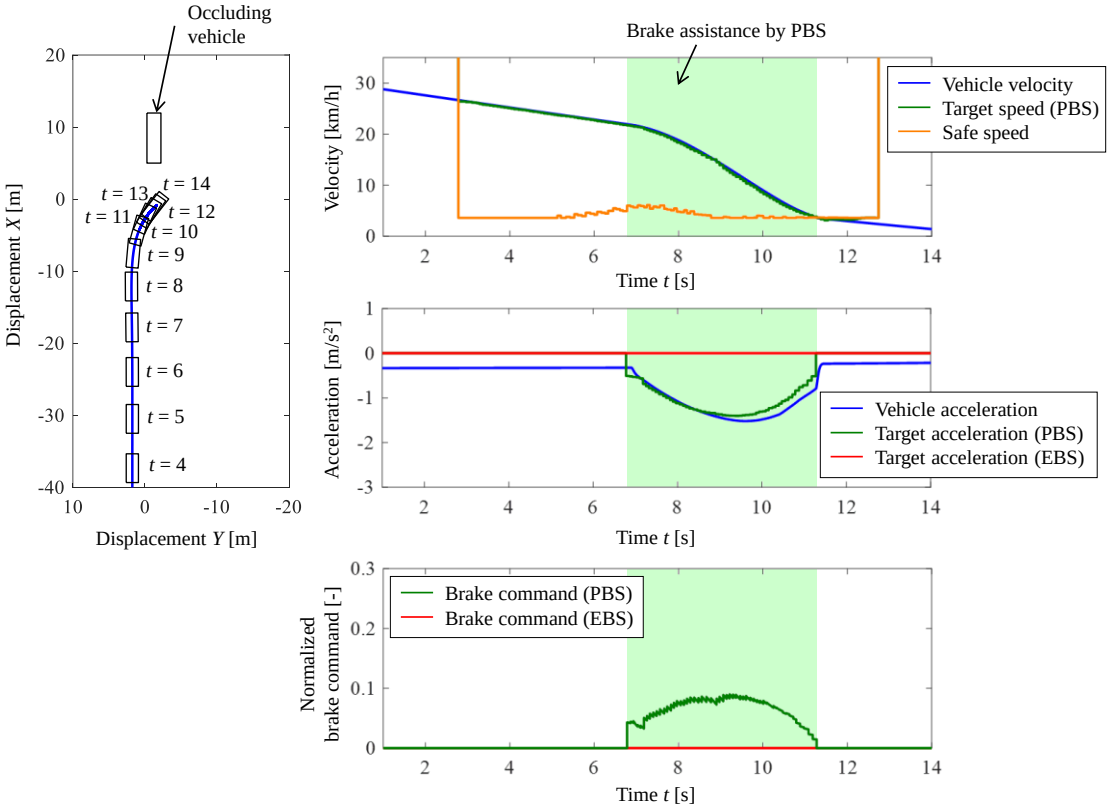

Fig. 4.4.26 Simulation results of the PBS without darting-out at the intersection with the crossing angle θ_{cross} = −90 [deg] and the position of occluding vehicle X_{occ_offset} = 2 [m].

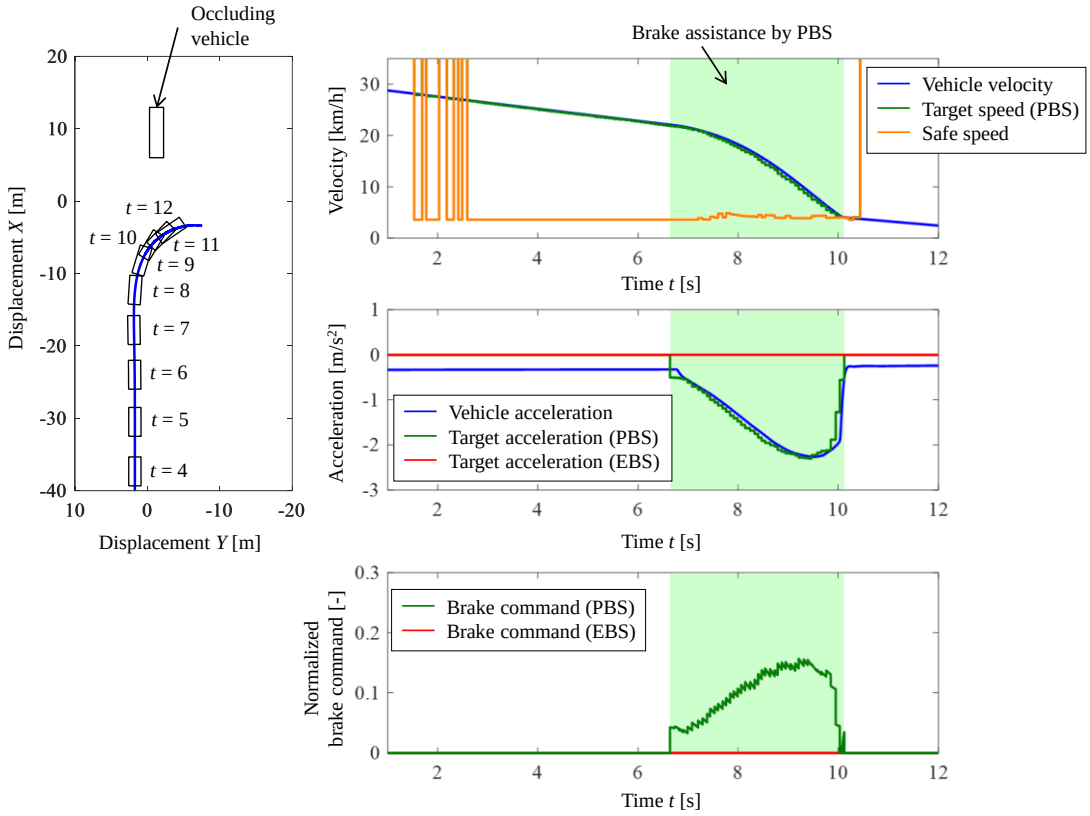

Fig. 4.4.27 Simulation results of the PBS without darting-out at the intersection with the crossing angle θ_{cross} = −120 [deg] and the position of occluding vehicle X_{occ_offset} = 2 [m].

From the results, the ego vehicle started to decelerate the vehicle speed before starting the turning at the intersection. And the brake assistance by PBS could follow the target speed and decelerate to the real-time calculated safe speed. At the beginning of the safe speed calculation, the calculated safe speeds were unstable and lower than the final safe speeds, however, the real-time calculation refined the safe speed when getting closer to the predicted conflict point, and the safe speeds became stable and higher value. Comparing the safe speeds between conditions, the calculated safe speed differed by the shape of the intersection and the position of occluding vehicle X_{occ_offset}. Especially the gaps between the conditions of positions of occluding vehicle were large. These indicated that the safe speeds became lower when the occluding vehicle was close, and the blind spot was large. Those facts explained qualitatively the proposed method could predict the potential risk. In addition, the minimum target deceleration and vehicle acceleration were suppressed higher than -2.5 m/s^2 in all of the conditions above, and the velocity curves and acceleration curves by the PBS were continuous and very smooth. Therefore, the system completed the deceleration only applying moderate and comfortable braking and it was expected that the braking assistance was not bothering assistance. The driver acceptance evaluation by the PBS intervention is presented in Chapter 5.

From Fig. 4.4.28 to Fig. 4.4.30 show the time historical results of the simulation regarding the three types of the intersection crossing angles θ_{cross}, where each parameter defined the simulation condition as follows: the offset position X_{obj_offset} = 0 [m], the position of the occlusion vehicle X_{occ_offset} = 2 [m], and the speed of the target object v_{obj} = 30 [km/h]. In the figures, subfigure (a) shows the result with the system only EBS, and subfigure (b) shows the result with the system PBS+EBS. Regarding the subfigure on the left that shows the trajectory of the ego vehicle and the darting-out object, the boxes show the position of

the vehicles will be colored in red when collisions had occurred.

From the figures, there were collisions in the vehicle equipped only EBS under the condition $\theta_{cross} = -60$ [deg] and $\theta_{cross} = -90$ [deg]. On the contrary, under the provided condition, no collision had occurred with the vehicle which equipped the PBS+EBS. From the figures, the PBS decelerated to the safe speed before the EBS applied the brake. This shows that the PBS completely lead the vehicle into a safe state before getting into the emergency situation as designed. Besides, because the PBS decelerated, the driving speeds of the vehicle equipped PBS+EBS were lower than ones with EBS therefore the braking times by the EBS became shorter and maximum decelerations were lower. These can expect to mitigate both the mental burden to the driver and the structural burden to the vehicle. In Fig. 4.4.29 and Fig. 4.4.30, the calculated values of the safe speed were jumping and discontinuous. This was because the system repeated to start and stop calculation sometimes. This phenomenon occurred only when the distance to the intersection was large, therefore, in the simulations, this phenomenon did not affect the results of the simulation.

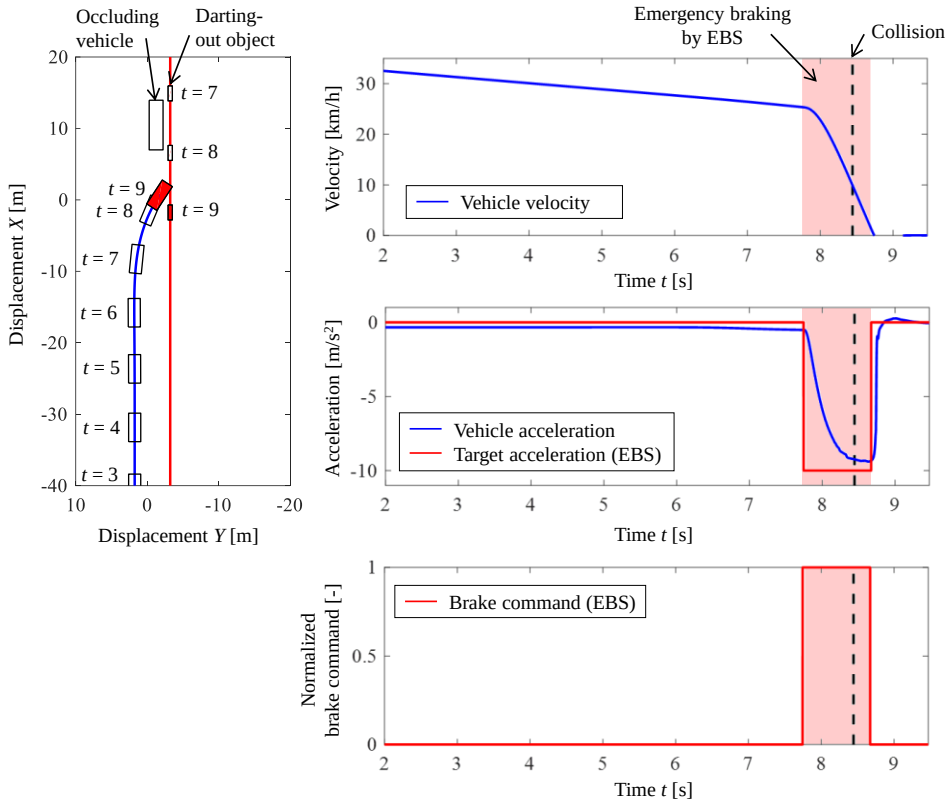

(a) EBS at intersection θ_{cross} = −60 [deg].

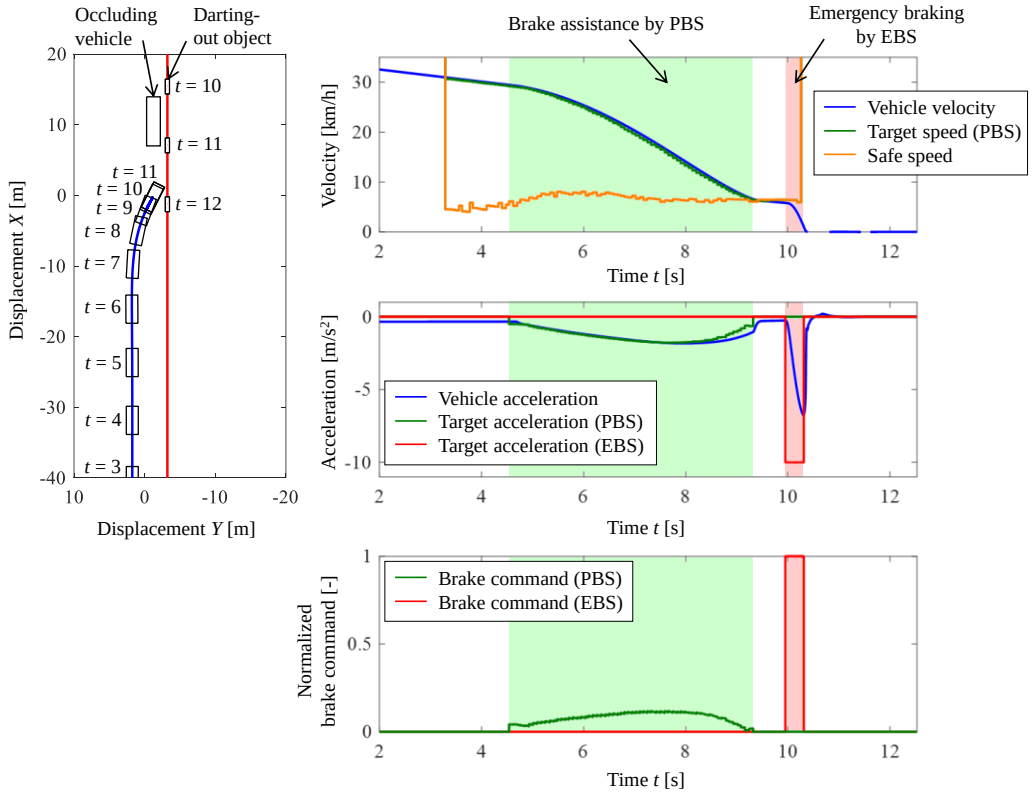

(b) PBS+EBS at intersection θ_{cross} = −60 [deg].

Fig. 4.4.28 Simulation results with darting-out (θ_{cross} = −60 [deg], X_{obj_offset} = 0 [m], X_{occ_offset} = 2 [m], v_{obj} = 30 [km/h]).

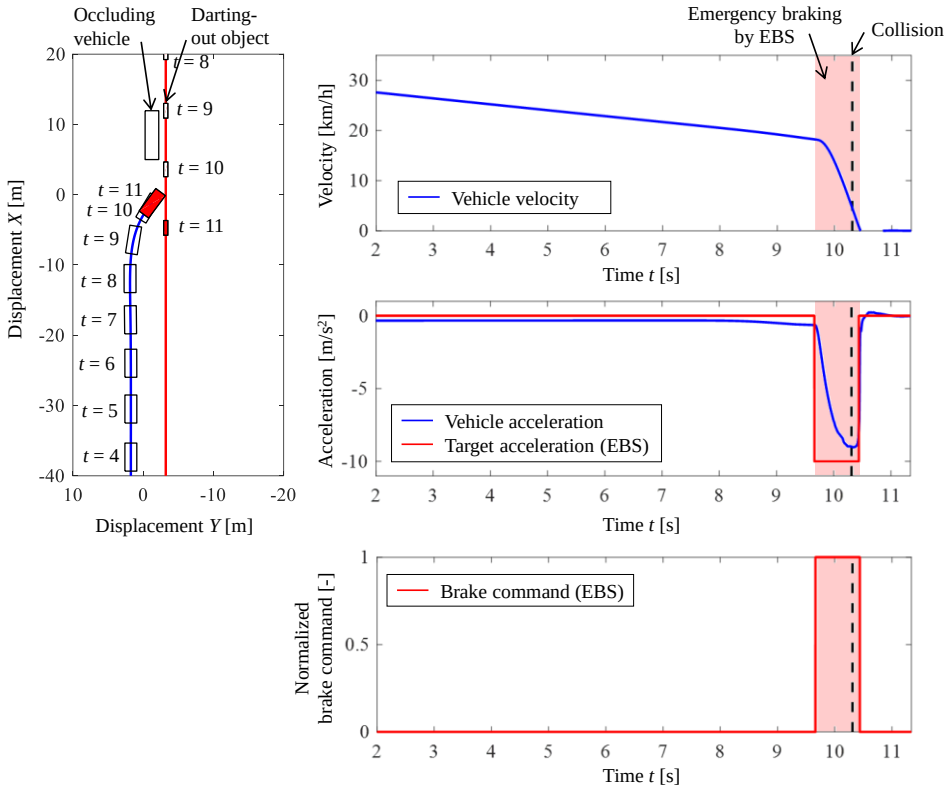

(a) EBS at intersection θ_{cross} = −90 [deg].

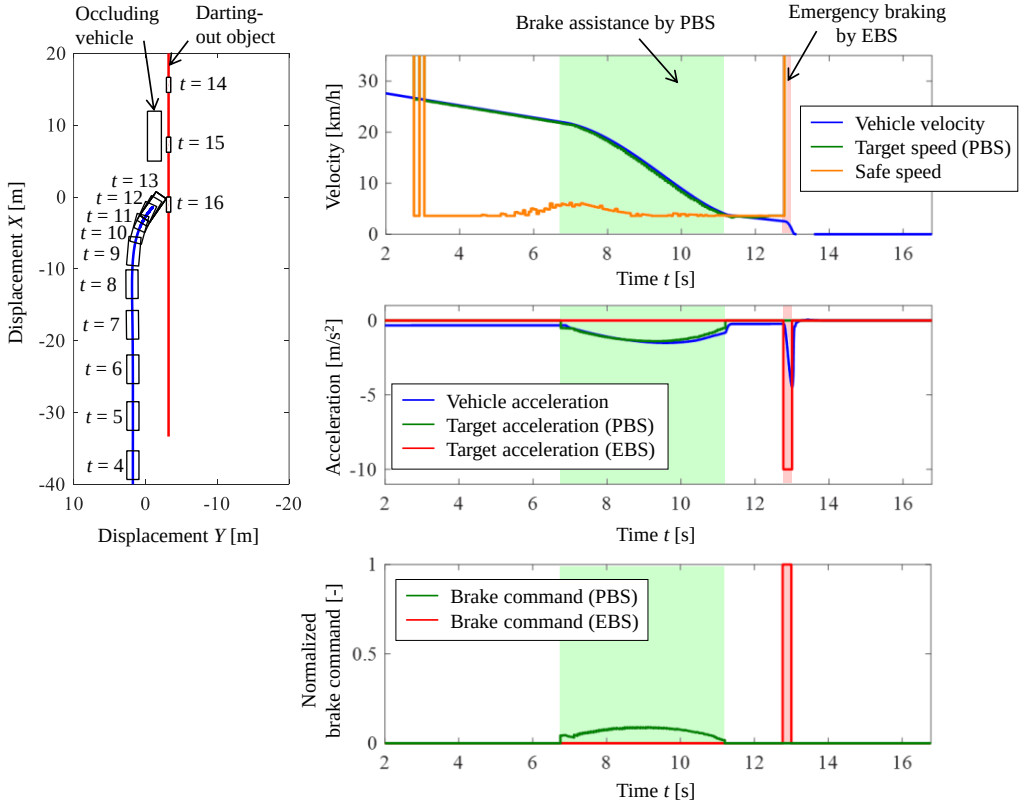

(b) PBS+EBS at intersection θ_{cross} = −90 [deg].

Fig. 4.4.29 Simulation results with darting-out (θ_{cross} = −90 [deg], X_{obj_offset} = 0 [m], X_{occ_offset} = 2 [m], v_{obj} = 30 [km/h]).

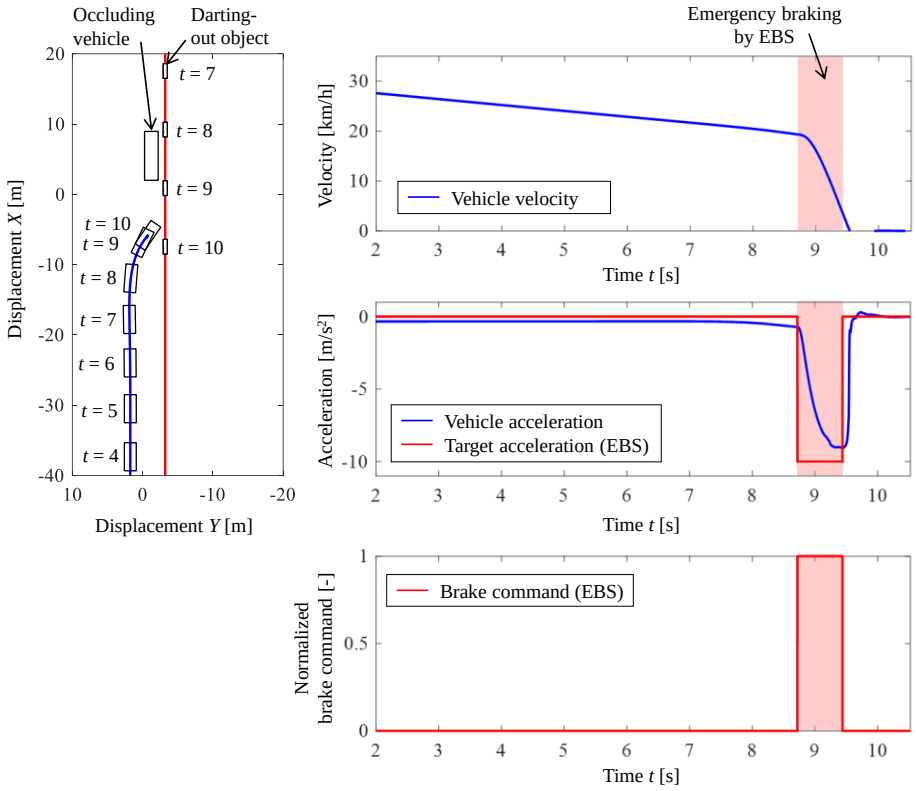

(a) EBS at intersection θ_{cross} = −120 [deg].

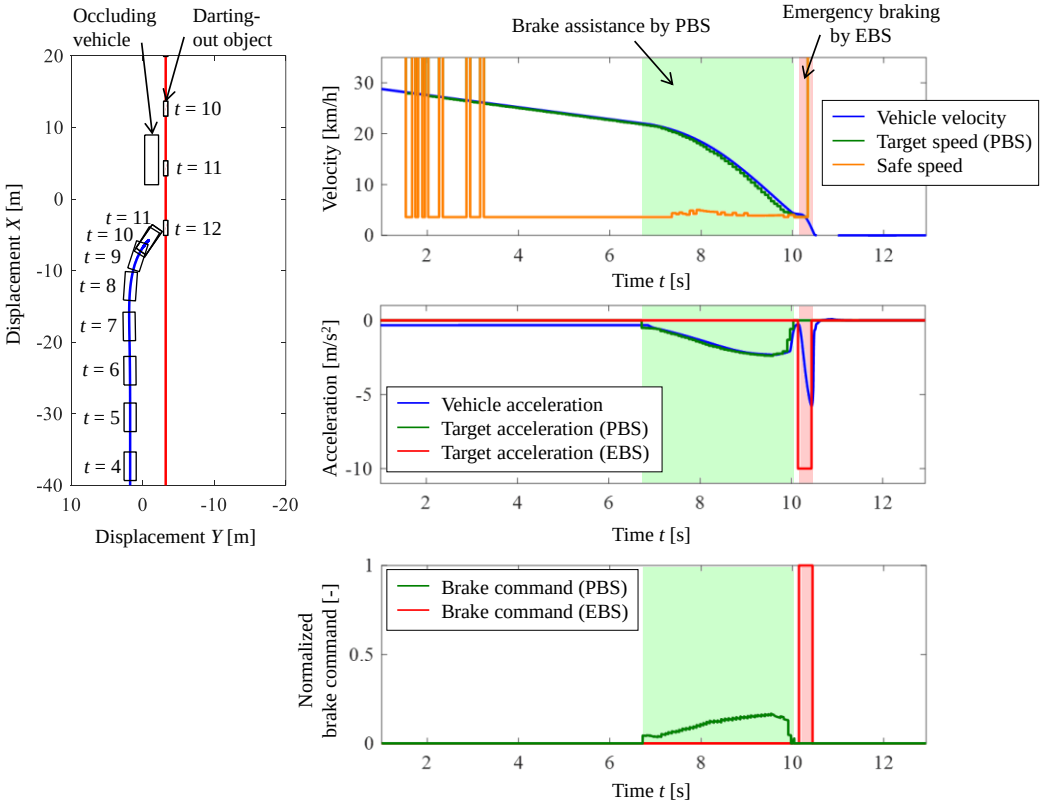

(b) PBS+EBS at intersection θ_{cross} = −120 [deg].

Fig. 4.4.30 Simulation results with darting-out (θ_{cross} = −120 [deg], X_{obj_offset} = 0 [m], X_{occ_offset} = 2 [m], v_{obj} = 30 [km/h]).

As comparisons of the system with the system only EBS and PBS+EBS, the collision avoidance performances at each condition when changed the offset position X_{obj_offset} and the occlusion vehicle position X_{occ_offset} were shown in the figures from Fig. 4.4.31 to Fig. 4.4.33. The darting-out speed v_{obj} was fixed to 30km/h. Subfigure (a) shows the result with the system only EBS, and subfigure (b) shows the result with the system PBS+EBS. Fig. 4.4.31 to Fig. 4.4.33 corresponds to results at the intersection crossing angles $\theta_{cross} = -60, -90, -120$ [deg]. In each figure, the x-axis shows the offset position of the target object, the y-axis shows the driving speed of the target object, and the gray cells with bold boxes show the collided conditions and white cells show the conditions that could avoid the collision.

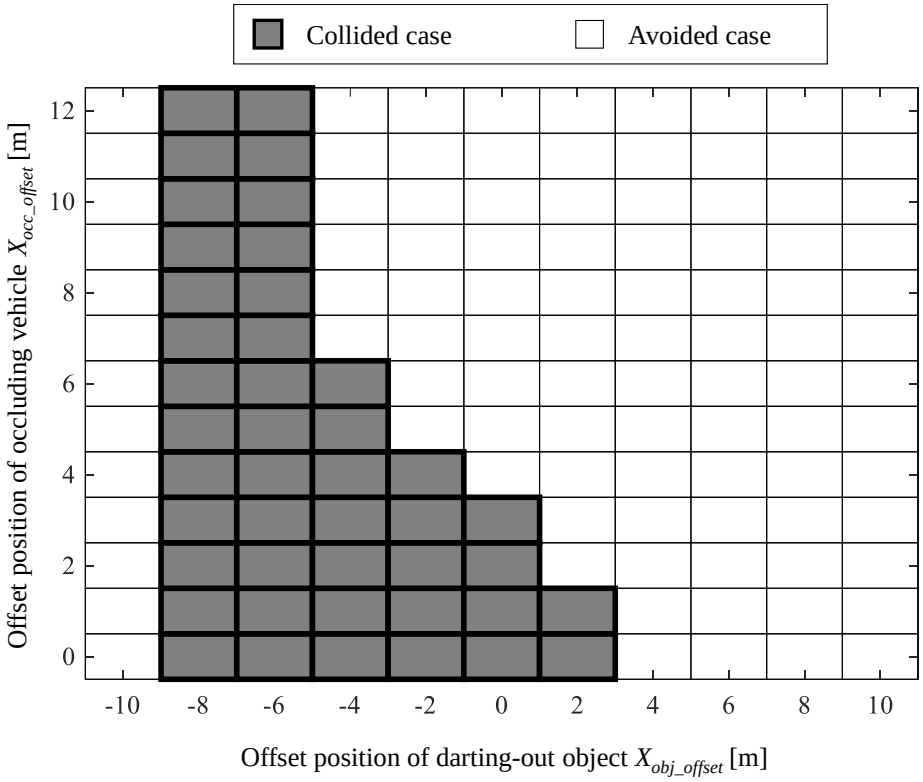

(a) EBS at intersection θ_{cross} = −60 [deg].

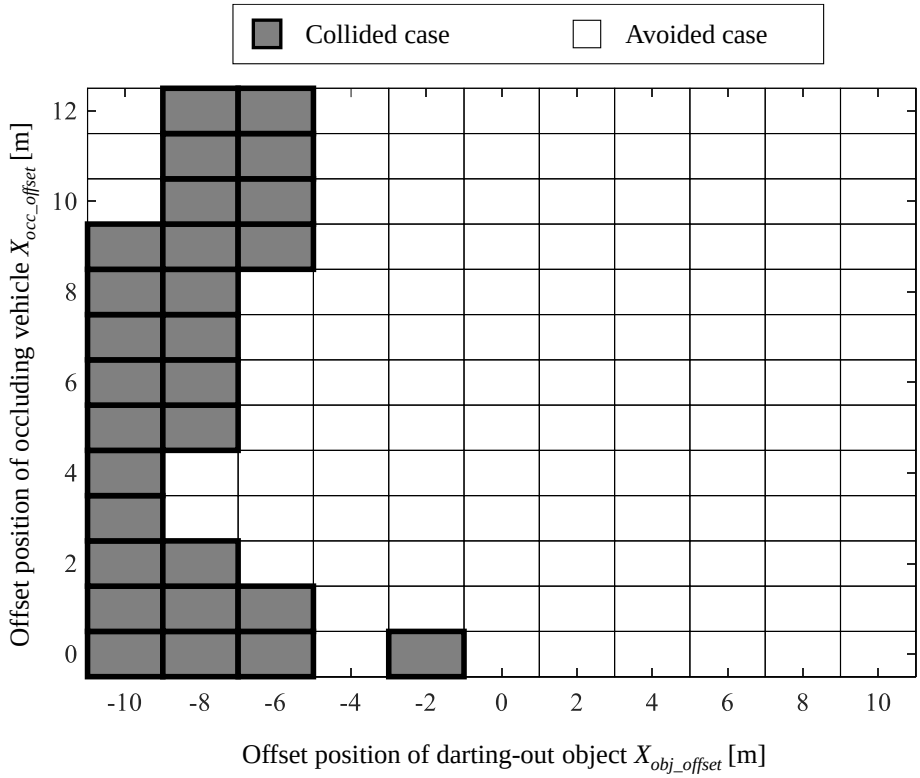

(b) PBS+EBS at intersection θ_{cross} = −60 [deg].

Fig. 4.4.31 The collision avoidance results under various conditions (θ_{cross} = −60 [deg], v_{obj} = 30 [km/h]).

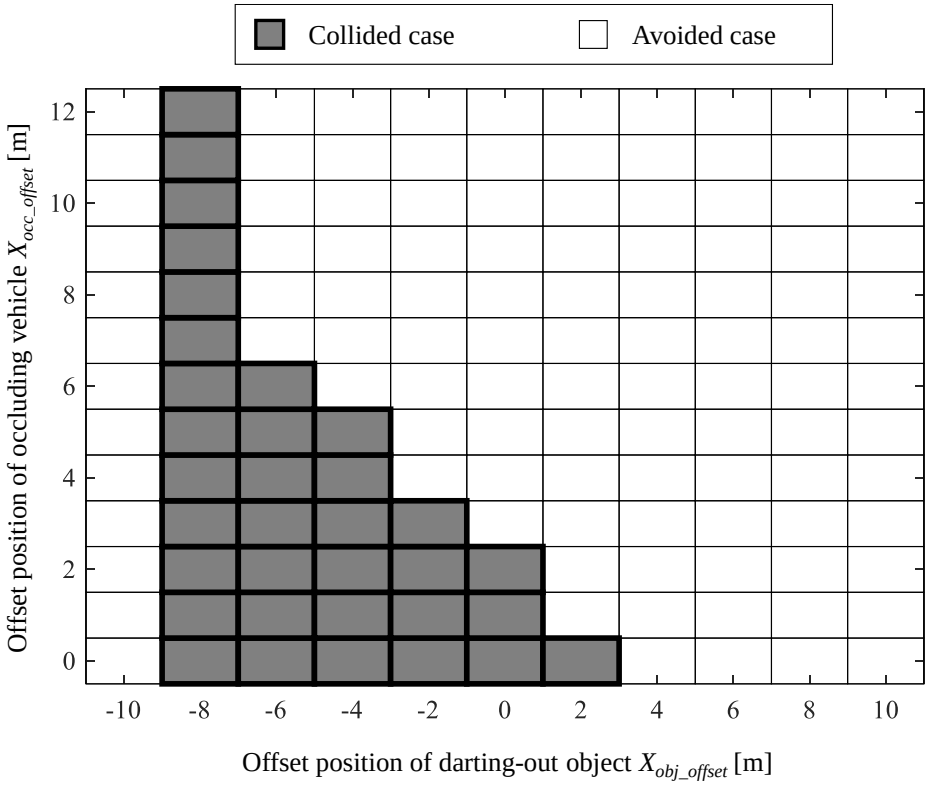

(a) EBS at intersection θ_{cross} = −90 [deg].

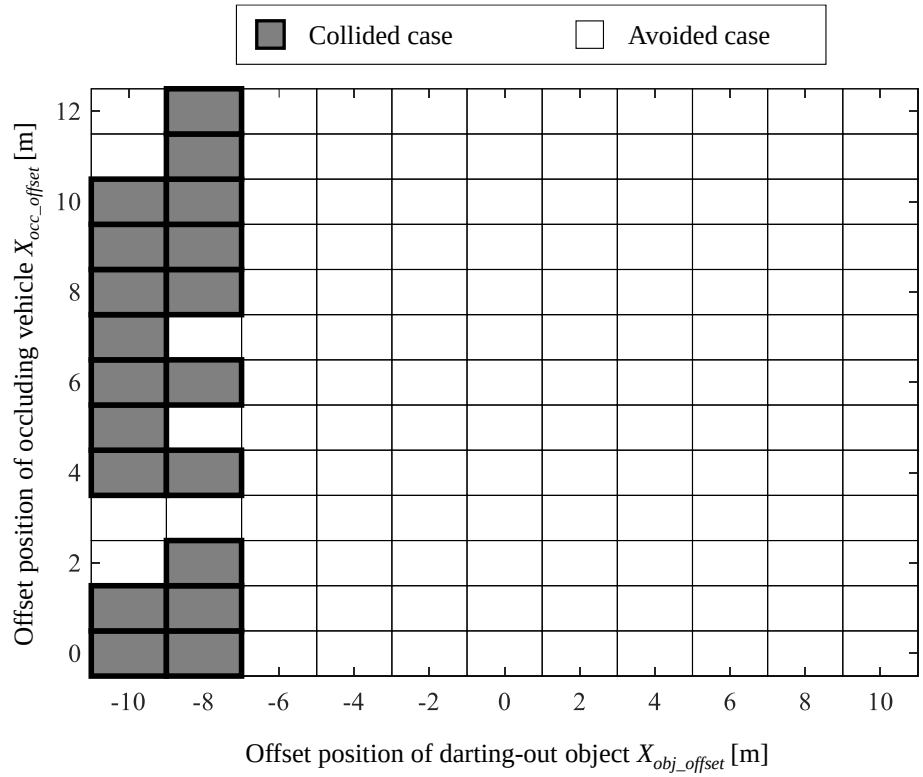

(b) PBS+EBS at intersection θ_{cross} = −90 [deg].

Fig. 4.4.32 The collision avoidance results under various conditions (θ_{cross} = −90 [deg], v_{obj} = 30 [km/h]).

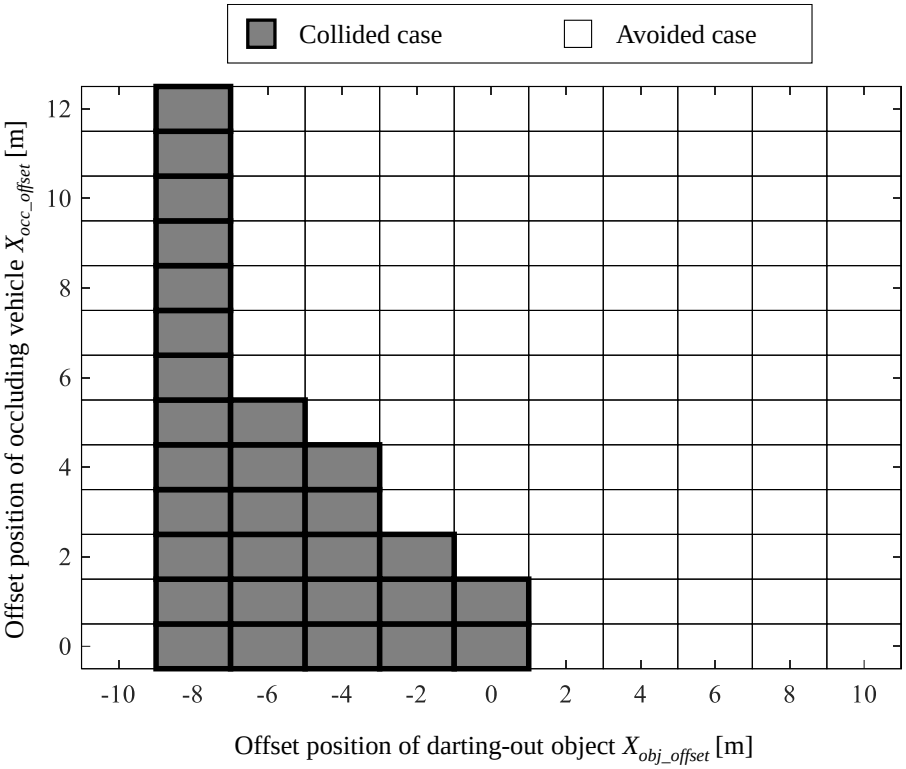

(a) EBS at intersection θ_{cross} = −120 [deg].

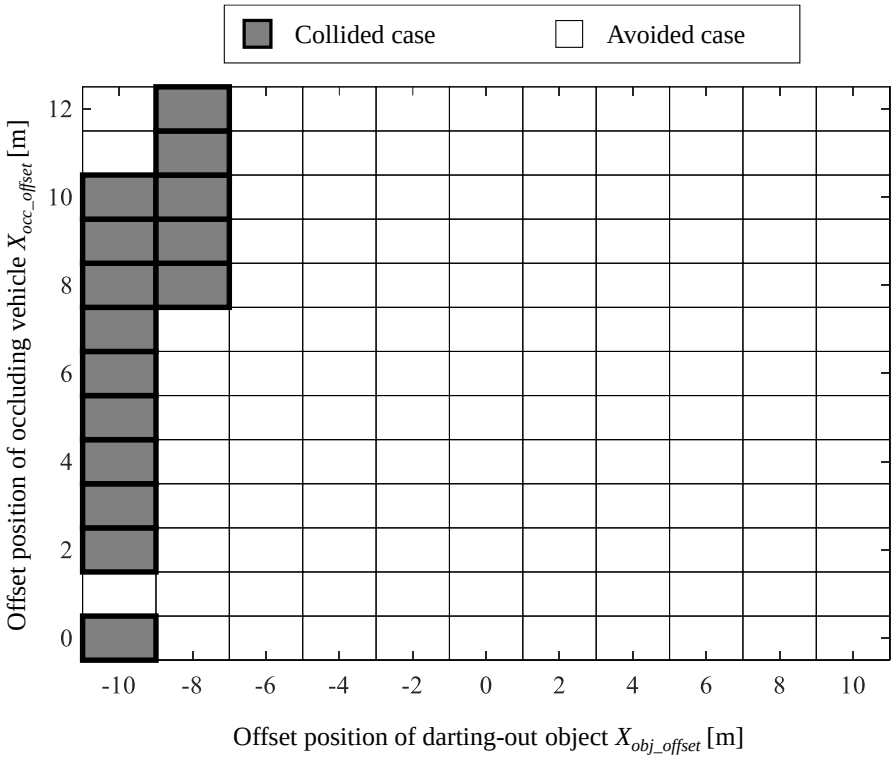

(b) PBS+EBS at intersection θ_{cross} = −120 [deg].

Fig. 4.4.33 The collision avoidance results under various conditions (θ_{cross} = −120 [deg], v_{obj} = 30 [km/h]).

Through the figures from Fig. 4.4.31 to Fig. 4.4.33, the numbers of collided cases with PBS+EBS were lower than the ones with EBS in every intersection shape. The most collided cases were biased to the left side in the figures, namely, more collisions had occurred when the offset position of the darting-out object was negative. Because when the offset position of the darting-out object is positive, the darting-out object already passed the conflict point while the vehicle reaches the conflict point therefore the collision does not occur. When X_{obj_occ} = -10 [m], there was no collision at the cases with EBS, but most cases at the case with PBS+EBS had a collision. The reason for this difference is because of the driving speed around the c,p. In the cases with EBS, the system did not decelerate the vehicle therefore the vehicle passed across the c.p. before the darting-out object reached the vehicle. On the other hand, the vehicle with PBS+EBS passes through the c.p. slower therefore, the darting-out object reached the vehicle and collided with the left-side wall of the vehicle. In the cases with EBS, when the X_{occ_offset} became shorter, more collisions had occurred. This was because as the occluding vehicle was closer, the blind spot became larger, and the safe speed became lower. Yet, the cases with PBS+EBS did not have this tendency. The PBS could decelerate the vehicle by considering the position of the surrounding object. Hence, the PBS+EBS could make the collision risk even regarding the occluding vehicle positions.

The figures from Fig. 4.4.34 to Fig. 4.4.36 show the collision velocity of the ego vehicle.

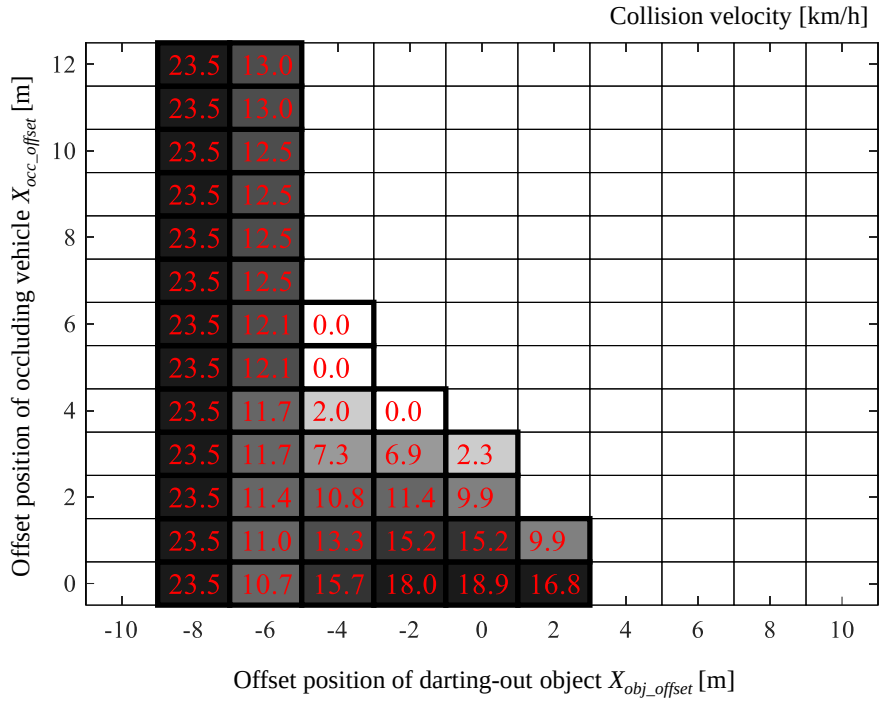

(a) EBS at intersection θ_{cross} = −60 [deg].

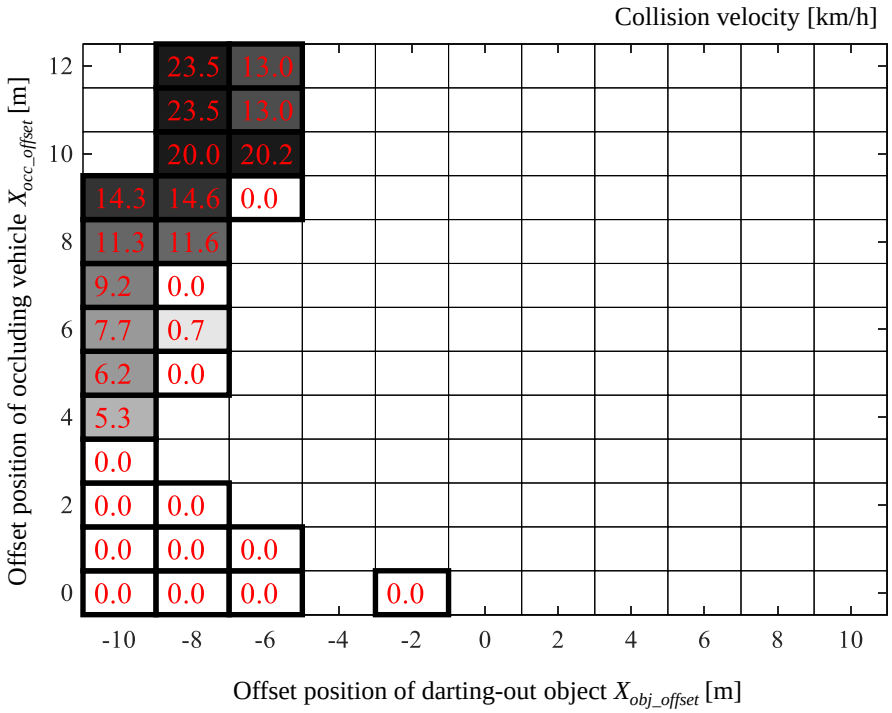

(b) PBS+EBS at intersection θ_{cross} = −60 [deg].

Fig. 4.4.34 The collision velocities under various conditions (θ_{cross} = −60 [deg], v_{obj} = 30 [km/h]).

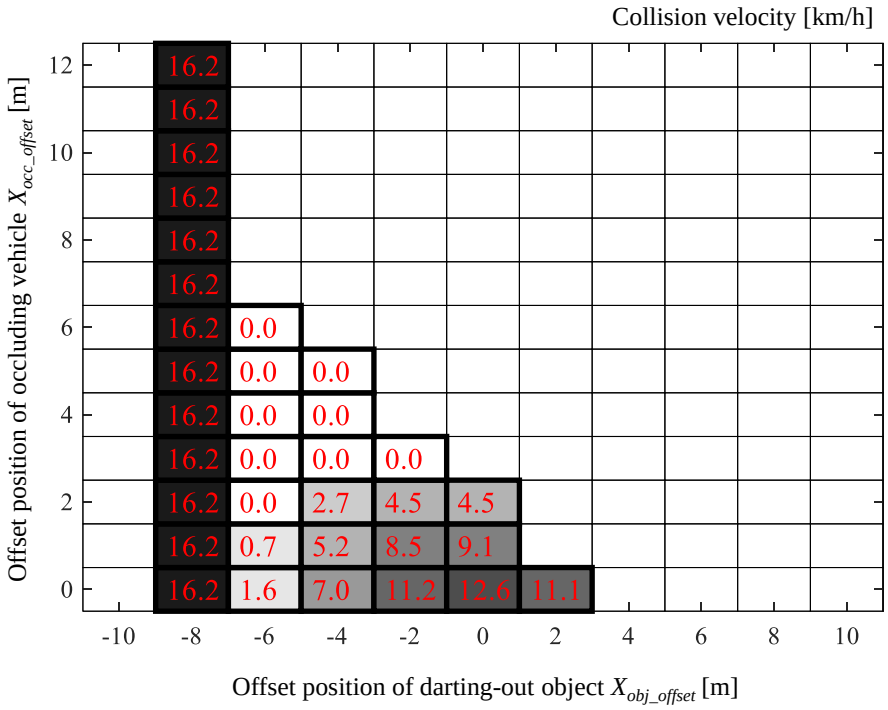

(a) EBS at intersection θ_{cross} = −90 [deg].

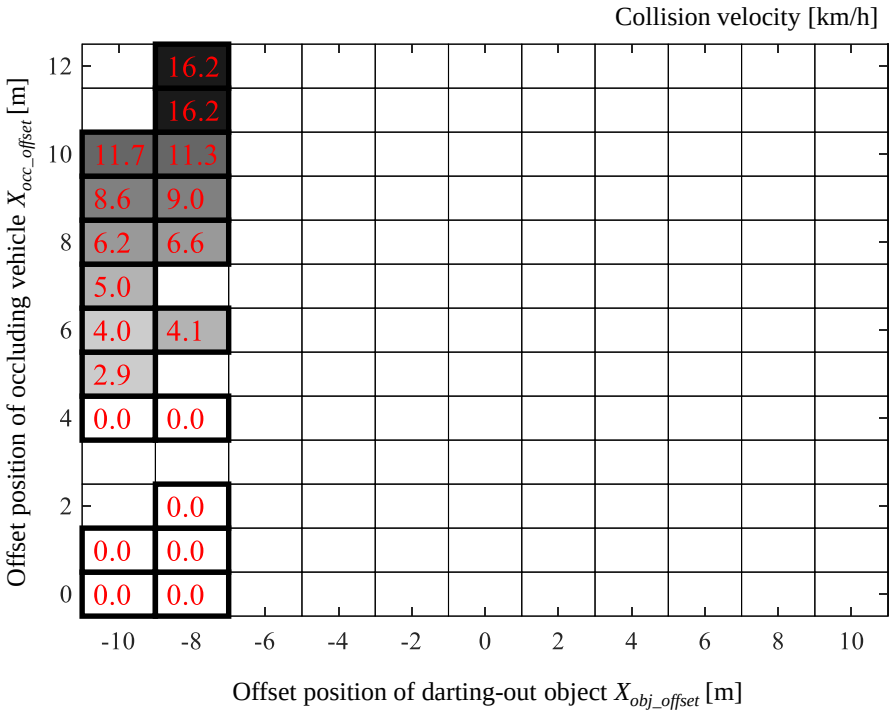

(b) PBS+EBS at intersection θ_{cross} = −90 [deg].

Fig. 4.4.35 The collision velocities under various conditions (θ_{cross} = −90 [deg], v_{obj} = 30 [km/h]).

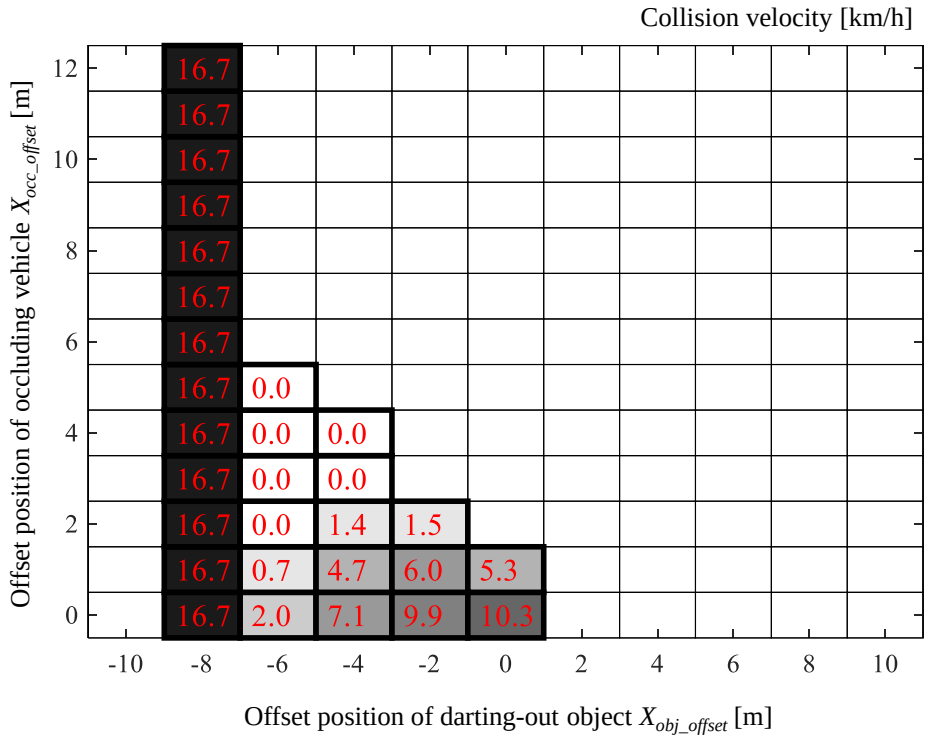

(a) EBS at intersection θ_{cross} = −120 [deg].

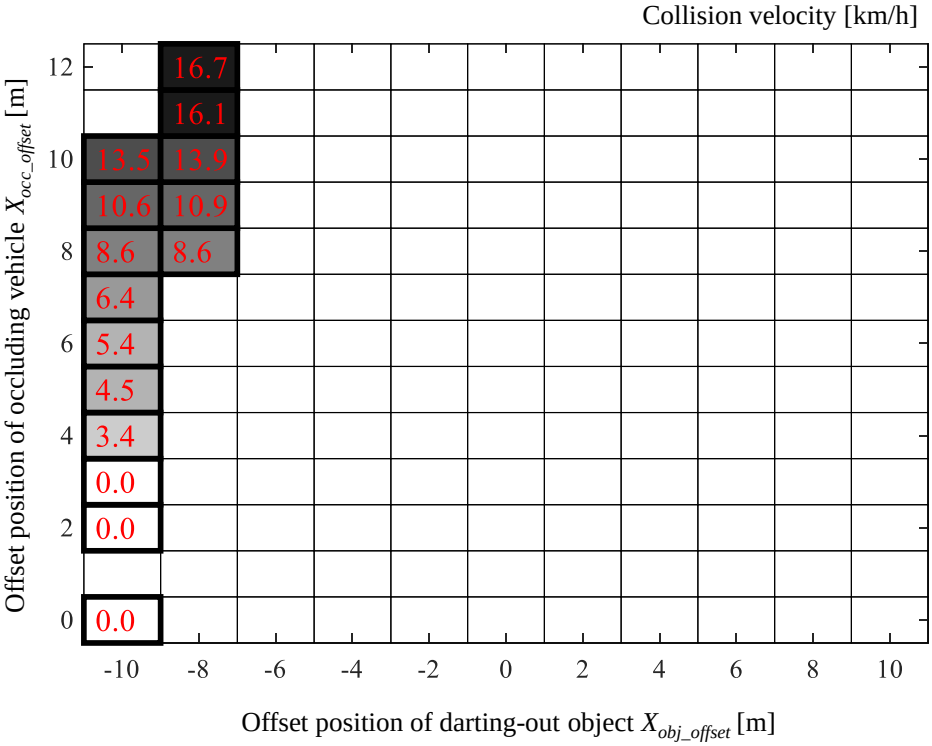

(b) PBS+EBS at intersection θ_{cross} = −120 [deg].

Fig. 4.4.36 The collision velocities under various conditions (θ_{cross} = −120 [deg], v_{obj} = 30 [km/h]).

When the TTC of the darting-out object of the collided data was larger than 2 seconds, we considered that the collision could be avoided by the darting-out object's collision avoidance maneuver. The figures from Fig. 4.4.37 to Fig. 4.4.39 show the simulation results of the collision velocity of the ego vehicle when the cases that have more than 2 seconds of TTC of the target object were eliminated. The simulations on the collision avoidance performances in the various conditions when the darting-out speed v_{obj} changed to 20km/h and 40km/h were also simulated. The results of the collision avoidance and collision velocity were appended to Appendices on this paper (Appendices 4-1, 4-2).

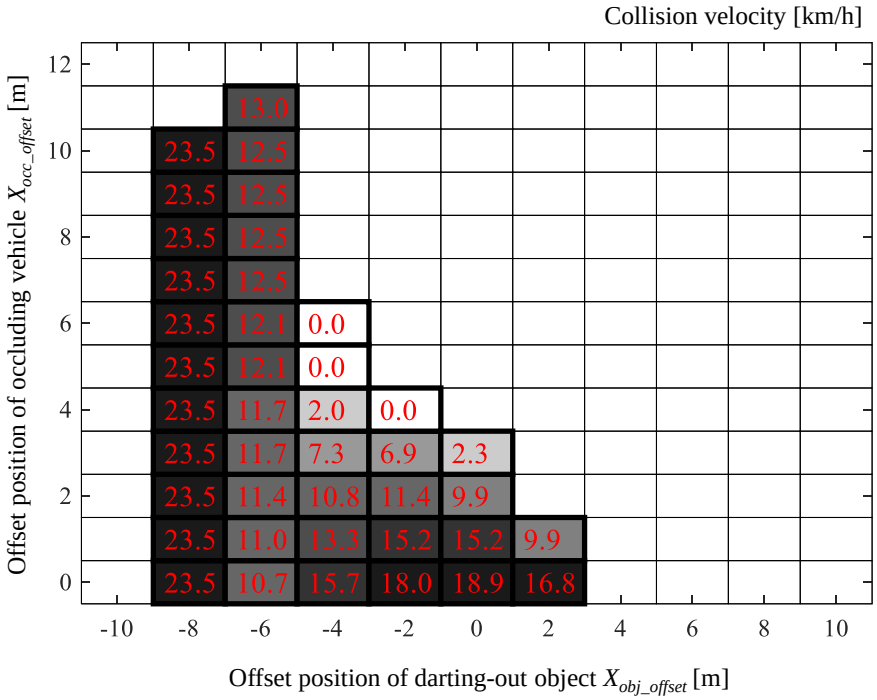

(a) EBS at intersection θ_{cross} = −60 [deg].

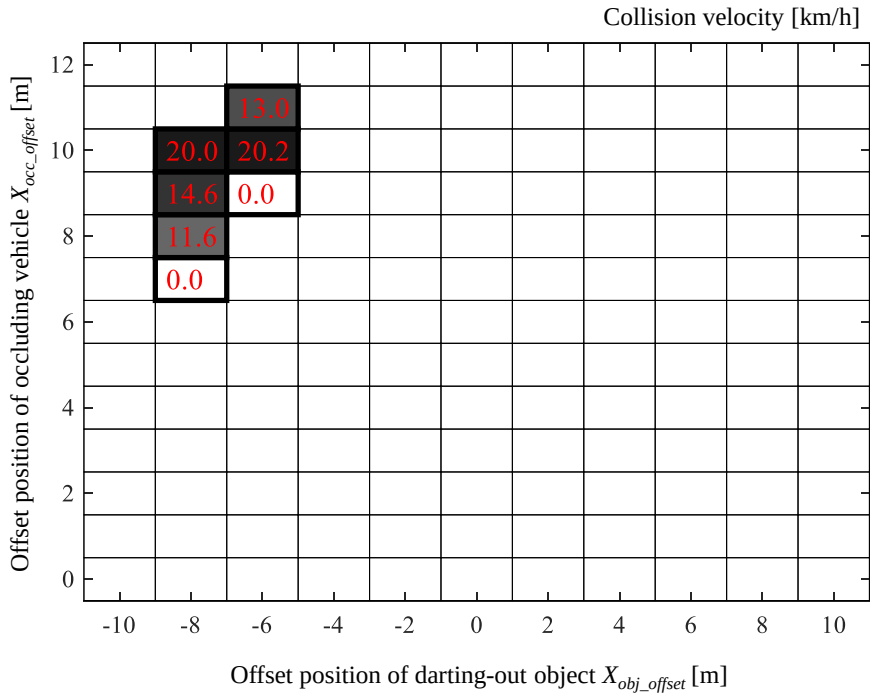

(b) PBS+EBS at intersection θ_{cross} = −60 [deg].

Fig. 4.4.37 The collision velocities when ttc > 2 [s] were eliminated under various conditions (θ_{cross} = −60 [deg], v_{obj} = 30 [km/h]).

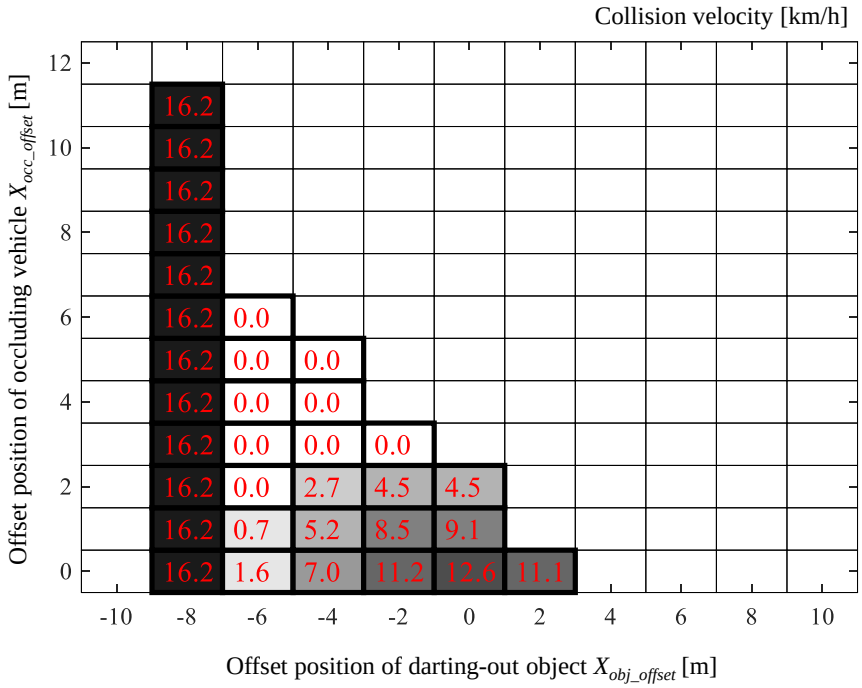

(a) EBS at intersection θ_{cross} = −90 [deg].

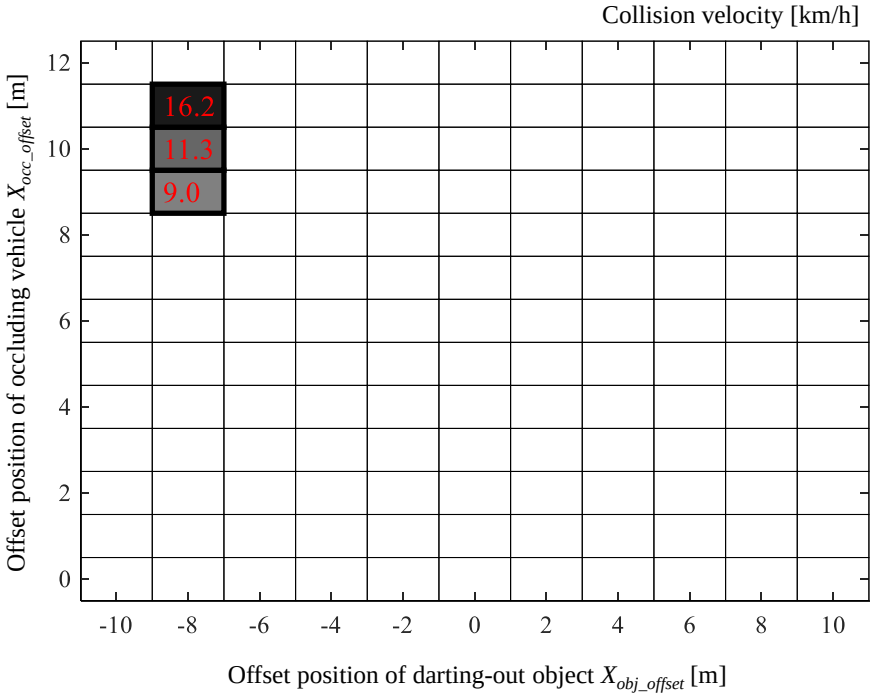

(b) PBS+EBS at intersection θ_{cross} = −90 [deg].

Fig. 4.4.39 The collision velocities when ttc > 2 [s] were eliminated under various conditions (θ_{cross} = −90 [deg], v_{obj} = 30 [km/h]).

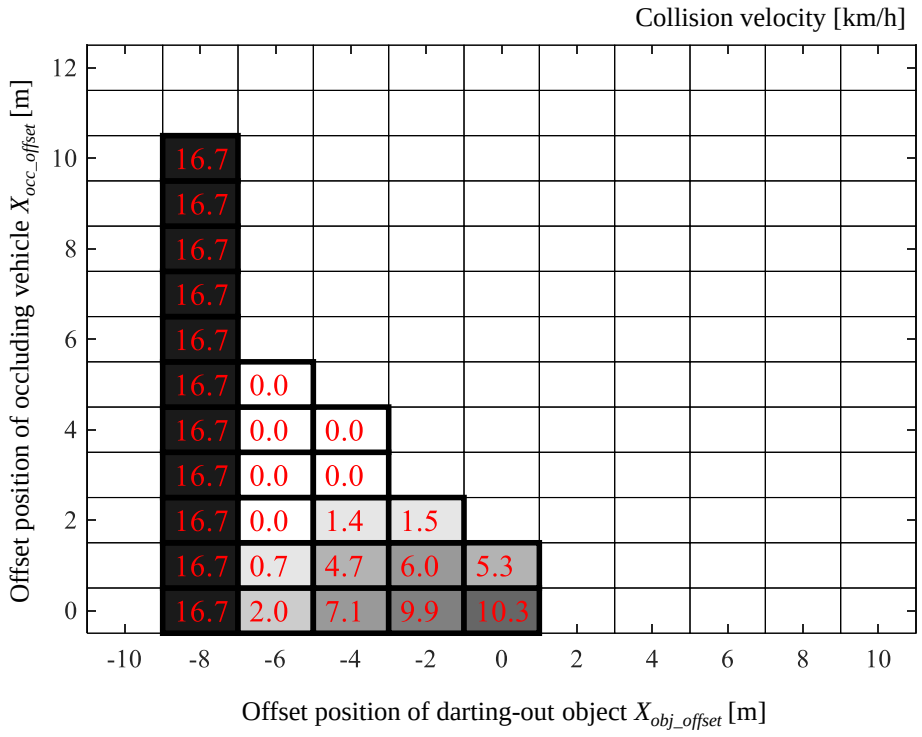

(a) EBS at intersection θ_{cross} = −120 [deg].

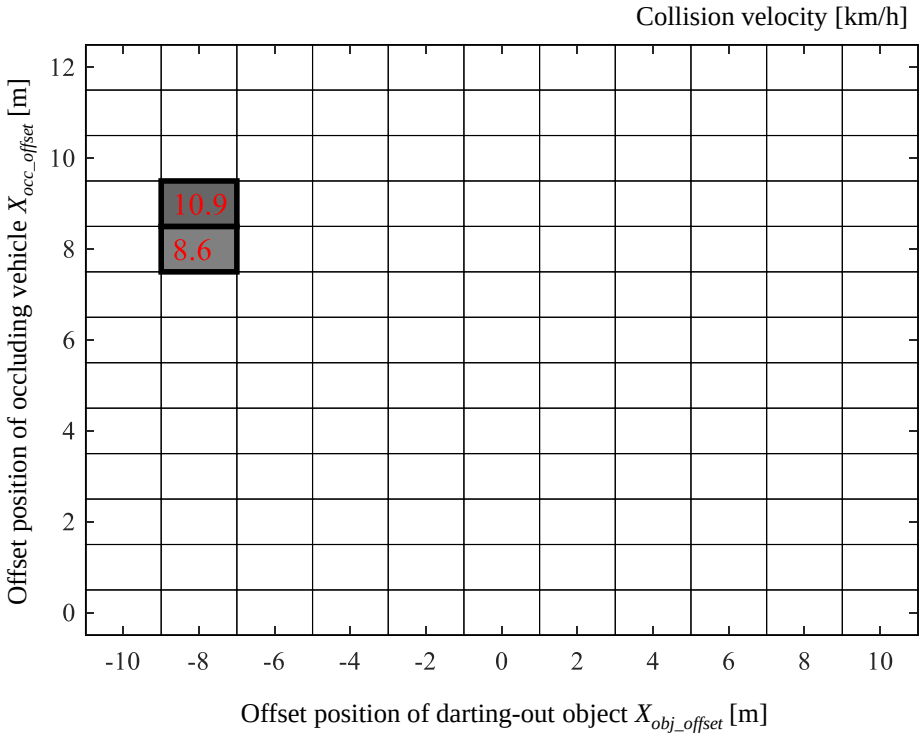

(b) PBS+EBS at intersection θ_{cross} = −120 [deg].

Fig. 4.4.39 The collision velocities when ttc > 2 [s] were eliminated under various conditions (θ_{cross} = −120 [deg], v_{obj} = 30 [km/h]).

From the figures above, PBS obviously enhanced the collision avoidance performance of the EBS. Especially the PBS affects the result largely when the offset position of the occluding vehicle is lower. And most of the collided cases with PBS+EBS decreased the collision velocity comparing to the collision velocity at only EBS. In addition, PBS+EBS could avoid the accident in most cases, therefore, the simulations confirmed the effectiveness of the safe speed calculation theory and appropriateness of the parameter settings for the target intersection scenario with the blind spot and darting-out.

4.5 Conclusion

To evaluate the “safety” performance of the proposed Proactive Braking System (PBS), this chapter presents the iterative full-vehicle simulations. Combining the PBS with an emergency braking function, the full-vehicle simulations proved the proposed method could moderately decelerate the vehicle to the safe speed and minimized the potential risk. In addition, the iterative full-vehicle simulations revealed that the proposed PBS definitely enhanced the collision avoidance performance and collision velocity in all of the conditions we prepared. Hence the proposed method was effective in terms of “safety”. The effectiveness evaluation on the “driver acceptance” of the proposed driver assistance system is presented in the next chapter.

This page is intentionally left blank.

5. Driver Acceptance Evaluation of Advanced Driver Assistance System

This chapter presents the evaluation of "driver acceptance" of the proposed Advanced Driver Assistance System (ADAS), Proactive Braking System (PBS). Section 5.1 explains the introduction of the driver acceptance evaluation. In Section 5.2, we present the acceptance evaluations by experimenting with a real test vehicle. Section 5.3 describes the problem revealed from the experiment in Section 5.2. Section 5.4 presents the acceptance evaluation by conducting the driving experiment with a driver-in-the-loop simulation using a driving simulator. Finally, Section 5.5 concludes this chapter.

5.1 Driver Acceptance Evaluation

Driver acceptance, which is an essential factor in designing the ADAS. Because in ADAS, the system requires monitoring by the driver, and most systems require some kind of control from the driver during the assistance. Thus, ADAS are required to cooperate with the driver. In order to avoid the conflict of the driver assistance system, the systems are recommended to not be too conservative or disturbing. Especially, our focusing scenario, the risk predictive driving requires high acceptability to the system because the system intervenes to minimize the potential risks therefore the system sometimes applies assistances that are unintended for the driver. In those scenarios, once the system becomes too conservative for safety, the driver may not accept the driver assistance system and may turn off the switch. This is a critical problem for the driver assistance system, because the system cannot accomplish "safety" any longer. Usually, the "safety" and the "driver acceptance" are in the trade-off relationships.

While the safety of the ADAS could be evaluated by the iterative full-vehicle simulations, the driver acceptance requires evaluations from human drivers. The evaluations of the driver acceptance of the ADAS have been conducted in a lot of research [85][97][111]-[113]. And an evaluation scale of the driver acceptance was invented by Van der Laan et.al. [114].

This research project also evaluates the driver acceptance of the proposed PBS. We conducted two individual subject driver experiments. The first experiment was the driving experiment with a real test vehicle. The second experiment was the driving experiment with a driver-in-the-loop simulation using a driving simulator. The former experiment can reconstruct the realistic scenario with the real vehicle. This method enables to obtain real driving data and also the subject driver can experience real driving feeling, acceleration, and intervention of the ADAS. The disadvantages of the method are the preparation time, cost, and difficulties to set the uniform conditions. On the other hand, the latter method with a driving simulator can shortcut the time for system implementation, preparation, and setting the uniform conditions even weather and time. The disadvantage of the latter method is the divergence from reality.

5.2 Conceptional Real Driving Experiment in Closed Test Track

To evaluate the impression to the braking assistance by PBS, we hypothesized that if the driver does not notice the brake assistance, the driver acceptance of the system will be higher, the subject participated in conceptional experiments with real experiment vehicle were in Germany. We implemented the PBS concept into an experiment vehicle. The concept was evaluated from the recorded driving data and questionnaire about the impression to the PBS. Notice that because the test location was in Germany, in

this section, the test was conducted in the intersection left-turn scenario for right-hand traffic. This section describes the conceptional experiment and brief results of the acceptance evaluation the full results of the experiment are described in [115].

5.2.1 Experiment Vehicle

The experiment vehicle TIAMO (Test Vehicle for Integrated Automation and Monitoring System) was used for the driving experiment [116]. As shown in Fig. 5.2.1, TIAMO equips enough equipment for the proposed driver assistance system such as a high precision ego localization system, environment perception sensors, and brake actuators. The test vehicle equipped only a Proactive Braking System (PBS) and no emergency braking functions. Therefore, only braking assistance by PBS was engaged before the darting-out object detection, and when the drivers recognized the darting-out, the drivers must avoid the collision by themselves.

Fig. 5.2.1 Experiment vehicle TIAMO [116].

5.2.2 Test Scenario

The experiments were conducted in a small city intersection with left-turn lanes in a test course in Braunschweig, Germany. The constructed scenario for the experiments is explained below. As shown in Fig. 5.2.2 and Fig. 5.2.3, the subject drivers drove the experiment vehicle (blue car in Fig. 5.2.2) and drove into the intersection for the left-turn, oncoming vehicles also came into the intersection and simulated a traffic jam as the leading oncoming vehicle had to stop behind the parking trailer. Here, the second vehicle (white van) yields a way to the subject driving vehicle to make a left turn. When the subject vehicle made the left-turn in the intersection, a bicycle darted out from the blind area of the occluding white van. In the experiment, a stuntman drove the bicycle and stopped before blocking the way of the test vehicle. Therefore, the darting-out was safely conducted.

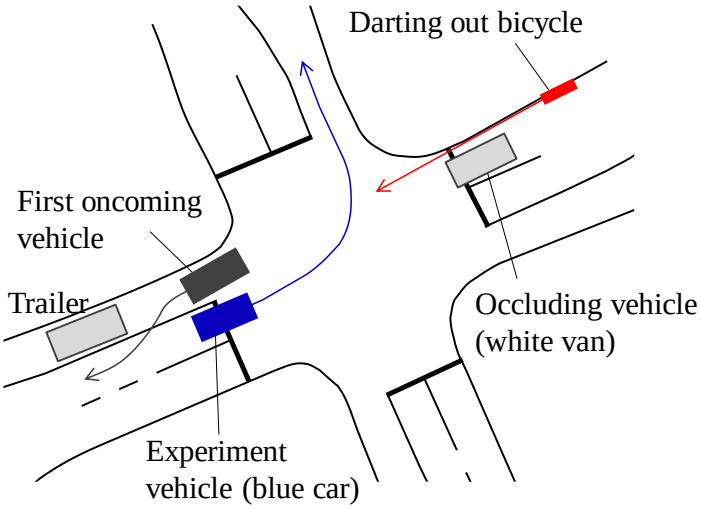

Fig. 5.2.2 The test intersection and surrounding objects.

Fig. 5.2.3 The test intersection in the real driving subject experiment.

5.2.3 Test Condition

In the experiment, to focus on the impression of the subject drivers to the system, the safe speed was set to the constant value, and the system applied the brake assistance to decelerate to the constant speed. The braking assistance was triggered when the ego vehicle entered the intersection.

18 subject drivers, who often drive a car in Germany, volunteered to participate in the experiments and drove the test vehicle in the test course. Subjects were divided into three condition groups. The groups allocated to three conditions as shown in Table 5.2.1 to evaluate the effectiveness and acceptance. All participants driving data of the intersection left-turn without bicycle darting out nor PBS assistance were also recorded before experiencing the darting-out cyclist and PBS assistance.

After the first lap of the experimental driving, we asked some questions about the risk predictive situation brake assistance system. The followings list the representative questions in the questionnaire:

(a) Do you think the intersection was dangerous?

(b) Did you notice the brake reaction of the vehicle?

(c) Do you think that the braking made the turning safer?

(d) Do you think braking in emergency situations would be effective?

(e) Would you like to have such a feature in your car?

In questions (a), (c), (d), and (e), the subjects answer the question from 7 grades “Yes, very”, “Yes”, “Slightly yes”, “Intermediate”, “Slightly no”, “No”, and “Not at all”. About question (b), the subjects answer the question from “Yes” or “No”, and if yes. Question (c) was asked only when the subjects

answered “Yes” in question (b).

Table 5.2.1 The experiment conditions.

Test lap	Group A 6 subjects		Group B 6 subjects		Group C 6 subjects	
	Darting-out bicycle	PBS engagement	Darting-out bicycle	PBS engagement	Darting-out bicycle	PBS engagement
1	Condition 1		Condition 2-2		Condition 3	
	✓	–	✓	✓ v_{safe} = 5 km/h	–	✓ v_{safe} = 5 km/h
2	Condition 2-1		Condition 1		–	
	✓	✓ v_{safe} = 10 km/h	✓	–		

5.2.4 Experiment Result and Evaluation

Fig. 5.2.4 shows the representative results at the first lap of the Group A. These results were under the conditions with darting-out bicycle and without PBS assistance (Condition 1). From the graphs in the figure, the driver drove into the intersection around 20km/h, and the driver used braking to stop the vehicle when detected the darting-out.

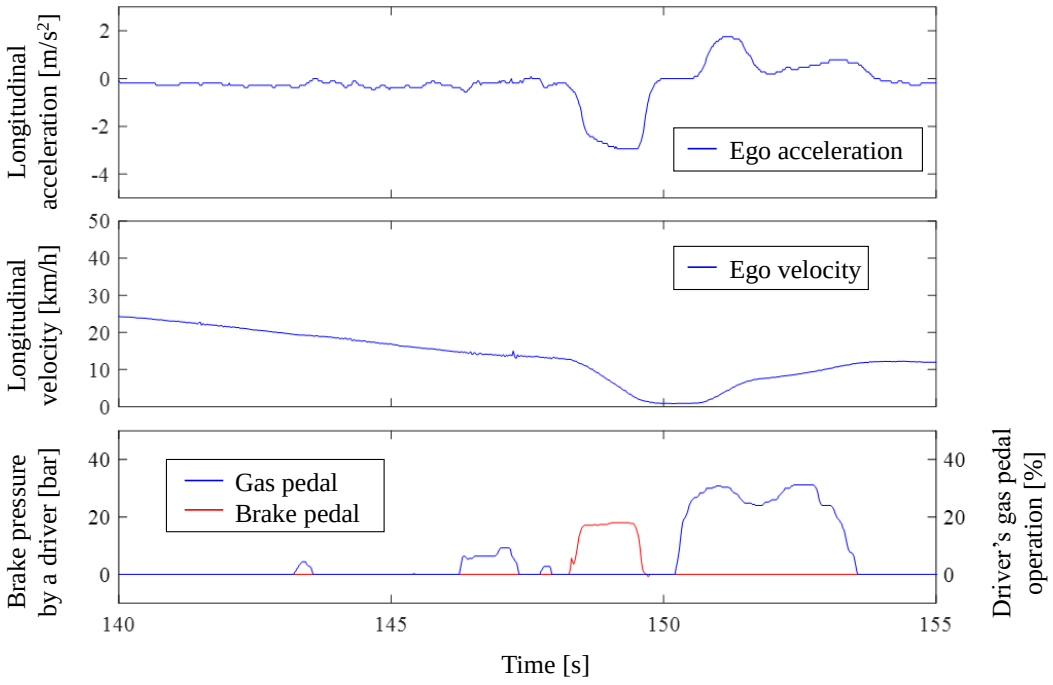

Fig. 5.2.4 Experiment results of the first lap of the subject from group A (condition 1).

Fig. 5.2.5 shows the representative results at the first lap of Group B. These results were under the conditions with darting-out bicycle and with PBS assistance (Condition 2-2). From the graphs, the driver decelerated the vehicle before driving into the intersection, and during the turn, the PBS engaged the brake

assistance. Later, the driver stopped the vehicle to avoid a collision. In this case, the PBS could not decelerate to the safe speed because the driver engaged the avoidance braking before the system decelerated to the safe speed.

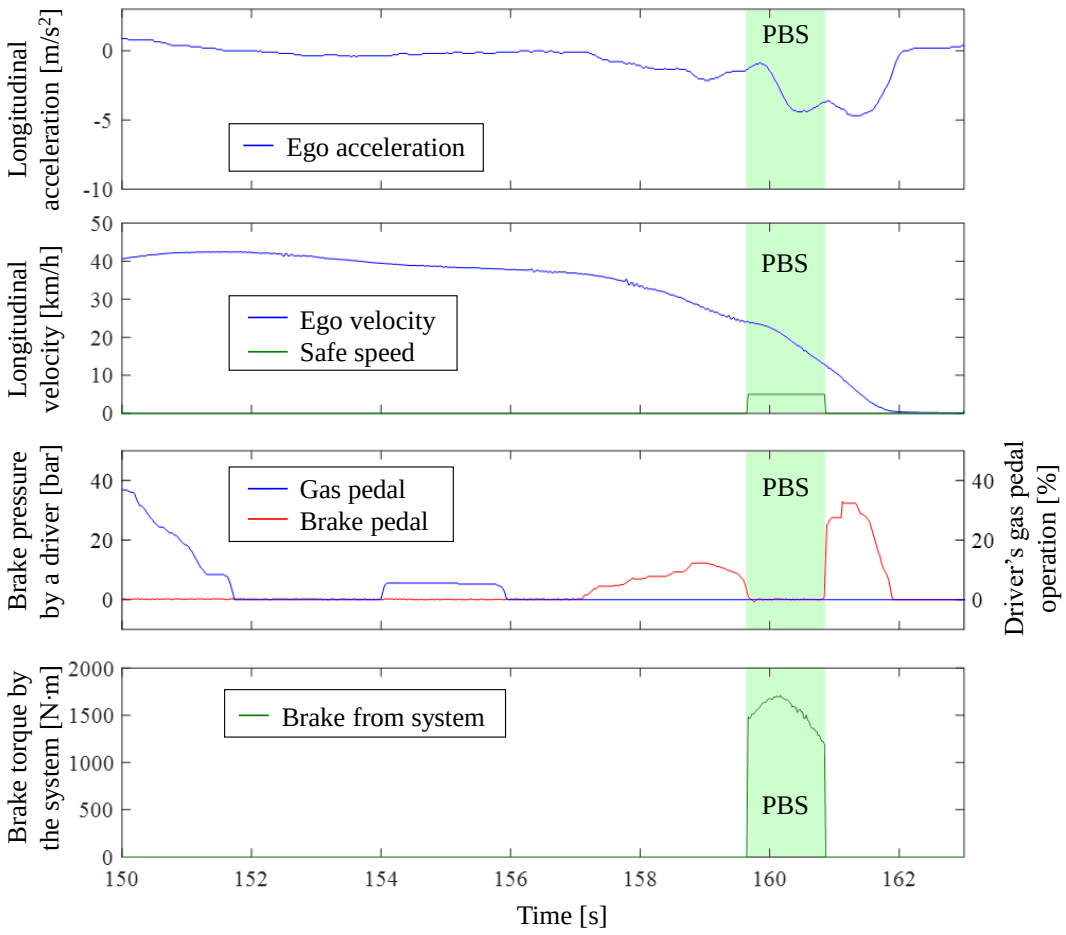

Fig. 5.2.5 Experiment results of the first lap of the subject from group B (condition 2-2).

Fig. 5.2.6 shows the representative results at the first lap of the Group C. These results were under the conditions without darting-out bicycle and with PBS assistance (Condition 3). From the graphs, the driver used a weak brake manually before turning. When the test vehicle drove into the intersection, the PBS applied the brake assistance to decelerate the vehicle, but while the brake assistance, the driver tried to reaccelerate the vehicle by using the gas pedal. Therefore, the system conflicted with the driver, and the brake assistance was canceled by the drive torque and could not decelerate to the safe speed.

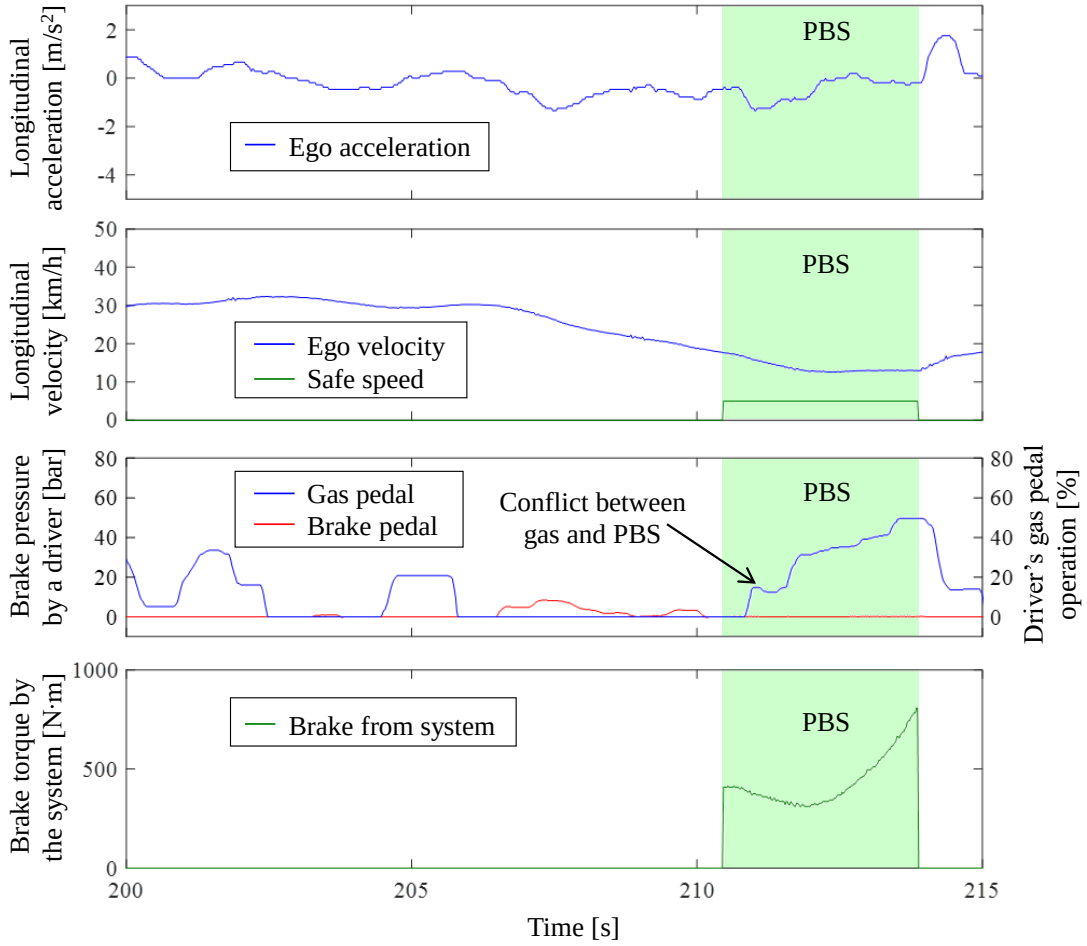

Fig. 5.2.6 Experiment results of the first lap of the subject from group C (condition 3).

From the results of the subject driver questionnaire about "Did you notice the brake reaction of the vehicle?", 6 subjects out of 6 from Group A and 5 subjects out of 6 from Group B did not notice the brake intervention from the PBS, on the other hand, 5 subjects out of 6 from Group C noticed the brake intervention. From those facts, it was estimated that the activation and beginning of brake assistance were unnoticeable interventions, but most subjects noticed the brake intervention in the latter part of the intervention.

To the subjects who noticed the brake assistance, we asked another question, "Do you think that the braking made the turning safer?". From the answers to the question, while a subject (out of one subject) from Group B answered, "Yes, very", 4 subjects out of 5 from Group C answered "No" and the rest of the subjects answered, "Slightly no". From these results, without the darting-out drivers may not be able to understand the meaning of the brake assistance.

In addition, 4 subjects out of 6 who noticed the driver assistance commented that they didn't notice the brake assistance at first but because the gas pedal was not working, they found there was the braking intervention.

5.3 Problem Statement of Proposed Method

The results of the conceptual experiment with the real test vehicle revealed that the brake intervention

itself was unnoticeable assistance, therefore, might not disturbing assistance, however, most subjects did not understand the assistance correctly and conflicted with the driver assistance system. The conflicts interfered with the system to decelerate to the safe speed. The most important knowledge we learned from the experiment was improving the recognition and understanding of the driver assistance system also plays an important role to improve driver acceptance.

5.4 Driver Acceptance Evaluation Experiments with Driver-in-the-Loop Simulation

This section describes the driver acceptance evaluation using the driver-in-the-loop simulation. The first subsection introduces the evaluation goal of the experiment. The second and third subsections explain the test equipment setups and conditions. The fourth subsection explains the experiment sequence and questionnaires. The fifth subsection presents the experiment results of the driver-in-the-loop simulations. And the last subsection evaluates the driver acceptances from the questionnaire results.

5.4.1 Evaluation Goal

The evaluation goal of the driver acceptance evaluation experiments with driver-in-the-loop simulation is simply to evaluate the “driver acceptance” via the subject driver driving experiment. To solve the problems stated in the previous section, we introduced visual information that enhances the understanding of the intention of the driver assistance system.

5.4.2 Test Equipment

As experimental equipment for the driver acceptance evaluation, we prepared a driving simulator with 4-axis motion (T3R Simulator). Fig. 5.4.1 shows the overview of the equipment. The driving simulator has a reclining driver seat, three pedals (gas, brake, clutch), a shifting lever, a steering wheel with a servo, a large wide display, a sound system, a computer for the dynamics calculation, and four motion actuators. The four motion actuators enable us to realize the lateral and longitudinal acceleration, the roll and pitch of the vehicle, and small vibration from the road surface in the simulation. This equipment enables the drivers to feel the realistic acceleration of the vehicle and intervention of the brake assistance from the driver assistance system.

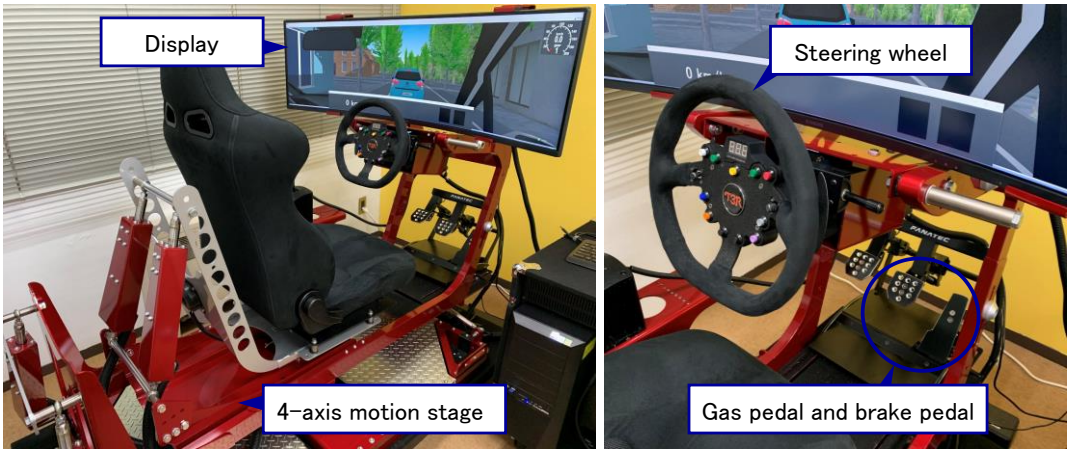

Fig. 5.4.1 Overview of the experimental equipment.

Fig. 5.4.2 shows the diagram of the whole setup of the experiment environment. The simulation scenery is reconstructed in the IPG CarMaker and the scenery is displayed on the display. The subject drivers watch the display and drive the simulator to drive the experimental course. Then the pedal and steering inputs from the driver transfer to the computer. From the transferred inputs, The IPG CarMaker and the MATLAB/Simulink compute the vehicle dynamics regarding the inputs and simulation environment data. When the sensor model detects the objects, the advanced driver assistance system calculated the appropriate command and inputs it to the vehicle model on the Simulink model.

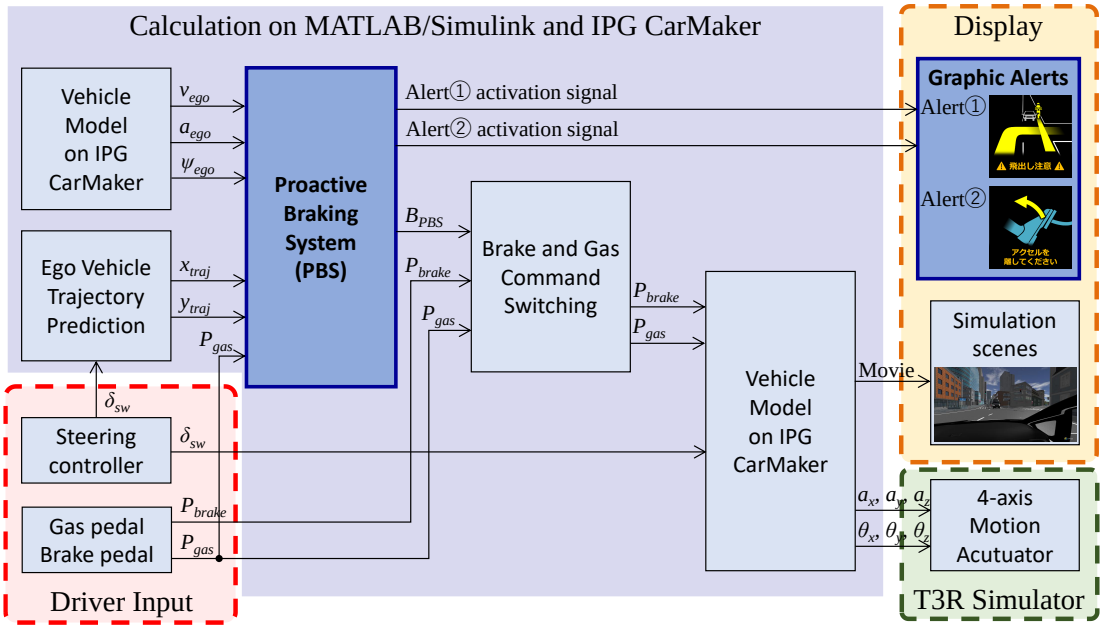

Variables

- Driver
  - P_{gas} Gas pedal input.
  - P_{brake} Brake pedal input.
  - δ_{sw} Steering wheel input.
- Vehicle
  - v_{ego} Ego vehicle longitudinal velocity.
  - a_{ego} Ego vehicle longitudinal acceleration.
  - ψ_{ego} Ego vehicle yaw angle.
  - a_x, a_y, a_z Ego vehicle acceleration (x, y, z-axis).
  - θ_x, θ_y, θ_z Ego vehicle rotation (x, y, z-axis).
- Trajectory prediction.
  - x_{traj} Predicted trajectory.
  - y_{traj} Predicted trajectory.
- Brake command
  - B_{PBS} Brake command from PBS.

Fig. 5.4.2 Diagram of the experiment environment setup.

To evaluate the validity of the driving simulator, we conducted experiments with a real vehicle to compare the characteristics between the real and the simulator. An experiment vehicle was prepared and put an IMU sensor (3DM-GX5-45) on the headrest of the driver's seat. To record the position of the vehicle, a GPS antenna was attached to the roof of the experiment vehicle. The vehicle drove in a test course and recorded the vehicle position, velocity, and accelerations. Fig. 5.4.3 shows the result of the vehicle velocity.

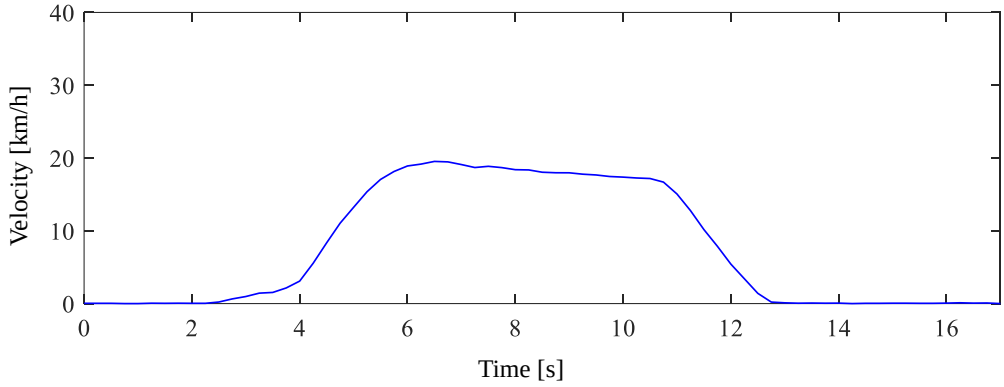

Fig. 5.4.3 Speed profile.

Adopting the vehicle velocity as a reference speed profile, the simulator moves the vehicle with the velocity profile. As same as the experiment vehicle, an IMU sensor (3DM-GX5-45) was mounted on the headrest of the driver's seat of the simulator. With activating the actuators of the simulator, the accelerations of the vehicle were recorded.

Fig. 5.4.4 shows the comparison between the real vehicle and the simulator. The left figure shows the comparison of acceleration and the right shows the comparison of the jerk of the vehicle. Those data were low pass filtered with a 25 Hz cut-off frequency.

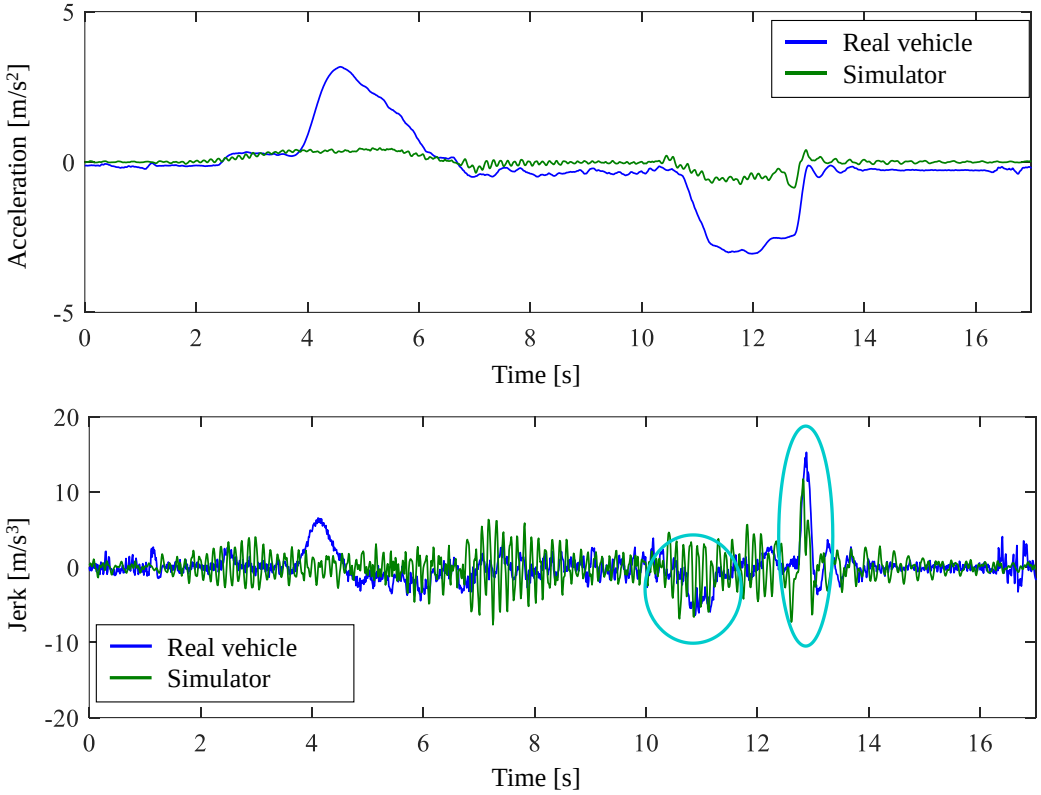

Fig. 5.4.4 Comparison between the real vehicle and simulator.

In the experiment, comparing with the real vehicle the driving simulator could not generate enough acceleration to imitate the motion of the real vehicle. The real vehicle accelerated with 3 m/s^3 decelerated

with -3 m/s^2. On the other hand, the simulator could generate an acceleration around 0.4 m/s^2 and -0.8 m/s^2 while decelerating. This is because to generate the acceleration with the simulator, it needs to rely on gravity, therefore, the actuators incline the seat to generate the acceleration. However, the angle the simulator can incline is structurally limited, thus, the simulator could not generate a large acceleration. Regarding the jerk, the simulator could imitate the motion of the real vehicle especially when decelerating. It is known that the human body is more sensitive to the jerk than acceleration when sensing the change of the motion [143]. Thus, we regarded that the simulator could give the realistic impact of the brake assistance to the subject drivers.

5.4.3 Test Scenario

Fig. 5.4.5 shows the test course of the evaluation experiments. The course contains typical city roads in Japan and combined several risk predictive scenes in the course. To construct the typical city roads, the course is fully controlled by traffic signals and traffic signs. In addition to them, buildings, houses, static cars, and dynamic traffics including pedestrians, cyclists, and cars are added to the course. Those static and dynamic objects make the risk predictive scenes. The followings list the risk predictive scenes in the experiment course:

① The residential area without safety fences.
② A road with two lanes in the same direction as other traffics.
③ A motorcycle weaves through the traffic.
④ A crossing pedestrian at the crosswalk.
⑤ Pedestrians and cyclists on the narrow street without pavements.
⑥ Parked vehicles on the roadside.
⑦ A small intersection with blind spots.
⑧ Intersection right-turn when oncoming traffic is congested.

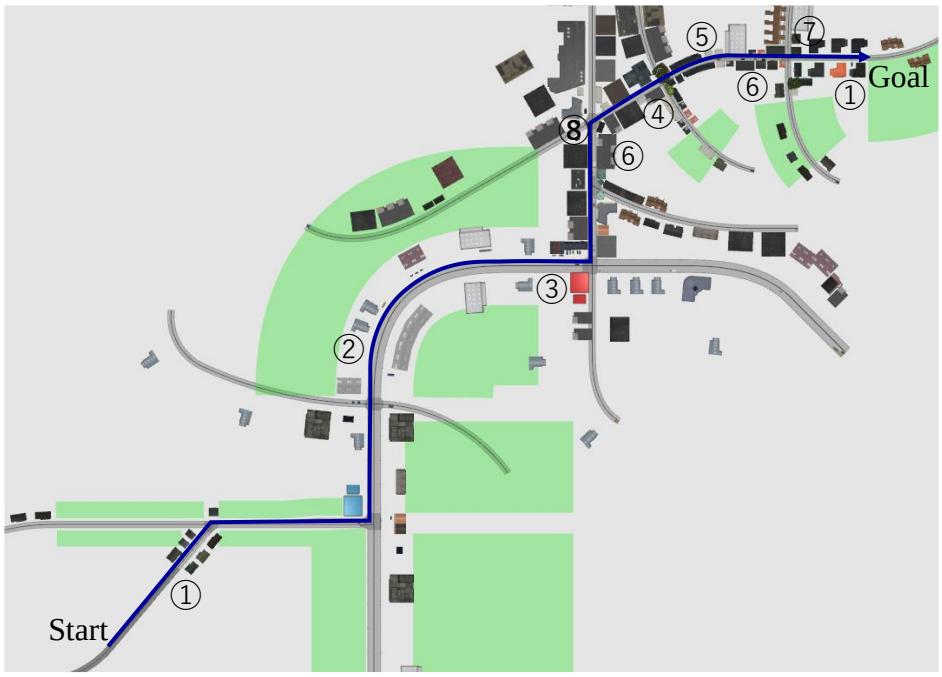

Fig. 5.4.5 The test course. The numbers on the course map are corresponding to the number of the list of risk predictive scenes above.

Fig. 5.4.6 shows the screenshot of the risk predictive scenes used in the experiments. In this study, to evaluate the proposed driver assistance system, the evaluation section was focused on the risk predictive scene "⑧ Intersection right-turn when oncoming traffic is congested".

① The residential area without safety fence.

② A road with two lanes in same direction with other traffics.

③ A motorcycle weaves through the traffic.

④ A crossing pedestrian at the crosswalk.

⑤ Pedestrians and cyclists on the narrow street without pavements.

⑥ Parked vehicles on the roadside.

⑦ A small intersection with blind spots.

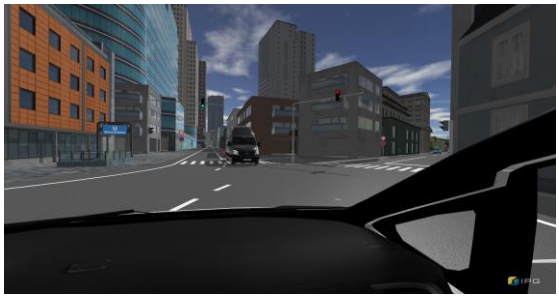

⑧ Intersection right-turn when oncoming traffic is congested.

Fig. 5.4.6 The risk predictive scenes in the experiment course.

Fig. 5.4.7 shows the target intersection. Two two-lane roads are crossing at 60 degrees and the intersection is controlled by the traffic signal. In the target scenario, the oncoming lane is congested with traffic and an oncoming vehicle at the entrance of the intersection is yielding for right-turning vehicles.

The subject follows a preceding vehicle that turns to the right at the intersection with higher speed. In this scenario, to catch up with the preceding vehicle, the subject drivers need to make the right cturn at a higher speed. To sum up, the focus of this scenario is to let the subject drivers intentionally hurry up and turn the intersection higher than the safe speed.

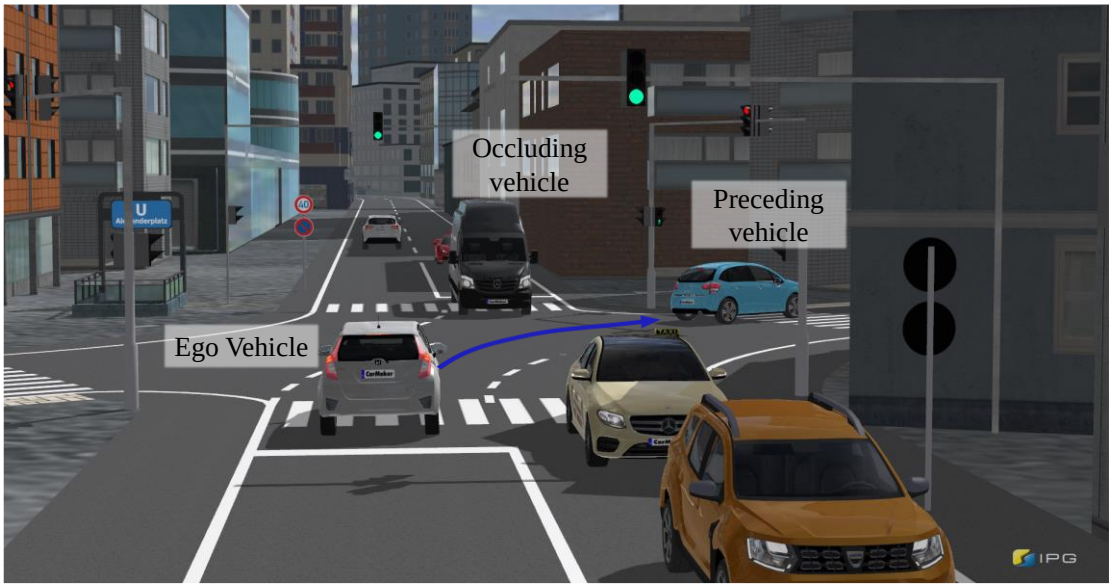

Fig. 5.4.7 The intersection right-turn scene when the oncoming traffic is congested and the oncoming vehicle making the blind spot.

5.4.4 Experiment Sequences and Acceptance Evaluation Questionnaire

A. Experiment Sequences

The subject driver experiments were conducted as the following sequences. The subjects joined the experiment for two days. The second day must be later than one day after the first day to avoid memorizing the driving course of the experiment.

Day 1

① Introduction of the research topic and the experiment equipment.
② Pre-experiment questionnaire.
③ Practice drive.
④ Data acquisition drive (without the driver assistance.)

Day 2

⑤ Practice drive.
⑥ Data acquisition drive (with the driver assistance.)
⑦ Post-experiment questionnaire.
⑧ Explanation of the driver assistance system.
⑨ Data acquisition drive (the equipment of the system was not provided to the subjects.)
⑩ Data acquisition drive (the equipment of the system was not provided to the subjects.)

The conditions of the data acquisition drives are shown in Table 5.4.1.

Table 5.4.1 Conditions of the data acquisition drives.

Index	Description	Equipment of driver assistance system	Provided information to subjects	Darting-out object
D-1	④ Data acquisition drive	None	Without assistance	-
D-2	⑥ Data acquisition drive	PBS Graphic warning	With assistance	-
D-3	⑨ Data acquisition drive	PBS Graphic warning	Nothing provided	-
D-4	⑩ Data acquisition drive	PBS Graphic warning	Nothing provided	✓
		None		

To acquire the acceptance of the drivers when they were ignorant about the driver assistance system, none of the information such as the focusing scenario, the experiment course, the functions of the driver assistance system, and the purpose of the experiment was provided before the data acquisition drive D-2. Only provided information about the research was "we are researching about the driver assistance system in the risk predictive scenario while driving automobiles." In the data acquisition drive D-4, a motorcycle darts out from the blind spot behind the occluding vehicle with a constant velocity. The existence of the darting-out object was not also provided to the subjects. In drive D-4, half of the subjects drive the vehicle equips the driver assistance system, and the rest of the subjects drive the vehicle without the driver assistance system.

B. Acceptance Evaluation Questionnaire

The acceptance was evaluated from the acquired driving data from the data acquisition drives and questionnaires. The subject drivers answered two questionnaires: pre-experiment questionnaire and post-experiment questionnaire. All questions from the questionnaires are appended to the appendices (in Appendices 5-1, 5-2. Only in Japanese). The pre-experiment questionnaire asks the subject about the driving experience, the experiences of driver assistance systems, and the basic postures to the driver assistance systems. The post-experiment questionnaire asks about the experience of the driver assistance system just after driving the data acquisition drive D-2.

5.4.5 Experiment Condition

A. Way to Drive Experiment Vehicle

The subject drivers operate the driving simulator. The subject drivers use only the gas pedal, brake pedal, and steering wheel to drive the vehicle. In the experiment, the drivers are asked to follow the preceding vehicle shown in Fig. 5.4.8. The driving course is not provided to the subjects in advance; therefore, the subjects are required to drive the car without losing the preceding vehicle.

Fig. 5.4.8 The preceding vehicle

To acquire the pure driving data, we asked the drivers to drive the vehicle as usual, and we asked the drivers that they do not need to follow strictly the traffic rules such as traffic signals or road signs in the experiment as if they drive as usual.

B. Driver Assistance System

In the acceptance evaluation experiments, the test vehicle equipped the driver assistance systems equips two functions that support safe driving in the risk predictive scenario: graphic warnings and brake assistance by PBS.

The first function, the graphic warnings, display when the vehicle drove into the risk predictive scenario. The system shows two images respectively on the information window. The information window in the experiment is shown in Fig. 5.4.9. And Fig. 5.4.10 shows the images of the graphic warnings. The first image in Fig. 5.4.10 (a) indicates the existence of the potential risk behind the occluding vehicle with the letter “飛出し注意 (be careful to the darting-out).” The image shows up when the PBS engages the brake assistance. When the graphic shows up, the system beeps a sound at the same time. This makes the driver easier recognize the risk predictive scenario. The second warning contains two images as in Fig. 5.4.10 (b). These images indicate the command to release the gas pedal with the letter “アクセルを離してください (please release gas pedal).” These images switch one another in one second period. This warning shows up when the driver operates the gas pedal during the brake assistance by the PBS.

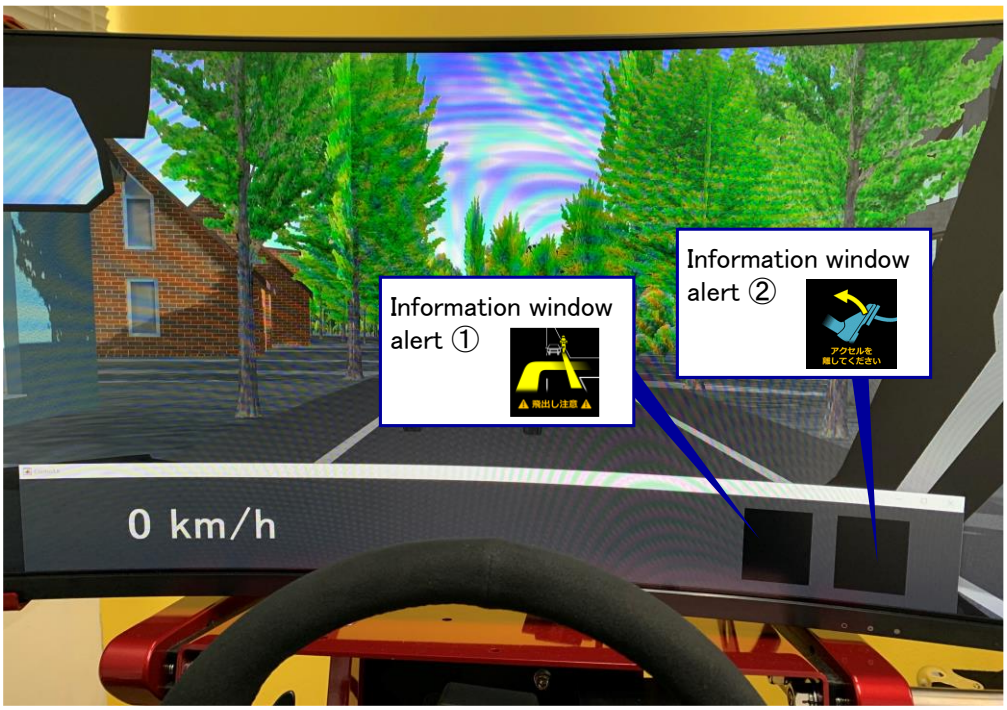

Fig. 5.4.9 The information window of the experiment vehicle.

(a) Warning① for the darting-out risk. (b) Warning② to release the gas pedal.

Fig. 5.4.10 The graphical warnings of the driver assistance system.

The second driver assistance system is the Proactive Braking System (PBS). The algorithm of the system is described in Chapters 2, 3, and 4. The Triclothoidal curve generation method was used to predict the right-turn trajectory. EBS was not equipped in all the data acquisition drives.

To avoid the gas pedal operation by the driver during the brake assistance, the PBS cut off the gas pedal input during the brake assistance. However, when the driver steps the gas pedal during the driver assistance, the vehicle tends to be vibrative because the system enables the gas pedal input when the vehicle velocity goes below the safe speed. To avoid this vibration, in addition to the graphical warning, the speed profile to define the target velocity is modified when operated the gas pedal during the brake assistance. When the gas pedal is operated, the equation (2.3.5) is modified to

$$\begin{cases} x(t) = v_0 t + \frac{1}{2} a_0' t^2 + \frac{1}{6} J_1 t^3 & (0 \le t \le t_1) \\ x(t) = x_1 + v_1 (t - t_1) + \frac{1}{2} a_1 (t - t_1)^2 + \frac{1}{6} J_2 (t - t_1)^3 & (t_1 < t \le t_2), \end{cases} \tag{5.4.1}$$

where

$$\begin{cases} a_0' = K_{gas} p_{gas} & \left(0 < p_{gas} \le 1\right) \\ a_0' = a_0 & \left(p_{gas} = 0\right), \end{cases} \tag{5.4.2}$$

provided that a_0' is the acceleration input to calculate the speed profile, K_{gas} is gain to define the acceleration, p_{gas} is the normalized gas pedal operation.

Introducing the equations (5.4.1) and (5.4.2), the system enables to increase the target speed without changing the safe speed. To do so, the system can delay the gas pedal cut-off hence the vibration can be suppressed.

To sum up, the driver assistance system that contains 2 functions: graphic warnings and PBS. The activation sequences and triggers to activate each function are explained in the flowchart in Fig. 5.4.11.

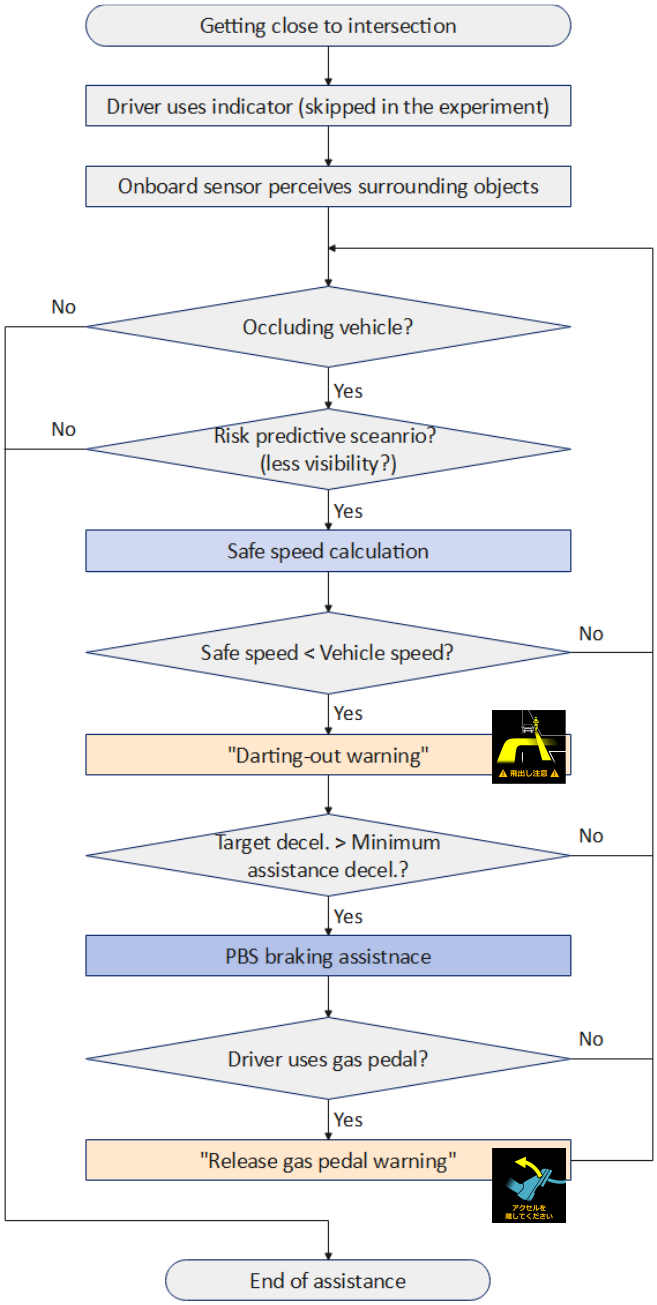

Fig. 5.4.11 Flowchart of the intervention of the driver assitance system in the experiment.

C. *Subject Drivers*

The subject drivers must fulfill the following conditions:

- Ignorant of the contents of the research.
- 20-year-old or more.
- Possession of a Japanese driver's license.
- More than 1 year passed after acquired the license.
- Driving experience on Japanese roads at least 1 time.
- Not be drunk or other states which are prohibited to drive by Japanese laws.

34 students and staff who were belonging to Tokyo University of Agriculture and Technology participated in the experiment. The gender, ages, and years after acquired the driver's license of the participated subjects are listed in Table 5.4.2. And the distribution of the yearly driving distance is shown in Fig. 5.4.12.

Table 5.4.2 Statistical features of the subject drivers.

Description	Male	Female	Age [years]	year after acquired driver's license [years]
Number of subjects	25	9	34	34
Minimum	-	-	21	1
Maximum	-	-	74	52
Median	-	-	25	4
Average	-	-	31.9	11.6
Standard division	-	-	13.9	14.2

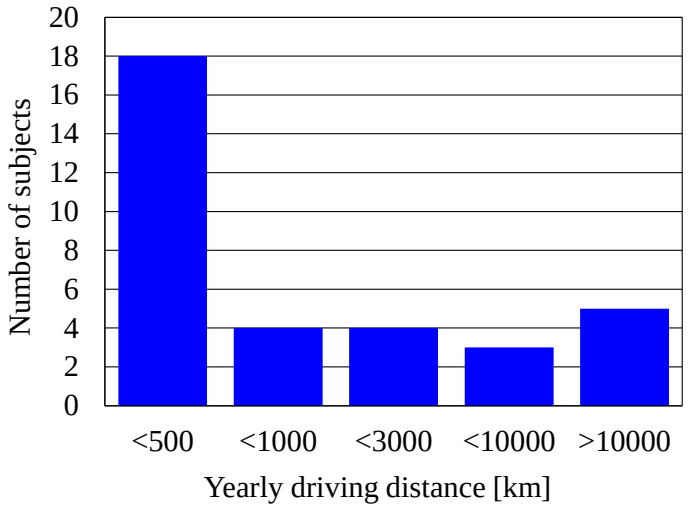

Fig. 5.4.12 Distribution of the subjects' yearly driving distance.

As the table and the figure, more than half of the subject drivers' driving experiences were less than 5 years and yearly driving distances were shorter than 500 km.

In the questions from the pre-experiment questionnaire "4. あなたが普段運転する道路はどのような道路ですか? (複数回答可) – Which types of the road do you drive frequently? (choose many if needed)", 21 out of 34 subjects answered "交通量が多い市街地道路(狭い道路) – City roads (narrow roads) with many traffics.", and 19 out of 34 subjects answered "交通量が少ない市街地道路(狭い道路) – City roads (narrow roads) with less traffics." Hence, more than half of the subjects frequently drove in the city while they drove a car.

D. Parameters

Tables from Table 5.4.3 to Table 5.4.5 respectively define the parameters of ego vehicle, simulation environments, and PBS. The same parameters in these tables are used in the experiments for all subjects.

Table 5.4.3 The parameters of ego vehicle and onboard sensor.

Description		Variable	Value	Unit
Ego vehicle	Length	L_{ego}	3.995	m
	Width	W_{ego}	1.695	m
	Height	H_{ego}	1.290	m
	Wheelbase	L_{wb}	2.530	m
	Distance from front-tip to rear-axle	L_{rax}	3.395	m
Sensor position	Lateral position	W_{sensor}	$W_{ego}/2 = 0.848$	m
	Vertical position	H_{sensor}	0.6	m
	Horizontal FoV	θ_{sensor_h}	150.0	deg
	Vertical FoV	θ_{sensor_v}	10.0	deg
	Detection range	R_{range}	150.0	m

Table 5.4.4 Parameters of the simulation environment.

Description		Variable	Value	Unit
Occluding vehicle	Vehicle length	L_{occ}	7.0	m
	Vehicle width	W_{occ}	2.0	m
Darting-out object	Vehicle length	L_{obj}	2.1	m
	Vehicle width	W_{obj}	0.6	m
	Darting-out speed	v_{obj}	20	km/h
Intersection	Crossing angle	θ_{cross}	−60	deg
	Size parameter	l_{in}	5.25	m
		l_{out}	5.25	m
	Estimated parameter	$\hat{d}_{pre}$	16.6	m

Table 5.4.5 Parameters of the PBS in the experiment.

Description	Variable	Value	Unit
Standard time to collision for PBS	t_{vir_d}	2.0	s
Distance from occluding vehicle to virtual darting-out object	D_{vir_occ}	1.0	m
Darting-out velocity of virtual darting-out object	v_{vir}	36	km/h
Expected emergency braking acceleration	a_{EBS}	−8.0	m/s^2
Safety margin	D_{safe}	1.0	m
Latency of PBS	τ	0.5	s
Control gain	K_{ff}	0.06	s^2/m
	K_v	0.05	s/m
	K_a	0.05	s^2/m
Maximum brake command	B_{PBS_max}	0.5	-
Minimum assistance velocity	v_{PBS_min}	3.6	km/h
Prediction time on speed profile	t_{pre}	0.3	s
Gain for speed profile when driver uses gas pedal	K_{gas}	9.8	m/s^2

5.4.6 Experiment Result

Fig. 5.4.13 shows the time historical results from the recorded data of one subject driver in the data acquisition driving. The time 0 in these figures defined as the time when the PBS started the brake assistance.

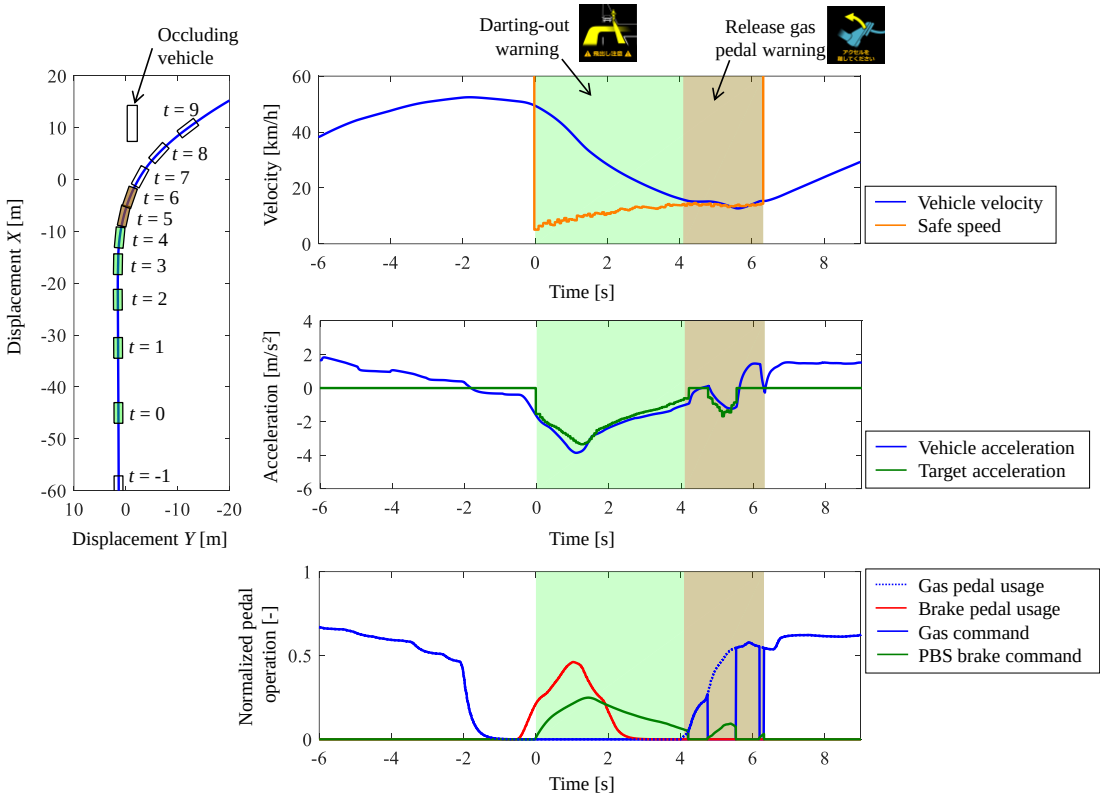

Fig. 5.4.13 Time historical results from the recorded data of one subject driver in the data acquisition driving (D-2).

The left figure in Fig. 5.4.13 shows the trajectory of the ego vehicle and the position of the occluding vehicle. The right three figures show the time historical results of the velocity, acceleration, and the normalized pedal operation by the driver and the driver assistance system. The sections that the driver assistance intervened in are colored in green, and the section “release gas pedal warning” was displayed is colored in red.

From the result, the driver approached the intersection at high speed and the velocity was about 45 km/h when the PBS started to intervention. The PBS calculated the safe speed and displayed the “darting-out warning” with the beep sound when the vehicle drove into the intersection. However, in this case, the driver used the brake pedal manually first, and it was overwhelming the amount of brake assistance by the PBS. Therefore, until about 2 seconds after the driver assistance system started the intervention, manual operation overrode the assistance. Later than that, the driver decreased the brake operation. Then, the PBS brake assistance overwhelmed and compensated the brake operation to decelerate to the safe speed. Later than 4 seconds after started the brake, the driver started to use the gas pedal to reaccelerate, but the vehicle did not pass through the risk predictive scenario, therefore, the driver assistance system displayed the “release gas pedal warning”. When the driver still used the gas pedal, the system cut the gas command and engaged brake assistance again. In this case, the driver did not recognize the “release gas pedal

warning", hence, the driver did not put off the foot from the pedal, however, the system could keep the ego vehicle velocity around the safe speed. The time historical results on D-2 of all subjects are appended in Appendices of this paper (Appendices 5-3).

Table 5.4.6 shows the summary of the experiment data of all subjects on D-2.

Table 5.4.6 The summary of the experiment in D-2 (34 subjects).

Description	PBS intervention time	"Gas pedal release warning" displayed time	Minimum acceleration during PBS	Maximum absolute jerk during PBS
Number of subjects	34	22	34	34
Unit	s	s	m/s^2	m/s^3
Minimum	3.04	0.15	-6.84	1.70
Maximum	18.12	13.95	-1.35	111.84
Median	4.34	1.43	-3.60	14.79
Average	5.43	2.35	-3.59	20.84
Standard division	2.79	2.85	1.27	21.56

Description	Vehicle speed when PBS engaged assistance	Vehicle speed when disengaged PBS ①	Safe speed when disengaged PBS ②	Error between vehicle speed and safe speed ①－②
Number of subjects	34	34	34	34
Unit	km/h	km/h	km/h	km/h
Minimum	27.72	9.49	7.59	-3.09
Maximum	56.28	20.22	18.76	3.88
Median	43.79	14.01	12.87	1.16
Average	43.24	14.40	13.25	1.15
Standard division	6.26	2.87	2.70	1.43

From the table, the PBS intervened in all of the driving cases on D-2, and the "gas pedal release warning" displayed 22 of 34 subjects. Average subjects approached the intersection with around 43 km/h and most drivers approached at the velocity between 35 to 50 km/h. And the PBS could successfully decelerate the vehicle speed to the safe speed and the errors were less than ±4 km/h in all subjects.

The following figures from Fig. 5.4.14 to Fig. 5.4.16 show the recorded driving data from all subject drivers. The red lines in the figure indicate the data from the data acquisition drive D-1: no PBS assistance condition. The blue lines indicate the data from the data acquisition drive D-2: the vehicle equipped with the PBS. The colored areas in Fig. 5.4.15 and Fig. 5.4.16 indicate the data within the standard deviation. The time 0 in these figures defined as the time when the vehicle reached the predicted conflict point (c.p.).

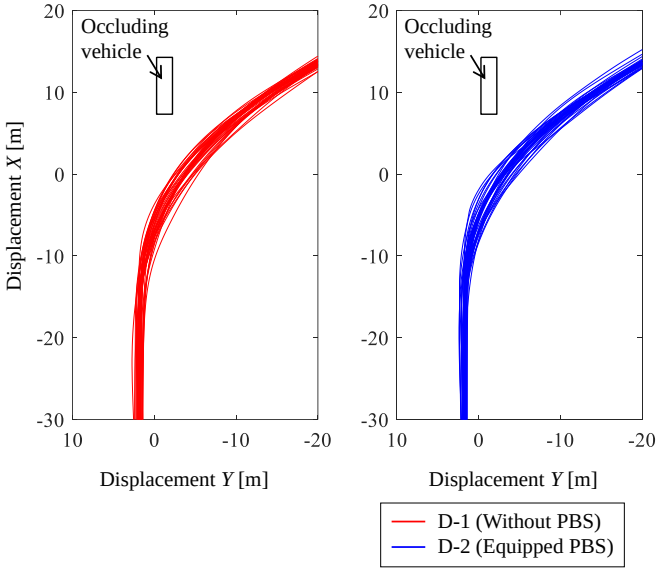

Fig. 5.4.14 Trajectories of the recorded driving data from the 34 subject drivers (D-1 vs D-2).

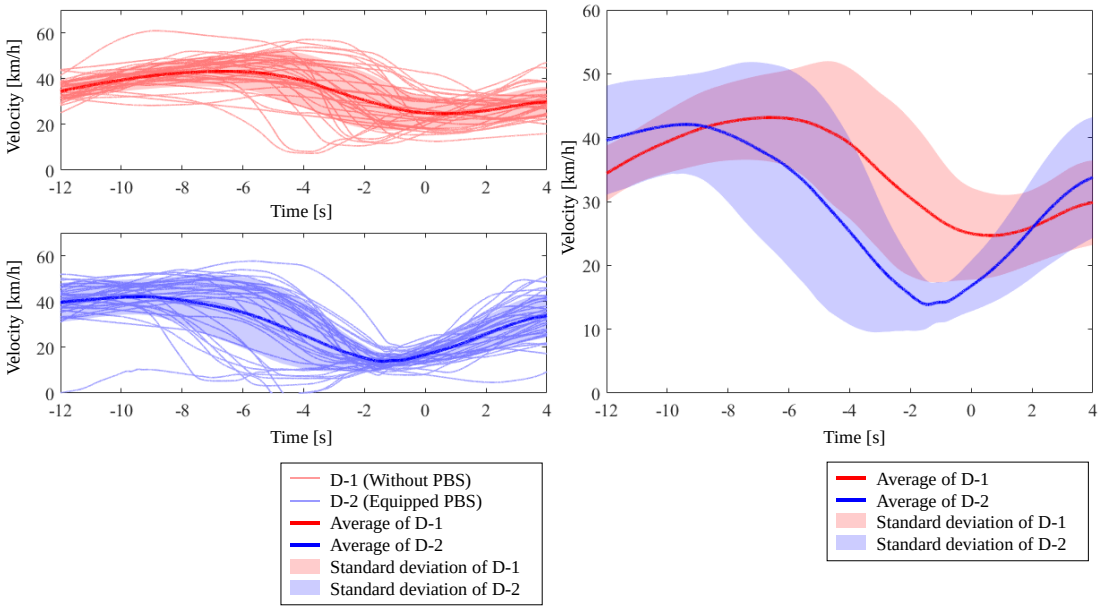

Fig. 5.4.15 Velocities of the recorded driving data from the 34 subject drivers (D-1 vs D-2).

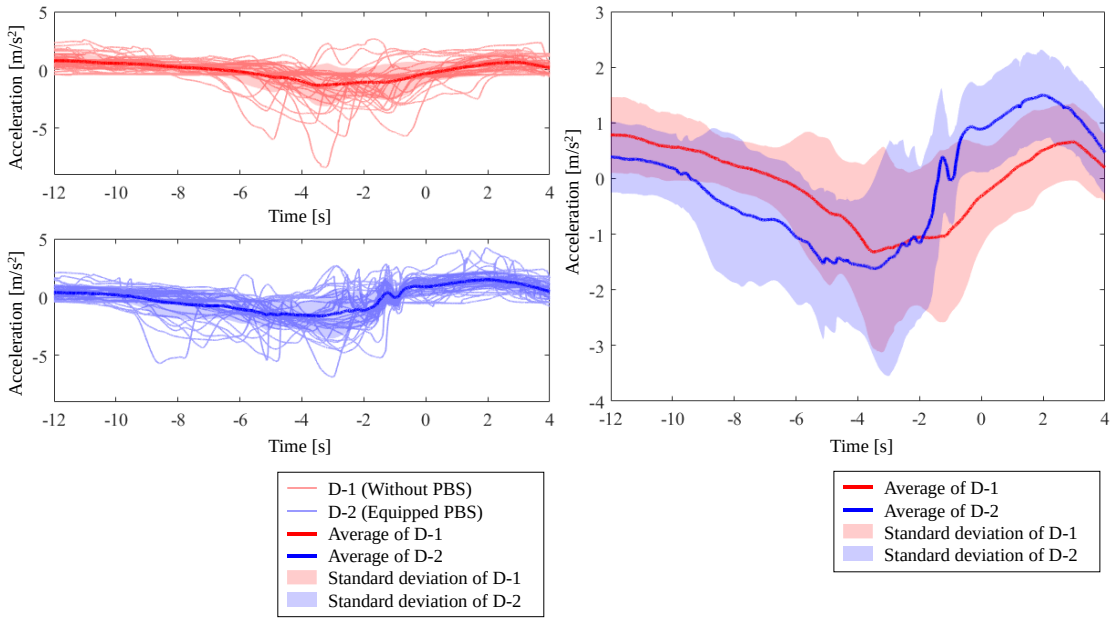

Fig. 5.4.16 Accelerations of the recorded driving data from the 34 subject drivers (D-1 vs D-2).

From Fig. 5.4.14, there was no large difference in the trajectory between the D-1 and D-2. Nevertheless, from Fig. 5.4.15 the average vehicle velocity of D-2 was lower than the one of D-1, especially, when the ego vehicle is close to the predicted c.p. In addition, PBS could lead to the negative peak of the velocity earlier around time t = -1 [s]. The deviation of the velocity was also reduced by the deceleration of PBS. This meant the system could decelerate the vehicle to a safe state evenly through the subjects. Regarding the acceleration, although the velocities in D-2 were slower than the ones in D-1, the magnitudes of the accelerations were not notably different. The point is that the PBS could start the deceleration earlier and decelerate to the safe speed with moderate acceleration.

From Fig. 5.4.17 to Fig. 5.4.19 compares the results of D-2 and D-3. In D-2, the subjects did not know anything about the driver assistance system, and this was the first time to drive the car with PBS. D-3 was the second time to experience the PBS and also the subjects knew about the purpose and contents of the PBS, provided that the subjects were ignorant whether the system was equipped or not to the test vehicle at D-3.

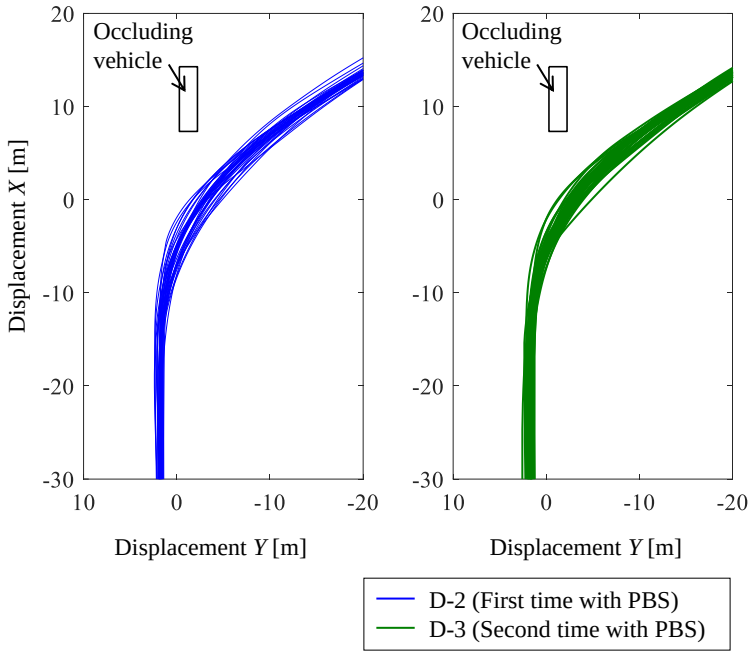

Fig. 5.4.17 Trajectories of the recorded driving data from the 34 subject drivers (D-2 vs D-3).

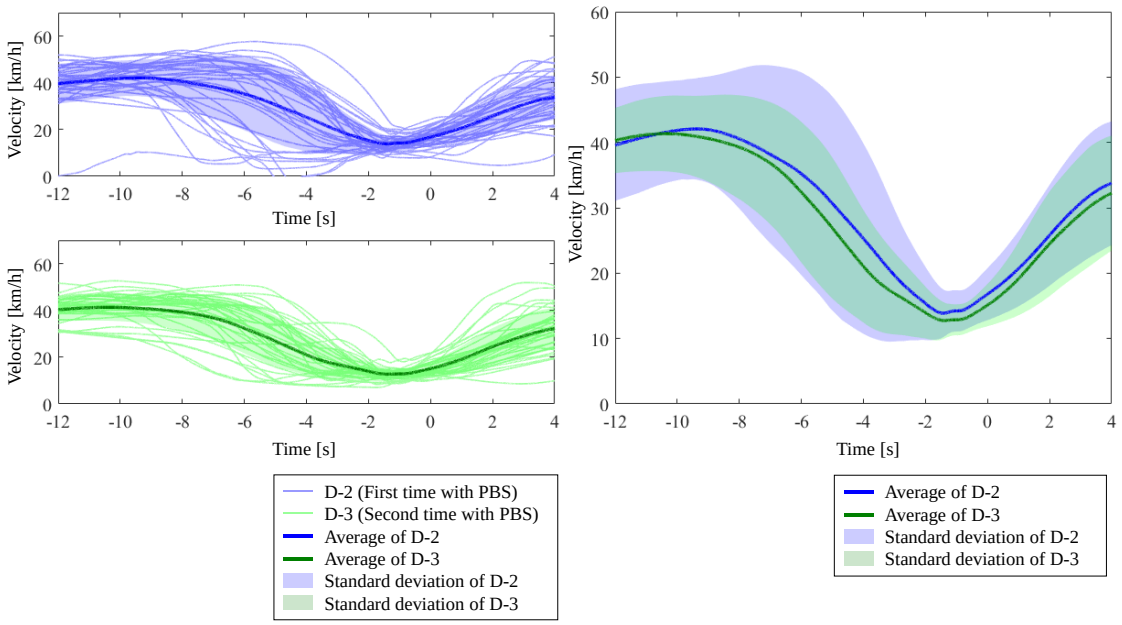

Fig. 5.4.18 Velocities of the recorded driving data from the 34 subject drivers (D-2 vs D-3).

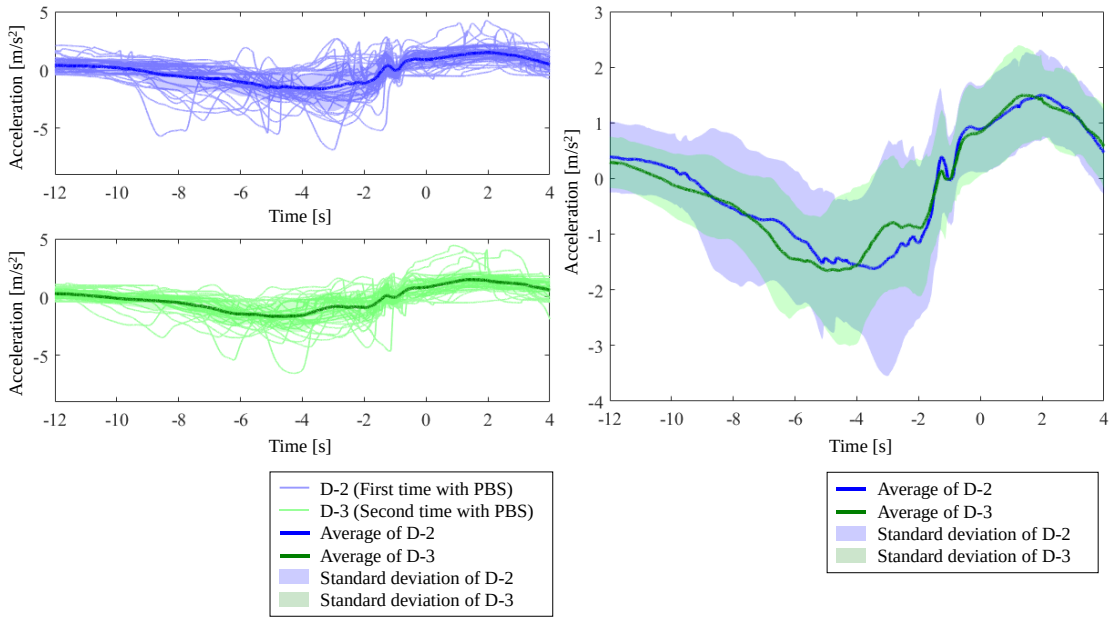

Fig. 5.4.19 Accelerations of the recorded driving data from the 34 subject drivers (D-2 vs D-3).

Comparing the results from D-2 and D-3, the mean velocity and acceleration were quite close values. This indicates when the system is enabled, the system could bring the vehicle to the safe speed regardless of the knowledge about the driver assistance system. In addition, the vehicle velocities of D-3 are less distributed compared to the velocities of D-2. Thus, the knowledge about the system affected guiding the driver to avoid excessive or deficient braking to the potential risks.

In the data acquisition drive D-4, 17 of 34 subjects drove the vehicle equipped with the driver assistance system and the rest of the subjects drove the vehicle without the driver assistance system. The collision avoidance results of the experiment are shown in the table below.

Table 5.4.7 Collision avoidance result (D-4).

Description	With driver assistance	Without driver assistance
Number of subjects	17	17
Collided cases	0	1
Avoided cases	17	16
Cases EBS engaged	9	5

With the driver assistance system, all subjects could avoid the collision with the darting-out object. On the other hand, a collision occurred in the condition without the driver assistance and collision velocity was 0 km/h. The driver assistance engaged EBS in that case, however, the EBS could not stop the vehicle before reaching the conflict point and the darting-out object collided with the vehicle. In the 9 out of 17 cases that with the driver assistance, EBS applied the emergency brake. On the other hand, 5 out of 17 cases without driver assistance engaged emergency braking to avoid the collision. The reason for the difference is not clear, but the approaching speed of the cases with the driver assistance tended to approach the intersection with higher speed (refer Fig. 5.4.20). Moreover, since the subject had already known about the feature of the driving assistance, the subjects may tend to leave the deceleration to brake assistance by PBS. Fig. 5.4.20 shows the recorded driving data from the subject drivers in D-4.

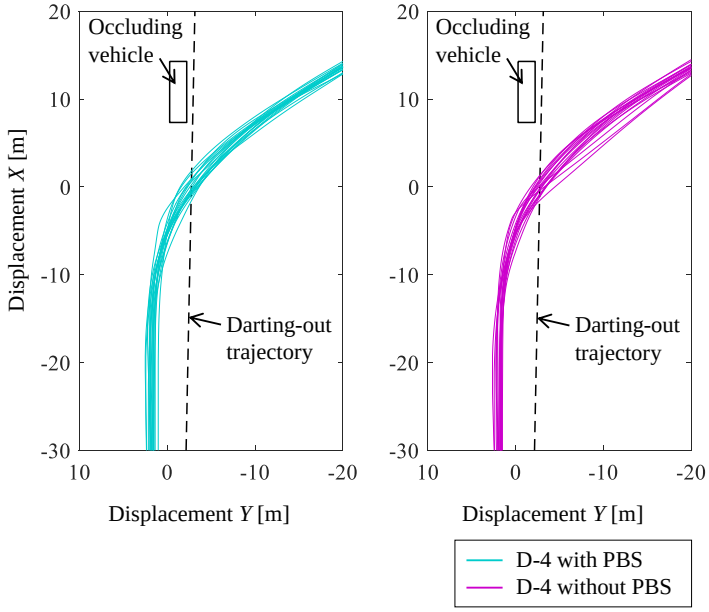

Fig. 5.4.20 Trajectories of the recorded driving data from the 34 subject drivers (D-4 with the driver assistance vs D-4 without the driver assistance).

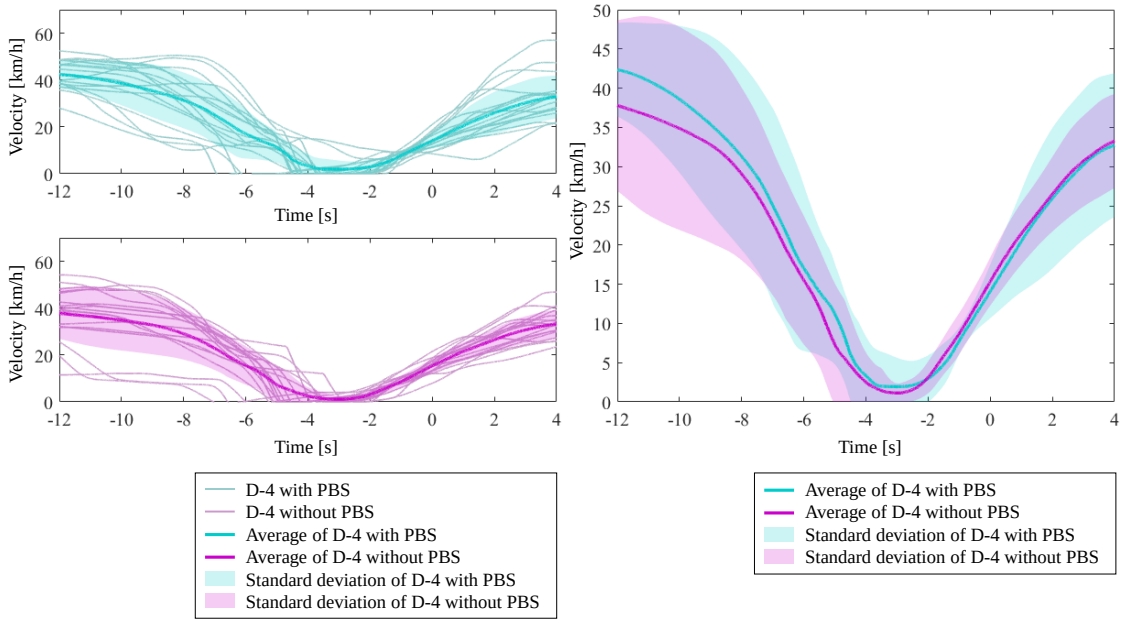

Fig. 5.4.21 Velocities of the recorded driving data from the 34 subject drivers (D-4 with the driver assistance vs D-4 without the driver assistance).

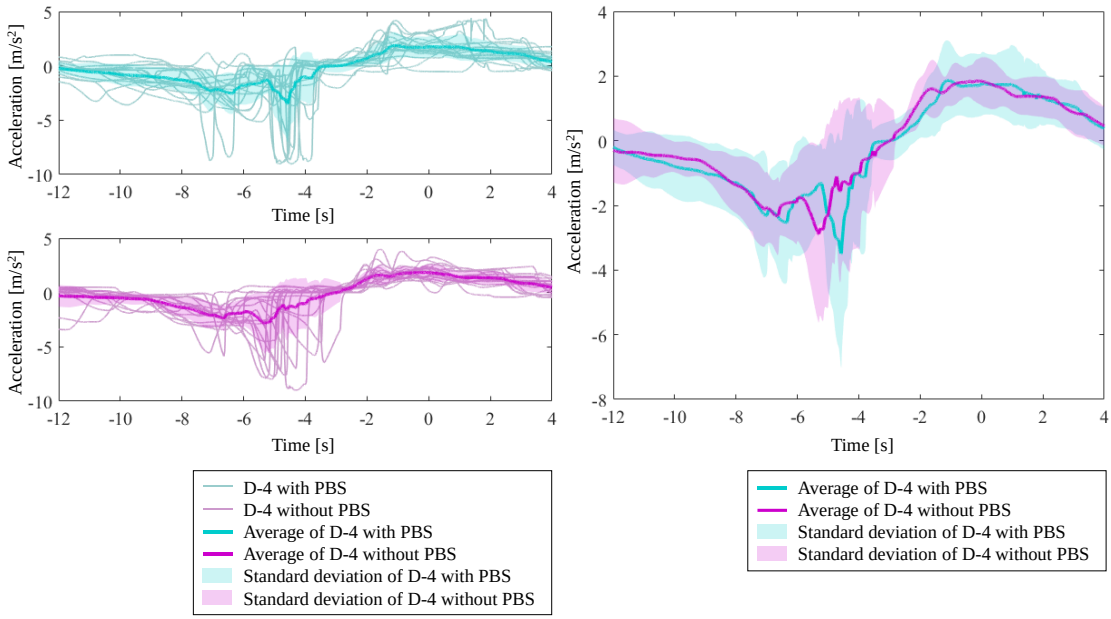

Fig. 5.4.22 Accelerations of the recorded driving data from the 34 subject drivers (D-4 with the driver assitance vs D-4 without the driver assistance).

The approach velocities of the cases with the driver assistance were tended to be higher than the cases without, however, there were not very big differences in the velocity and acceleration between the conditions while the driver assistance system engaged. Because the drivers had already known about the purpose and focus of the experiment and experienced the driver assistance, drivers drove the intersection safely regardless of the existence of the driver assistance system.

5.4.7 Questionnaire Results and Driver Acceptance Evaluation

The followings describe the results of the post-experiment questionnaire. The subjects answered the questionnaire just after the experiment D-2.

The questions and the answers to the questions from 1 to 3 are listed below and shown in Fig. 5.4.23:

- Question 1, Did you feel any kind of driver assistance?
- Question 2, Did you find the graphic image warning from the driver assistance system?
- Question 3, Did you find the deceleration assistance by the driver assistance system?

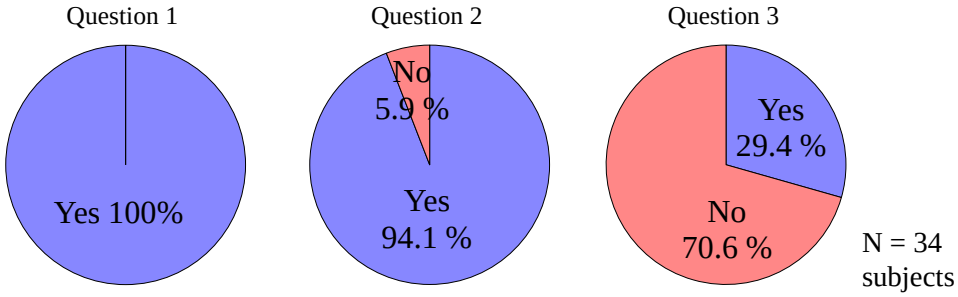

Fig. 5.4.23 The pie chart of the answer to questions from 1 to 3.

Regarding question 1, all of the subjects felt the interventions from the driver assistance system. Form

question 2, 94% of the subjects recognized the graphic warnings. In contrast, only 29% of the subjects recognized brake assistance.

Question 4 asked about the understanding of the system. The result of the question is shown in Fig. 5.4.24.

- Question 4, In which situation did the driver assistance assisted, and what is the purpose of the assistance?

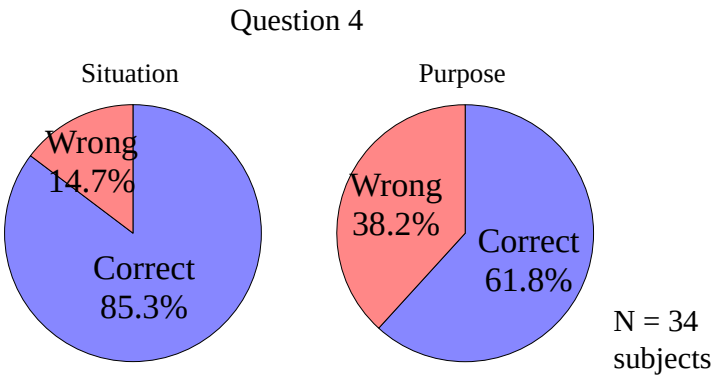

Fig. 5.4.24 The pie chart of the answer to question 4.

From the results, 85% of the subjects correctly understood the situation where the driver assistance system assisted, and 62% of the subjects correctly understood the purpose of the assistance. To evaluate the driver acceptance fairly, the following questionnaire results were the answers from 29 out of 34 subjects who correctly understood the situation where the driver assistance system assisted the driver.

Questions from 5 to 10 asked the general acceptance of the driver assistance system. Questions from 5 to 10 are listed below:

- Question 5, Did you feel that you could drive safely because of the assistance?
- Question 6, Did you drive at ease because of the assistance?
- Question 7, Did you feel that you attempted to confirm safety because of the assistance?
- Question 8, Did you feel that you needed a turn-off switch?
- Question 9, Do you want to equip this function for your own vehicle?
- Question 10, Do you need that assistance function for yourself now?

Here, Fig. 5.4.25 shows the results of the questions.

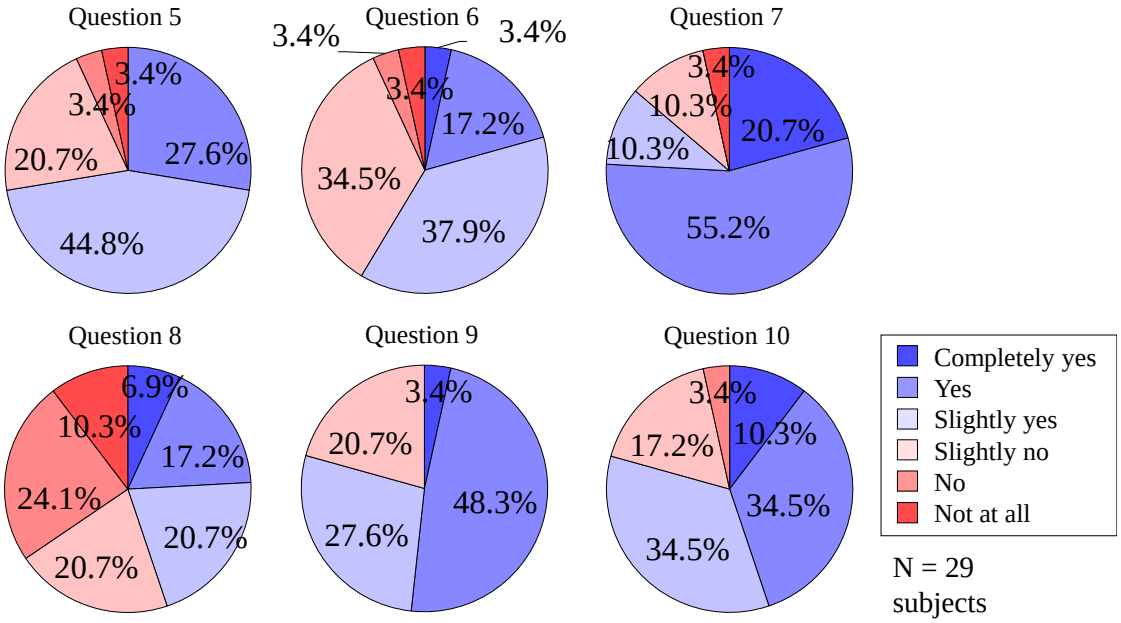

Fig. 5.4.25 The pie chart of the answer to the questions from 5 to 10.

From the results of the questionnaire, more than half of the subjects positively evaluated the driver assistance system in all of the questions. Notice that regarding question 8, more than half of the subjects answered negatively, but this meant more than half of the subjects did not require the turn-off switch. Especially, from the result of question 7, more than 75% of the subjects answered “Yes” or “Completely yes”, hence the assistance affected to most drivers drive safely in the risk predictive scenario. Moreover, more than 50% and 45% of the subjects answered “Yes” or “Completely yes” for questions 9 and 10 respectively. From above, most subject drivers felt the effectiveness of the driver assistance and they thought the driver assistance had a positive effect on their driving, and most subjects were positive to equip the system to their own vehicle, and the subjects themselves recognized the system was needed for themselves now. Thus, the driver assistance system in the scenario was generally accepted by the subject drivers.

Focusing on the braking assistance by PBS. From the answers to question 3, 29.4% (= 10 subjects) felt the deceleration assistance. To evaluate the understanding of the assistance, the following question was asked to the subjects.

- Question 11, For which purpose did the braking assistance assist?

  The results of question 11 are shown in Fig. 5.4.26.

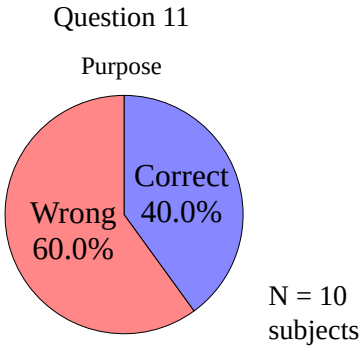

Fig. 5.4.26 The pie chart of the answer to question 11.

From the results, 4 subjects out of 10 correctly understood the purpose and situation of the brake assistance. According to the comment, three subjects understood the brake assistance for keeping the safe distance between preceding vehicle, a subject understood the brake assistance to stop the vehicle safely, a subject understood the brake assistance to prevent the miss pedal usage, and a subject understood the brake assistance to prevent the lane departure while driving the curve. To evaluate the driver acceptance fairly, results from the following questions from 18 to 23 were the answers from four subjects who correctly understood the purpose of the brake assistance.

Fig. 5.4.27 and the list below describe the question and the answer to the questions regarding acceptance of the braking system:

- Question 18, Did you feel the braking assistance convenient?
- Question 19, Did you feel the braking assistance uncomfortable?
- Question 21, Did you feel the braking assistance interrupted your drive?
- Question 23, Did you feel the braking assistance made you anxious?

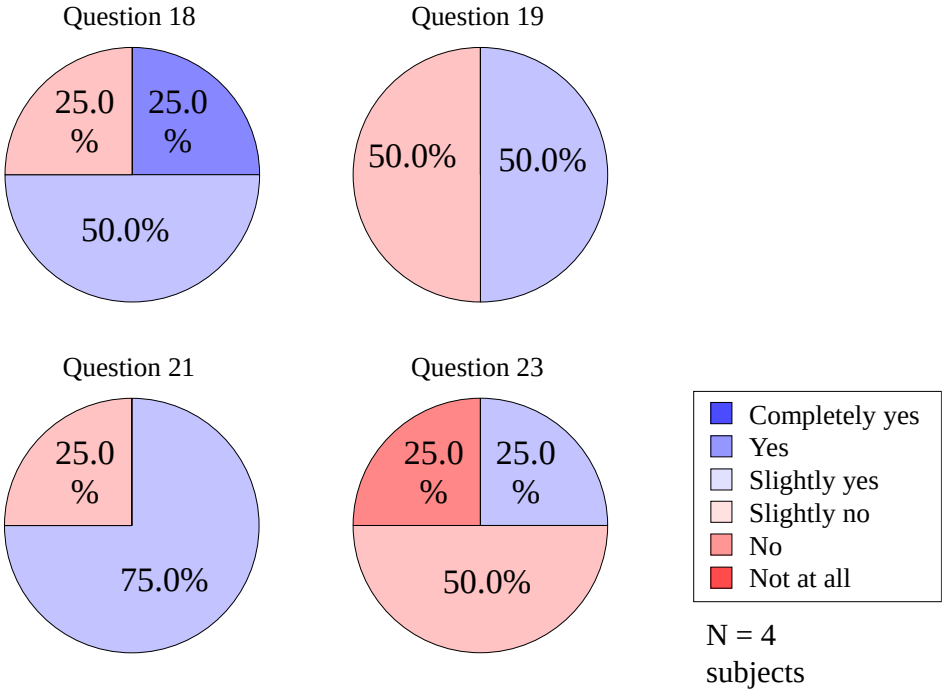

Fig. 5.4.27 The pie chart of the answer to the questions 18, 19, 21, and 23.

From the results, more subjects felt the brake assistance convenient and less anxious, however, due to the number of the subjects who felt the brake assistance is quite low, we could not acquire a clear tendency in those questions. Besides, none of the subjects answered “Completely yes” or “Not at all”, therefore, the brake assistance might be less impressive. An important point of the result was that despite there was brake assistance, most drivers did not recognize the brake assistance. Because, by considering the current acceleration of the vehicle to the speed profile, the initial brake assistance was smooth and continuous (see also Section 2.3.4 and acceleration of Fig. 5.4.13). Besides, during the brake assistance, the target acceleration changes continuously and moderately therefore it might be hard to find when the brake assistance intervened. Hence, when the subjects could not find the brake intervention, it should be handled as the system was accepted. To sum up, the brake assistance was widely accepted by the subjects.

As explained in Section 5.4.2, the acceleration that the simulator generated was lower than the real environment, therefore, the result might be different in the real environment. However, as presented in Section 5.3, in the real environment, most of the subjects also did not notice the brake assistance, thus, it is expected that most drivers also do not realize the driver assistance in the real environment.

Focusing on the graphic warnings. From the answers to question 2, 94.1% (= 32 subjects) recognized the graphic warnings. On the other hand, 29 subjects understood the driver assistance from the question 4. These 29 subjects belonged to the 32 subjects who recognized the graphic warnings. Thus, focusing on the 29 subjects for the following question. To evaluate the recognition of the assistance, the following question were asked.

- Question 25, What did the graphic warnings display?

  The results of the question 25 are shown in Fig. 5.4.28.

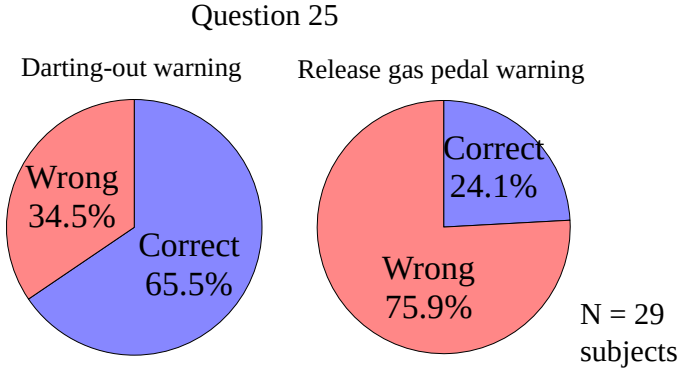

Fig, 5.4.28 The pie chart of the answer to question 25.

From the results, 65% of the subjects correctly recognized the “darting-out warning”, on the other hand, 24% of the subjects correctly recognized the “Release gas pedal warning”. The main reason for the result is the time that the “Release gas pedal warning” is relatively shorter than the “Daring-out warning” (see also Table 5.4.6).

As a problem of the graphic warnings, because the display time was short and also the drivers are watching ahead of the vehicle. Since the brake assistance actively decelerates to the safe speed, this misunderstanding would not be critical for safety, however, the misunderstandings might lead decline in the driver acceptance of the driver assistance. The problem remained the task to warn the potential risks and release the gas pedal correctly without losing the acceptance.

Despite some of the subjects wrongly recognized the graphic warnings, all of those subjects correctly understood the intervention location. Therefore, the following questions are evaluated with the results from the 29 subjects.

The list below describes the questions regarding acceptance of the graphic warnings:

- Question 30, Did you feel the graphic warnings convenient?
- Question 31, Did you feel the graphic warnings interrupted your drive?
- Question 33, Did you feel the graphic warnings made you anxious?

The results of questions 30, 31, and 33 are shown in Fig. 5.4.28.

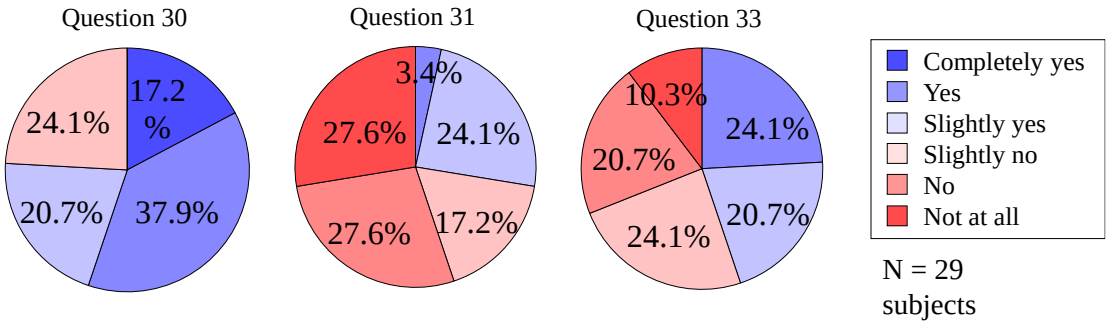

Fig. 5.4.28 The pie chart of the answer to questions 30, 31, and 33.

The result of question 30 indicates that the graphic warnings were highly supported by the subjects about its convenience. From the result of the question 31, 72% of the subjects answered that the graphic warnings did not interrupt the driving, and 28% of the subjects were not interrupted at all. Regarding question 33, More than half of the subjects answered the warnings did not make them anxious, however, 45 % of the subjects felt anxiety by the graphic warnings. The reasons for the feeling of anxiety were the pictograms showed up suddenly, the subject did not understand why the warnings were displayed, and the subject did not figure out the timing of the object darting out. Concluding the graphic warnings, the graphic warnings were mostly accepted by the subjects in terms of convenience, less interruptive, and less anxiety.

5.5 Conclusion

This chapter evaluated the “driver acceptance” of the proposed Proactive Braking System (PBS). This paper described two individual driver acceptance evaluations with subject drivers. Considering the problem of the first driver experiment, the second experiment installed the graphical warnings while the PBS engages the brake assistance. From the evaluation of the second experiment, the braking assistance by PBS was accepted by most subjects.

This page is intentionally left blank.

6. Generalization of Advanced Driver Assistance System for Risk Predictive Driving in Urban Areas

In real driving situations, especially driving in the urban area, there is no exaggeration to say that the road is full of potential risks not only in the intersection turning scenario. By generalizing the concept of the proposed Proactive Braking System (PBS), the PBS can mitigate the collision risk in the other risk predictive scenarios in the urban areas. This chapter presents the generalization of the advanced driver assistance system and simulates the collision avoidance by the proposed advanced driver assistance system in several risk predictive scenarios. In section 6.1, the generalization of the PBS is explained. Section 6.2 lists up several example cases of the risk predictive driving scenarios in the urban area and gives the definitions to accomplish the driver assistance system to decelerate the vehicle to the safe speed. Besides this section mentions the simulation and its results. And section 6.3 concludes the chapter.

6.1 Generalization of Proactive Braking System (PBS)

This section explains the algorithms to generalize the functions to adapt to the other darting-out scenarios. The important point to guarantee the accuracy of the safe speed, as explained in Chapters 2 and 3, is to predict the conflict point with high accuracy. Thus, to adopt the function to other risk predictive scenarios, we must redefine the trajectory of the virtual darting-out object and the predicted trajectory of the ego vehicle. Fig. 6.1.1 and Fig. 6.1.2 respectively define the parameters of the virtual darting-out trajectory and ego vehicle Triclothoidal trajectory.

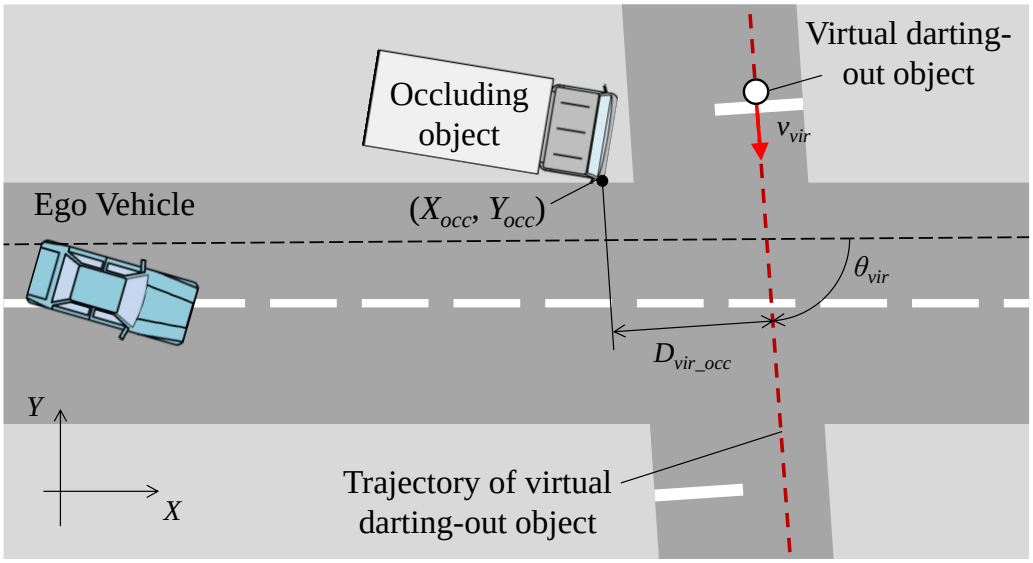

Fig. 6.1.1 Definitions of the parameters that define the trajectory of the virtual darting-out object.

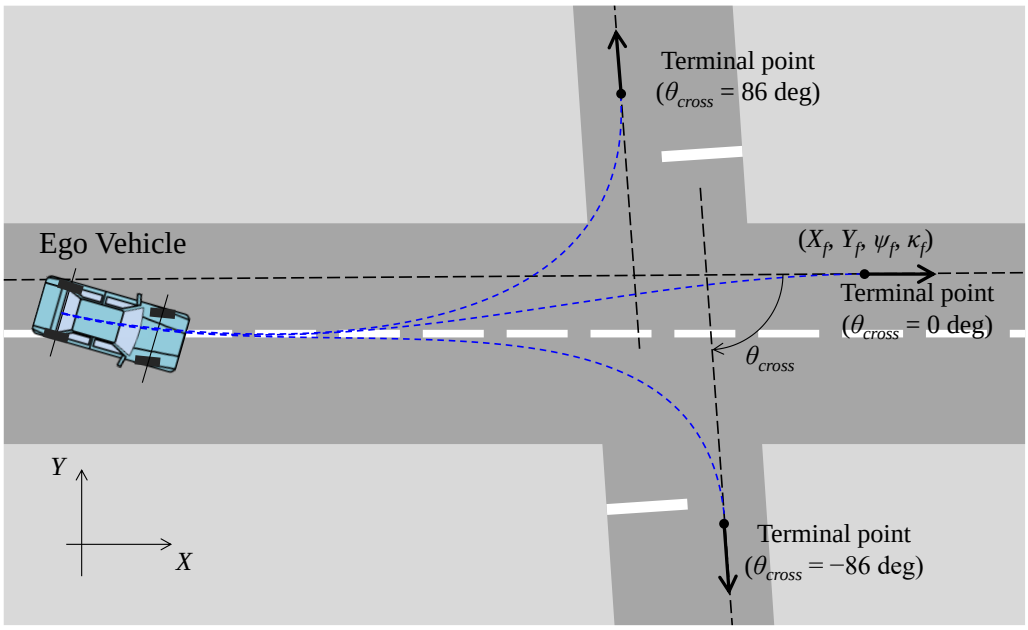

Fig. 6.1.2 Definitions of the parameters that define the Triclothoidal trajectory of the ego vehicle.

To correctly predict the conflict point, first, we must define the darting-out direction of the virtual darting-out object. As shown in Fig. 6.1.1, the direction of the crossing road defines the darting-out direction of the virtual darting-out object. Then, the corner position of the occluding object (X_{occ}, Y_{occ}) can be defined as the position of the corner that an object may dart out. Usually, this position can be decided as the closest corner point from both the ego vehicle predicted trajectory and the crossing road. The lateral offset D_{vir_occ} of the virtual darting-out object is a predefined parameter. This parameter differs by the situation. When an object may dart out from the very close position to the occluding object, this parameter must be smaller. From those directions and positions, the trajectory can be defined. Another parameter that differs by the situation is the velocity of the virtual darting-out object v_{vir}.

Next, the ego trajectory prediction. Fig. 6.1.2 shows the definitions of the trajectory prediction of the ego vehicle. The Triclothoidal curve was designed to predict the trajectory by giving the conditions on the initial point and terminal point. Therefore, this prediction method also can be used for the other cases without changing the algorithm. An important point is how to define the terminal conditions. To generalize the trajectory prediction, the terminal point position and direction are defined as follows. When ego vehicle goes straight, the terminal point position is on the lane-center of the driving lane and when ego vehicle intends to turn right or left at intersections (e.g., when a driver uses a turn-indicator), the terminal point positions are defined as a point on the central part of the escaping road of the intersection as same as Section 3.3.3. To define the positions of the terminal point (X_f, Y_f). This chapter uses the distance parameter d_{pre} and defines the positions (X_f, Y_f). Besides, when the ego vehicle is going on the curve, the turning curvature at the terminal point can be considered to predict the trajectory.

To sum up, the PBS enables to engage the brake assistance in the other risk predictive scenarios by simply giving the following parameters regarding each risk predictive scenario: the darting-out direction, positions of the darting-out trajectory of the virtual object, the darting-out velocity of the virtual object, corner point positions of the occluding object, terminal point positions, terminal point direction, and terminal point curvature.

6.2 Practical Examples on Risk Predictive Driving Scenarios in Urban Area

This section provides several practical examples where PBS possibly reduce the traffic accident by predict the potential risk and decelerate the vehicle to the safe speed. This section also demonstrates the PBS function in the example cases on the full-vehicle simulation using IPG CarMaker.

6.2.1 Right-turn at Large Intersection

As examples of the large intersections, 2 scenarios were prepared as shown in Fig. 6.2.1 (a) and Fig. 6.2.2 (a). Scenario (i) is a scenario that the opposite lanes are full of traffic and a motorcycle darts out from the blind spot of the left-lane vehicle. The trajectory of the virtual darting-out object and the terminal conditions of this case are defined as indicated in Fig. 6.2.1 (b). Scenario (ii) is a scenario that the center-lane of the opposite lanes is congested but the left-lane is not occupied. In this scenario, an object in the center-lane may dart out from the blind spot of the center-lane-vehicle with higher velocity. The trajectory of the virtual darting-out object and the terminal conditions of this case are defined as indicated in Fig. 6.2.2 (b).

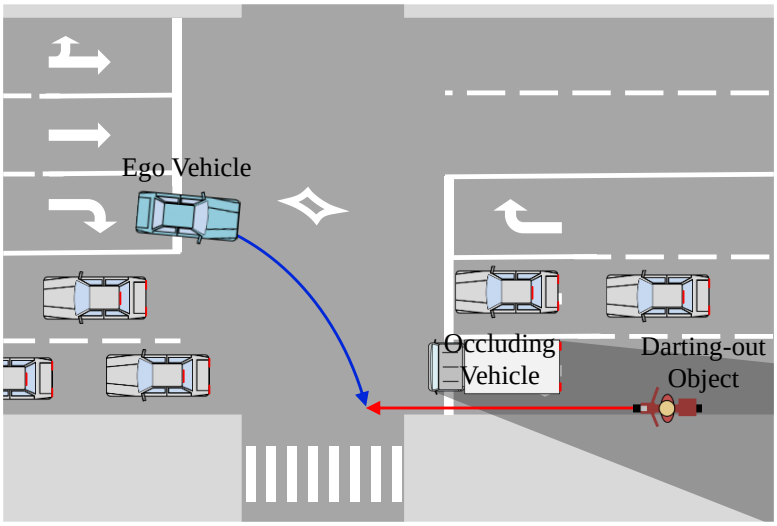

(a) Bird's eye view of the scenario.

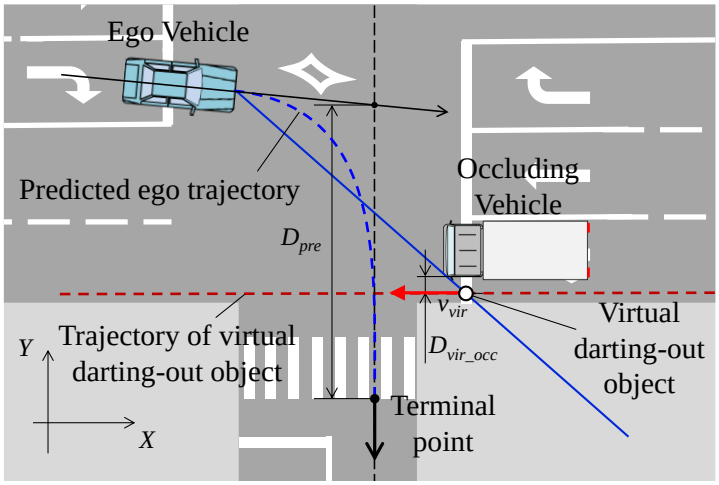

(b) Schematic definitions of the trajectory of the virtual darting-out object and terminal point.

Fig. 6.2.1 Right-turn at a large intersection scenario (i). A motorcycle may dart out when opposite lanes are full of traffic.

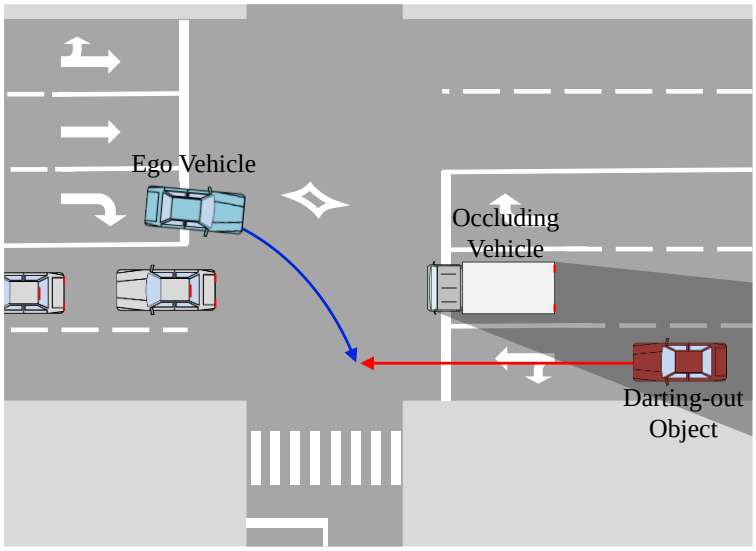

(a) Bird's eye view of the scenario.

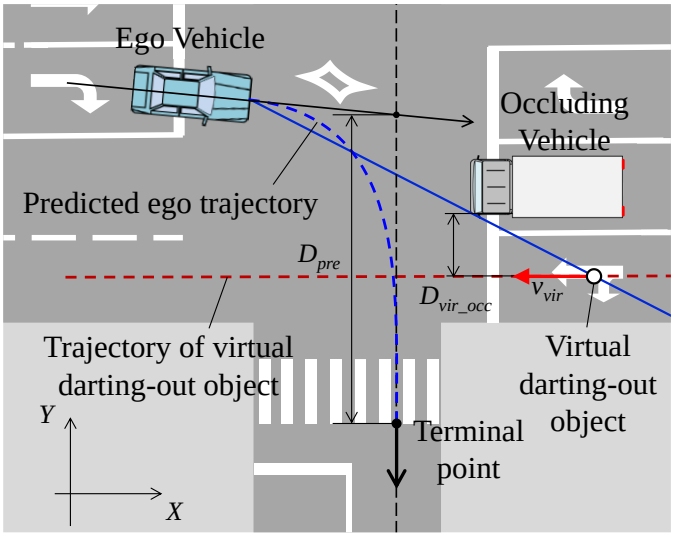

(b) Schematic definitions of the trajectory of the virtual darting-out object and terminal point.

Fig. 6.2.2 Right-turn at a large intersection scenario (ii). A motor vehicle may dart out when the center-lane of the opposite lanes is congested but the left-lane is not occupied.

Under these scenarios, the vehicle which equips only an autonomous emergency braking system (EBS) cannot avoid the collision with the darting-out object when the drivers do not correctly predict the potential risk at the scenario. The simulations with IPG CarMaker show the example cases that generalized PBS enabled the collision avoidance by the moderate brake assistance. Table 6.2.1 and Table 6.2.2 show the defined parameters to realize the PBS assistance in these scenarios. Fig. 6.2.3 and Fig. 6.2.4 show the results of the simulations on the scenario (i) and (ii). Subfigure (a) and (b) respectively show the results of the conditions without and with PBS.

Table 6.2.1 Simulation conditions at scenario (i).

Description		Symbol	Value	Unit
Virtual darting-out object	Offset from the occluding object to trajectory	D_{vir_occ}	1.0	m
	Darting-out velocity	v_{vir}	10.0	m/s
	Darting-out direction	θ_{vir}	−180.0	deg
Terminal point	Direction	θ_{cross}	−90.0	deg
	Distance parameter	d_{pre}	28.3	m
	Curvature	κ_f	0.0	1/m

Table 6.2.2 Simulation conditions at scenario (ii).

Description		Symbol	Value	Unit
Virtual darting-out object	Offset from the occluding object to trajectory	D_{vir_occ}	3.0	m
	Darting-out velocity	v_{vir}	16.7	m/s
	Darting-out direction	θ_{vir}	−180.0	deg
Terminal point	Direction	θ_{cross}	−90.0	deg
	Distance parameter	d_{pre}	28.3	m
	Curvature	κ_f	0.0	1/m

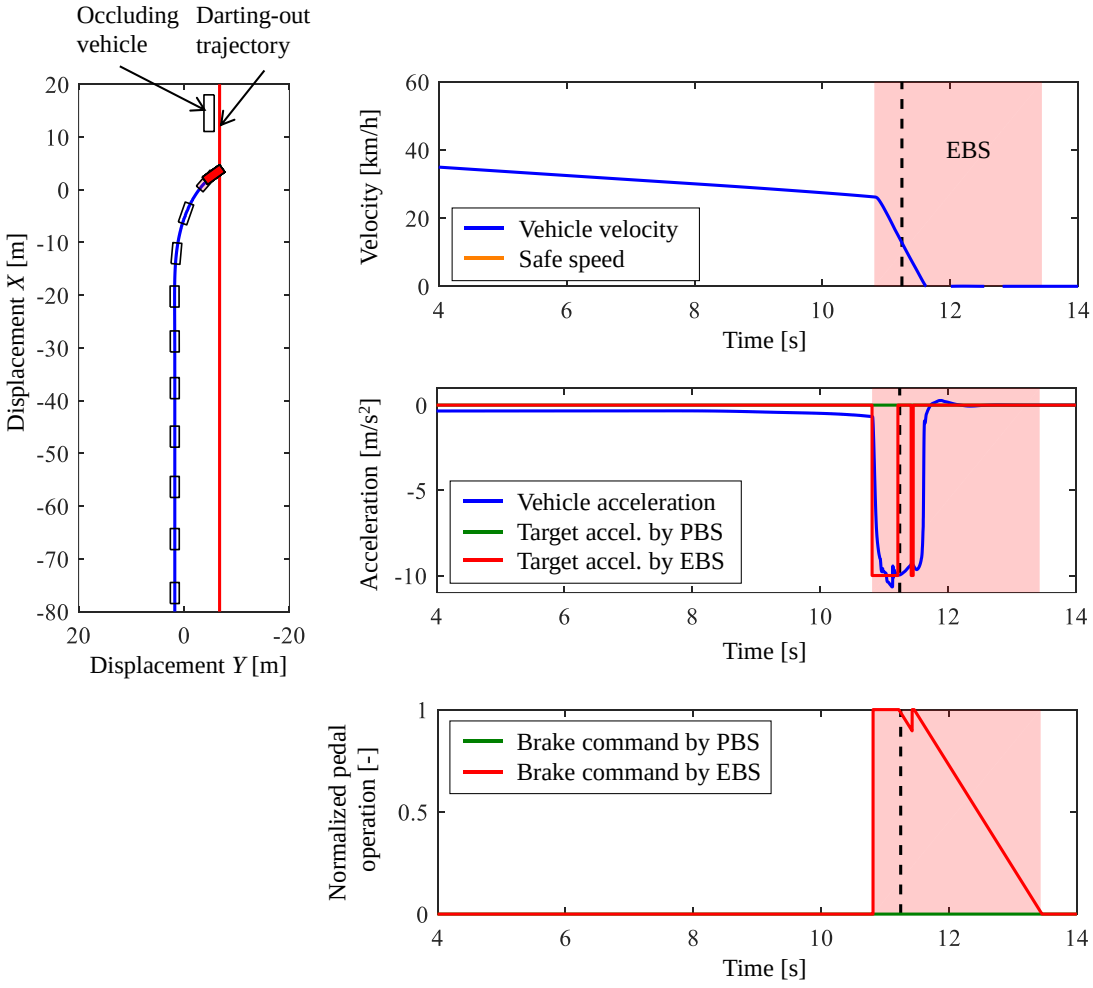

(a) The results with only EBS.

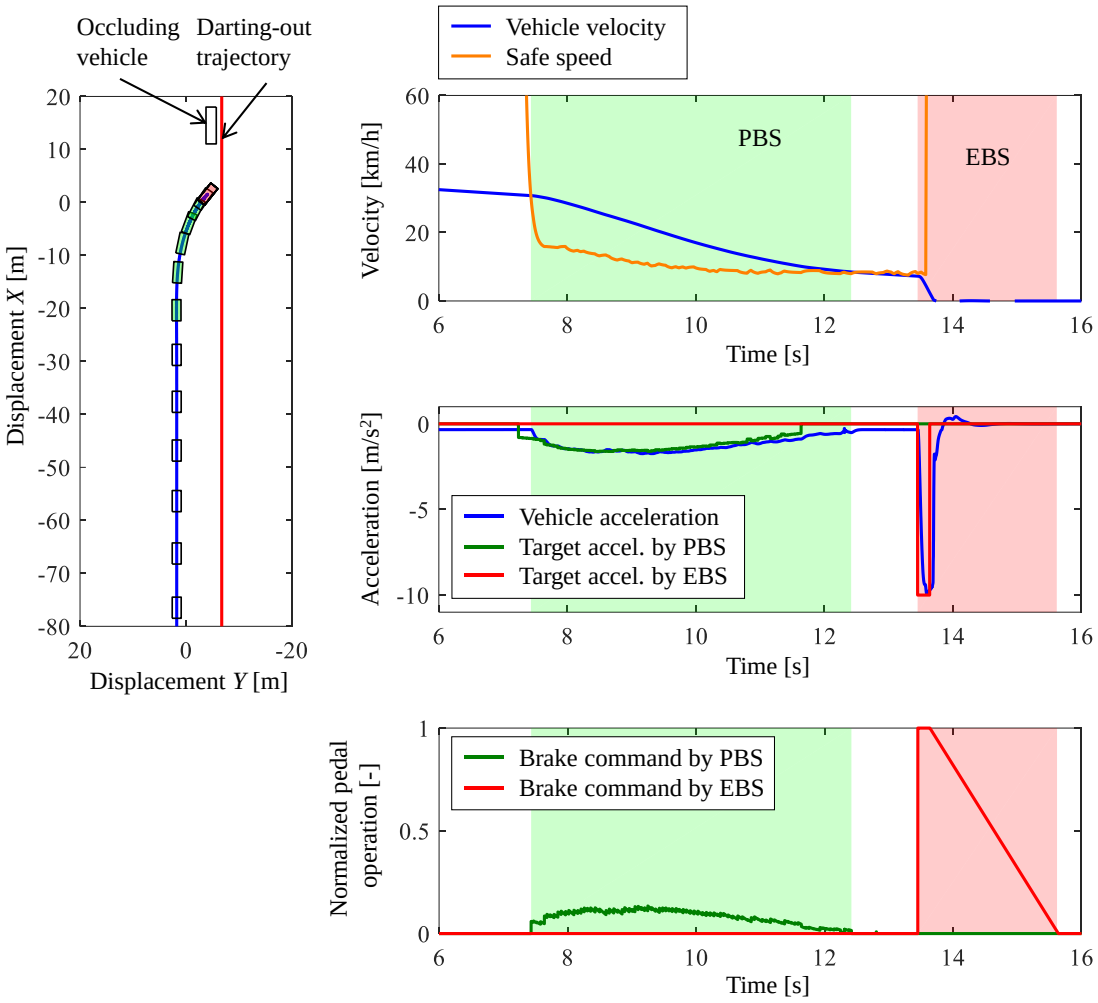

(b) The results with PBS+EBS.

Fig. 6.2.3 Right-turn at a large intersection scenario (i).

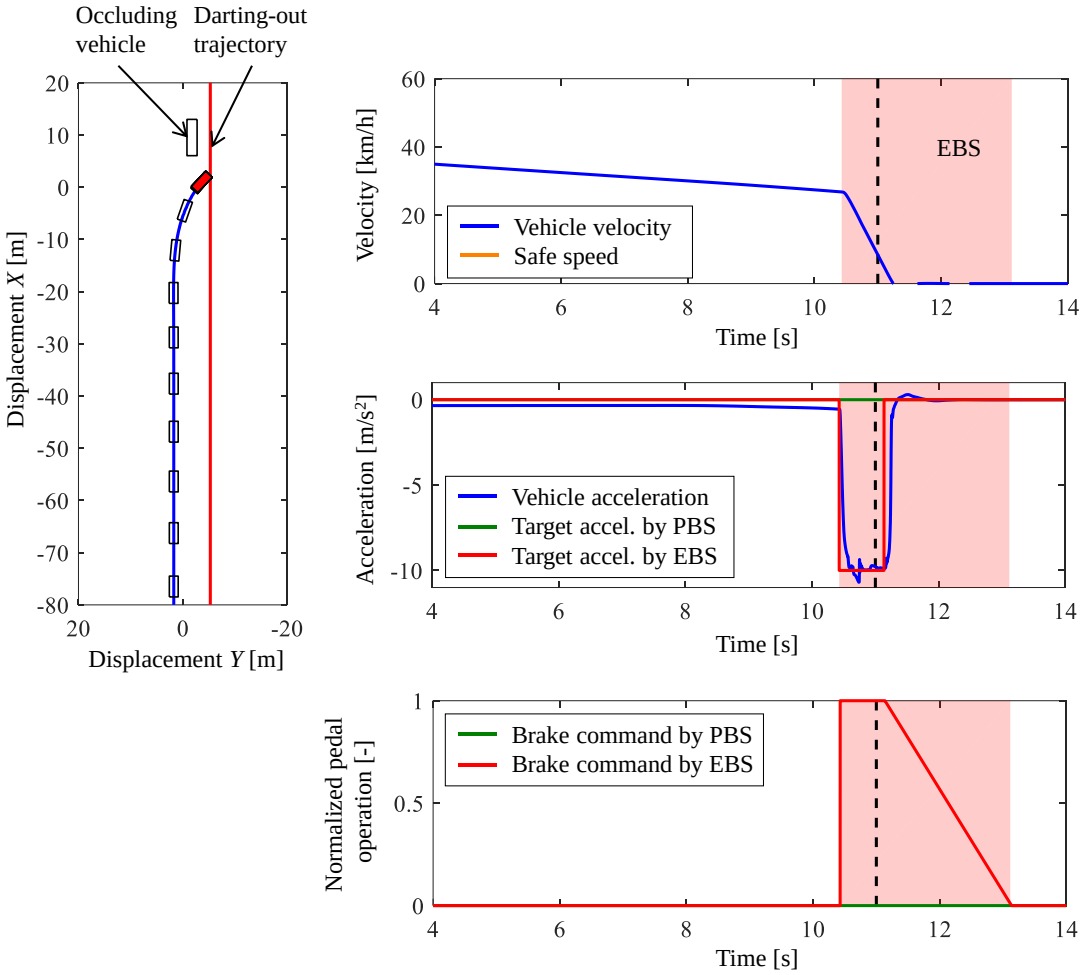

(a) The results with only EBS.

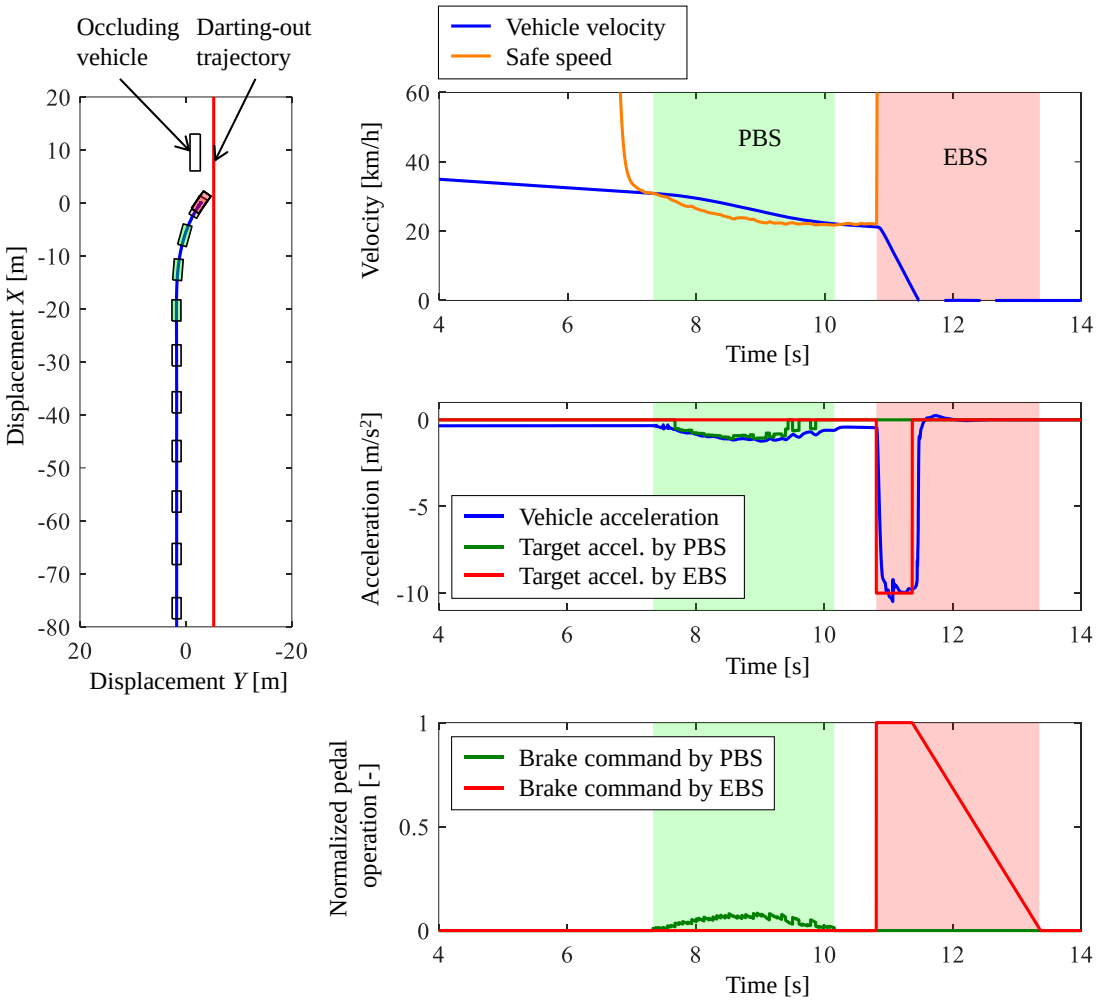

(b) The results with PBS+EBS.

Fig. 6.2.4 Right-turn at a large intersection scenario (ii).

Form both results in Fig. 6.2.3 and Fig. 6.2.4 showed the PBS could assist to decelerate the vehicle speed to the safe speed to avoid the collision in both scenarios. Comparing the safe speed between the scenarios, despite the definition of the virtual darting-out velocity was higher in scenario (ii), the safe speed in scenario (ii) was higher than the one in scenario (i). Because in scenario (ii), since the vehicle yaw angle was lower and the offset D_{vir_occ} was larger, scenario (ii) had more visibility and enough distance to stop the vehicle to avoid the collision by emergency braking.

6.2.2 Going Straight on Blind Intersection in Narrow Road

Fig. 6.2.5 (a) shows a scenario when the vehicle going straight at the small unsignalized intersection. In this scenario, a building is standing on the left side of the road and making a blind spot. The trajectory of the virtual darting-out object and the terminal conditions of this case are defined as indicated in Fig. 6.2.5 (b). In this scenario, the distance parameter $\hat{d}_{pre}$ cannot be defined from the estimation equation (see Section 3.4), thus the terminal point position is defined as a point on the lane-center of ego-lane that has distance d_{pre}.

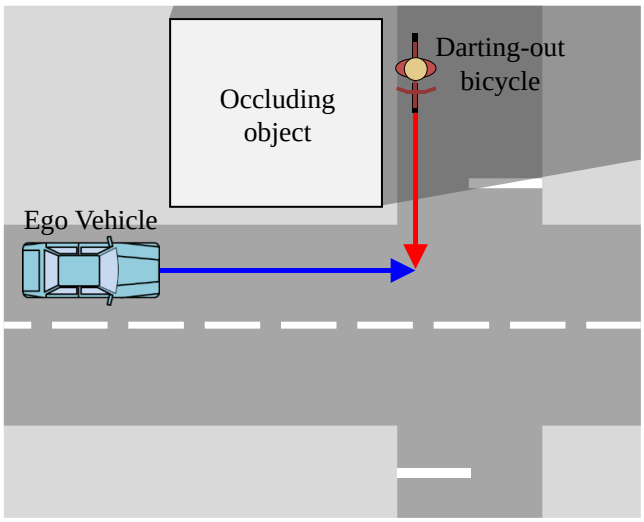

(a) Bird's eye view of the scenario.

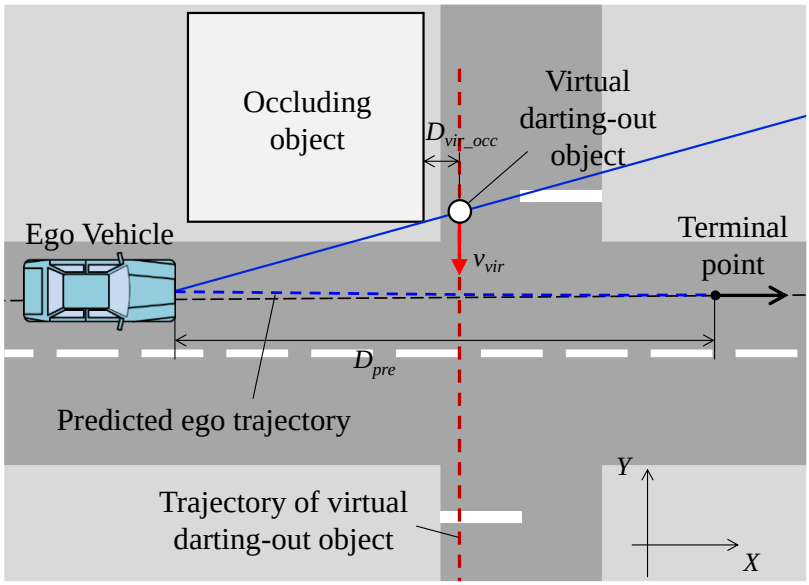

(b) Schematic definitions of the trajectory of the virtual darting-out object and terminal point.

Fig. 6.2.5 Going straight at small unsignalized intersection. An object may dart out from the blind spot behind the occluding object.

Under the scenarios, the vehicle which equips only an autonomous emergency braking system (EBS) cannot avoid the collision with the darting-out object when the drivers do not correctly predict the potential risk at the scenario. The simulations show the example cases that generalized PBS enabled collision avoidance by the moderate brake assistance. Table 6.2.3 shows the defined parameters to realize the PBS assistance in these scenarios. Fig. 6.2.6 shows the results of the simulations on the scenario. Subfigure (a) and (b) respectively show the results of the conditions without and with PBS.

Table 6.2.3 Simulation conditions.

Description		Symbol	Value	Unit
Virtual darting-out object	Offset from the occluding object to trajectory	D_{vir_occ}	1.0	m
	Darting-out velocity	v_{vir}	10.0	m/s
	Darting-out direction	θ_{vir}	−90.0	deg
Terminal point	Direction	θ_{cross}	0.0	deg
	Distance parameter	d_{pre}	80.0	m
	Curvature	κ_f	0.0	1/m

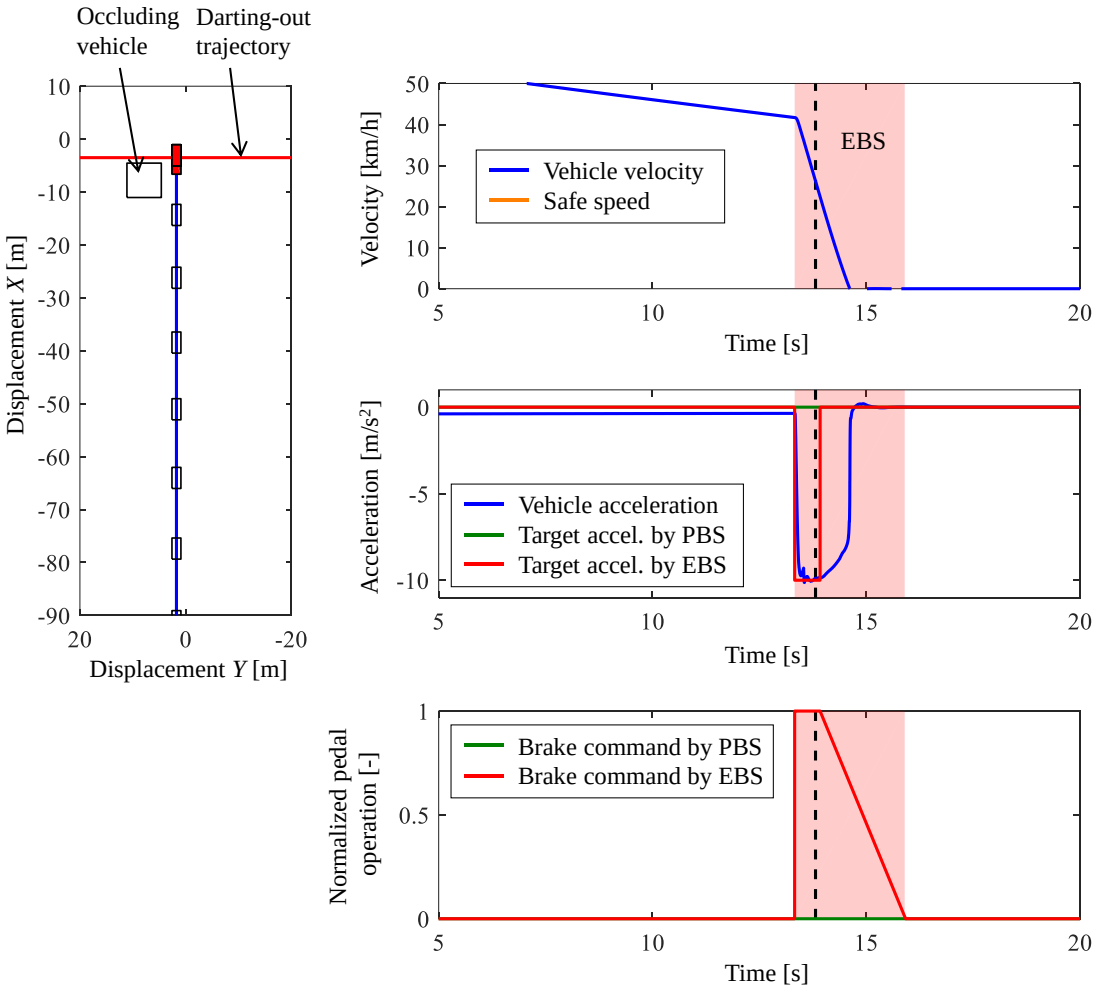

(a) The results with only EBS.

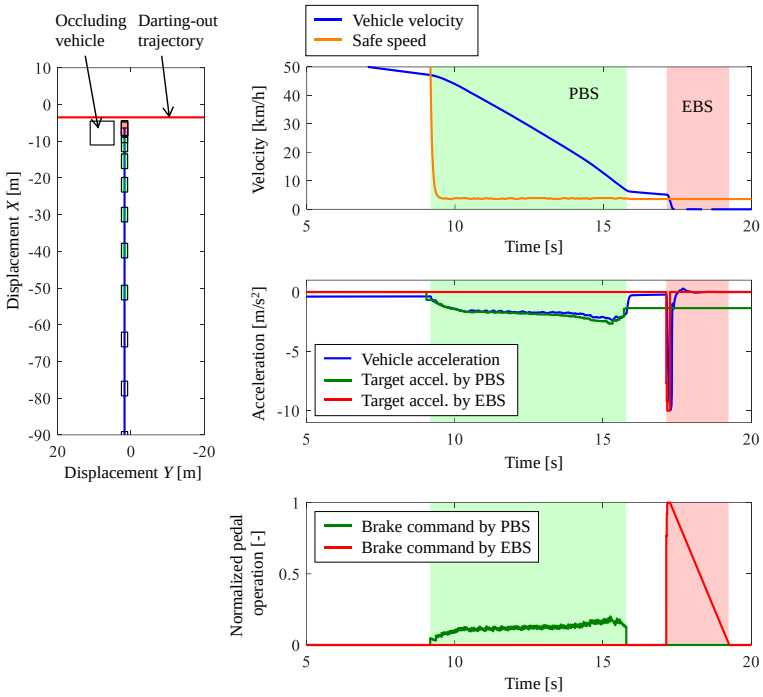

(b) The results with PBS+EBS.

Fig. 6.2.6 Simulation results: going straight at small unsignalized intersection.

The results showed the PBS could assist to decelerate the vehicle speed to the safe speed to avoid the collision. From the results, PBS could effectively function in the risk predictive scenario when the vehicle going straight at the intersection by simply changing the parameters.

6.2.3 Overtaking Parked Vehicle

Fig. 6.2.7 (a) shows a scenario when the vehicle going straight on the street and overtaking a vehicle parking on the roadside. In this scenario, a pedestrian may dart out from the blind spot of the parked vehicle. The trajectory of the virtual darting-out object and the terminal conditions of this case are defined as indicated in Fig. 6.2.7 (b). The overtaking trajectory is simply predicted by using the characteristics of the Triclothoidal curve that consider the terminal position conditions and ego vehicle steering wheel input. Thus, definitions for the terminal point of the trajectory predictions are quite the same as the definitions in Section 6.2.2. The defined parameters are listed in Table 6.2.4.

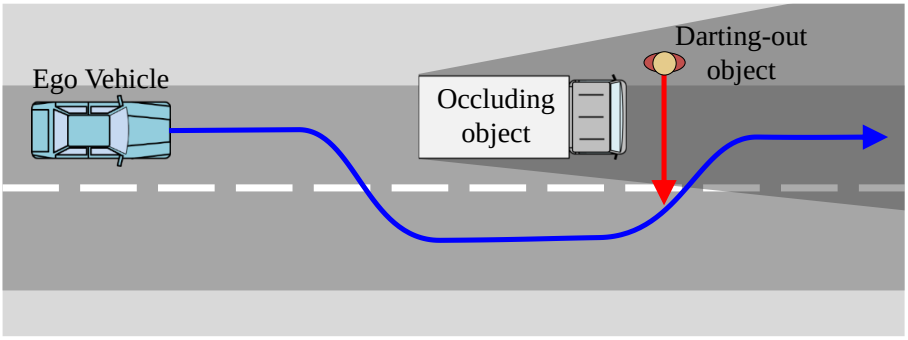

(a) Bird's eye view of the scenario.

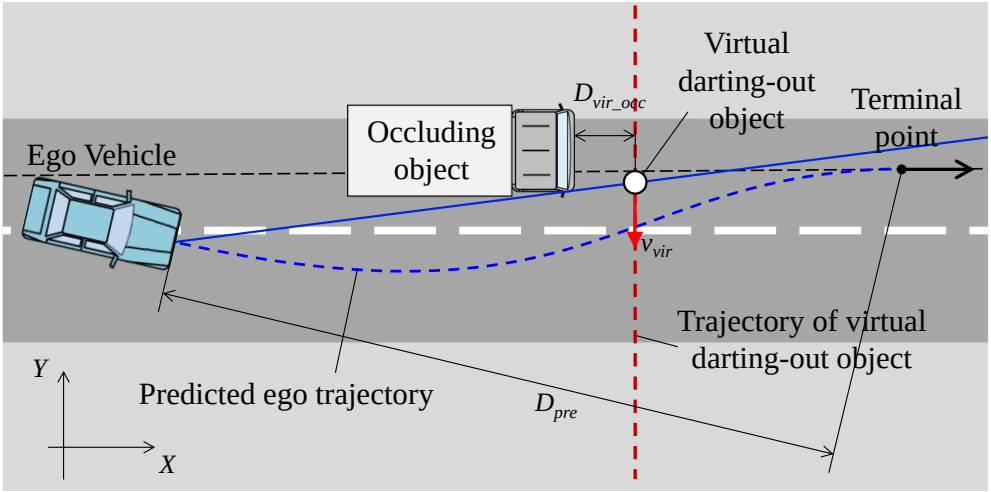

(b) Schematic definitions of the trajectory of the virtual darting-out object and terminal point.

Fig. 6.2.7 Overtaking a parked vehicle. An object may dart out from the blind spot behind the occluding object.

Under the scenarios, the vehicle which equips only an autonomous emergency braking system (EBS) cannot avoid the collision with the darting-out object when the drivers do not correctly predict the potential risk at the scenario. The simulations show the example cases that generalized PBS enabled collision avoidance by the moderate brake assistance. Table 6.2.4 shows the defined parameters to realize the PBS assistance in these scenarios. Fig. 6.2.8 shows the results of the simulations on the scenario. Subfigure (a) and (b) respectively show the results of the conditions without and with PBS.

Table 6.2.4 Simulation conditions.

Description		Symbol	Value	Unit
Virtual darting-out object	Offset from the occluding object to trajectory	D_{vir_occ}	1.0	m
	Darting-out velocity	v_{vir}	3.0	m/s
	Darting-out direction	θ_{vir}	−90.0	deg
Terminal point	Direction	θ_{cross}	0.0	deg
	Distance parameter	d_{pre}	80.0	m
	Curvature	κ_f	0.0	1/m

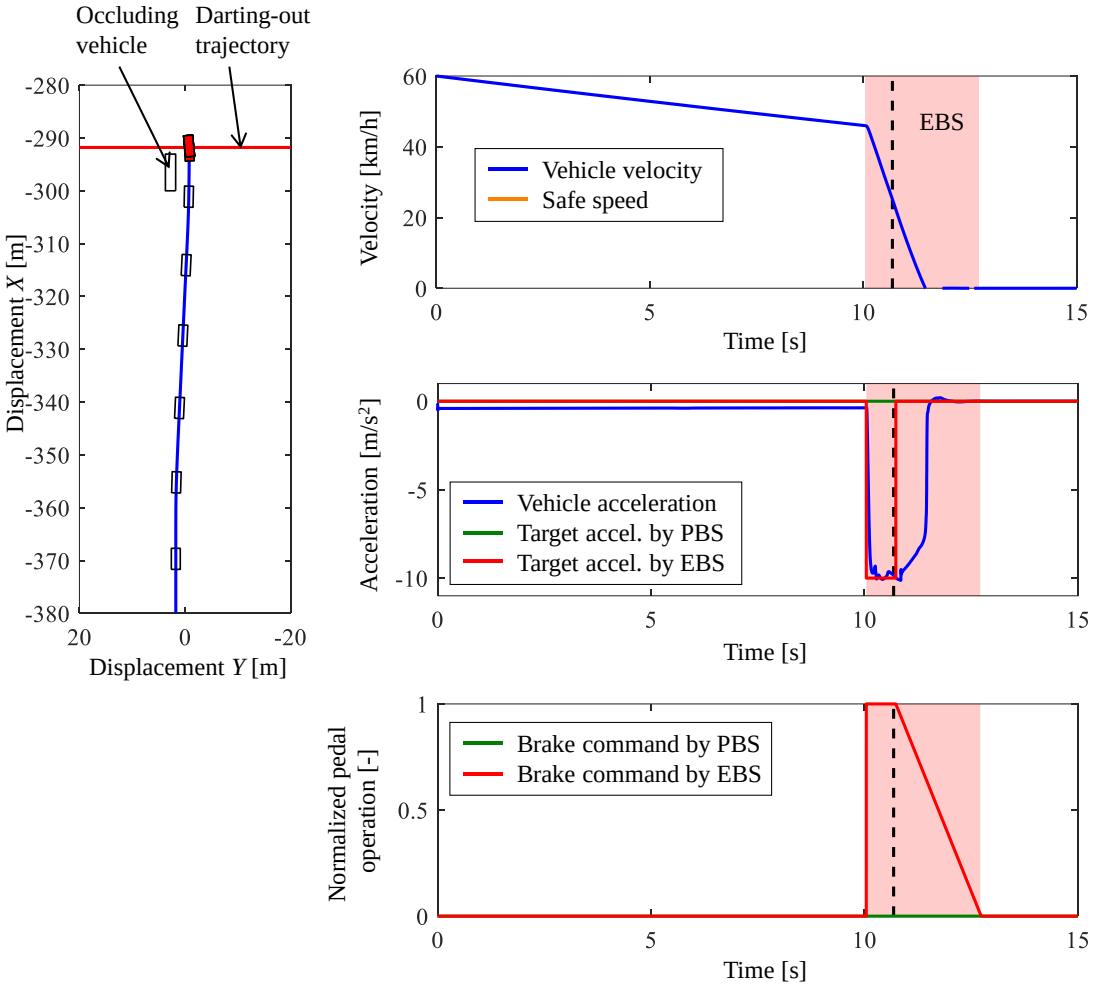

(a) The results with only EBS.

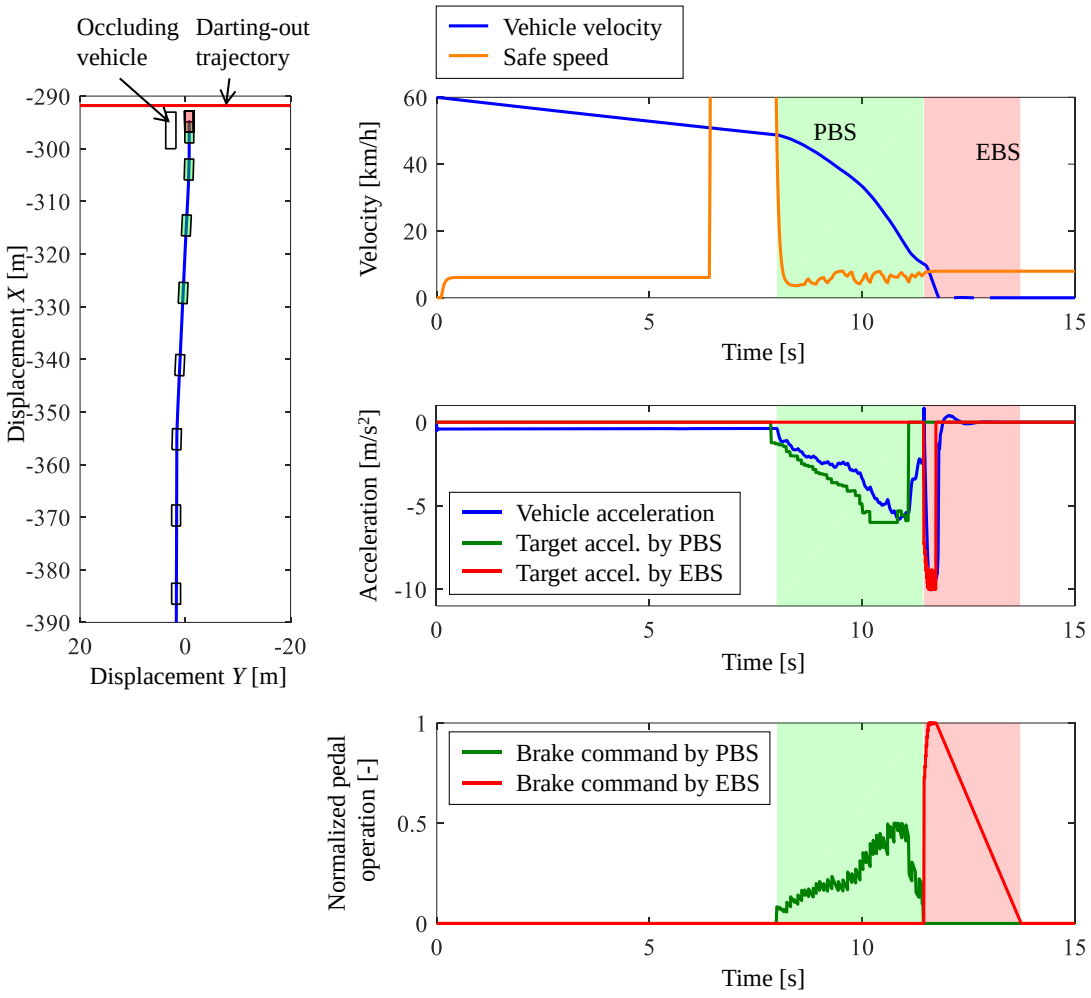

(b) The results with PBS+EBS.

Fig. 6.2.8 Simulation results: overtaking the parked vehicle.

The results showed the PBS could assist to decelerate the vehicle speed to the safe speed to avoid the collision in the overtaking scenario. As indicated in the figure of velocity, the safe speed is not very unstable despite the difficulty of the trajectory prediction at the overtaking scenario. This indicates that the Triclothoidal curve was effective not only for predicting the right-turn trajectory but also for the overtaking scenario.

6.2.4 Blind Curve

Fig. 6.2.9 (a) shows a scenario when the vehicle going into the left-curve and there is an intersection during the curve. By the intersection, an obstacle is standing on the left side of the road and making a blind spot. In this scenario, a vehicle may cross the ego-lane from the blind spot of the crossing road at the intersection. The trajectory of the virtual darting-out object and the terminal conditions of this case are defined as indicated in Fig. 6.2.9 (b). The virtual darting-out object was set to dart out from the crossing road parallelly to the direction of the crossing road. The terminal point of the Triclothoidal curve is defined that the point on the lane-center of the ego-lane. And the turning curvature at the terminal point is defined as the curvature of the curve. Table 6.2.5 shows the parameters defined for driver assistance in the scenario.

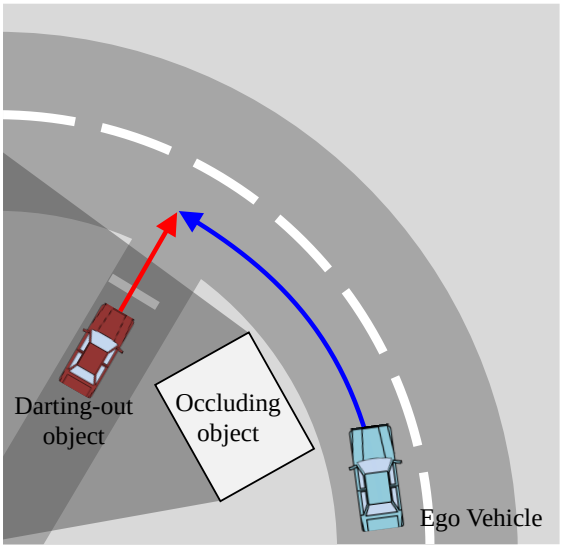

(a) Bird's eye view of the scenario.

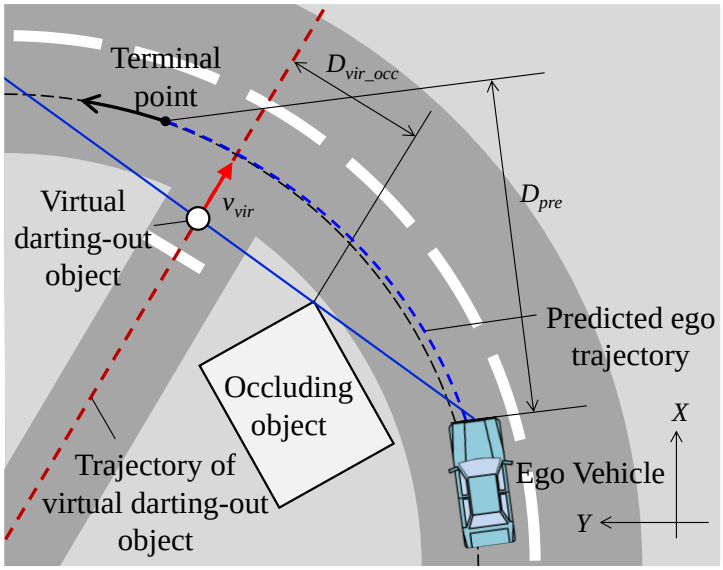

(b) Schematic definitions of the trajectory of the virtual darting-out object and terminal point.

Fig. 6.2.9 Left curve with a blind spot. A vehicle may cross the ego-lane from the blind spot of the crossing road at the intersection.

Under the scenarios, the vehicle which equips only an autonomous emergency braking system (EBS) cannot avoid the collision with the darting-out object when the drivers do not correctly predict the potential risk at the scenario. The simulations show the example cases that generalized PBS enabled collision avoidance by the moderate brake assistance. Table 6.2.5 shows the defined parameters to realize the PBS assistance in these scenarios. Fig. 6.2.9 shows the results of the simulations on the scenario. Subfigure (a) and (b) respectively show the results of the conditions without and with PBS.

Table 6.2.5 Simulation conditions.

Description		Symbol	Value	Unit
Virtual darting-out object	Offset from the occluding object to trajectory	D_{vir_occ}	3.0	m
	Darting-out velocity	v_{vir}	10.0	m/s
	Darting-out direction	θ_{vir}	−90	deg
Terminal point	Direction	θ_{cross}	60	deg
	Distance parameter	d_{pre}	80.0	m
	Curvature	κ_f	0.0102	1/m

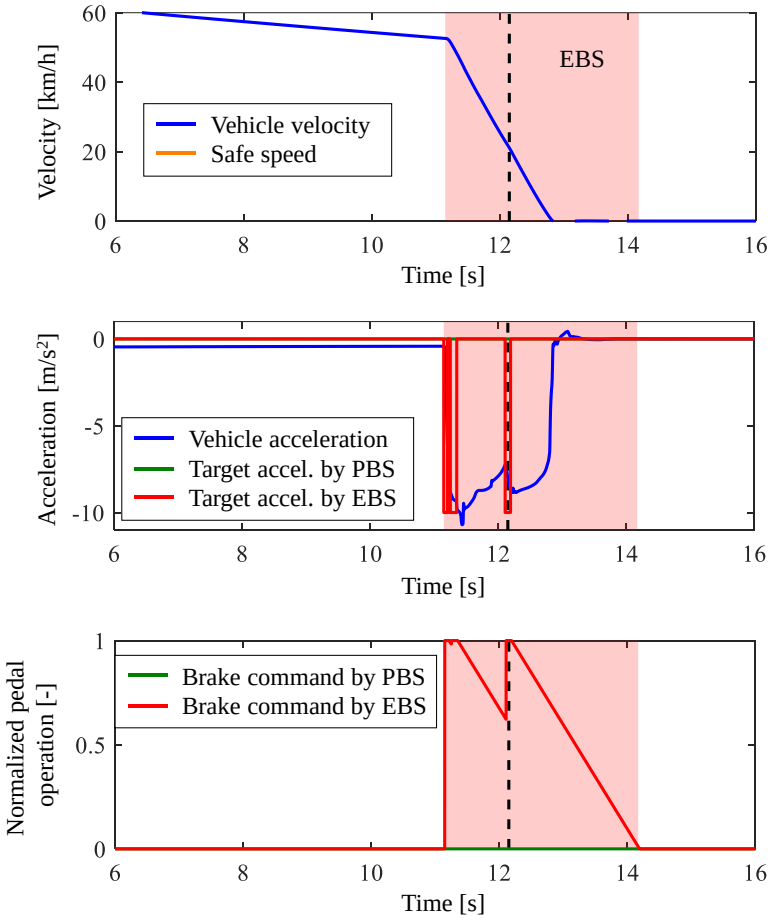

(a) The results with only EBS.

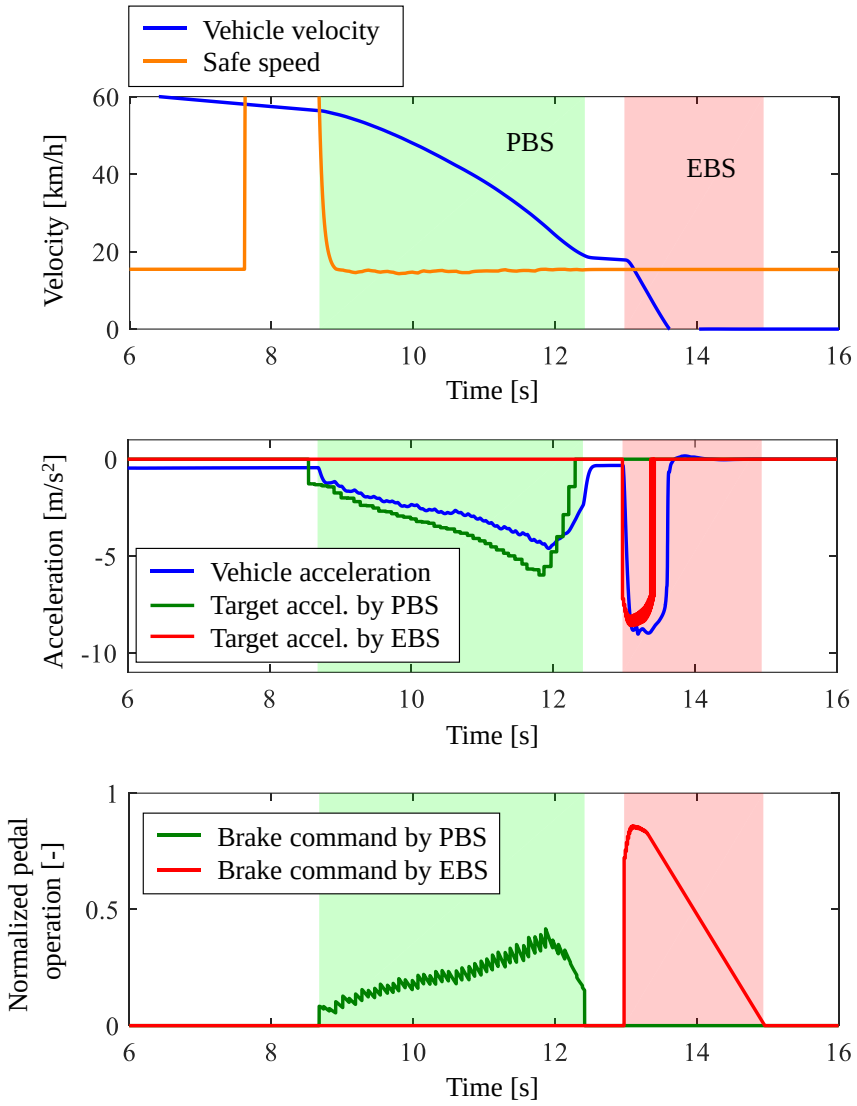

(b) The results with PBS+EBS.

Fig. 6.2.10 Simulation results: a curve with a blind spot.

The results showed that the PBS could effectively reduce the collision risk by deceleration assistance in the curve area. Also, the calculated safe speed was very stable even in the curve scenario. Because the course was a continuous curve with a constant turning radius, and the Triclothoidal curve can also predict the circular curve trajectory by considering the terminal curvature.

6.2.5 Passing Through Traffic Jam in Large Intersection

The last scenario is a scenario passing through a large intersection with a traffic jam. As shown in Fig. 6.2.11 (a), when a right-side lane is congested, and a left-lane (ego-lane) is not, sometimes vehicles on the left-lane go into the intersection at high speed. However, an oncoming vehicle may make a right turn at the intersection and may across the ego-lane and it causes a serious accident. This scenario is the same as scenario (ii) in Section 6.2.1, but the situation is the opposite. In this case, PBS also can assist the safe driving before causing an accident. As same as the definitions in Section 6.2.2, the occluding object and the direction of the crossing road define the trajectory of the virtual darting-out object. To simplify the

problem, the virtual darting-out trajectory defines the straight trajectory. The terminal point positions of the Triclothoidal curve are defined as the center position of the ego-lane and the point that has a distance d_{pre} from the ego vehicle position as shown in Fig. 6.2.11 (b).

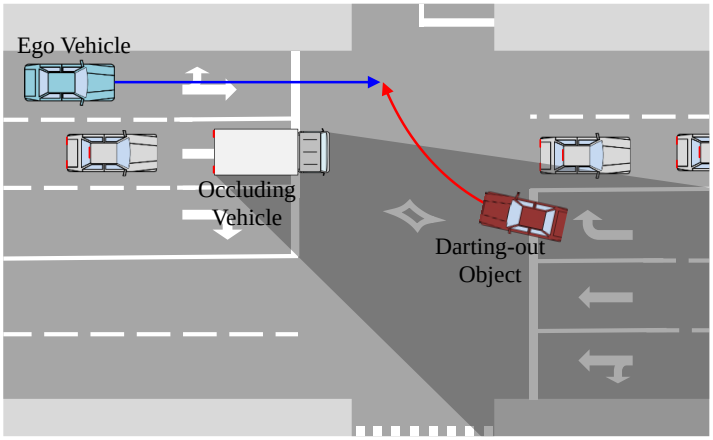

(a) Bird's eye view of the scenario.

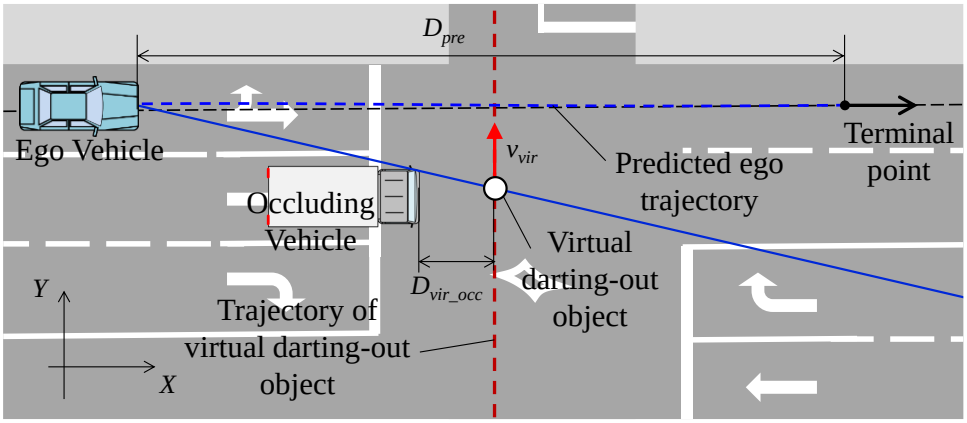

(b) Schematic definitions of the trajectory of the virtual darting-out object and terminal point.

Fig. 6.2.11 Passing through a traffic jam in a large Intersection. An oncoming vehicle may make a right-turn and dart out from the blind spot behind the traffic jam.

Under the scenarios, the vehicle which equips only an autonomous emergency braking system (EBS) cannot avoid the collision with the darting-out object when the drivers do not correctly predict the potential risk at the scenario. The simulations show the example cases that generalized PBS enabled collision avoidance by the moderate brake assistance. Table 6.2.6 shows the defined parameters to realize the PBS assistance in these scenarios. Fig. 6.2.12 shows the results of the simulations on the scenario. Subfigure (a) and (b) respectively show the results of the conditions without and with PBS.

Table 6.2.6 Simulation conditions.

Description		Symbol	Value	Unit
Virtual darting-out object	Offset from the occluding object to trajectory	D_{vir_occ}	3.0	m
	Darting-out velocity	v_{vir}	10.0	m/s
	Darting-out direction	θ_{vir}	90	deg
Terminal point	Direction	θ_{cross}	0	deg
	Distance parameter	d_{pre}	80.0	m
	Curvature	κ_f	0	1/m

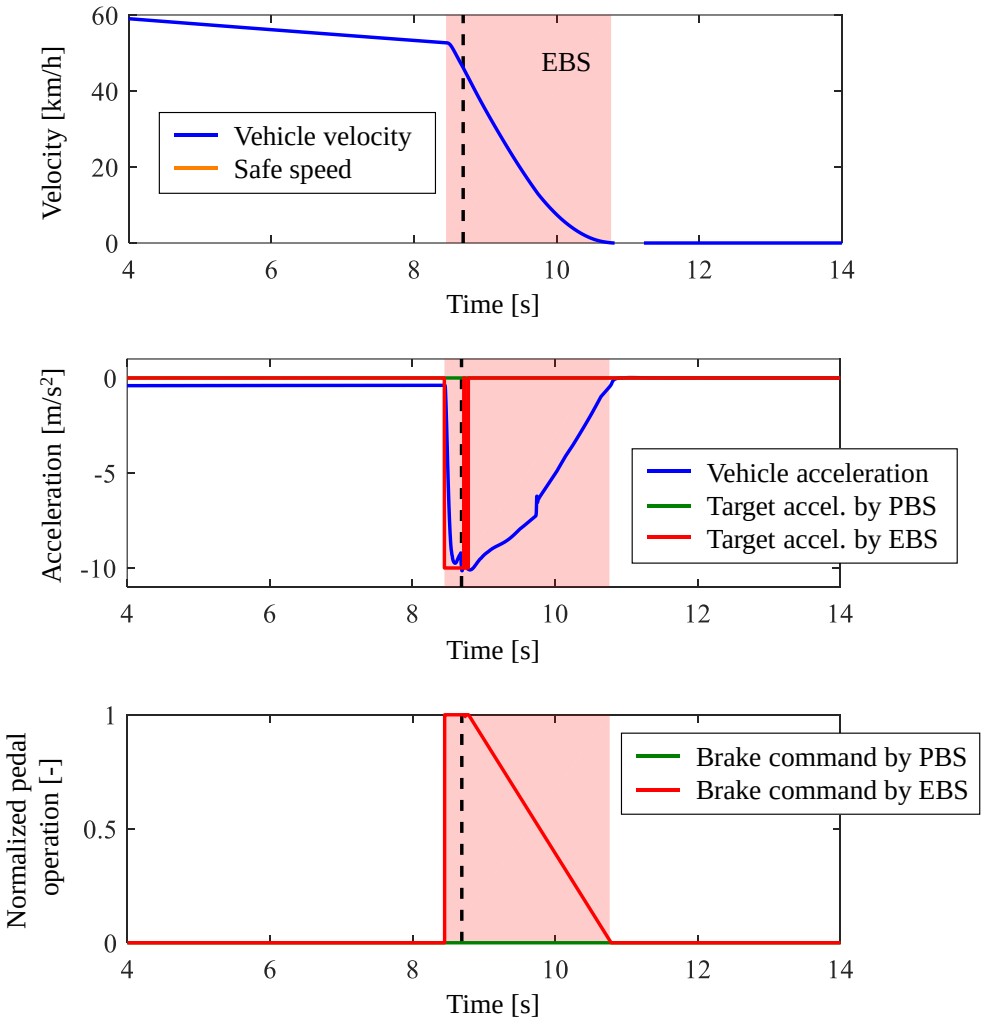

(a) The results with only EBS.

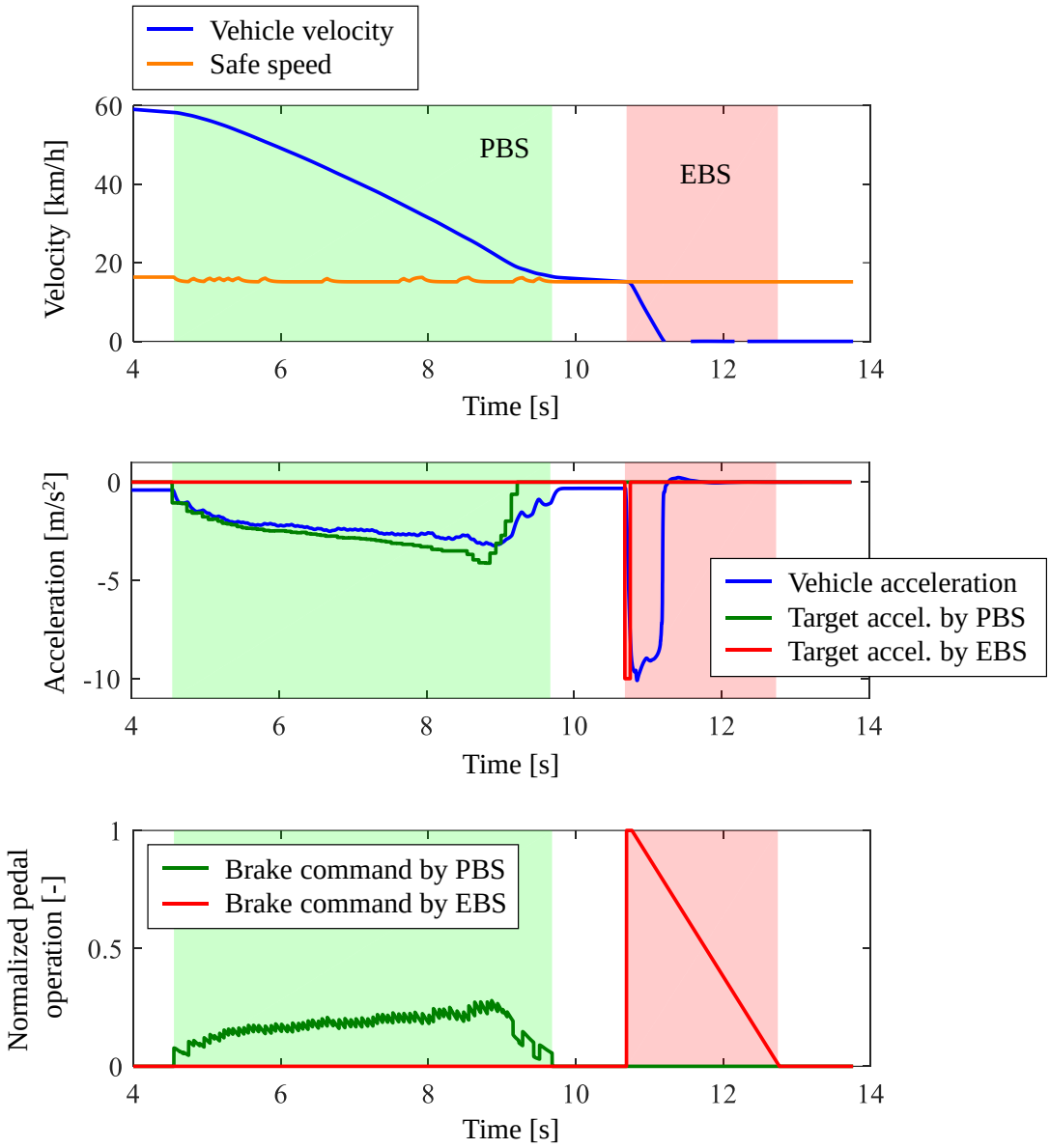

(b) The results with PBS+EBS.

Fig. 6.2.12 Simulation results: passing through a large intersection with a traffic jam.

The results showed the PBS could assist to decelerate the vehicle speed to the safe speed with moderate braking. The safe speed was calculated by simplifying the virtual darting trajectory to the straight trajectory. Thus, the accuracy of the safe speed may not be high, however, by combining the warnings, the collision avoidance effect can be expected. Moreover, if the oncoming traffic that makes a right-turn also equips the PBS, the traffic accidents at the right-turn scenario with blind spot will be firmly avoided.

6.3 Conclusion

To generalize the Proactive Braking System (PBS), this chapter redesigned the function to adapt to the other possible risk predictive scenarios not only in the right-turn scenarios. The proposal enables the function adoptive to the other cases by defining the several parameters that defining the darting-out

trajectory of the virtual darting-out object and the terminal point of the Triclothoidal curve. To demonstrate the collision avoidance with the generalized PBS, we prepared the representative risk predictive driving scenarios with a blind spot in an urban area on the full-vehicle simulations. The full-vehicle simulations showed the proposals effectively reduced the speed to the calculated safe speed at each risk predictive scenario. And the proposals could assist the collision avoidance by the moderate braking before the darting-out object detection. From those results, the proposed advanced driver assistance system expected to make the driving intersections are much safer even there have blind spots.

This page is intentionally left blank.

7. Summary and Outlook

7.1 Summary

Reducing road traffic accidents is a worldwide topic for human beings. The number of traffic accident fatalities tends to be decreasing in Japan, United States, and Europe; however, the number of fatalities is still enormous. In order to accomplish a society with zero traffic accident fatality and heavy injury, Vision Zero has been adopted by many countries.

Focusing on the locations of road traffic fatal accidents, most traffic accident fatalities have died on the non-motorway roads. Therefore, reducing traffic accidents on non-motorway roads is effective to reduce total traffic accident fatalities. Especially, in the non-motorway roads such as urban roads or rural roads, statistics revealed that the turnings at the intersections are one of the riskiest scenarios.

As to be the countermeasure to reduce the worldwide social and health problem, road traffic accidents, plenty of challenges to develop Advanced Driver Assistance Systems (ADAS) have been conducted. And currently, a lot of ADAS are now on the market. However, most of those commercialized ADAS have been biased to the normal driving function in no risk condition or emergency function. On the other hand, to drive the urban roads safely, it is important to predict the potential risks before getting into an emergency situation. We called this driving skill “risk predictive driving” and focused on the risk predictive scenarios.

As the related research especially focusing on the risk predictive driving scenario, two groups of the ADAS were presented: the system using V2V/V2I communication and the system without depending on the communication technology.

This thesis focused on the latter technology without communication. We defined the target scenario which is a motorcycle darting-out scenario from the blind spot of the stopping oncoming vehicle while the ego vehicle makes an intersection right-turn (in left-hand traffic). And proposed an ADAS that assists the driver to make a safe intersection right turning by potential risk prediction. As to design the ADAS, the following questions were addressed in this thesis:

- How can the system define and predict the darting-out risk quantitatively before detecting the darting-out?
- How can the system be consistent with both “safety” and “driver acceptance” simultaneously?
- How can the “safety” and “driver acceptance” of the ADAS be proved by the simulation?

Those questions are solved by the following proposals.

Our proposal ADAS, Proactive Braking System (PBS) was designed to minimize the potential risk in the target scenario in the intersection right-turn. When the ego vehicle intends to make a right turn at the intersection, assuming a virtual darting-out object is darting-out from the blind spot. By predicting the conflict point between the ego vehicle and the virtual darting-out object, the safe speed that can stop the collision by emergency braking if the virtual darting-out object darts out can be geometrically derived. This safe speed is the physically highest speed that can be avoided by the emergency braking if there is a darting-out, thus, the question, *How can the system define and predict the darting-out risk quantitatively before detecting the darting-out?*, was solved by defining the potential risk as a darting-out of the virtual darting-out object and quantitatively predicted the risk by introducing the safe speed.

Reducing the excessive intervention opportunity is one solution to enhance the “driver acceptance” of the system. In order to reduce that opportunity, the system must calculate the safe speed accurately. In other words, we must calculate the safe speed as high as possible but can guarantee safety. Therefore, the

important point to calculate the safe speed accurately is obtaining the high accuracy conflict point prediction. To predict the conflict point, accurately, we proposed an ego trajectory prediction method by applying the Triclothoidal curve. This curve generates a smooth curve to connect to the terminal position considering the steering input of the ego vehicle. The prediction accuracy of the trajectory prediction with the Triclothoidal curve was evaluated by the driving data acquired from the data acquisition driving in the real city traffic. From the evaluations, the accuracy of the Triclothoidal trajectory was higher than the conventional trajectory prediction methods. As an answer to the question, *How can the system be consistent with both "safety" and "driver acceptance" simultaneously?*, we accomplished the proposal to be consistent with both "safety" and "acceptable", by calculating the safe speed with high accuracy and minimizing the invention opportunity.

To answer the question *How can the "safety" and "driver acceptance" of the ADAS be proved by the simulation?*, by using the proposed ADAS above, we evaluated the effectiveness of the system from two aspects: "safety" and "driver acceptance". Regarding the evaluation of "safety", to conduct the effectiveness evaluations in various conditions in a short time, all of the evaluations were conducted in the virtual world using the full-vehicle simulation. These simulation conditions covered the various combinations of the intersection shapes, positions of the occluding vehicle, darting-out speeds, and collision positions. About 1300 simulation cases were conducted. Conducting this number of experiments with a real test vehicle requires a large effort. In terms of "safety", these simulations covered very wide ranges of daring-out scenarios, thus it can be said that the "safety" of the PBS is accepted. In terms of the "driver acceptance", we conducted the subject driver acceptance experiments with the real experiment vehicle and the driving simulator. Two experiments revealed that most subjects did not realize the PBS intervention itself, but when the drivers did not understand the system correctly there were conflicts between the system and the driver, and the acceptance became lower. In the second driver acceptance experiment that used the driving simulator, the results indicated that the proposed driver assistance system is highly accepted.

7.2 Outlook

- Implying the PBS to a passenger vehicle and Vehicle-in-the-Loop experiments in the test track.

We conducted the experiments with the real experiment vehicle as described in Section 5.2 in Chapter 5, but the experiment focused on the driver acceptance of the concept of the PBS. Therefore, problems on the object detection, ego localization, and validity of system parameter setting have not been clear yet. Implying the PBS to a real passenger vehicle with the emergency braking for intersection turning may give us the solutions to the problems. Besides, the implementation of the PBS enables us to conduct the vehicle-in-the-loop (VIL) simulations for further evaluations. By applying the darting-out object in the virtual world, the collision avoidance evaluations can safely evaluate the validity of the system parameter settings.

- Further discussions on the tasks to put the PBS into the market.

This thesis did not cover the tasks to be commercialized. Further discussions on the tasks to put the PBS into the market may point out the following topics. How to obtain the intersection geometry parameters, the validity of the speed of virtual darting-object, price, the necessity of the additional sensors, and system handling when GNSS is not available.

Acknowledgment

I would like to express the deepest gratitude to the people who have helped me undertake this research, complete this dissertation, and supported my student life. The following researchers particularly help and support to accomplish the research goal and to complete this dissertation paper:

Smart Mobility Research Center, Tokyo University of Agriculture and Technology

My supervisors **Prof. Pongsathorn Raksincharoensak** and **Prof. Hiroshi Mouri**, have brought me consistent guidance and advice for six years since I had been an undergraduate student. Their advice helped me many times, not only about the research but also about the attitude as a professional scientist, engineer, and mature person.

My committee members **Prof. Yasutaka Tagawa**, **Prof. Takayoshi Kamada**, and **Assoc. Prof. Masayoshi Wada** advised me to write my dissertation a good one.

Prof. Masao Nagai brought me ideas for my research and future decisions (especially regarding my internship in Germany).

Dr. Shunsaku Arita, National Defense Academy of Japan, contributed very deeply to my research. His accurate advice always helped me understand the problem correctly and essentially.

Dr. Xingguo Zhang gave me many ideas for the future research plan. And thank you very much for helping me when I moved to the new place. I'm glad to have a very kind and splendid colleague and neighbor :)

Dr. Xun Shen lectured me on optimal control. Thank you for sharing the many ideas that directed my future research topic. Shen-san, I am looking forward to researching with you.

Ms. Yoko Hojo cooperated in my experiments as voice guidance. Due to the COVID-19 pandemic, we used recorded audio guidance during the experiments to avoid conversation. She has recorded and prepared the audio guidance.

Assoc. Prof. Yasuhiro Akagi, Nagoya University, and **Dr. Keisuke Kazama**, Seikei University, helped me prepare the experiment vehicle.

And laboratory staffs and students: **Ms. Yoko Homma**, **Mr. Yutaka Hamaguchi**, **Mr. Rei Kato**, **Mr. Yuki Sekimoto**, **Mr. Hidetoshi Takemura**, **Mr. Shoi Furukawa**, **Mr. Sota Ishimoto**, **Mr. Toshinori Kojima**, **Mr. Takumi Takahashi**, **Mr. Ryota Abe**, **Mr. Yusuke Iyobe**, **Mr. Itsuki Miyazaki**, **Mr. Yo Sanogawa**, **Ms. Yuri Sugitan**, **Mr. Hiraki Watanabe**, **Dr. Mitsunobu Fujita**, **Ms. Yukiko Okita**, **Mr. Masaki Nazumi**, **Dr. Shigeyoshi Tsutsumi** (Mie University), **Dr. Akito Yamasaki** (Meijo University), **Dr. Yuichi Saito** (University of Tsukuba), **Dr. Keisuke Shimono** (University of Tokyo) and more.

Institut für Fahrzeugtechnik (IfF), Technische Universität Braunschweig

A thank you to the following members of IfF for the academic supports, hospitality, and the best friendship.

Especially I thank **apl. Prof. -Ing. Roman Henze** and **Prof. Dr.-Ing. Ferit Küçükay** for bringing me the great opportunity to do the international collaborative research project at TU Braunschweig. I could not finish my Ph.D. work without their cooperation.

Dr. -Ing. Adrian Sonka advised my research project from various aspects and helped me prepare for the experimental environment. I am waiting the day to do bouldering again in "Greifhaus" :D

Mr. Florian Krauns, Volkswagen AG, and **Mr. Toni Lubiniecki** helped me set up and conduct the

experiment.
Mr. Holger Znamiec, Volkswagen AG, supported me not only in the research. I still remember the day clearly when we were driving with Volvo on the Autobahn.
Mr. Maximilian Flormann supported my daily life in Braunschweig. It was a nice opportunity that I could help translate your application into Japanese.
And laboratory staffs (Mitarbeiter): **Mr. Thorsten Meister**, **Ms. Silvia Thal**, and **Mr. Marcel Kascha**.

Continental, Continental Japan, Continental Teves

Collaborative researches with Continental and Continental Japan gave me many opportunities to complete my project. Internship experience in Continental Teves was a great chance to learn the cutting-edge technologies in automotive engineering. I would like to express the appreciation for the following researchers: **Mr. Rolf Adomat** (Continental), **Mr. Dirk Ulbricht** (Continental), **Dr. Noriaki Itagaki** (Continental Japan), **Mr. Kazuhiro Oda** (Continental Japan), **Mr. Tetsuya Ehira** (Continental Japan), **Dr. Matthias Schreier** (Continental Teves), **Mr. Gary Parks** (Continental Japan), **Mr. Judhi Hallim** (Continental), and **Mr. Robert Morris** (Continental USA).

Finally, I am extremely thankful to my **family**. I could have kept going in the long and competitive student years because I always had big cheer from my loving family, and I had a house to come back to. Once I proposed to go to a doctor course to my family, no one stopped me, even slowed me down. I could not have completed the doctor's work and this dissertation without the support from my family. Thank you very much.

This research was financially supported as a JSPS Research Fellows by **JSPS KAKENHI Grant Number JP19J13748**.

Reference

[1] World Health Organization, “Road traffic injuries,” https://www.who.int/news-room/fact-sheets/detail/road-traffic-injuries [Accessed on 2020/11/10].

[2] World Health Organization, “Global Status Report on Road Safety 2018,” 2018, pp. 3-18.

[3] World Health Organization, “Road safety: a public health issue,” https://www.who.int/features/2004/road_safety/en/ [Accessed on 2020/11/10].

[4] 警察庁交通局, “令和元年中の交通死亡事故の発生状況及び道路交通法違反取締り状況等について,” pp.2, 2020. (In Japanese)

[5] Cabinet Office, “White Paper on Traffic Safety,” 2019, pp. 4.

[6] 内閣府, “令和 2 年版交通安全白書,” 2020, pp. 47-48. (In Japanese)

[7] 内閣府, “平成 20 年度版交通安全白書,” 2009, pp. 22-34. (In Japanese)

[8] Eurostat, “Road accident fatalities - statistics by type of vehicle,” https://ec.europa.eu/eurostat/statistics-explained/index.php/Road_accident_fatalities_-_statistics_by_type_of_vehicle [Accessed on 2020/11/10].

[9] Eurostat, “Persons killed in road accidents by type of vehicle (CARE data),” https://ec.europa.eu/eurostat/databrowser/view/tran_sf_roadve/default/table?lang=en [Accessed on 2020/11/10].

[10] European Parliament, “Road fatality statistics in the EU (infographic),” https://www.europarl.europa.eu/news/en/headlines/society/20190410STO36615/road-fatality-statistics-in-the-eu-infographic [Accessed on 2020/11/10].

[11] National Highway Traffic Safety Administration (NHTSA), “Early Estimate of Motor Vehicle Traffic Fatalities in 2019,” 2020, pp. 1-3.

[12] International Transport Forum (ITF), “Road Safety Annual Report 2019,” 2019, pp. 8-15.

[13] International Transport Forum (ITF), “Road Safety Annual Report 2019 France,” 2019, pp. 1-19.

[14] International Transport Forum (ITF), “Road Safety Annual Report 2019 Germany,” 2019, pp. 1-14.

[15] International Transport Forum (ITF), “Road Safety Annual Report 2019 Italy,” pp. 1-14, 2019.

[16] International Transport Forum (ITF), “Road Safety Annual Report 2019 Japan,” 2019, pp.1-13.

[17] International Transport Forum (ITF), “Road Safety Annual Report 2019 Korea,” 2019, pp. 1-14.

[18] International Transport Forum (ITF), “Road Safety Annual Report 2019 Spain,” 2019, pp. 1-16.

[19] International Transport Forum (ITF), “Road Safety Annual Report 2019 Sweden,” 2019, pp. 1-18.

[20] International Transport Forum (ITF), “Road Safety Annual Report 2019 United Kingdom,” pp.1-14, 2019.

[21] International Transport Forum (ITF), “Road Safety Annual Report 2019 USA,” 2019, pp. 1-18.

[22] International Transport Research Documentation, “Government Status Report of Republic of Korea,” https://trid.trb.org/view/1498057 [Accessed on 2020/11/16].
[23] C. Tingvall and N Haworth, “Vision Zero - An Ethical Approach to Safety and Mobility,” in the 6th ITE International Conference Road Safety & Traffic Enforcement: Beyond 2000, Melbourne, 1999.
[24] World Health Organization, “Global Status Report on Road Safety 2018,” 2018, pp. 14-21.
[25] 警察庁交通局, “令和元年中の交通死亡事故の発生状況及び道路交通法違反取締り状況等について,” pp.33, 2020. (In Japanese)
[26] National Highway Traffic Safety Administration (NHTSA), “Traffic Safety Facts 2017 A Compilation of Motor Vehicle Crash Data,” 2019, pp.74.
[27] National Highway Traffic Safety Administration (NHTSA), Crash Factors in Intersection-Related Crashes: An On-Scene Perspective, 2010, pp. 1-23.
[28] H. Gstalter and W. Fastenmeier, “Reliability of drivers in urban intersections,” Accident Analysis & Prevention, Volume 42 (1), 2010, pp. 225-234, https://doi.org/10.1016/j.aap.2009.07.021.
[29] 公益財団法人交通事故総合分析センター (ITARDA), “信号交差点における事故発生状況と人的要因分析—四輪車から見た事故発生要因の分析—,” 2012, pp. 1-173. (In Japanese)
[30] R. Kala, “On-Road Intelligent Vehicles,” Butterworth-Heinemann, 2016, Ch. 4, Pages 59-82, https://doi.org/10.1016/B978-0-12-803729-4.00004-0.
[31] SAE International, “SAE Standards News: J3016 automated-driving graphic update,” https://www.sae.org/news/2019/01/sae-updates-j3016-automated-driving-graphic [Accessed on 2020/11/10].
[32] Yano Research Institute Ltd., “Global Market of ADAS & Autonomous Driving Systems: Key Research Findings 2019,” Press Release, No. 2134, https://www.yanoresearch.com/en/press-release/show/press_id/2134 [Accessed on 2020/11/10].
[33] Euro NCAP, “2020 Assisted Driving Tests,” https://www.euroncap.com/en/vehicle-safety/safety-campaigns/2020-assisted-driving-tests/ [Accessed on 2020/11/10].
[34] Euro NCAP, “Euro NCAP 2025 Roadmap,” 2017, pp. 1-19.
[35] Euro NCAP, “2018 Automated Driving Tests,” https://www.euroncap.com/en/vehicle-safety/safety-campaigns/2018-automated-driving-tests/ [Accessed on 2020/11/10].
[36] W. Vlakveld, “Hazard Anticipation of Young Novice Drivers,” SWOV, 2011, pp. 13-20.
[37] P. Raksincharoensak, I. Iwasawa and M. Nagai, “Hazard-Anticipatory Braking Assistance System in Unsignalized Intersection Based on Driving Data of Expert Drivers,” Transactions of the Japan Society of Mechanical Engineers Series C, 2013, Vol. 79, pp. 4802-4817, https://doi.org/10.1299/kikaic.79.4802.
[38] A. Mahmood, W.E. Zhang and Q.Z. Sheng, “Software-Defined Heterogeneous Vehicular Networking: The Architectural Design and Open Challenges,” Future Internet 2019, 2019, Vol. 11 (3), pp. 1-17. https://doi.org/10.3390/fi11030070
[39] J. Wang, Y. Shao, Y. Ge and R. Yu, “A Survey of Vehicle to Everything (V2X) Testing,” Sensors 2019, Vol. 19 (2), pp. 1-20, https://doi.org/10.3390/s19020334.
[40] J. Harding, G. Powell, R. Yoon et al., “Vehicle-to-Vehicle Communications: Readiness of

V2V Technology for Application," DOT HS 812 014, 2014, pp. 119-132.

[41] F. Li, R. Zhang and F. You, "Fast pedestrian detection and dynamic tracking for intelligent vehicles within V2V cooperative environment," IET Image Processing, 2017, Vol. 11 (10), pp. 833-840, http://dx.doi.org/10.1049/iet-ipr.2016.0931.

[42] R. Dang, J. Ding, B. Su, Q. Yao, Y. Tian and K. Li, "A lane change warning system based on V2V communication," 17th International IEEE Conference on Intelligent Transportation Systems (ITSC), Qingdao, 2014, pp. 1923-1928, doi: 10.1109/ITSC.2014.6957987.

[43] K. Emara, "Safety-aware Location Privacy in Vehicular Ad-hoc Networks," Ph.D. Thesis, Fakultät für Informatik, Technische Universität München, 2016, pp. 1-40, https://www.researchgate.net/publication/312499042_Safety-aware_Location_Privacy_in_Vehicular_Ad-hoc_Networks [Accessed on 2020/11/10].

[44] J. Ibanez-Guzman, S. Lefevre, A. Mokkadem and S. Rodhaim, "Vehicle to vehicle communications applied to road intersection safety, field results," 13th International IEEE Conference on Intelligent Transportation Systems, Funchal, 2010, pp. 192-197, doi: 10.1109/ITSC.2010.5625246.

[45] M. Abudulla, H. Wymeersch, "Fine-Grained Reliability for V2V Communications around Suburban and Urban Intersections," IEEE Transactions on Wireless Communications, 2017, pp. 1-27, https://arxiv.org/abs/1706.10011.

[46] United States Department of Transportation, "Cooperative Intersection Collision Avoidance Systems (CICAS)", https://www.its.dot.gov/research_archives/cicas/ [Accessed on 2020/11/16].

[47] V. Milanés, S. E. Shladover, J. Spring, C. Nowakowski, H. Kawazoe and M. Nakamura, "Cooperative Adaptive Cruise Control in Real Traffic Situations," in IEEE Transactions on Intelligent Transportation Systems, 2014, Vol. 15, No. 1, pp. 296-305, doi: 10.1109/TITS.2013.2278494.

[48] J. Ploeg, B. T. M. Scheepers, E. van Nunen, N. van de Wouw and H. Nijmeijer, "Design and experimental evaluation of cooperative adaptive cruise control," 2011 14th International IEEE Conference on Intelligent Transportation Systems (ITSC), Washington, DC, 2011, pp. 260-265, doi: 10.1109/ITSC.2011.6082981.

[49] B. van Arem, C. J. G. van Driel and R. Visser, "The Impact of Cooperative Adaptive Cruise Control on Traffic-Flow Characteristics," in IEEE Transactions on Intelligent Transportation Systems, 2006, Vol. 7, No. 4, pp. 429-436, doi: 10.1109/TITS.2006.884615.

[50] Z. Wang, G. Wu and M. J. Barth, "A Review on Cooperative Adaptive Cruise Control (CACC) Systems: Architectures, Controls, and Applications," 2018 21st International Conference on Intelligent Transportation Systems (ITSC), Maui, HI, 2018, pp. 2884-2891, doi: 10.1109/ITSC.2018.8569947.

[51] I. H. Zohdy, R. K. Kamalanathsharma and H. Rakha, "Intersection management for autonomous vehicles using iCACC," 2012 15th International IEEE Conference on Intelligent Transportation Systems, Anchorage, AK, 2012, pp. 1109-1114, doi: 10.1109/ITSC.2012.6338827.

[52] L. Wang, A. Afanasyev, R. Kuntz, R. Vuyyueu, R. Wakikawa and L. Zhang, "Rapid Traffic Information Dissemination Using Named Data," NoM '12: Proceedings of the 1st ACM workshop on Emerging Name-Oriented Mobile Networking Design - Architecture,

Algorithms, and Applications, 2012, pp. 7-12, https://doi.org/10.1145/2248361.2248365.
[53] B. Maitipe, U. Ibrahim and M. I. Hayee, “Development and Field Demonstration of DSRC Based V2V-Assisted V2I Traffic Information System for the Work Zone,” Intelligent Transportation Systems Institute, Center for Transportation Studies, University of Minnesota, 2012, pp. 1-31.
[54] V. D. Khairnar, S. N. Pradhan, “V2V Communication Survey - (Wireless Technology),” International Journal of Computer Technology & Applications, 2014, Vol. 3 (1), pp. 370-373.
[55] J. Jang, K. Choi and H. Cho, “A Fixed Sensor-Based Intersection Collision Warning System in Vulnerable Line-of-Sight and/or Traffic-Violation-Prone Environment,” in IEEE Transactions on Intelligent Transportation Systems, 2012, Vol. 13, No. 4, pp. 1880-1890, doi: 10.1109/TITS.2012.2207952.
[56] A. Colombo and H. Wymeersch, “Cooperative Intersection Collision Avoidance in a Constrained Communication Environment,” 2015 IEEE 18th International Conference on Intelligent Transportation Systems, Las Palmas, 2015, pp. 375-380, doi: 10.1109/ITSC.2015.70.
[57] Ching-Yao Chan, “Defining Safety Performance Measures of Driver-Assistance Systems for Intersection Left-Turn Conflicts,” 2006 IEEE Intelligent Vehicles Symposium, Tokyo, 2006, pp. 25-30, doi: 10.1109/IVS.2006.1689600.
[58] L. Le, A. Festag, R, Baldessari and W. Zhang, “V2X Communication and Intersection Safety,” 13th International Forum on Advanced Microsystems for Automotive Applications 2009, Germany 2009, 97-103.
[59] A. Kaadan and H. H. Refai, “iICAS: Intelligent intersection collision avoidance system,” 2012 15th International IEEE Conference on Intelligent Transportation Systems, Anchorage, AK, 2012, pp. 1184-1190, doi: 10.1109/ITSC.2012.6338750.
[60] M. Maile and L. Delgrossi, “Cooperative Intersection Collision Avoidance System for Violations (CICAS-V) for Avoidance of Violation-Based Intersection Crashes”, 2009, pp. 1-14.
[61] M. Maile et al., “Objective testing of a cooperative intersection collision avoidance system for traffic signal and stop sign violation,” 2011 IEEE Intelligent Vehicles Symposium (IV), Baden-Baden, 2011, pp. 130-137, doi: 10.1109/IVS.2011.5940431.
[62] S. Nakamura, H. Suganua, K. Kikuchi, R. Homma, “Effect Evaluation of Vehicle-Infrastructure Cooperative Right-Turn Collision Prevention System,” 自動車技術会論文集, 2015, Vol. 46, No. 2, pp. 449-454, https://doi.org/10.11351/jsaeronbun.46.449. (In Japanese)
[63] T. Maeda, S. Morita, M. Ikawa, Y. Tsuda, “DSSS on Board Unit,” Mitsubishi Denki Giho, 2010, Vol. 84, No. 9. (In Japanese)
[64] B. Roessler, K. Fuerstenberg, “Cooperative Intersection Safety – The EU project INTERSAFE-2,” Advanced Microsystems for Automotive Applications 2009, VDI-Buch Springer, 2009, pp. 77-86, https://doi.org/10.1007/978-3-642-00745-3_6.
[65] O. Aycard et al., "Intersection safety using lidar and stereo vision sensors," 2011 IEEE Intelligent Vehicles Symposium (IV), Baden-Baden, 2011, pp. 863-869, doi: 10.1109/IVS.2011.5940518.
[66] F. Krauns, R. Henze, F. Küçükay and P. Raksincharoensak, “Objectification of Automated Driving at Intersections,” in Proc. the 5th International Symposium on Future Active Safety

Technology toward Zero Accidents (FAST-zero ’19), Sept. 2019, Blacksburg, VA, USA.
[67] X. Zhao, J. Wang, G. Yin and K. Zhang, “Cooperative Driving for Connected and Automated Vehicles at Non-signalized Intersection based on Model Predictive Control,” 2019 IEEE Intelligent Transportation Systems Conference (ITSC), Auckland, New Zealand, 2019, pp. 2121-2126, doi: 10.1109/ITSC.2019.8916786.
[68] A. Weimerskirch, “V2X Security & Privacy: The Current State and Its Future,” in Proc. of 18th ITS World Congress, Orlando, 2011.
[69] Y. Yang, Z. Wei, Y. Zhang, H. Lu, K. R. Choo and H. Cai, “V2X security: A case study of anonymous authentication,” Pervasive and Mobile Computing, 2017, Vol. 41, pp. 259-269, https://doi.org/10.1016/j.pmcj.2017.03.009.
[70] F. A. Teixeira, V. F. e Silva, J. L. Leoni, D. F. Macedo, J. M.S. Nogueira, “Vehicular networks using the IEEE 802.11p standard: An experimental analysis,” Vehicular Communications, 2014, Vol. 1 (2), Pages 91-96, ttps://doi.org/10.1016/j.vehcom.2014.04.001.
[71] J. Engdahl (ed.) EG8 final report, “Final Review of draft UNI DSRC Specifications,” Prepared by Expert Group 8 working with support of the European Commission DG TREN on the work in Directive 2004/52/EC, 2005.
[72] Association of Radio Industries and Businesses (ARIB), “Dedicated Short-Range Communication System,” ARIB STANDARD, ARIB STD－T75, Ver. 1.0, 2001.
[73] ETC 総合情報ポータルサイト, “ETC 2.0 について”, https://www.go-etc.jp/etc2/index.html [Accessed on 2020/11/10]. (In Japanese)
[74] Qualcomm, “Cellular-V2X Technology Overview,” https://www.qualcomm.com/media/documents/files/c-v2x-technology-overview.pdf [Accessed on 2020/11/10].
[75] M. T. Kawser, M. S. Fahad, S. Ahmed, S. S. Sajjad and H. A. Rafi, “The Perspective of Vehicle-to-Everything (V2X) Communication towards 5G,” International Journal of Computer Science and Network Security (IJCSNS), 2019, Vol. 19, No. 4, pp. 146-155.
[76] Qualcomm, “Introduction to Cellular V2X,” https://www.qualcomm.com/media/documents/files/introduction-to-c-v2x.pdf [Accessed on 2020/11/16].
[77] TOYOTA, “ITS Connect,” https://toyota.jp/technology/safety/itsconnect/ [Accessed on 2020/11/10]. (In Japanese)
[78] HONDA, “信号情報活用運転支援システムの公道実証実験を 2014 年 4 月より開始～商品化に向けてシステムの効果を検証～,” ニュースリリース, 2014, https://www.honda.co.jp/news/2014/4140328.html [Accessed on 2020/11/10]. (In Japanese)
[79] 警察庁, “警察における ITS ,” https://www.npa.go.jp/bureau/traffic/seibi2/annzen-shisetu/utms/utms.html#syuryou [Accessed on 2020/11/10]. (In Japanese)
[80] G. Schildbach, M. Soppert and F. Borrelli, “A collision avoidance system at intersections using Robust Model Predictive Control,” 2016 IEEE Intelligent Vehicles Symposium (IV), Gothenburg, 2016, pp. 233-238, doi: 10.1109/IVS.2016.7535391.
[81] H. Yoshitake, M. Shino, “Risk assessment based on driving behavior for preventing collisions with pedestrians when making across-traffic turns at intersections,” IATSS Research, 2018, Vol. 42 (4), Pages 240-247, https://doi.org/10.1016/j.iatssr.2018.02.001.
[82] G. R. de Campos, A. H. Runarsson, F. Granum, P. Falcone and K. Alenljung, “Collision

avoidance at intersections: A probabilistic threat-assessment and decision-making system for safety interventions," 17th International IEEE Conference on Intelligent Transportation Systems (ITSC), Qingdao, 2014, pp. 649-654, doi: 10.1109/ITSC.2014.6957763.

[83] C. Rodemerk, H. Winner and R. Kastner, "Predicting the driver's turn intentions at urban intersections using context-based indicators," 2015 IEEE Intelligent Vehicles Symposium (IV), Seoul, 2015, pp. 964-969, doi: 10.1109/IVS.2015.7225809.

[84] M. Bareiss, J. Scanlon, R. Sherony and H. C. Gabler, "Crash and injury prevention estimates for intersection driver assistance systems in left turn across path/opposite direction crashes in the United States," Traffic Injury Prevention, 2019, Vol. 20, No. S1, pp. S133–S138, https://doi.org/10.1080/15389588.2019.1610945.

[85] Y. Saito and P. Raksincharoensak, "Shared Control in Risk Predictive Braking Maneuver for Preventing Collisions with Pedestrians," in IEEE Transactions on Intelligent Vehicles, 2016, Vol. 1, No. 4, pp. 314-324, doi: 10.1109/TIV.2017.2700210.

[86] T. Ito, M. Soya, K. Tohriyama, Y. Saito, T. Shimizu, A. Yamasaki, M. Nagai, H. Inoue and M. Kamata, "Evaluation of Acceptability of Adaptive Proactive Braking Intervention System Based on Risk Map for Elderly Drivers," International Journal of Automotive Engineering, 2020, Vol. 11, No. 2, pp. 40-48, https://doi.org/10.20485/jsaeijae.11.2_40.

[87] T. Shimizu and P. Raksincharoensak, "Motion planning via optimization of risk quantified by collision velocity accompanied with AEB activation," 2017 IEEE International Conference on Vehicular Electronics and Safety (ICVES), Vienna, 2017, pp. 19-25, doi: 10.1109/ICVES.2017.7991895.

[88] P. Raksincharoensak and Y. Akamatsu, "Development of Collision Avoidance System in Right Turn Maneuver Using Vehicle-in-the-Loop Simulation," Journal of Robotics and Mechatronics, 2015, Vol. 27, No. 6, pp. 627-635, https://doi.org/10.20965/jrm.2015.p0627.

[89] R. Matsumi, P. Raksincharoensak and M. Nagai, "Development of Autonomous Intelligent Driving System to Enhance Safe and Secured Traffic Society for Elderly Drivers – Autonomous Collision Avoidance System with Hazard Anticipation Driver Characteristics –," J. Robot. Mechatron., 2013, Vol.25, No.6, pp. 966-972, doi: 10.20965/jrm.2013.p0966.

[90] SUBARU, "SUBARU の総合安全," https://www.subaru.jp/safety/eyesight/ [Accessed on 2020/11/10]. (In Japanese)

[91] SUBARU, "新型「レヴォーグ」プロトタイプを世界初公開～新世代アイサイトや新開発水平対向エンジンを搭載～," ニュースリリース, 2019, https://www.subaru.co.jp/press/news/2019_10_23_7922/ [Accessed on 2020/11/10]. (In Japanese)

[92] Audi Media Center, "Driver assistance systems," 2017, https://www.audi-mediacenter.com/en/technology-lexicon-7180/driver-assistance-systems-7184 [Accessed on 2020/11/10].

[93] VOLVO, "Intersection Support", 2012, https://www.media.volvocars.com/global/en-gb/media/photos/43940 [Accessed on 2020/11/10].

[94] VOLVO, "ボルボの先進安全・運転支援機能「インテリセーフ」を XC90 全車に標準装備," https://www.volvocars.com/jp/cars/new-models/xc90/intellisafe#intellisafe [Accessed on 2020/11/10]. (In Japanese)

[95] Panasonic, " "CASE"時代を迎えた自動車のトレンドと技術課題(4)～コネクテッドカー

～,” https://industrial.panasonic.com/jp/ss/technical/t4 [Accessed on 2020/11/17]. (In Japanese)
[96] Smart Drive Magazine, “次世代自動車のカギ！車とすべてのモノを繋ぐ「V2X」とは,” https://smartdrivemagazine.jp/technology/v2x/#V2X-2 [Accessed on 2020/11/10]. (In Japanese)
[97] National Highway Traffic Safety Administration (NHTSA), “Evaluation of an Automotive Rear-End Collision Avoidance System,” DOT HS 810 569, 2006, Chapter 5.
[98] M. Fujita, P. Raksincharoensak and M. Nagai, “Comparison between Low-Speed and High-Speed Rear-End Incidents Using a Near-Miss Incident Database,” in Proc. 12th International Symposium on Advanced Vehicle Control (AVEC’14), 2014, p. 1-6.
[99] R. Futagami, R. Tsuboi, H. Mouri and K. Kazama, “Factor analysis of pedestrian accidents based on driver’s eye movement and the time that drivers attract pedestrian at right turn in an intersection with traffic lights,” Transactions of the JSME, 2020, Vol. 86, No. 883, pp. 1-11, https://doi.org/10.1299/transjsme.19-00047. (In Japanese)
[100] J. Pérez, J. Godoy, J. Villagrá and E. Onieva, “Trajectory generator for autonomous vehicles in urban environments,” 2013 IEEE International Conference on Robotics and Automation, Karlsruhe, 2013, pp. 409-414, doi: 10.1109/ICRA.2013.6630608.
[101] D. González, J. Pérez, V. Milanés and F. Nashashibi, “A Review of Motion Planning Techniques for Automated Vehicles,” in IEEE Transactions on Intelligent Transportation Systems, 2016, Vol. 17, No. 4, pp. 1135-1145, doi: 10.1109/TITS.2015.2498841.
[102] J. Wiest, M. Höffken, U. Kreßel and K. Dietmayer, “Probabilistic trajectory prediction with Gaussian mixture models,” 2012 IEEE Intelligent Vehicles Symposium, Alcala de Henares, 2012, pp. 141-146, doi: 10.1109/IVS.2012.6232277.
[103] S. Annell, A. Gratner and L. Svensson, “Probabilistic collision estimation system for autonomous vehicles,” 2016 IEEE 19th International Conference on Intelligent Transportation Systems (ITSC), Rio de Janeiro, 2016, pp. 473-478, doi: 10.1109/ITSC.2016.7795597.
[104] J. Eggert and T. Puphal, “Continuous Risk Measures for ADAS and AD,” 4th International Symposium on Future Active Safety Technology toward zero-traffic-accident (FAST-zero’17), 2017, TuA-P1-1.
[105] B. B. Kimia, I. Frankel and A. M. Popescu, “Euler Spiral for Shape Completion,” in International Journal of Computer Vision, Springer, 2003, Vol. 54, No. 1, pp. 159-182.
[106] M. Brezak and I. Petrovic, “Real-time Approximation of Clothoids With Bounded Error for Path Planning Applications,” in IEEE Transactions on Robotics, 2014, Vol. 30, No. 2, pp. 507-515, doi: 10.1109/TRO.2013.2283928.
[107] E. Bertolazzi and M. Frego, “G^1 fitting with clothoids,” in Mathematical Methods in the Applied Sciences, 2014, Vol. 38 (5), pp.881-897, https://doi.org/10.1002/mma.3114.
[108] Velodyne Lidar, “HDL-32E,” https://velodynelidar.com/products/hdl-32e/ [Accessed on 2020/11/10].
[109] OxTS, “How does a GNSS receiver work?,” https://www.oxts.com/gnss-receiver/ [Accessed on 2020/11/10].
[110] 国土地理院, “地理院地図 Vector,” https://maps.gsi.go.jp/vector/#11.768/35.689541/139.691659/&ls=vstd&disp=1&d=l [Accessed on 2020/11/8]. (In Japanese)

[111] G. S. Larue, A. Rakotonirainy, N. L. Haworth and M. Darvell, “Assessing driver acceptance of Intelligent Transport Systems in the context of railway level crossings,” Transportation Research Part F: Traffic Psychology and Behaviour, 2015, Vol. 30, pp. 1-13, https://doi.org/10.1016/j.trf.2015.02.003.

[112] J. Son, M. Park, B. B. Park, “The effect of age, gender and roadway environment on the acceptance and effectiveness of Advanced Driver Assistance Systems,” Transportation Research Part F: Traffic Psychology and Behaviour, 2015, Vol. 31, pp. 12-24, https://doi.org/10.1016/j.trf.2015.03.009.

[113] M. M. Rahman, L. Strawderman, M. F. Lesch, W. J. Horrey, K. Babski-Reeves and T. Garrison, "Modelling driver acceptance of driver support systems," Accident Analysis & Prevention, 2018, Vol. 121, pp. 134-147, https://doi.org/10.1016/j.aap.2018.08.028.

[114] J. D. Van Der Laan, A. Heino and D. De Waard, "A simple procedure for the assessment of acceptance of advanced transport telematics," Transportation Research Part C: Emerging Technologies, 1997, Vol. 5 (1), pp. 1-10, https://doi.org/10.1016/S0968-090X(96)00025-3.

[115] Y. Fujinami, P. Raksincharoensak, A. Sonka, F. Krauns, T. Lubiniecki and R. Henze, “Effectiveness Assessment of Proactive Braking System for Intersection Collision Avoidance,” in Proc. 14th International Symposium on Advanced Vehicle Control (AVEC’18), 2018, TuB2-6.

[116] A. Sonka, L. Liesner, T. Pawellek et al., “Environment Perception and Event Detection for Object Prediction in Traffic,” in Proc. of FAST-zero’15, 2015, pp. 79-83.

[117] Euro NCAP, “TEST PROTOCOL – AEB Car-to-Car systems,” 2019, https://cdn.euroncap.com/media/56143/euro-ncap-aeb-c2c-test-protocol-v302.pdf [Accessed on 2020/11/12].

[118] Euro NCAP, “TEST PROTOCOL – AEB VRU systems,” 2020, https://cdn.euroncap.com/media/58226/euro-ncap-aeb-vru-test-protocol-v303.pdf [Accessed on 2020/11/12].

[119] IPG Automotive, “CarMaker: Virtual testing of automobiles and light-duty vehicles,” https://ipg-automotive.com/products-services/simulation-software/carmaker/#driver [Accessed on 2020/11/12].

[120] S. Arita and P. Raksinchroensak, “A path planning method with specification of curvatures of boundary conditions based on clothoidal curve elements”, Transactions of the JSME, 2019, Vol. 85, No. 878, pp. 1-15, doi: 10.1299/transjsme.19-00090. (In Japanese)

[121] K. Mori, M. Homma and T. Saito, “Modeling of Gap Acceptance Characteristics of Right-Turning Vehicles at Signalized Intersections,” Infrastructure Planning Review, 1996, Vol. 13, pp. 901-906. (In Japanese)

[122] K. Watanabe and H. Nakamura, “Gap acceptance analysis of right-turn vehicle considering positions of opposing through vehicles,” 交通工学論文集, 2016. Vol. 2, No. 2, pp. A_85-A_91, https://doi.org/10.14954/jste.2.2_A_85. (In Japanese)

[123] T. Sato and M, Akamatsu, “運転行動データベースを利用したドライバー右折準備行動の解析,” 自動車技術会論文集, 2006, Vol. 37, No. 2, pp. 167-172. (In Japanese)

[124] T. Sato and M, Akamatsu, “Investigation on aging of elderly driver’s preparatory behavior before making a right turn,” 日本人間工学会大会講演集, 2009, Vol. 45, 日本人間工学会第 50 回記念大会, セッション ID O5-2, pp. 136-137,

https://doi.org/10.14874/jergo.45spl.0.136.0. (In Japanese)
[125] S. Lefèvre, R. Bajcsy and C. Laugier, “Probabilistic decision making for collision avoidance systems: Postponing decisions,” 2013 IEEE/RSJ International Conference on Intelligent Robots and Systems, Tokyo, 2013, pp. 4370-4375, doi: 10.1109/IROS.2013.6696983.
[126] Y. Kojima, “Driving Characteristics of Novice and Experienced Drivers -Part 1: Characteristics of Visual Search-,” 自動車技術会論文集, 1997, Vol. 28, No. 2, pp. 73-78. (In Japanese)
[127] M. Ishibashi, R. Yamashita and I. Kageyama, “A Study on Performance Test for Attention Allocation Ability in a Simulated Right Turn Situatinon,” 自動車技術会論文集, 2018, Vol. 49, No. 4, pp. 825-831, https://doi.org/10.11351/jsaeronbun.49.825. (In Japanese)
[128] T. Hosokawa, M. Shino, M. Kamata, et al., “Classification of Aged Drivers Based on Their Daily Driving and Prediction Method for the Classification using Right Turn Driving Parameters,” 自動車技術会論文集, 2008, Vol. 39, No. 4, pp. 4_141-4_146, https://doi.org/10.11351/jsaeronbun.39.4_141. (In Japanese)
[129] K, Suzuki, Y. Ida and K. Yamada, “Construction of Right-turning Driver Model at Intersection and Analysis Concerning the Effects of Information Presentation for Avoiding the Right-turning Collision,” 自動車技術会論文集, 2009, Vol. 40, No. 3, pp. 925-932, https://doi.org/10.11351/jsaeronbun.40.925. (In Japanese)
[130] M. Hiramatsu, T. Sunda, G. Abe, et al. “A Study of a Method for Quantifying Drivers’ Near-miss Risk in Right Turns at Intersections,” 自動車技術会論文集, 2014, Vol. 45, No. 6, pp. 1129-1134, https://doi.org/10.11351/jsaeronbun.45.1129. (In Japanese)
[131] M. Nagai, Y. Kojima, H. Sato, “Driver’s Decision and Control Process During Right-Turning at Intersection (Application of Fuzzy Linguistic Model for Accident Analysis), Proceedings of the 4th International Pacific Conference on Automotive Engineering, 1987, No. 871250.
[132] P. Raksincharoensak, M. Tago, M. Nagai, et al. “Analysis on Environmental Hazard and Safety Confirmation in Right Turn Behavior using Continuous Sensing Drive Recorder - Evaluation of Collision Hazard with Pedestrians and Bicycles -,” 自動車技術会論文集, 2010, Vol. 41, No. 4, pp. 909-914, https://doi.org/10.11351/jsaeronbun.41.909. (In Japanese)
[133] K. Nobukawa, “A Model Based Approach to the Analysis of Intersection Conflicts and Collision Avoidance Systems,” Dissertation, The University of Michigan, 2011, pp. 1-123, http://hdl.handle.net/2027.42/89791.
[134] Y. Fujinami, P. Raksincharoensak, D. Ulbricht and R. Adomat, “Risk Predictive Driver Assistance System for Collision Avoidance in Intersection Right Turns,” Journal of Robotics and Mechatronics, Fuji Technology Press, 2018, Vol. 30 No. 1, pp. 15-23, https://doi.org/10.20965/jrm.2018.p0015.
[135] Y. Fujinami, S. Arita, R. Yoshida and P. Raksincharoensak, “Safe Speed Planning Method with Risk Prediction for Intersection Right-Turn Assistance System —Trajectory Prediction Based on Triclothoidal Curves—,” Fifth International Symposium on Future Active Safety Technology Toward zero traffic accidents (FAST-zero’19), 2019, Blacksburg, VA, USA.
[136] K. C. Fuerstenberg and B. Roessler, “Advanced Intersection Safety - The EC project INTERSAFE,” 2006 IEEE Intelligent Vehicles Symposium, Tokyo, 2006, pp. 89-93, doi: 10.1109/IVS.2006.1689610.
[137] 国土交通省自動車交通局 先進安全自動車推進検討会, “先進安全自動車(ASV)推進計画

報告書—第 4 期 ASV 計画における活動成果について—”, 2011, pp. 69-184. (In Japanese)
[138] A. Ohtani, K. Fujita, M. Noguchi and Y. Nakamura, “Discussion on Human Machine Interfaces in Vehicle-Infrastructure Cooperative Safe Driving Support Systems (Second Report),” 自動車技術会論文集, 2010, Vol. 41, No. 2, pp. 431-436, https://doi.org/10.11351/jsaeronbun.41.431. (In Japanese)
[139] TOYOTA, “ヤリス 安全性能,” https://toyota.jp/yaris/feature/ [Accessed on 2020/11/18]. (In Japanese)
[140] DLR Verkehr, “Digitaler Knoten 4.0,” https://verkehrsforschung.dlr.de/de/projekte/digitaler-knoten-40 [Accessed on 2020/11/18]. (In German)
[141] Technische Universität Braunschweig, “Digitaler Knoten 4.0,” Magazin: Forschung, https://magazin.tu-braunschweig.de/m-post/digitaler-knoten-4-0-automatisiertes-fahren/ [Accessed on 2020/11/18]. (In German)
[142] The KITTI Vision Benchmark Suite, “Multi-Object Tracking and Segmentation (MOTS) Evaluation,” http://www.cvlibs.net/datasets/kitti/eval_mots.php [Accessed on 2021/01/20].
[143] N. Henmi, “Measurement Method of Jerk,” Journal of the Japan Society for Precision Engineering, 2014, Vol. 80, No. 11, pp. 995-998. (In Japanese)

Appendices

4. Collision Avoidance Ability Evaluation with Full-Vehicle Simulation

4-1 Simulation results on collision avoidance performance and collision velocity at darting-out velocity v_{obj} = 20 km/h.

(1) Intersection S60 (θ_{cross} = −60 [deg], v_{obj} = 20 [km/h]).

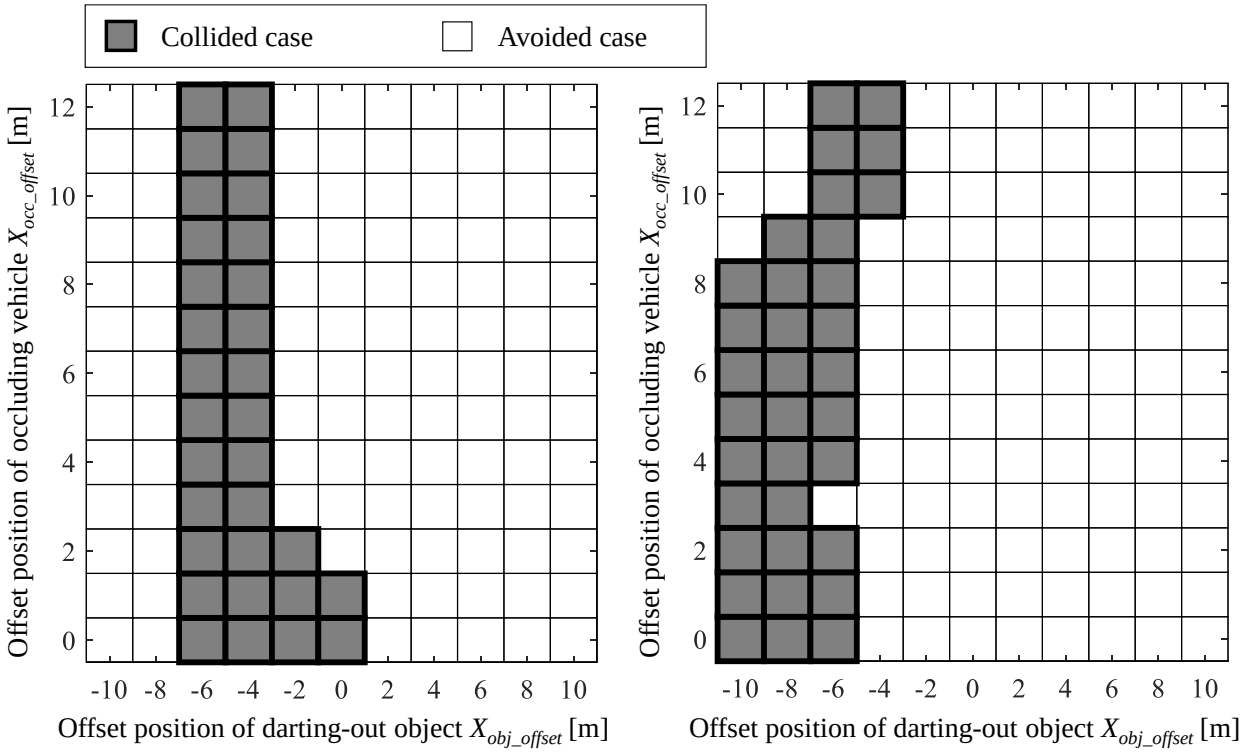

(a) EBS (b) PBS+EBS

Fig. 4-1.1 Collision avoidance results.

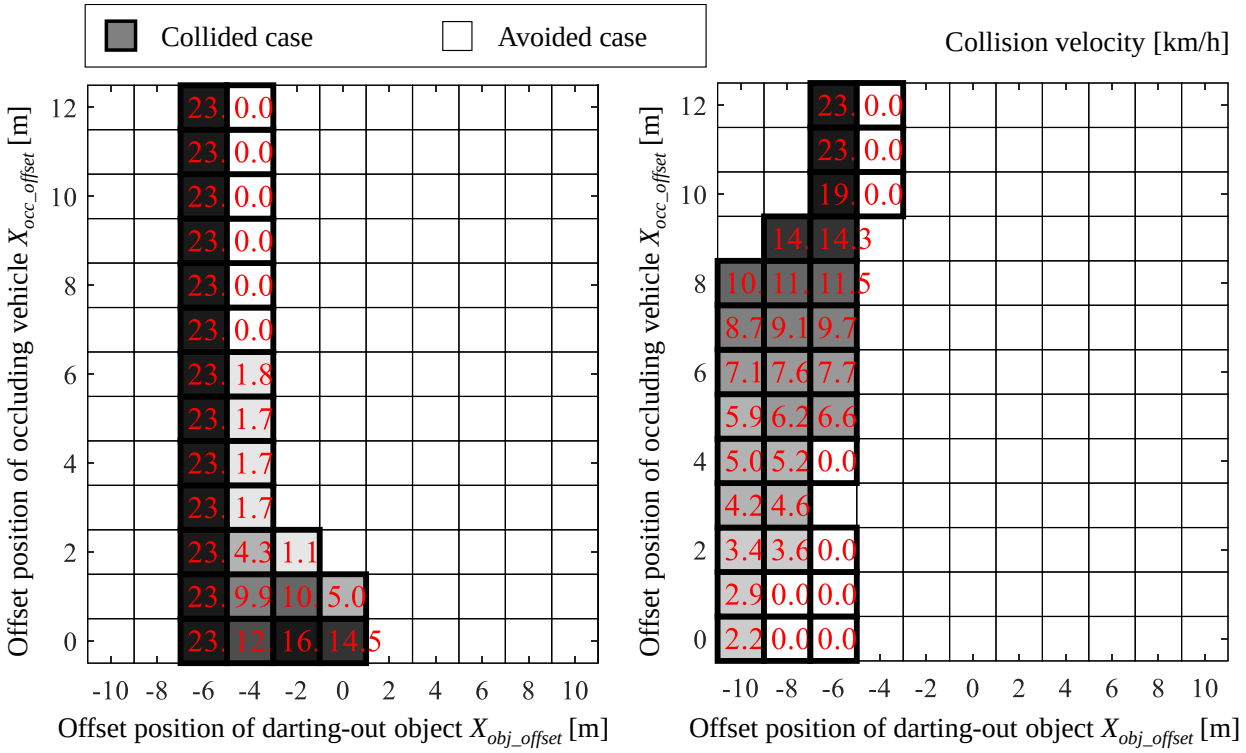

(a) EBS (b) PBS+EBS

Fig. 4-1.2 Collision velocities.

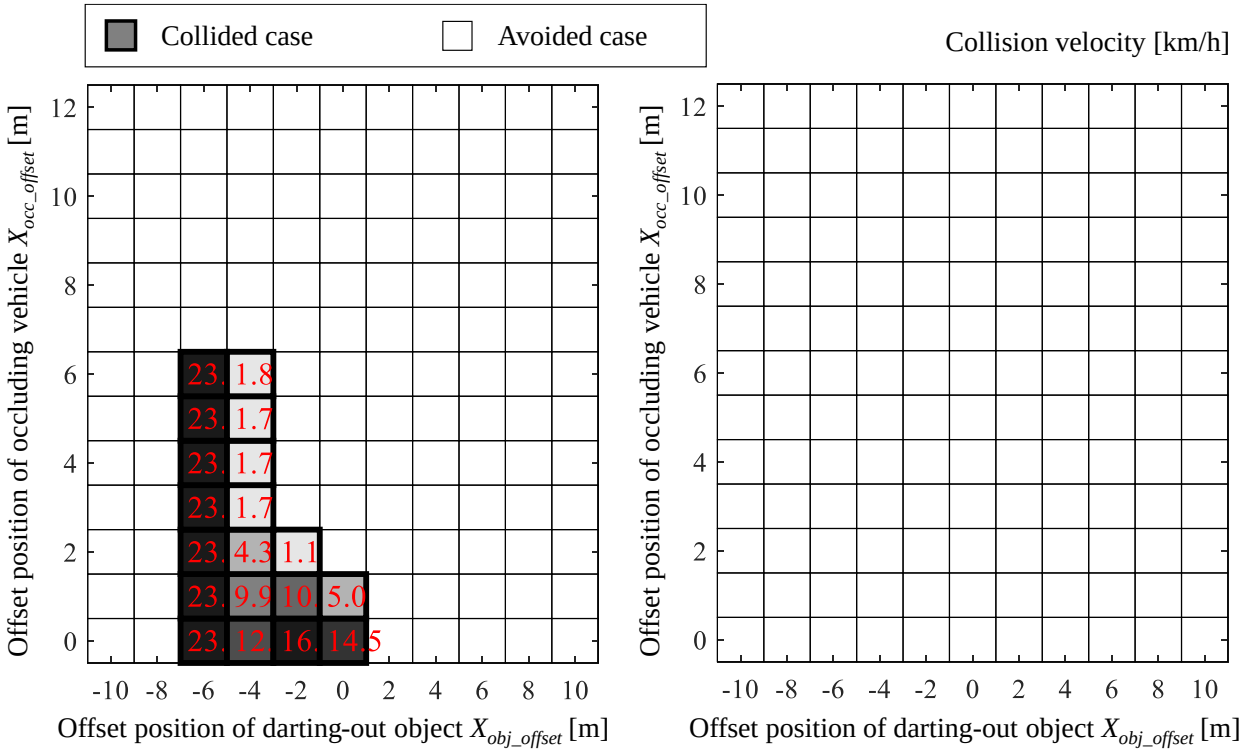

(a) EBS (b) PBS+EBS

Fig. 4-1.3 Collision velocities when ttc > 2 [s] were eliminated.

(2) Intersection S90 (θ_{cross} = −90 [deg], v_{obj} = 20 [km/h]).

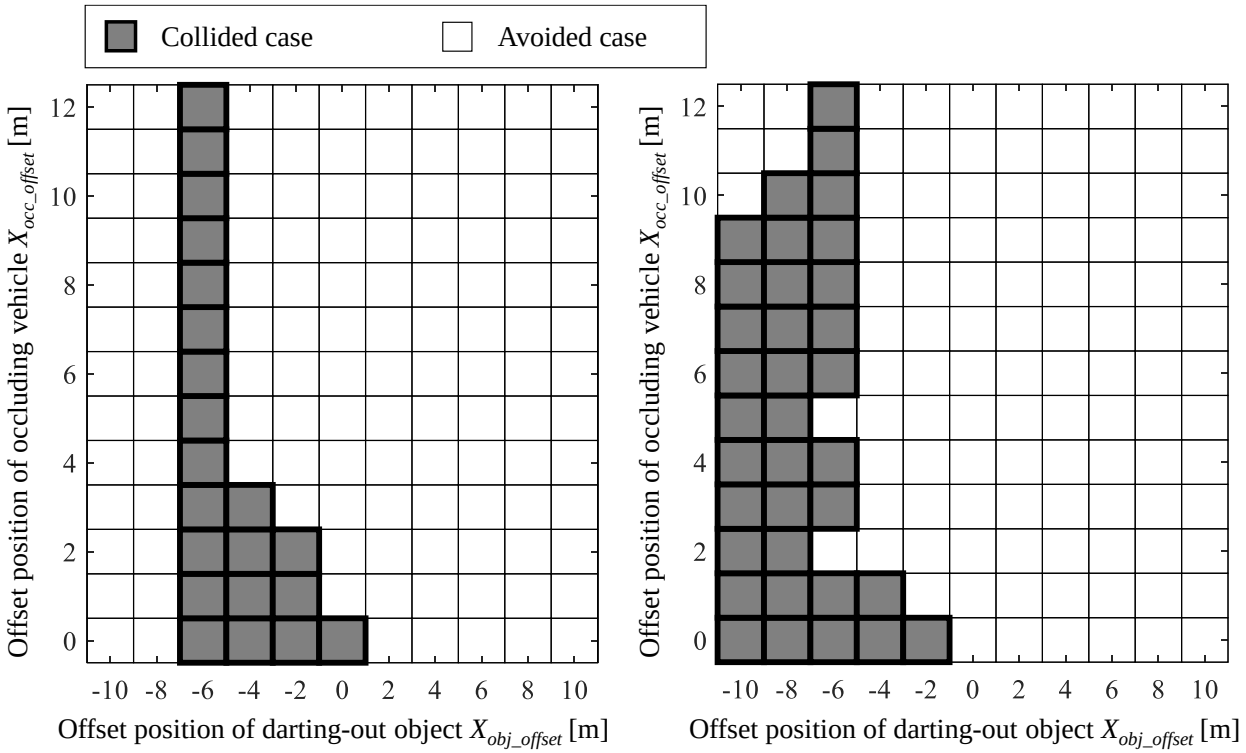

Fig. 4-1.4 Collision avoidance results.

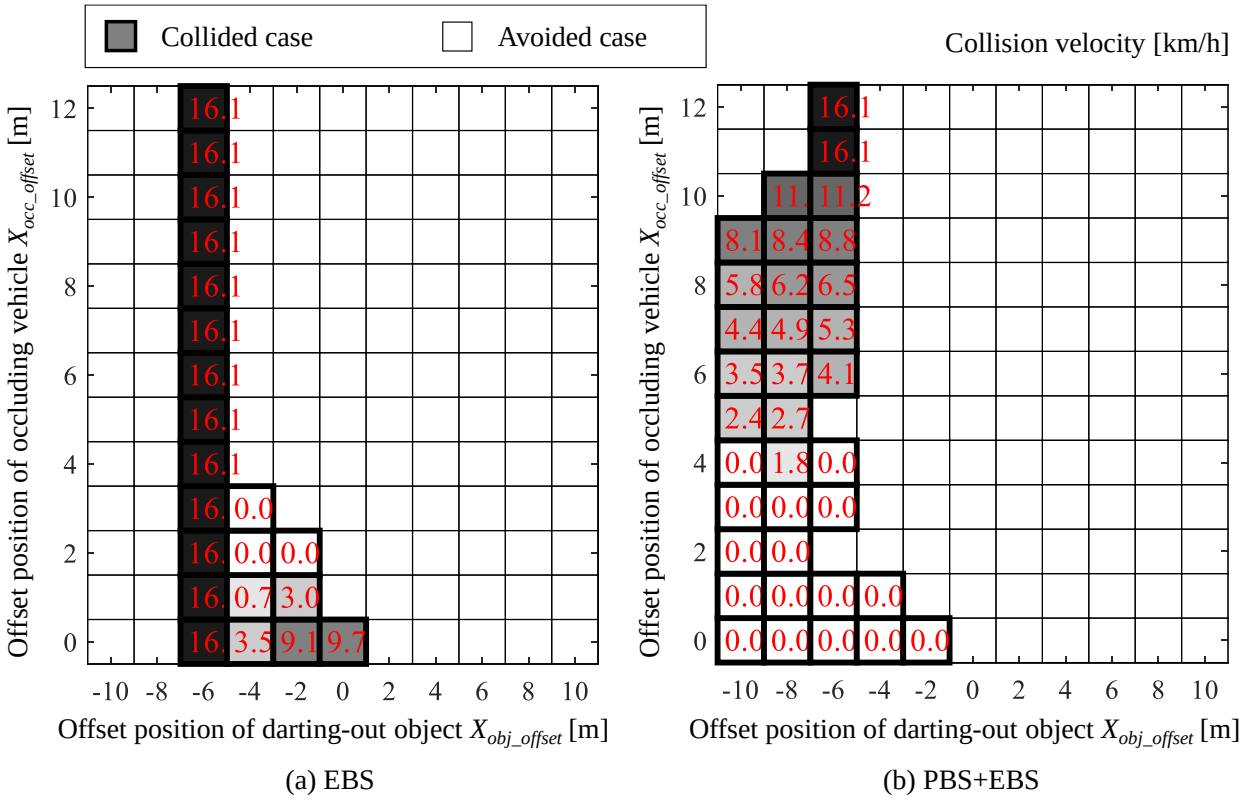

Fig. 4-1.5 Collision velocities.

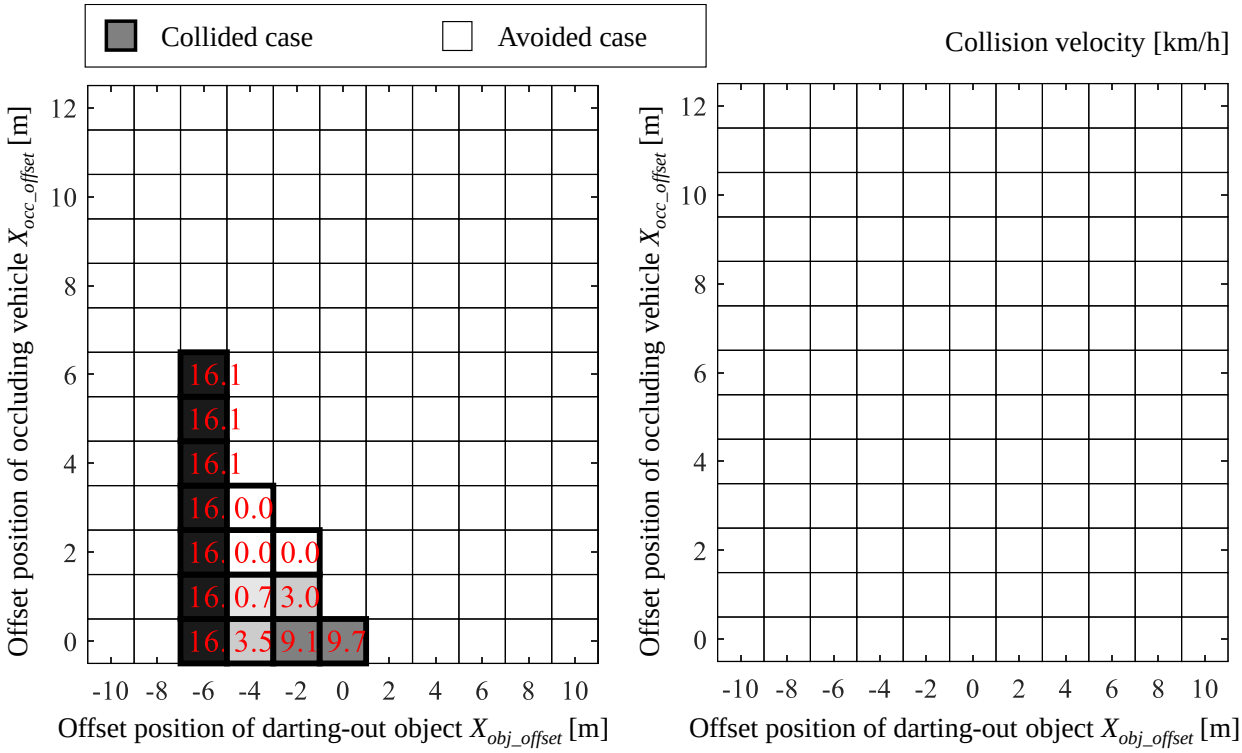

(a) EBS (b) PBS+EBS

Fig. 4-1.6 Collision velocities when ttc > 2 [s] were eliminated.

(3) Intersection S120 (θ_{cross} = −120 [deg], v_{obj} = 20 [km/h]).

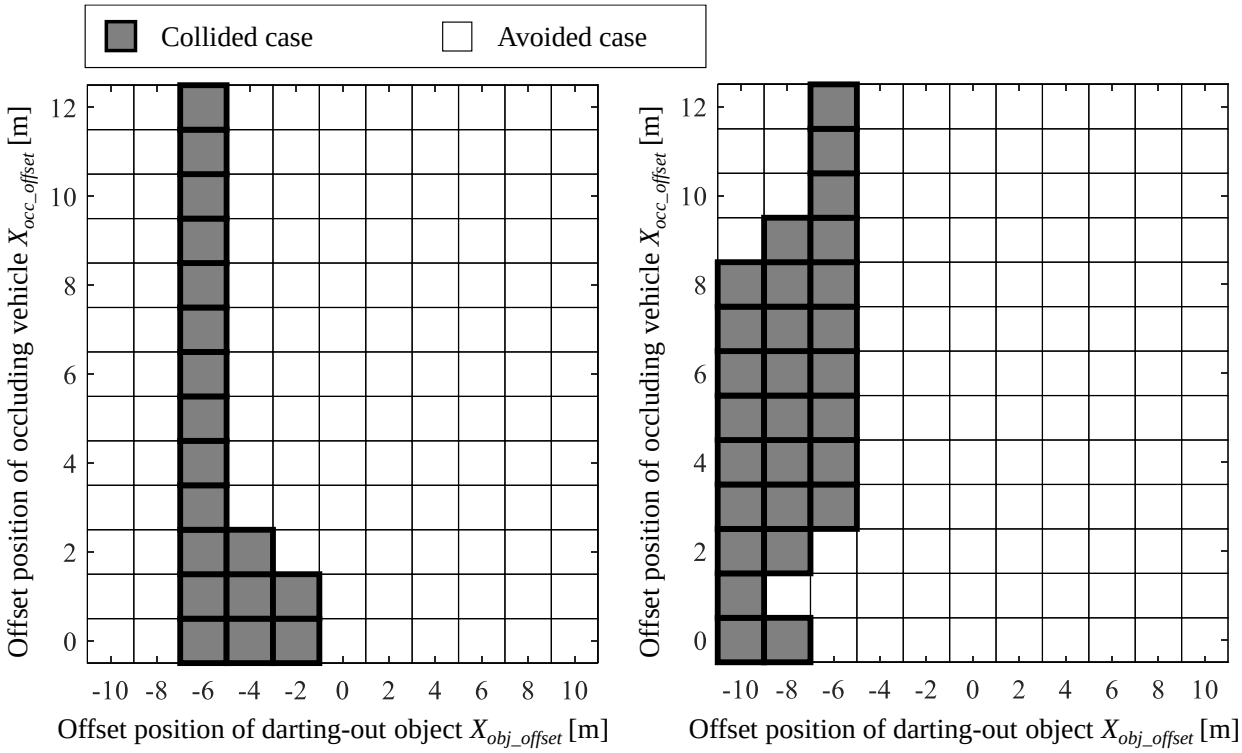

(a) EBS (b) PBS+EBS

Fig. 4-1.7 Collision avoidance results.

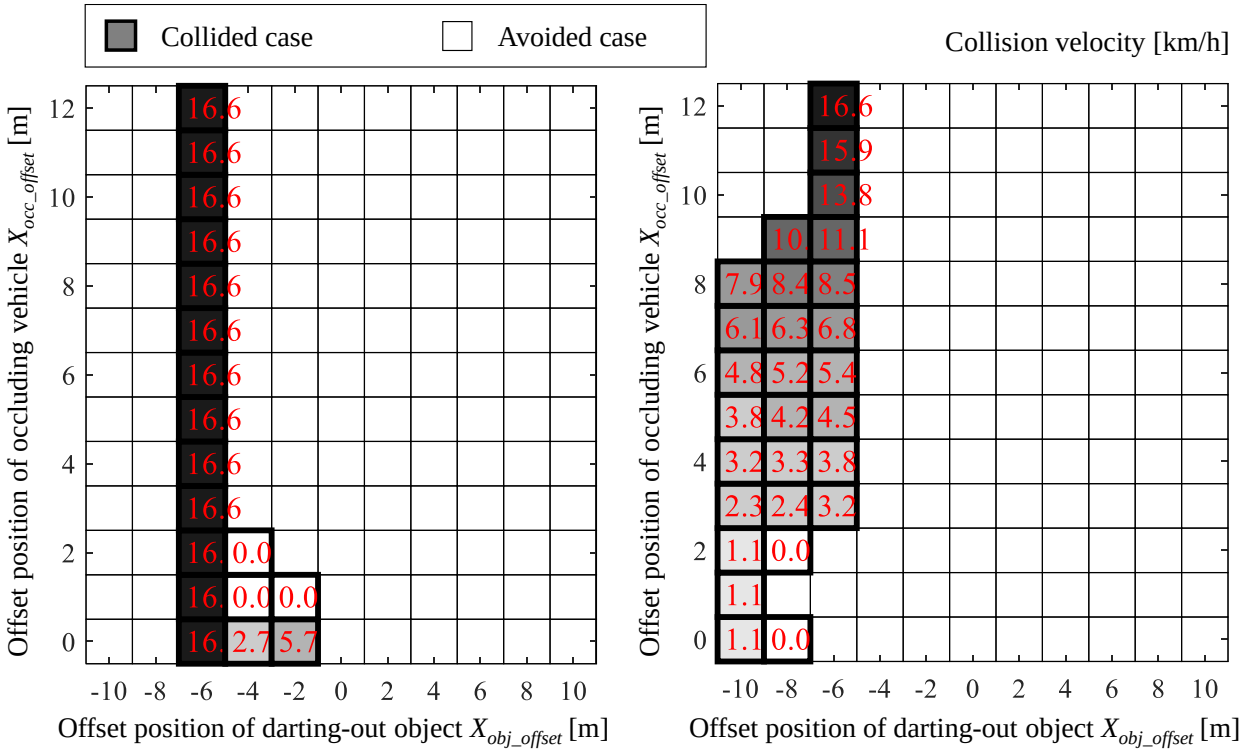

(a) EBS (b) PBS+EBS

Fig. 4-1.8 Collision velocities.

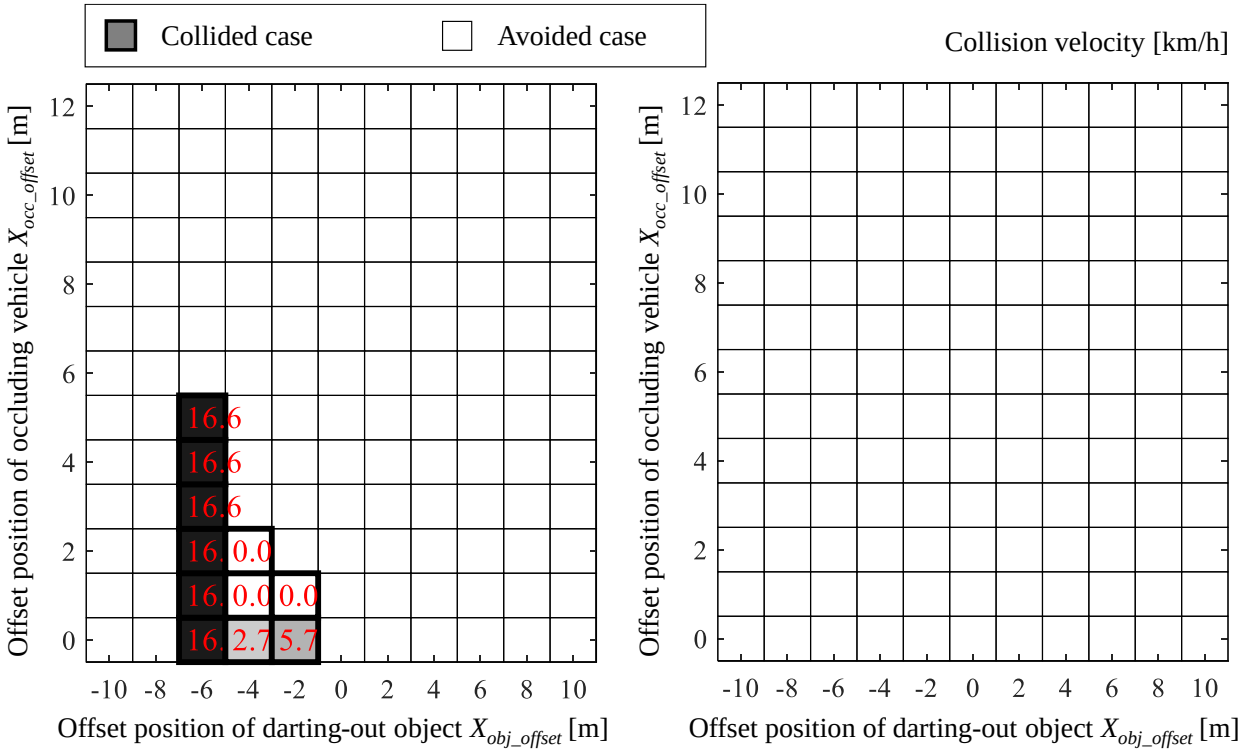

(a) EBS (b) PBS+EBS

Fig. 4-1.9 Collision velocities when ttc > 2 [s] were eliminated.

4-2 Simulation results on collision avoidance performance and collision velocity at darting-out velocity v_{obj} = 70 km/h.

(1) Intersection S60 (θ_{cross} = −60 [deg], v_{obj} = 40 [km/h]).

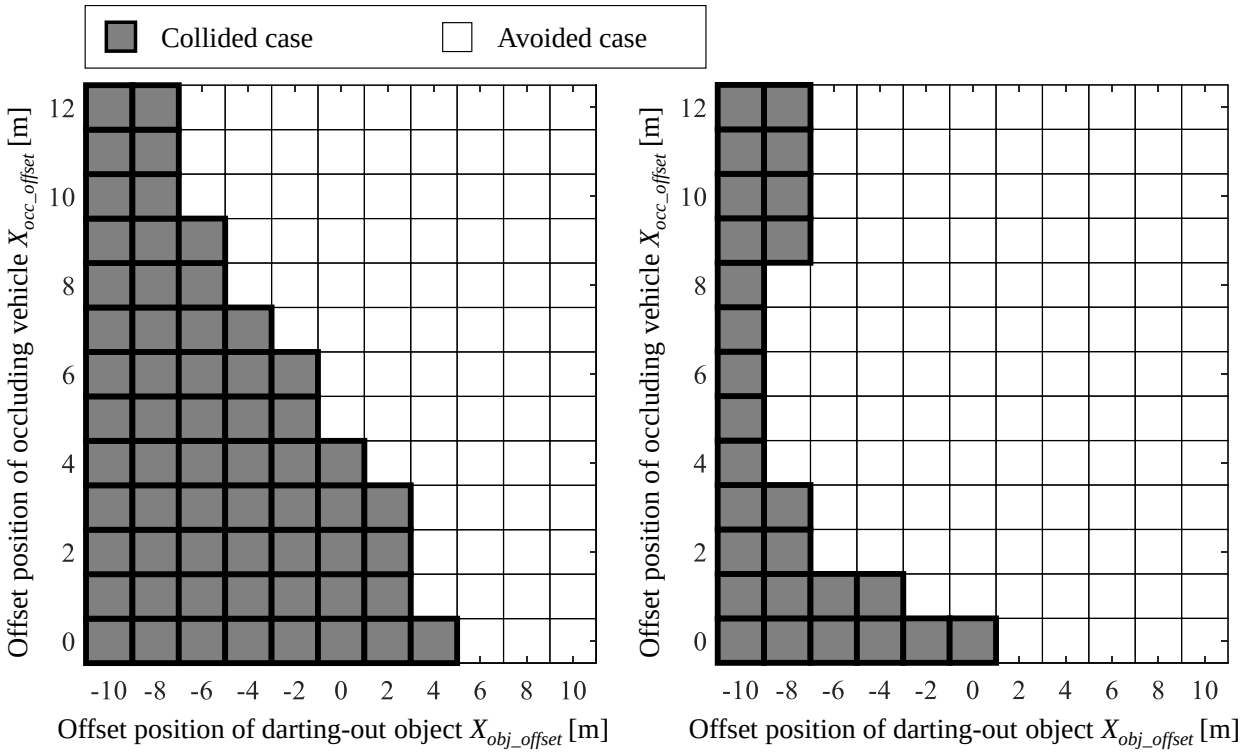

(a) EBS (b) PBS+EBS

Fig. 4-2.1 Collision avoidance results.

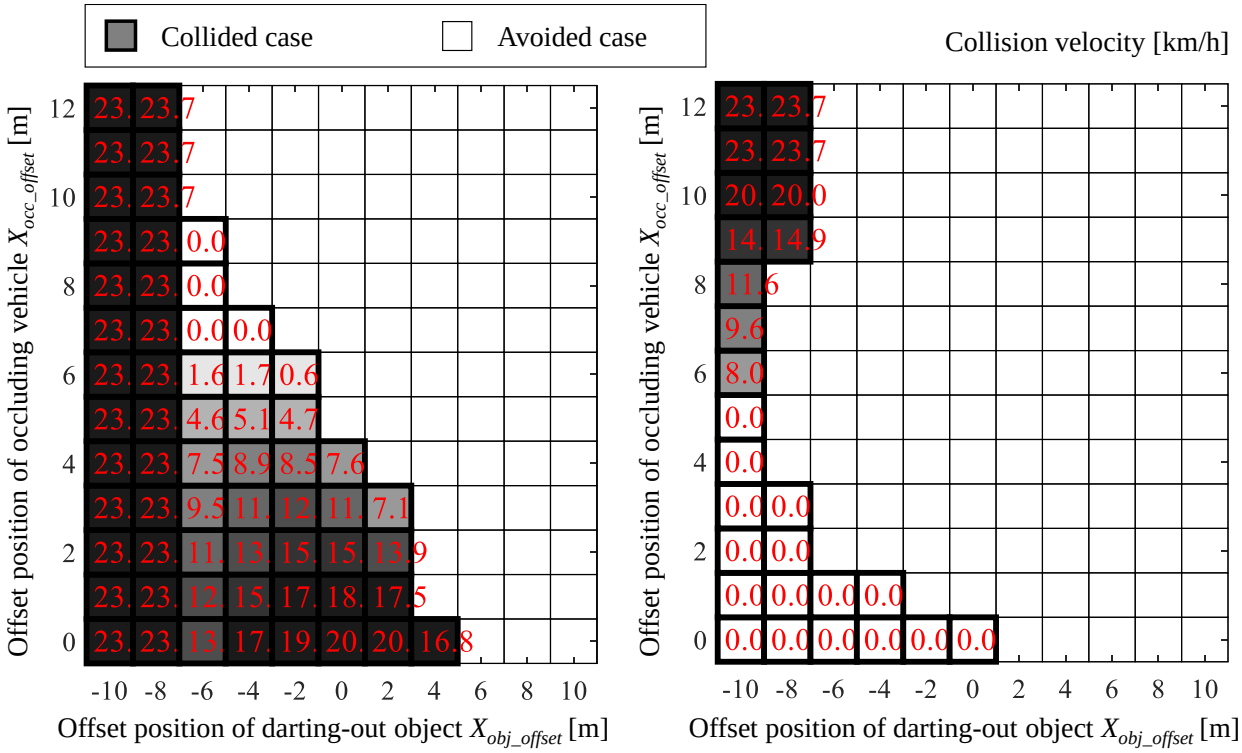

(a) EBS (b) PBS+EBS

Fig. 4-2.2 Collision velocities.

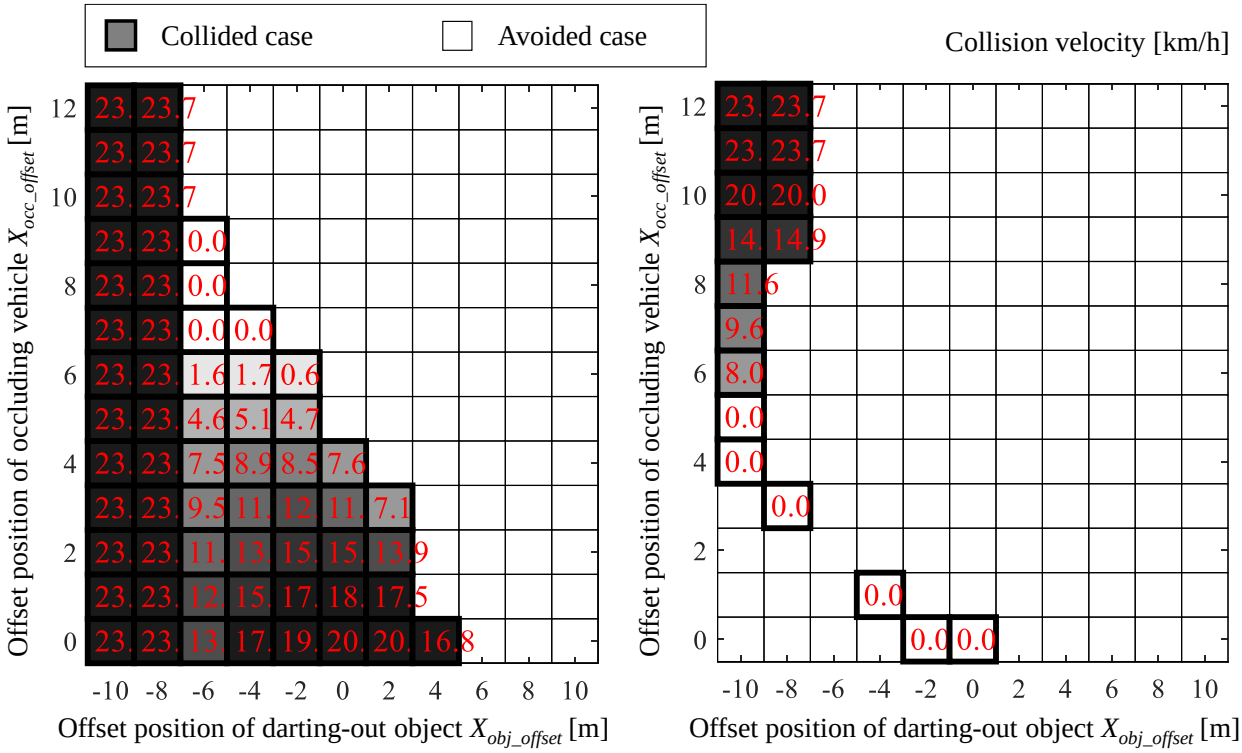

(a) EBS (b) PBS+EBS

Fig. 4-2.3 Collision velocities when ttc > 2 [s] were eliminated.

(2) Intersection S90 (θ_{cross} = −90 [deg], v_{obj} = 40 [km/h]).

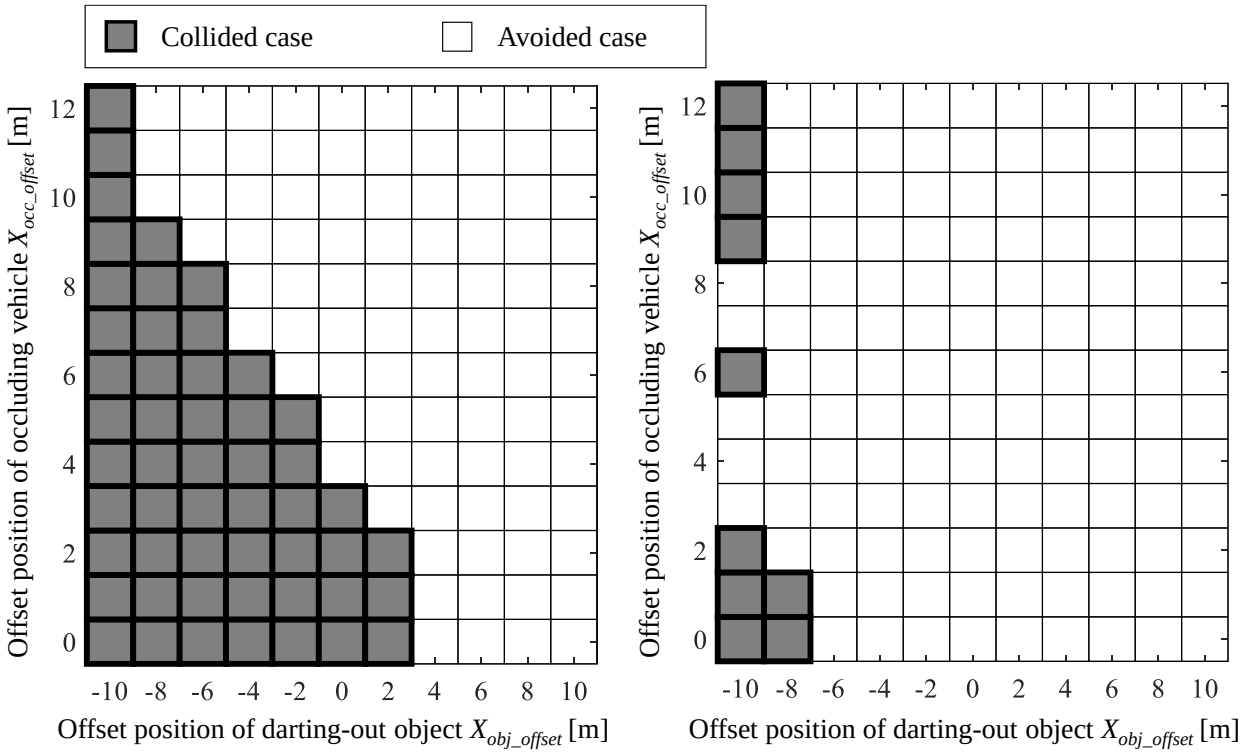

Fig. 4-2.4 Collision avoidance results.

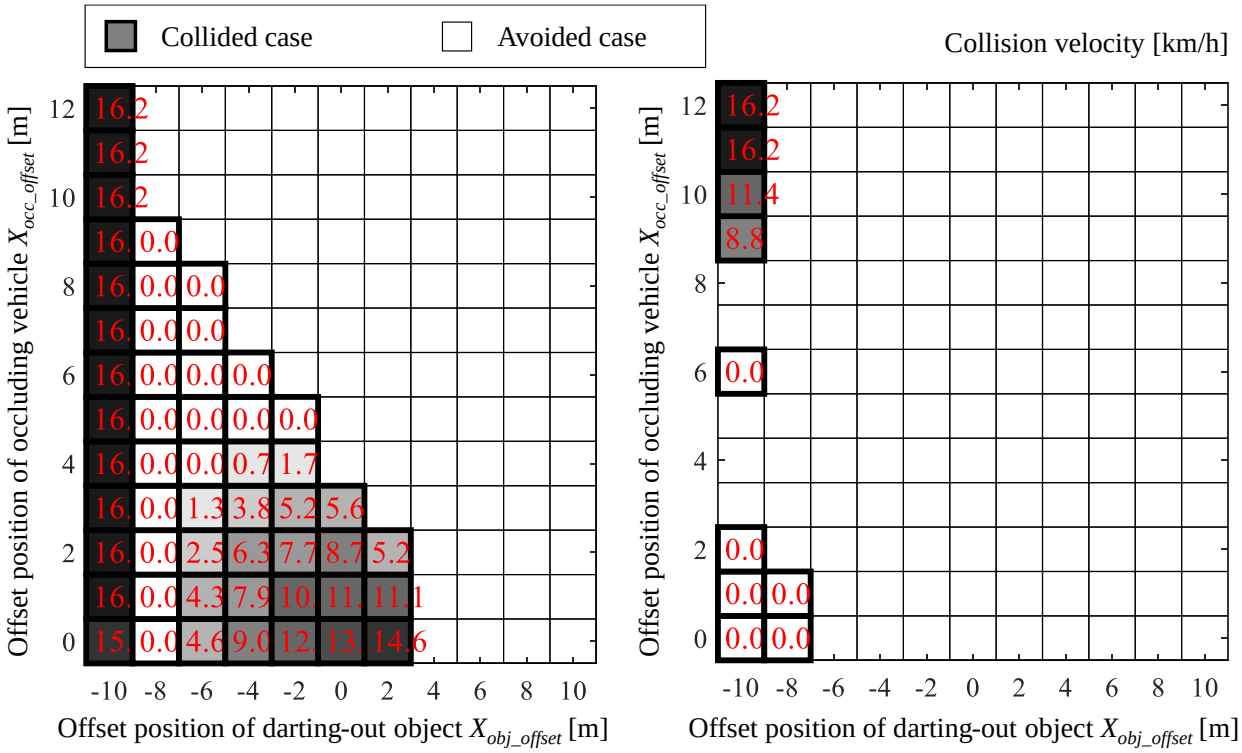

Fig. 4-2.5 Collision velocities.

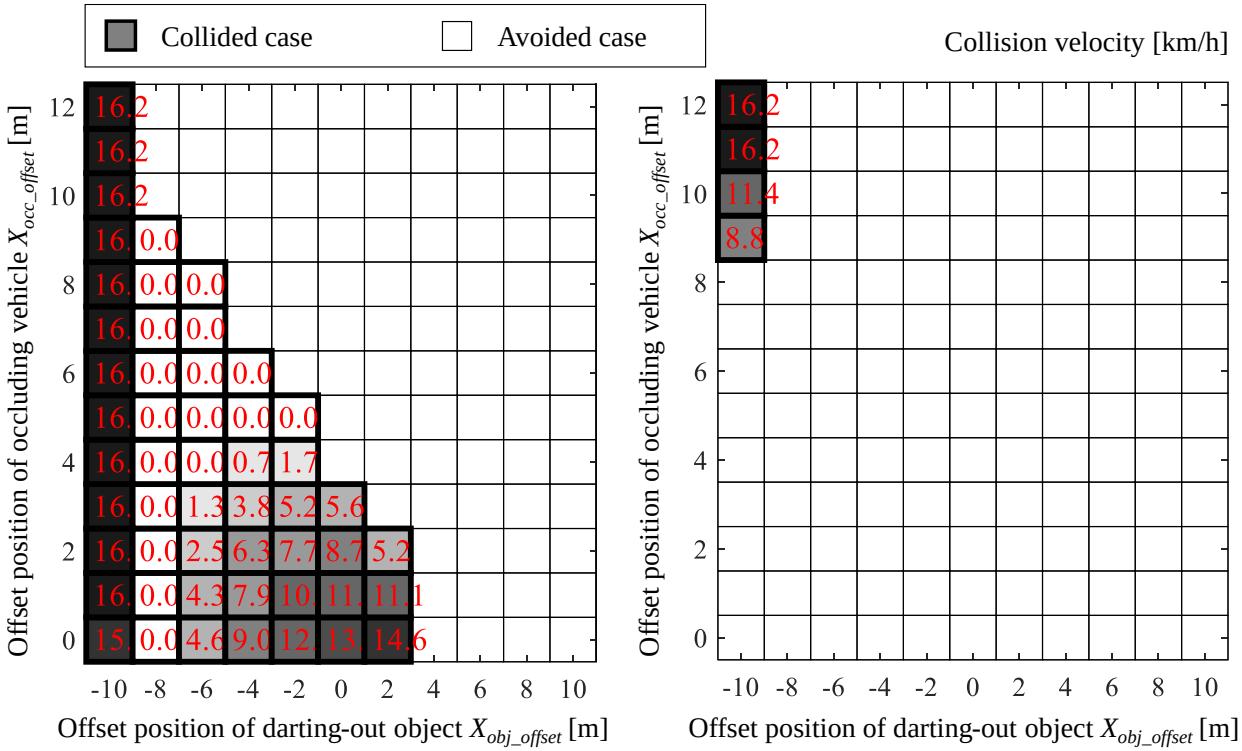

Fig. 4-2.6 Collision velocities when ttc > 2 [s] were eliminated.

(3) Intersection S120 (θ_{cross} = −120 [deg], v_{obj} = 40 [km/h]).

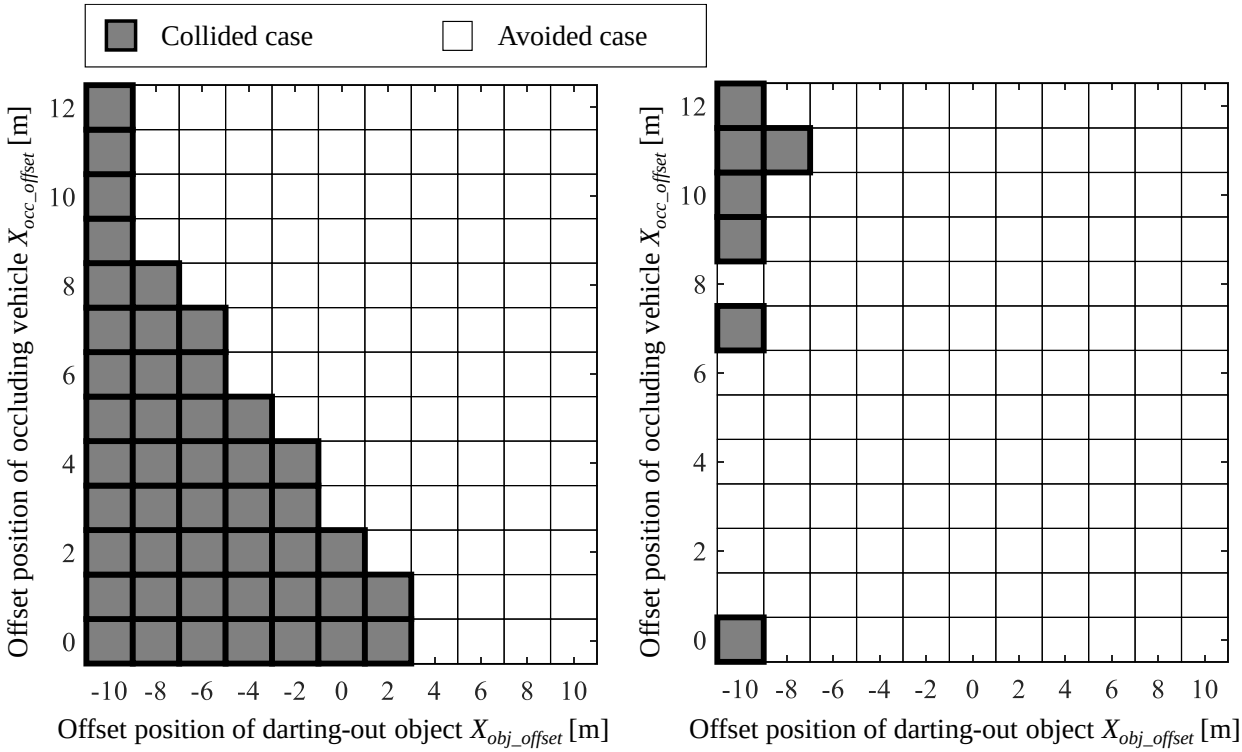

Fig. 4-2.7 Collision avoidance results.

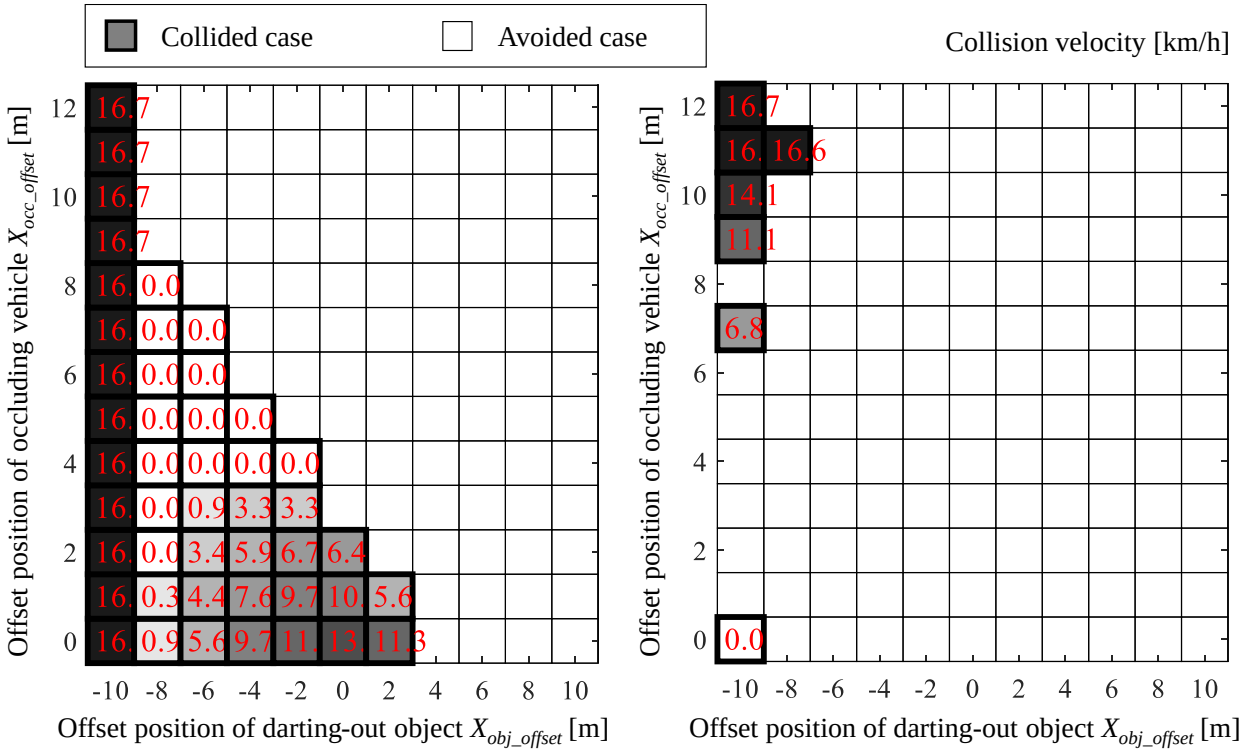

(a) EBS (b) PBS+EBS

Fig. 4-2.8 Collision velocities.

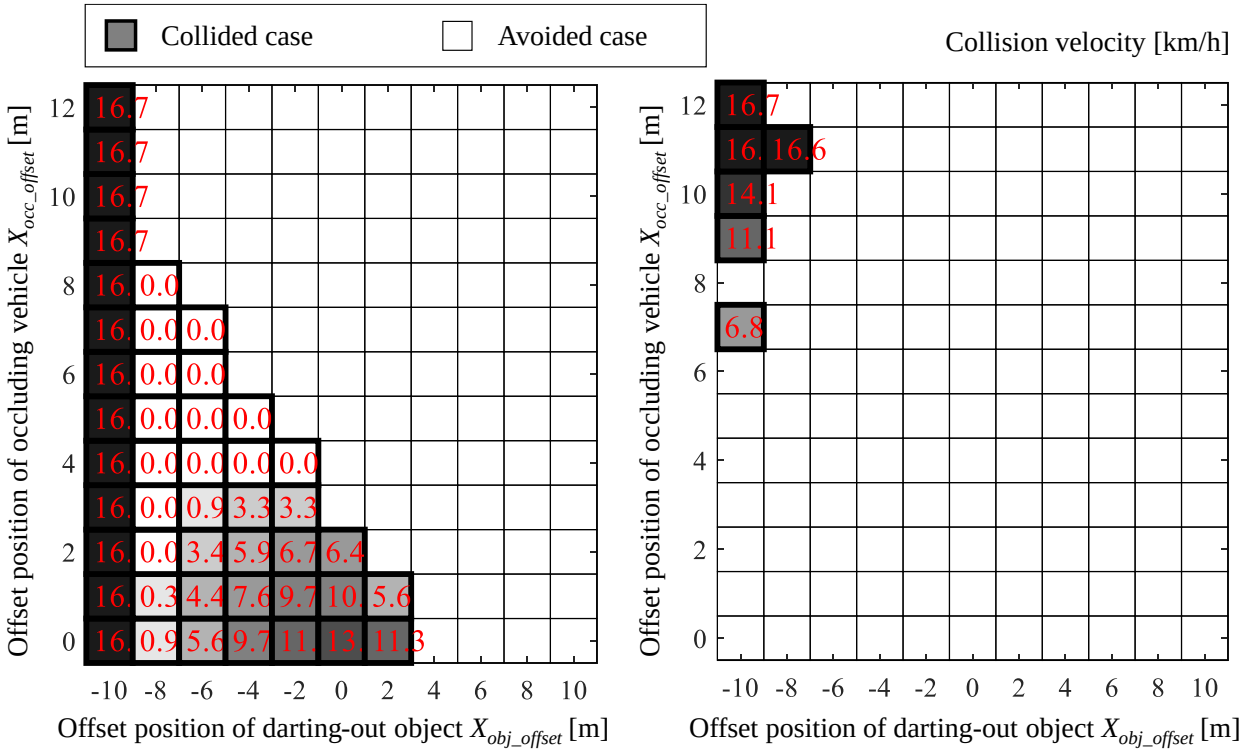

(a) EBS (b) PBS+EBS

Fig. 4-2.9 Collision velocities when ttc > 2 [s] were eliminated.

5. Driver Acceptance Evaluation of Advanced Driver Assistance System

5-1 Pre-experiment questionnaire.

The contents of the questionnaire are on the next pages.

東京農工大学 ポンサトーン研究室
自動車運転支援システム受容性評価実験
実験前アンケート

年齢 _____歳

性別 （ 男 ・ 女 ）

1. あなたが運転免許を取得したのはいつですか？
   運転免許証の左下の日付をご確認のうえご記入ください。
   ［ 昭和 ・ 平成 ・ 西暦 ］_____年

2. あなたの運転頻度はどのくらいですか？

□ ほとんど毎日	1 週間に約_____日運転する。
□ 週に数回	1 週間に約_____日運転する。
□ 月に数回	1 か月間に約_____日運転する。
□ 年に数回	1 年間に約_____日運転する。
□ ほとんどしない	

3. あなたの年間運転距離はどのくらいですか？

□ 0～500km
□ 501～1000km
□ 1001～3000km
□ 3001km～10000km
□ 10001km 以上

4. あなたが普段運転する道路はどのような道路ですか？(複数回答可)

□ 高速道路
□ 交通量が多い国道(広い道路)
□ 交通量が少ない国道(広い道路)
□ 交通量が多い市街地道路(狭い道路)
□ 交通量が少ない市街地道路(狭い道路)
□ 山道
□ 見通しの良い道路(建物の少ない平坦地)
□ その他(不整地など)

5. あなたが高速道路を運転する頻度はどれくらいですか？

□ ほとんど毎日
□ 週に数回
□ 月に数回
□ 年に数回
□ ほとんどしない

6. あなたが市街地道路を運転する頻度はどれくらいですか？

□ ほとんど毎日
□ 週に数回
□ 月に数回
□ 年に数回
□ ほとんどしない

7. 普段運転される際の１日あたりの運転時間を教えてください
_____ ［ 分 ・ 時間 ］くらい。
※「分」または「時間」に〇をつけてください。

8. あなたが普段運転する車のトランスミッションはどちらですか？

□ MT(マニュアル車)
□ AT(オートマチック車)
□ 両方

9. あなたが普段運転する車の種類はなんですか？(複数回答可)

□ 軽自動車
□ コンパクトカー
□ クーペ
□ セダン
□ ワゴン
□ ＳＵＶ
□ ミニバン
□ その他（_____）

10. もしわかれば、あなたが普段運転する車の名称をお教えください。
複数ある場合はわかる範囲ですべてご記入ください。

11. あなたは普段、どのような目的で車を運転しますか？(複数回答可)

□ 買い物に利用するため
□ 通学・通勤に利用するため
□ 仕事で利用するため
□ ドライブなど、運転そのものを楽しむため
□ 旅行など休日の遊び目的の移動のため
□ 趣味や習い事の移動のため
□ 家族の送り迎えなど、自分以外の人の移動のため
□ その他（＿＿＿＿＿＿＿＿＿＿＿＿＿＿＿＿＿＿＿＿＿＿＿＿＿＿＿＿＿＿）

12. あなたの運転スタイルはどのような感じですか？

□ 大胆な運転
□ 少し大胆な運転
□ 中間
□ 少し慎重な運転
□ 慎重な運転

13. あなたが普段運転するときに特に気を付ける場面はどこですか？
次の項目の中で最も気を付けるものから順に**1から5までの番号を振ってください。**

	車線変更		長い下り坂
	後退(バック)駐車		坂道発進
	交差点左折		歩道のない道路
	交差点右折		見通しの悪い交差点
	高速道路の合流		動いている自転車の追い越し
	信号のない横断歩道		動いている自動車の追い越し
	急カーブ		駐車車両の追い越し

14. 次の安全運転を支援する技術について、「これまで日常的に利用していた自動車についていたか」と「車を新しくした際に欲しいと思うか」の 2 つの質問に両方ご回答ください。

回答例

- エアバッグ
  交通事故などの際に袋のようなものが膨らみ、それによってドライバに及ぶ衝撃を軽減する技術。

☑ ついていた	☑ 欲しいと思う
☐ ついていない	☐ 欲しいと思わない
☐ よく分からない	☐ よく分からない

- エアバッグ
  交通事故などの際に袋のようなものが膨らみ、それによってドライバに及ぶ衝撃を軽減する技術。

☐ ついていた	☐ 欲しいと思う
☐ ついていない	☐ 欲しいと思わない
☐ よく分からない	☐ よく分からない

- カーナビゲーションシステム
  運転席に取り付ける電子機器で、地図情報を表示したり、音声による道案内を行ったりする装置。

☐ ついていた	☐ 欲しいと思う
☐ ついていない	☐ 欲しいと思わない
☐ よく分からない	☐ よく分からない

- 追突防止警報
  前方の車両との車間距離が短くなり、追突の危険性が高くなった際に警報を鳴らす装置。

☐ ついていた	☐ 欲しいと思う
☐ ついていない	☐ 欲しいと思わない
☐ よく分からない	☐ よく分からない

- 緊急自動ブレーキ
  衝突の危険性が高まっているにもかかわらずドライバがブレーキを踏まない場合に、自動車が自動的に車両を急停止させる技術。

☐ ついていた	☐ 欲しいと思う
☐ ついていない	☐ 欲しいと思わない
☐ よく分からない	☐ よく分からない

- レーンキープアシストまたは車線逸脱防止支援システム（LKAS）
  高速道路などを走行中に、車両が車線を逸脱するのを防ぐために、自動車がハンドル操作をサポートする技術。

□　ついていた	□　欲しいと思う
□　ついていない	□　欲しいと思わない
□　よく分からない	□　よく分からない

- アダプティブクルーズコントロール（ACC）
  前方の車両との車間距離を一定に保つように、自動車が自動的にアクセルおよびブレーキを行う技術。

□　ついていた	□　欲しいと思う
□　ついていない	□　欲しいと思わない
□　よく分からない	□　よく分からない

15. あなたが車を新しくする際に、あったら欲しいと思う安全運転支援は以下のどの場面ですか？次の項目の中ものから欲しいと思う順に**1から番号を振ってください。**（最大5個まで）

	車線変更		長い下り坂
	後退(バック)駐車		坂道発進
	交差点左折		歩道のない道路
	交差点右折		見通しの悪い交差点
	高速道路の合流		動いている自転車の追い越し
	信号のない横断歩道		動いている自動車の追い越し
	急カーブ		駐車車両の追い越し

アンケートは以上です。ご協力ありがとうございます。

ここまでのご回答が終わりましたら、担当者をお呼びください。

5-2 Post-experiment questionnaire.

The contents of the questionnaire are on the next pages.

東京農工大学 ポンサトーン研究室

自動車運転支援システム受容性評価質問票

ただ今、運転シミュレータで運転した場面について以下の質問にお答えください。なお、全ての質問に質問番号の順番にお答えいただき、前の質問に戻って回答を修正したり、次のページの質問の内容を先に確認したりしないようにご協力お願いいたします。

わからないことがございましたら担当者をお呼びください。

1. 以下の質問に対し、最も該当するものを一つ選んで回答してください。
   運転支援システムによる何かしらの支援を実感しましたか？

感じた	□
全く感じなかった	□

2. 以下の質問に対し、最も該当するものを一つ選んで回答してください。
   運転支援システムによる注意喚起の画像表示に気が付きましたか？

気が付いた	□
全く気が付かなかった	□

3. 以下の質問に対し、最も該当するものを一つ選んで回答してください。
   運転支援システムによる減速支援を実感しましたか？

感じた	□
全く感じなかった	□

・他に感じた支援がありましたら以下に自由に記述してください.

記入欄

ここまでのご回答が終わりましたら、担当者をお呼びください。

4. 以下の質問に対し、回答を具体的に記述してください。
運転支援システムはどのような場面で、どのような目的で支援を行ったと感じましたか？

記入欄

5. 以下の質問に対し、最も該当するものを一つ選んで回答してください。
この支援システムによる支援のおかけで安全に運転できたと感じましたか？

非常にそう感じた	□
そう感じた	□
少しそう感じた	□
あまりそう感じなかった	□
そう感じなかった	□
全くそう感じなかった	□

6. 以下の質問に対し、最も該当するものを一つ選んで回答してください。
この支援システムによる支援のおかげで安心して運転できたと感じましたか？

非常にそう感じた	□
そう感じた	□
少しそう感じた	□
あまりそう感じなかった	□
そう感じなかった	□
全くそう感じなかった	□

7. 以下の質問に対し、最も該当するものを一つ選んで回答してください。
運転支援システムの支援のおかげで、支援の行われた場所での安全確認をしたいと感じましたか？

非常にそう感じた	□
そう感じた	□
少しそう感じた	□
あまりそう感じなかった	□
そう感じなかった	□
全くそう感じなかった	□

次のページに続きます。

8. 以下の質問に対し、最も該当するものを一つ選んで回答してください。
この支援システムの作動 OFF スイッチが欲しいと感じましたか？

非常にそう感じた	□
そう感じた	□
少しそう感じた	□
あまりそう感じなかった	□
そう感じなかった	□
全くそう感じなかった	□

9. 以下の質問に対し、最も該当するものを一つ選んで回答してください。
この運転支援システムを自分の車に導入したいと感じましたか？

非常にそう感じた	□
そう感じた	□
少しそう感じた	□
あまりそう感じなかった	□
そう感じなかった	□
全くそう感じなかった	□

10. 以下の質問に対し、最も該当するものを一つ選んで回答してください。
この支援システムは今の自分に必要と感じましたか？

非常にそう感じた	□
そう感じた	□
少しそう感じた	□
あまりそう感じなかった	□
そう感じなかった	□
全くそう感じなかった	□

担当者をお呼びください。次の質問用紙をお渡しいたします。

運転支援システムにおける**減速支援**について以下の質問にご回答ください.

11. 以下の質問に対し、回答を具体的に記述してください。
減速支援はどのような運転支援のために行われたと思いますか？

記入欄

12. 以下の質問に対し、最も該当するものを一つ選んで回答してください。
減速支援のタイミングはいかがでしたか？

早すぎる	☐
少し早い	☐
ちょうどよい	☐
少し遅い	☐
遅すぎる	☐
気が付かなかった	☐

13. 以下の質問に対し、最も該当するものを一つ選んで回答してください。
減速支援の強さはいかがでしたか？

強すぎる	☐
少し強い	☐
ちょうどよい	☐
少し弱い	☐
弱すぎる	☐
気が付かなかった	☐

次のページに続きます。

14. 以下の質問に対し、最も該当するものを一つ選んで回答してください。
減速支援により、アクセルペダルを離そうと感じましたか？

非常にそう感じた	□
そう感じた	□
少しそう感じた	□
あまりそう感じなかった	□
そう感じなかった	□
全くそう感じなかった	□

15. 質問 14. で**「あまりそう感じなかった」「そう感じなかった」「全くそう感じなかった」を選択した方のみ**ご回答ください。以下の質問に対し、該当するものを選んで回答してください。
減速支援により、アクセルペダルを踏もうと感じましたか？

非常にそう感じた	□
そう感じた	□
少しそう感じた	□
あまりそう感じなかった	□
そう感じなかった	□
全くそう感じなかった	□

16. 以下の質問に対し、最も該当するものを一つ選んで回答してください。
減速支援により、ブレーキペダルを踏もうと感じましたか？

非常にそう感じた	□
そう感じた	□
少しそう感じた	□
あまりそう感じなかった	□
そう感じなかった	□
全くそう感じなかった	□

17. 質問 16. で**「あまりそう感じなかった」「そう感じなかった」「全くそう感じなかった」を選択した方のみ**ご回答ください。以下の質問に対し、該当するものを選んで回答してください。
減速支援により、ブレーキペダルを離そうと感じましたか？

非常にそう感じた	□
そう感じた	□
少しそう感じた	□
あまりそう感じなかった	□
そう感じなかった	□
全くそう感じなかった	□

18. 以下の質問に対し、最も該当するものを一つ選んで回答してください。
この減速支援機能は便利だと感じましたか？

非常にそう感じた	□
そう感じた	□
少しそう感じた	□
あまりそう感じなかった	□
そう感じなかった	□
全くそう感じなかった	□

19. 以下の質問に対し、最も該当するものを一つ選んで回答してください。
減速支援は不快と感じましたか？

非常にそう感じた	□
そう感じた	□
少しそう感じた	□
あまりそう感じなかった	□
そう感じなかった	□
全くそう感じなかった	□

20. 質問 19. で**「非常にそう感じた」「そう感じた」「少しそう感じた」を選択した方のみ**ご回答ください。以下の質問に対し、該当するものを選んで回答してください。（複数回答可）
なぜ不快と感じましたか？

突然減速したため	□
自分で減速するよりも速度が低下したため	□
自分で減速するよりも速度が低下しなかったため	□
なぜ減速したかわからなかったため	□
どこで減速しているかわからなかったため	□
その他　※その他の場合には下記に理由をご記入ください	□

記入欄

次のページに続きます。

21. 以下の質問に対し、最も該当するものを一つ選んで回答してください。
減速支援によって運転を邪魔されたと感じましたか？

非常にそう感じた	□
そう感じた	□
少しそう感じた	□
あまりそう感じなかった	□
そう感じなかった	□
全くそう感じなかった	□

22. 質問 21. で**「非常にそう感じた」「そう感じた」「少しそう感じた」を選択した方のみ**ご回答ください。以下の質問に対し、該当するものを選んで回答してください。（複数回答可）
なぜ運転を邪魔されたと感じましたか？

突然減速したため	□
自分で減速するよりも速度が低下したため	□
自分で減速するよりも速度が低下しなかったため	□
なぜ減速したかわからなかったため	□
どこで減速しているかわからなかったため	□
その他　※その他の場合には下記に理由をご記入ください	□

記入欄

次のページに続きます。

23. 以下の質問に対し、最も該当するものを一つ選んで回答してください。
減速支援によって不安を感じましたか？

非常にそう感じた	□
そう感じた	□
少しそう感じた	□
あまりそう感じなかった	□
そう感じなかった	□
全くそう感じなかった	□

24. 質問 23. で**「非常にそう感じた」「そう感じた」「少しそう感じた」を選択した方のみ**ご回答ください。以下の質問に対し、該当するものを選んで回答してください。（複数回答可）
なぜ不安を感じましたか？

突然減速したため	□
自分で減速するよりも速度が低下したため	□
自分で減速するよりも速度が低下しなかったため	□
なぜ減速したかわからなかったため	□
どこで減速しているかわからなかったため	□
その他　※その他の場合には下記に理由をご記入ください	□

記入欄

ここまでのご回答が終わりましたら、担当者をお呼びください。

運転支援システムにおける**画像表示機能**について以下の質問にご回答ください.

25. 以下の質問に対し、回答を具体的に記述してください。
運転支援システムによる注意喚起の画像表示には何が表示されていましたか？

記入欄

26. 以下の質問に対し、最も該当するものを一つ選んで回答してください。
表示画像により、アクセルペダルを離そうと感じましたか？

非常にそう感じた	☐
そう感じた	☐
少しそう感じた	☐
あまりそう感じなかった	☐
そう感じなかった	☐
全くそう感じなかった	☐

27. 質問 26. で**「あまりそう感じなかった」「そう感じなかった」「全くそう感じなかった」を選択した方のみ**ご回答ください。以下の質問に対し、該当するものを選んで回答してください。
表示画像により、アクセルペダルを踏もうと感じましたか？

非常にそう感じた	☐
そう感じた	☐
少しそう感じた	☐
あまりそう感じなかった	☐
そう感じなかった	☐
全くそう感じなかった	☐

次のページに続きます。

28. 以下の質問に対し、最も該当するものを一つ選んで回答してください。
表示画像により、ブレーキペダルを踏もうと感じましたか？

非常にそう感じた	□
そう感じた	□
少しそう感じた	□
あまりそう感じなかった	□
そう感じなかった	□
全くそう感じなかった	□

29. 質問 28. で**「あまりそう感じなかった」「そう感じなかった」「全くそう感じなかった」を選択した方のみ**ご回答ください。以下の質問に対し、該当するものを選んで回答してください。
表示画像により、ブレーキペダルを離そうと感じましたか？

非常にそう感じた	□
そう感じた	□
少しそう感じた	□
あまりそう感じなかった	□
そう感じなかった	□
全くそう感じなかった	□

30. 以下の質問に対し、最も該当するものを一つ選んで回答してください。
この画像表示機能は便利だと感じましたか？

非常にそう感じた	□
そう感じた	□
少しそう感じた	□
あまりそう感じなかった	□
そう感じなかった	□
全くそう感じなかった	□

次のページに続きます。

31. 以下の質問に対し、最も該当するものを一つ選んで回答してください。
表示された画像によって運転を邪魔されたと感じましたか？

非常にそう感じた	☐
そう感じた	☐
少しそう感じた	☐
あまりそう感じなかった	☐
そう感じなかった	☐
全くそう感じなかった	☐

32. 質問 31. で**「非常にそう感じた」「そう感じた」「少しそう感じた」を選択した方のみ**ご回答ください。以下の質問に対し、該当するものを選んで回答してください。（複数回答可）
なぜ運転を邪魔されたと感じましたか？

突然表示されたため	☐
注意が散漫になったため	☐
表示がしつこいため	☐
表示が眩しすぎたため	☐
どうして表示されたか理解できなかったため	☐
その他　※その他の場合には下記に理由をご記入ください	☐

記入欄

次のページに続きます。

33. 以下の質問に対し、最も該当するものを一つ選んで回答してください。
表示された画像によって不安を感じましたか？

非常にそう感じた	☐
そう感じた	☐
少しそう感じた	☐
あまりそう感じなかった	☐
そう感じなかった	☐
全くそう感じなかった	☐

34. 質問 33. で**「非常にそう感じた」「そう感じた」「少しそう感じた」を選択した方のみ**ご回答ください。以下の質問に対し、該当するものを選んで回答してください。（複数回答可）
なぜ不安を感じましたか？

突然表示されたため	☐
注意が散漫になったため	☐
表示がしつこいため	☐
表示が眩しすぎたため	☐
どうして表示されたか理解できなかったため	☐
その他　※その他の場合には下記に理由をご記入ください	☐

記入欄

次のページに続きます。

画像表示機能には画像①と画像②が表示されていました(表示されない場合もあります)。これらの画像表示に関する以下の質問について回答してください。

画像①　右折時の飛出し注意表示

画像②　アクセルペダル解除の指示表示

35. 以下の質問に対し、画像①、画像②のそれぞれについて最も該当するものを一つ選んで回答してください。
表示された画像に気が付きましたか？

	画像①	画像②
気が付いた	☐	☐
全く気が付かなかった	☐	☐

36. 以下の質問に対し、画像①、画像②のそれぞれについて最も該当するものを一つ選んで回答してください。
画像が表示されるタイミングはいかがでしたか？

	画像①	画像②
早すぎる	☐	☐
少し早い	☐	☐
ちょうどよい	☐	☐
少し遅い	☐	☐
遅すぎる	☐	☐
気が付かなかった	☐	☐

37. 以下の質問に対し、画像①、画像②のそれぞれについて最も該当するものを一つ選んで回答してください。
画像が表示される頻度はいかがでしたか？

	画像①	画像②
多すぎる	☐	☐
少し多い	☐	☐
ちょうどよい	☐	☐
少し少ない	☐	☐
少なすぎる	☐	☐
気が付かなかった	☐	☐

38. 以下の質問に対し、画像①、画像②のそれぞれについて最も該当するものを一つ選んで回答してください。
画像が表示される時間の長さはいかがでしたか？

	画像①	画像②
長すぎる	☐	☐
少し長い	☐	☐
ちょうどよい	☐	☐
少し短い	☐	☐
短すぎる	☐	☐
気が付かなかった	☐	☐

39. 以下の質問に対し、画像①、画像②のそれぞれについて最も該当するものを一つ選んで回答してください。
画像表示画面に表示された画像の内容は理解しやすかったですか？

	画像①	画像②
非常にそう感じた	☐	☐
そう感じた	☐	☐
少しそう感じた	☐	☐
あまりそう感じなかった	☐	☐
そう感じなかった	☐	☐
全くそう感じなかった	☐	☐
気が付かなかった	☐	☐

40. 質問 39. で**「全くそう感じなかった」を選択した方のみ**ご回答ください。以下の質問に対し、回答を具体的に記述してください。（両方の画像に対して「全くそう感じなかった」と答えた場合はそれぞれの図について記述してください。）
運転中に画像表示画面に表示された画像をどのような画像として理解しましたか？

記入欄

ここまでのご回答が終わりましたら、担当者をお呼びください。

5-3 Time historical results of the driver acceptance experiment (D-2)

To anonymize the results, the data were unlabeled, and sequences of the figures are not corresponding to the experiment order.

(1)

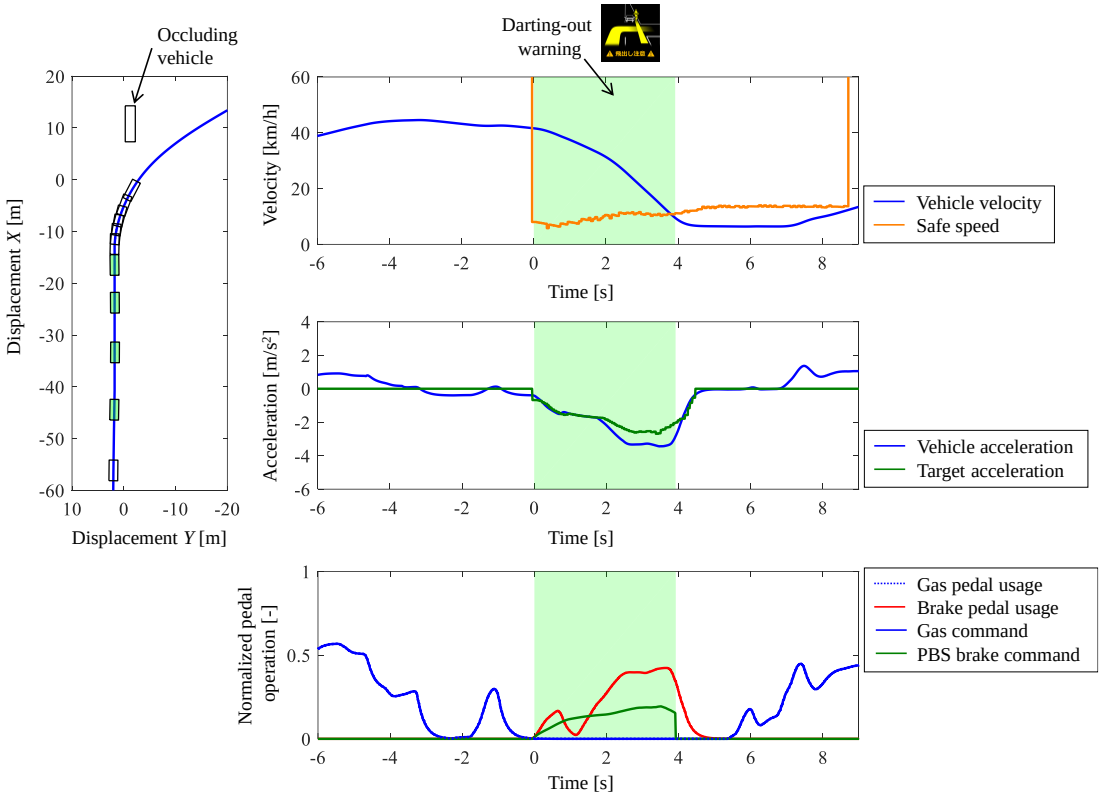

(2)

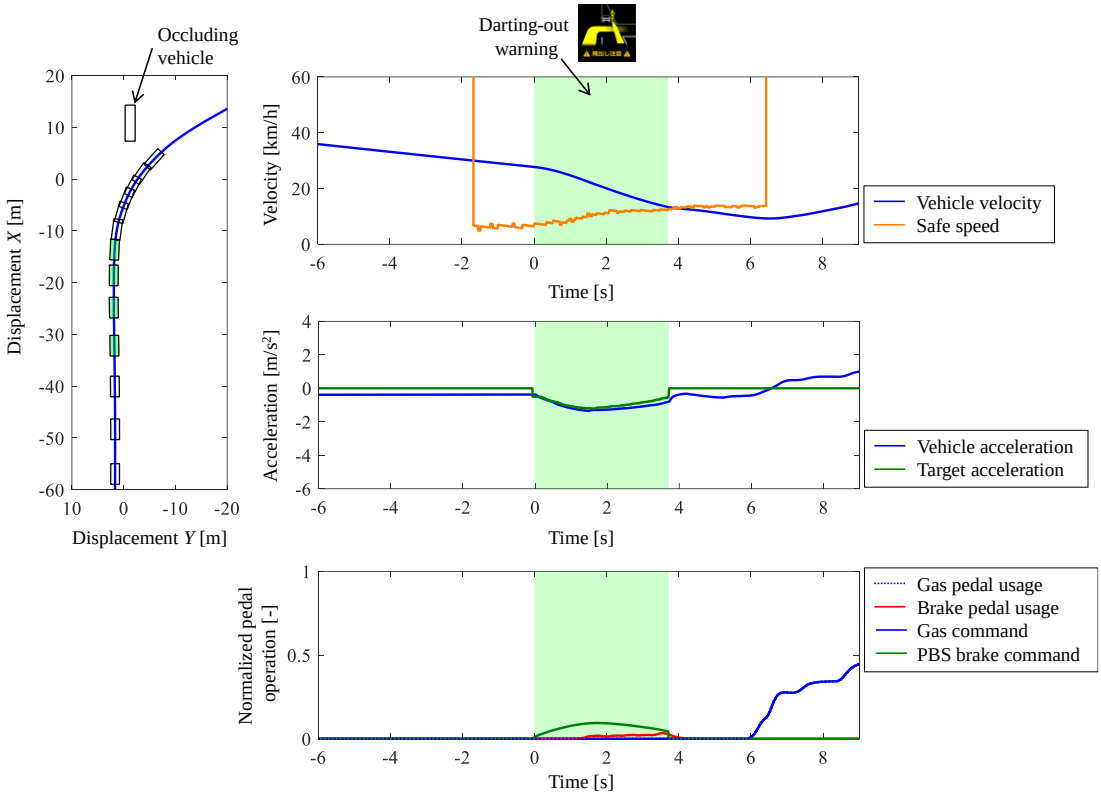
Occluding vehicle
Darting-out warning
Displacement X [m]
Displacement Y [m]
Velocity [km/h]
Time [s]
Vehicle velocity
Safe speed
Acceleration [m/s²]
Vehicle acceleration
Target acceleration
Normalized pedal operation [-]
Gas pedal usage
Brake pedal usage
Gas command
PBS brake command

(3)

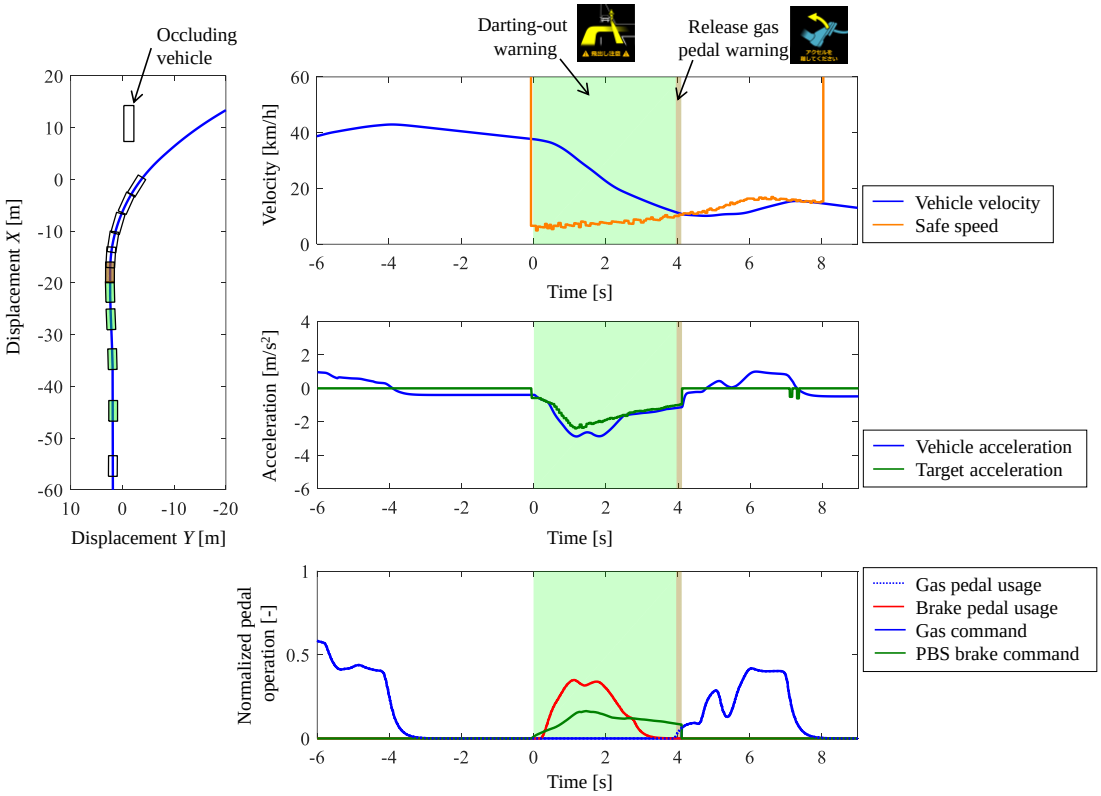
Occluding vehicle
Darting-out warning
Release gas pedal warning
Displacement X [m]
Displacement Y [m]
Velocity [km/h]
Time [s]
Vehicle velocity
Safe speed
Acceleration [m/s²]
Vehicle acceleration
Target acceleration
Normalized pedal operation [-]
Gas pedal usage
Brake pedal usage
Gas command
PBS brake command

(4)

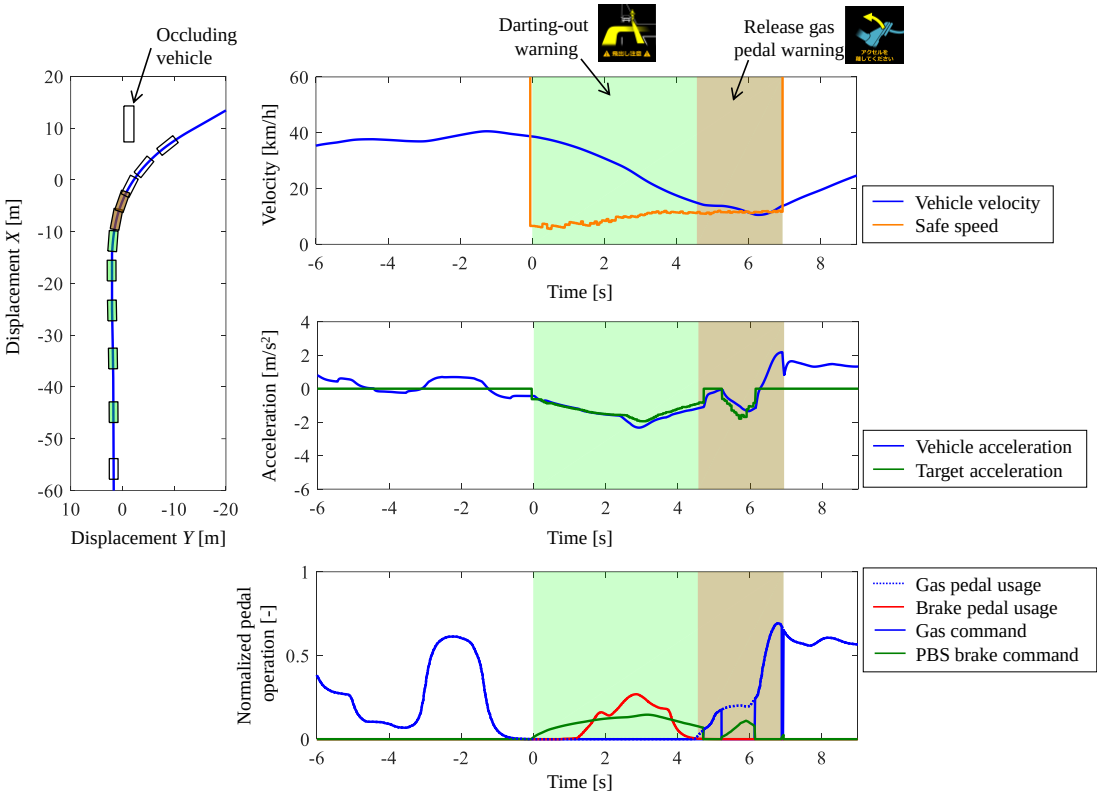
Occluding vehicle
Darting-out warning
Release gas pedal warning
Displacement X [m]
Displacement Y [m]
Velocity [km/h]
Time [s]
Vehicle velocity
Safe speed
Acceleration [m/s²]
Vehicle acceleration
Target acceleration
Normalized pedal operation [-]
Gas pedal usage
Brake pedal usage
Gas command
PBS brake command

(5)

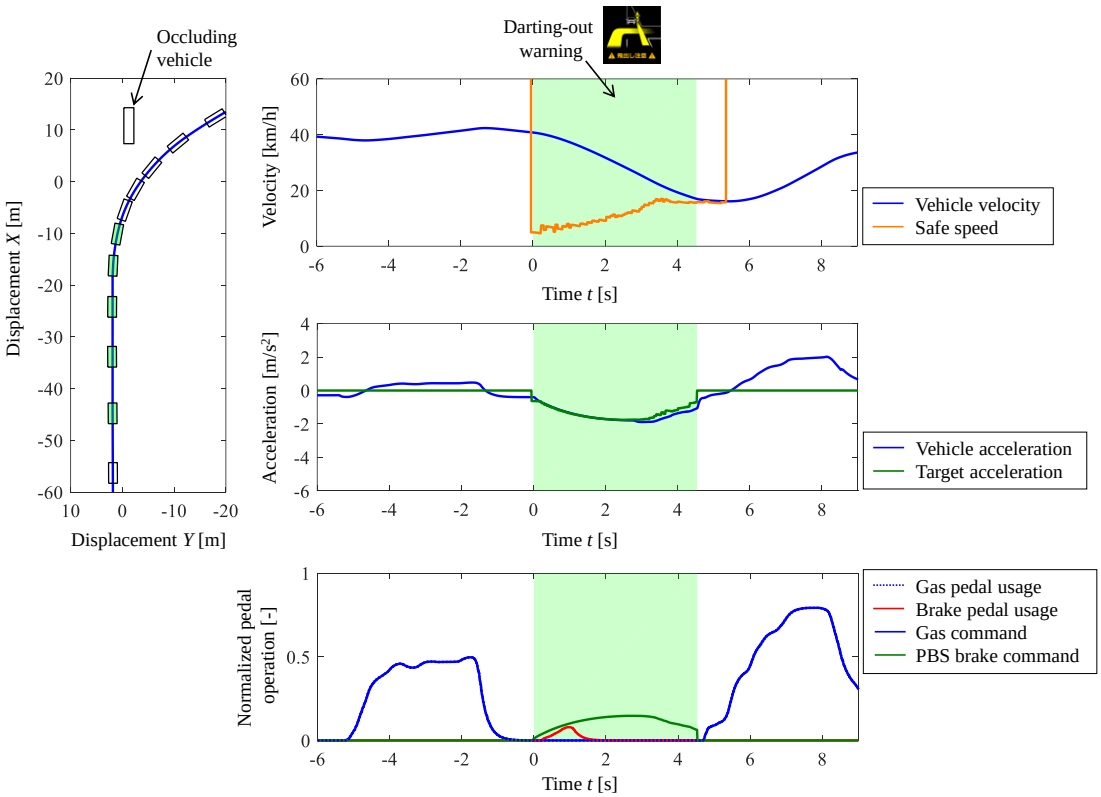
Occluding vehicle
Darting-out warning
Displacement X [m]
Displacement Y [m]
Velocity [km/h]
Time t [s]
Vehicle velocity
Safe speed
Acceleration [m/s²]
Vehicle acceleration
Target acceleration
Normalized pedal operation [-]
Gas pedal usage
Brake pedal usage
Gas command
PBS brake command

(6)

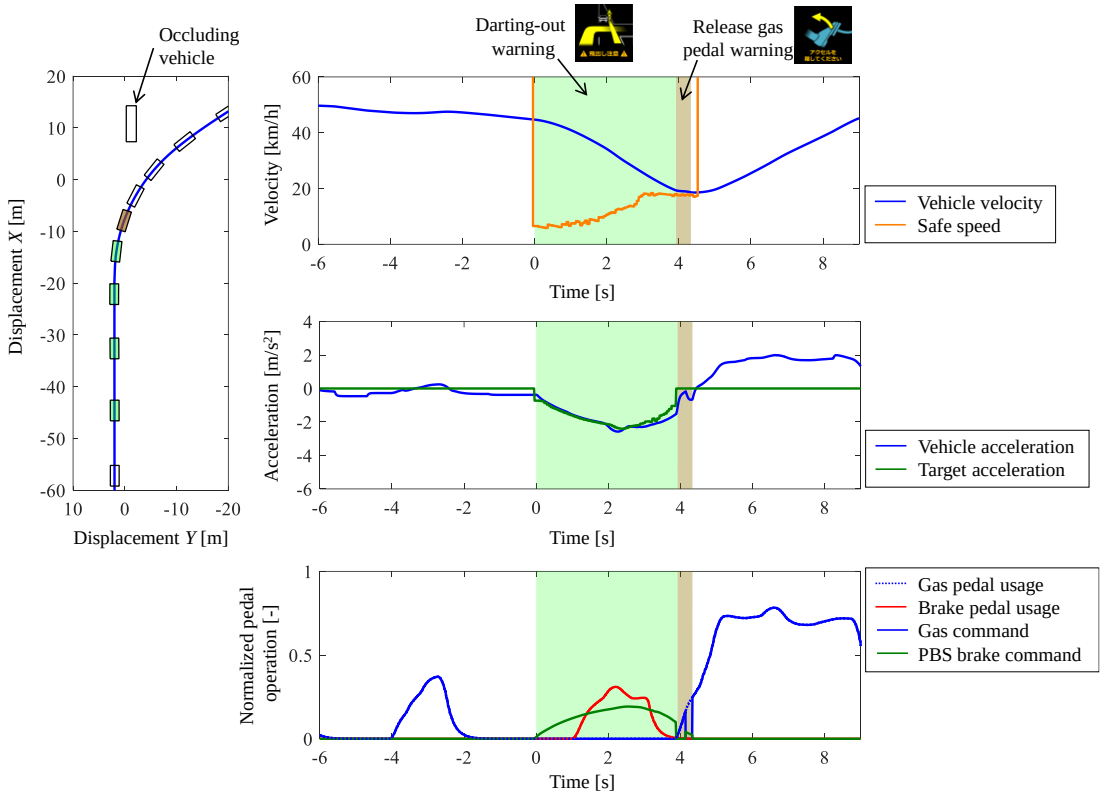
Occluding vehicle
Darting-out warning
Release gas pedal warning
Displacement X [m]
Displacement Y [m]
Velocity [km/h]
Time [s]
Vehicle velocity
Safe speed
Acceleration [m/s²]
Vehicle acceleration
Target acceleration
Normalized pedal operation [-]
Gas pedal usage
Brake pedal usage
Gas command
PBS brake command

(7)

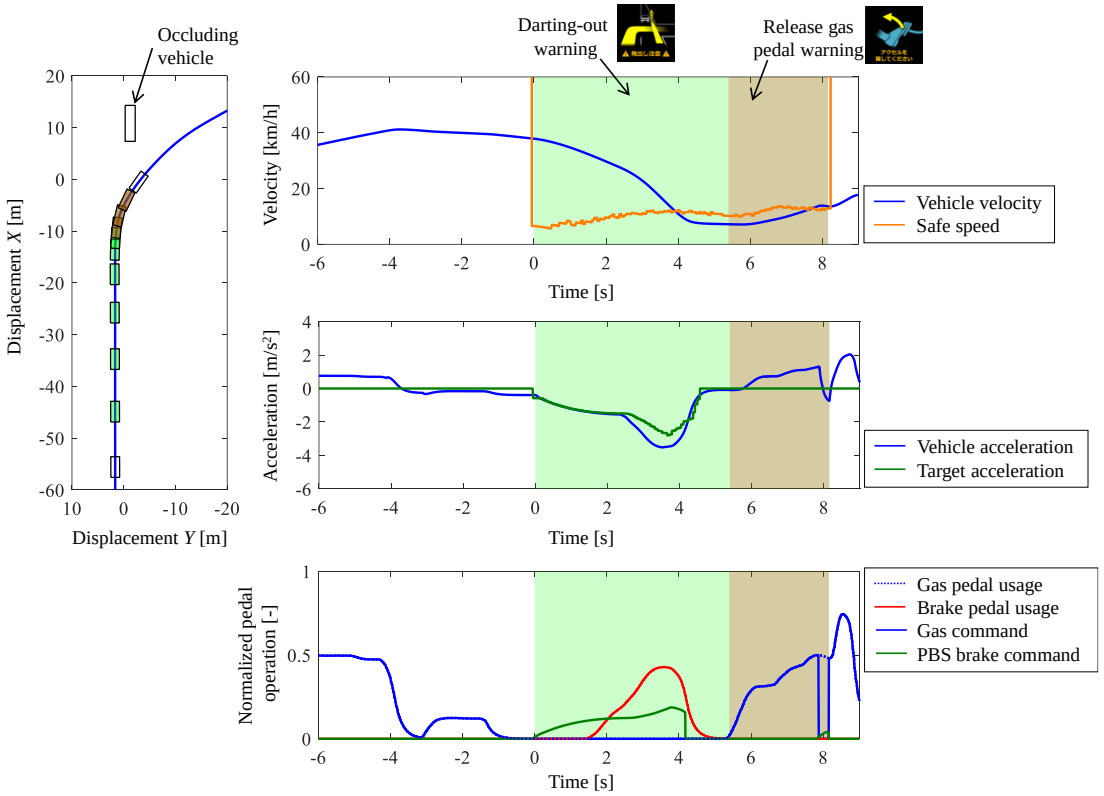
Occluding vehicle
Darting-out warning
Release gas pedal warning
Displacement X [m]
Displacement Y [m]
Velocity [km/h]
Time [s]
Vehicle velocity
Safe speed
Acceleration [m/s²]
Vehicle acceleration
Target acceleration
Normalized pedal operation [-]
Gas pedal usage
Brake pedal usage
Gas command
PBS brake command

(8)

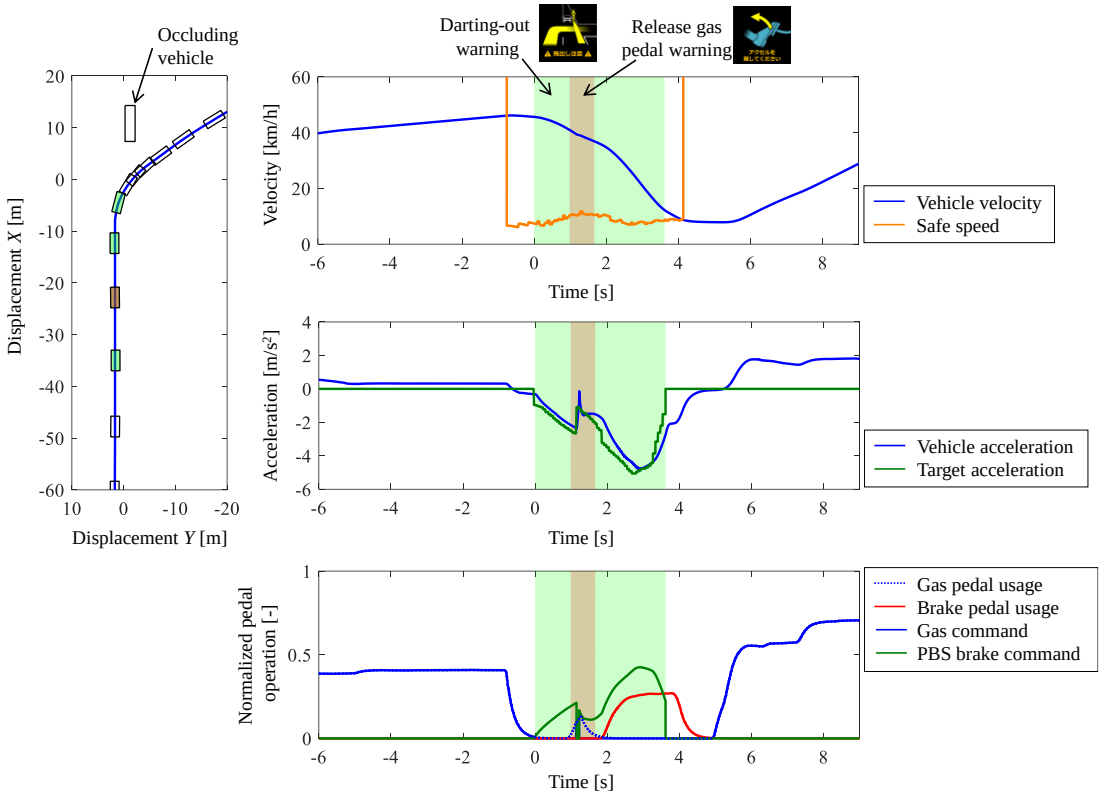
Occluding vehicle
Darting-out warning
Release gas pedal warning
Displacement X [m]
Displacement Y [m]
Velocity [km/h]
Time [s]
Vehicle velocity
Safe speed
Acceleration [m/s²]
Vehicle acceleration
Target acceleration
Normalized pedal operation [-]
Gas pedal usage
Brake pedal usage
Gas command
PBS brake command

(9)

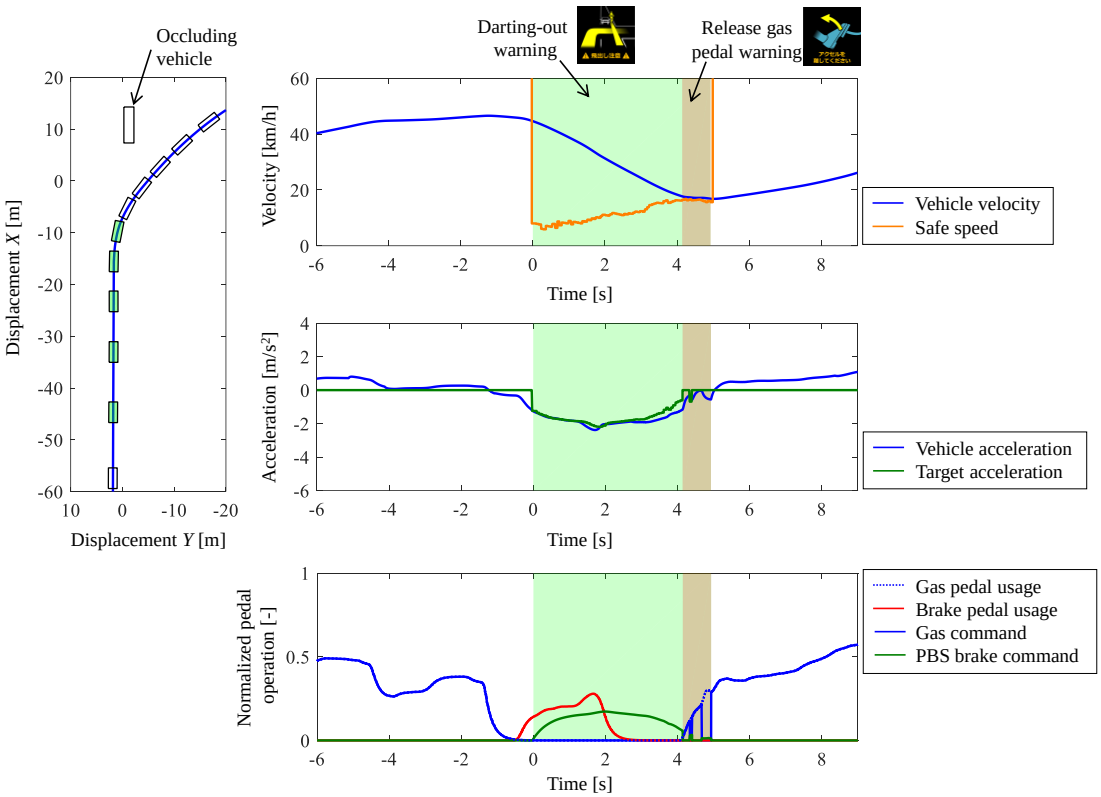
Occluding vehicle
Darting-out warning
Release gas pedal warning
Displacement X [m]
Displacement Y [m]
Velocity [km/h]
Time [s]
Vehicle velocity
Safe speed
Acceleration [m/s²]
Vehicle acceleration
Target acceleration
Normalized pedal operation [-]
Gas pedal usage
Brake pedal usage
Gas command
PBS brake command

(10)

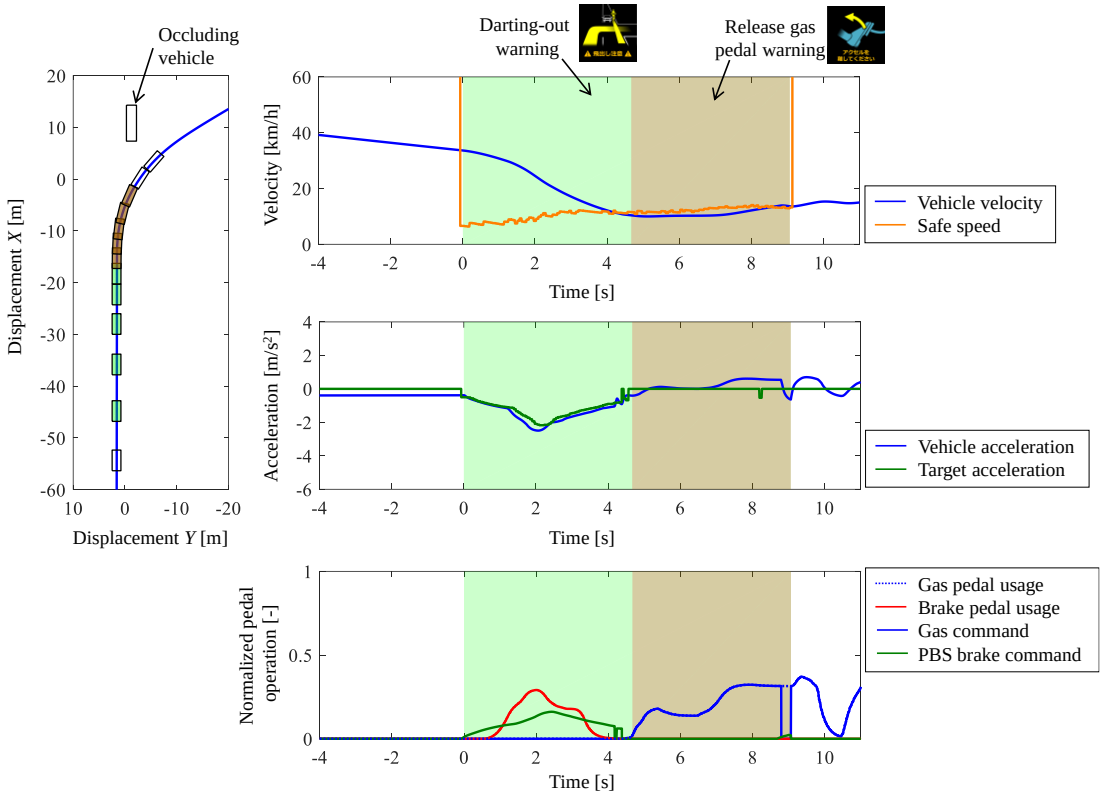
Occluding vehicle
Darting-out warning
Release gas pedal warning
Displacement X [m]
Displacement Y [m]
Velocity [km/h]
Time [s]
Vehicle velocity
Safe speed
Acceleration [m/s²]
Vehicle acceleration
Target acceleration
Normalized pedal operation [-]
Gas pedal usage
Brake pedal usage
Gas command
PBS brake command

(11)

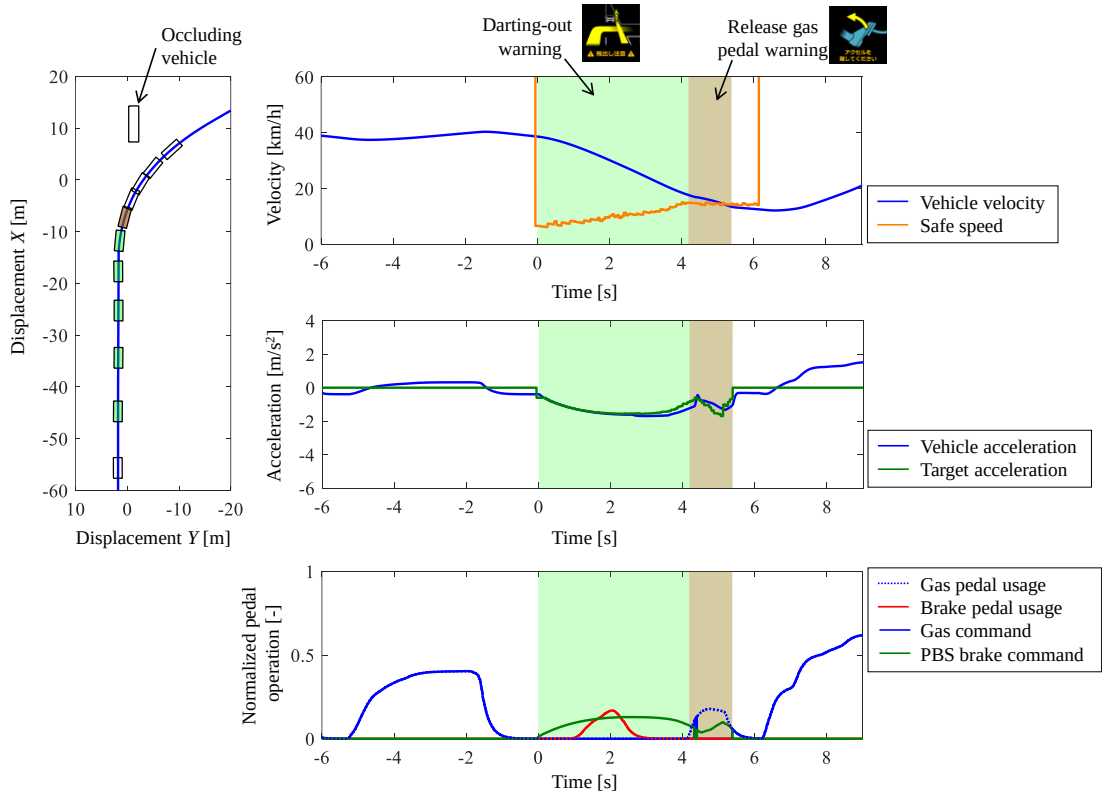
Occluding vehicle
Darting-out warning
Release gas pedal warning
Displacement X [m]
Displacement Y [m]
Velocity [km/h]
Time [s]
Vehicle velocity
Safe speed
Acceleration [m/s²]
Vehicle acceleration
Target acceleration
Normalized pedal operation [-]
Gas pedal usage
Brake pedal usage
Gas command
PBS brake command

(12)

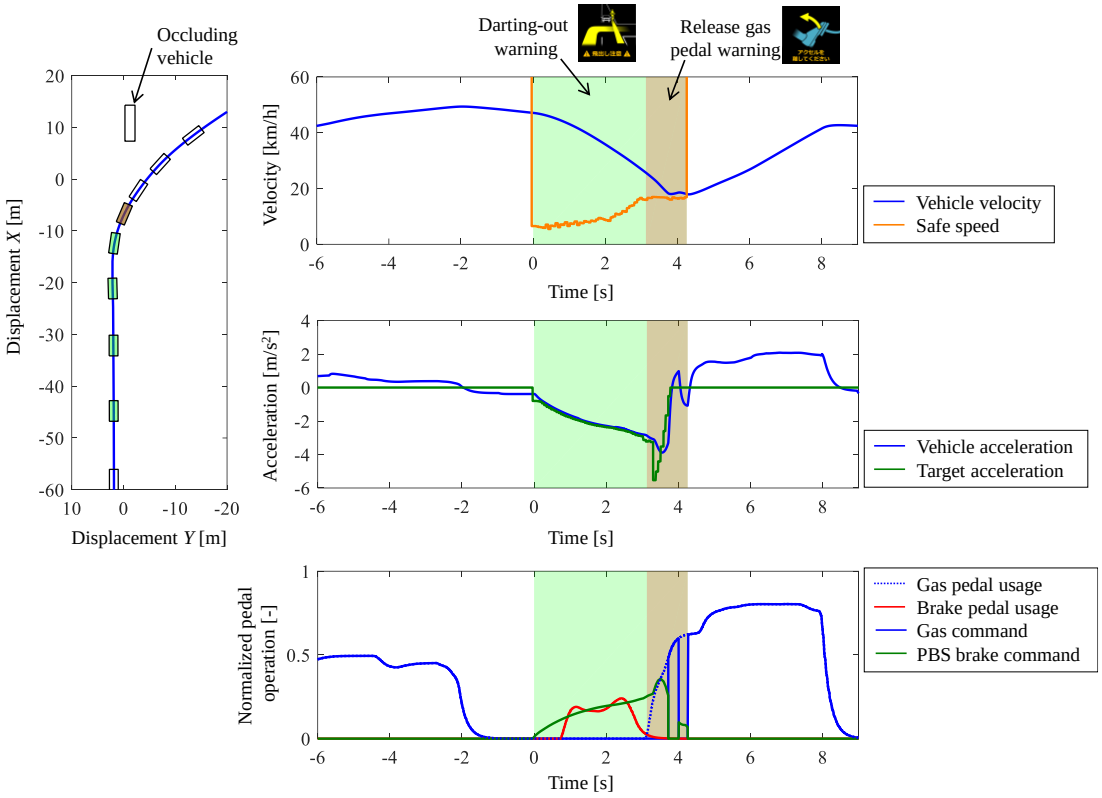
Occluding vehicle
Darting-out warning
Release gas pedal warning
Displacement X [m]
Displacement Y [m]
Velocity [km/h]
Time [s]
Vehicle velocity
Safe speed
Acceleration [m/s²]
Vehicle acceleration
Target acceleration
Normalized pedal operation [-]
Gas pedal usage
Brake pedal usage
Gas command
PBS brake command

(13)

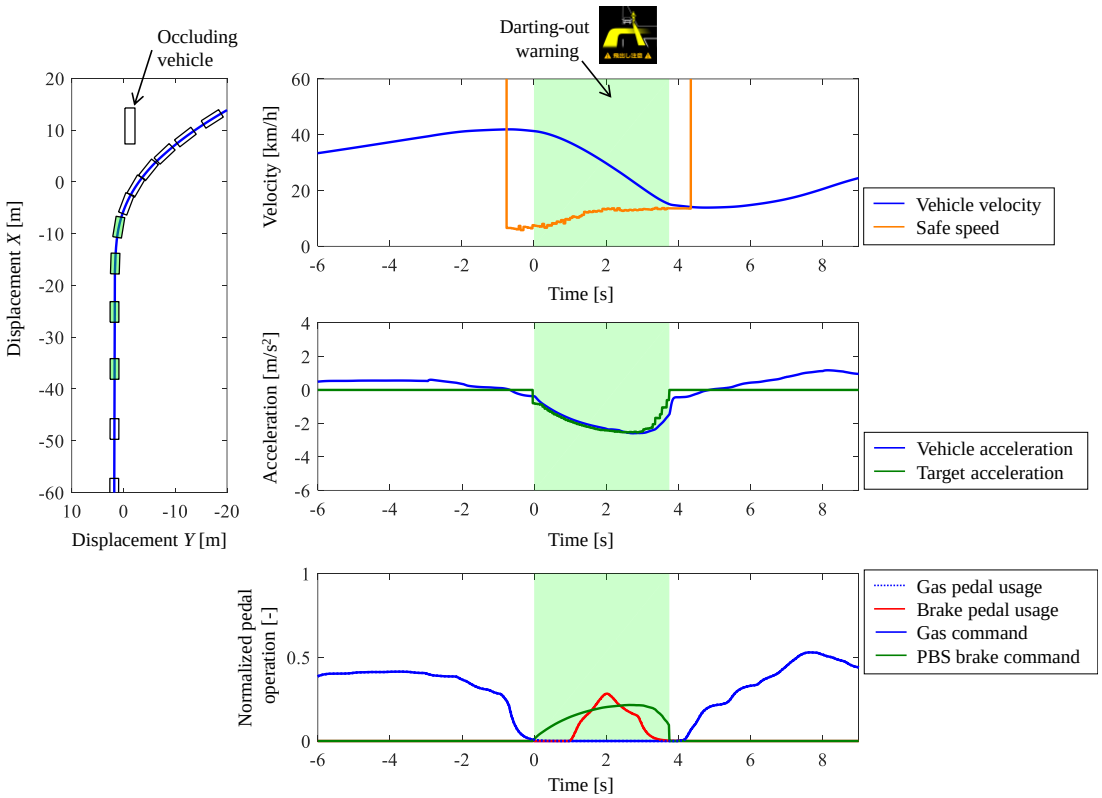
Occluding vehicle
Darting-out warning
Displacement X [m]
Displacement Y [m]
Velocity [km/h]
Time [s]
Vehicle velocity
Safe speed
Acceleration [m/s²]
Vehicle acceleration
Target acceleration
Normalized pedal operation [-]
Gas pedal usage
Brake pedal usage
Gas command
PBS brake command

(14)

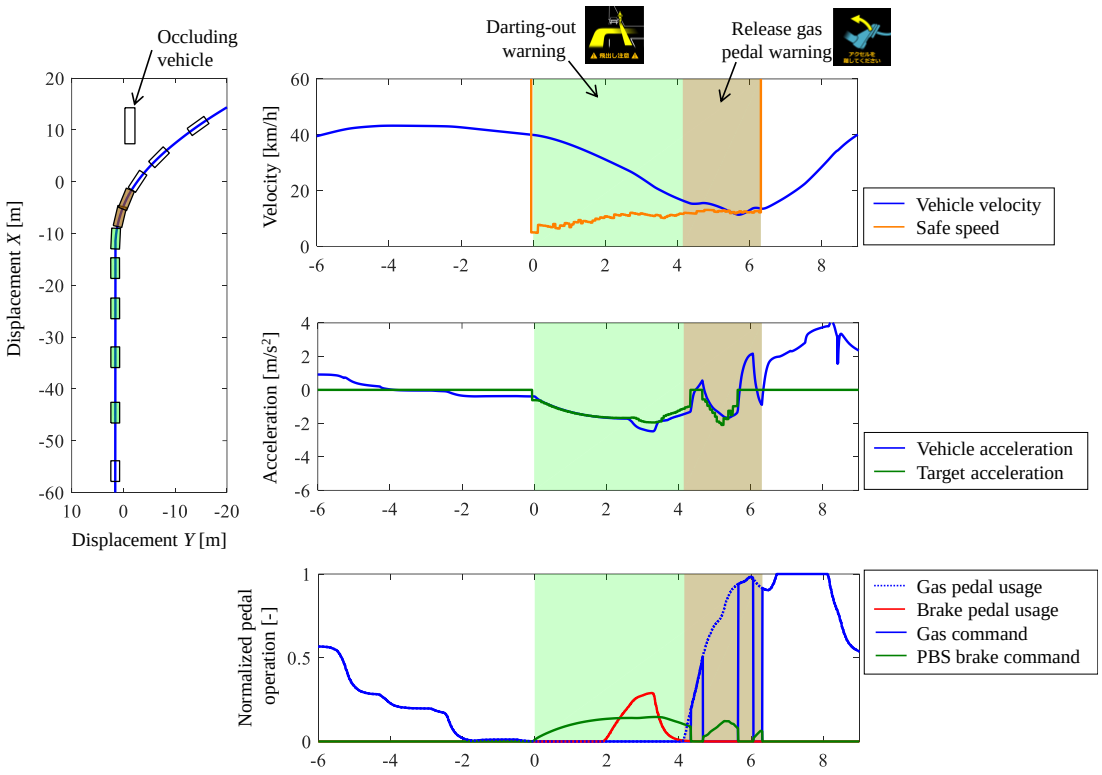
Occluding vehicle
Displacement X [m]
Displacement Y [m]
Darting-out warning
Release gas pedal warning
Velocity [km/h]
Vehicle velocity
Safe speed
Acceleration [m/s²]
Vehicle acceleration
Target acceleration
Normalized pedal operation [-]
Gas pedal usage
Brake pedal usage
Gas command
PBS brake command

(15)

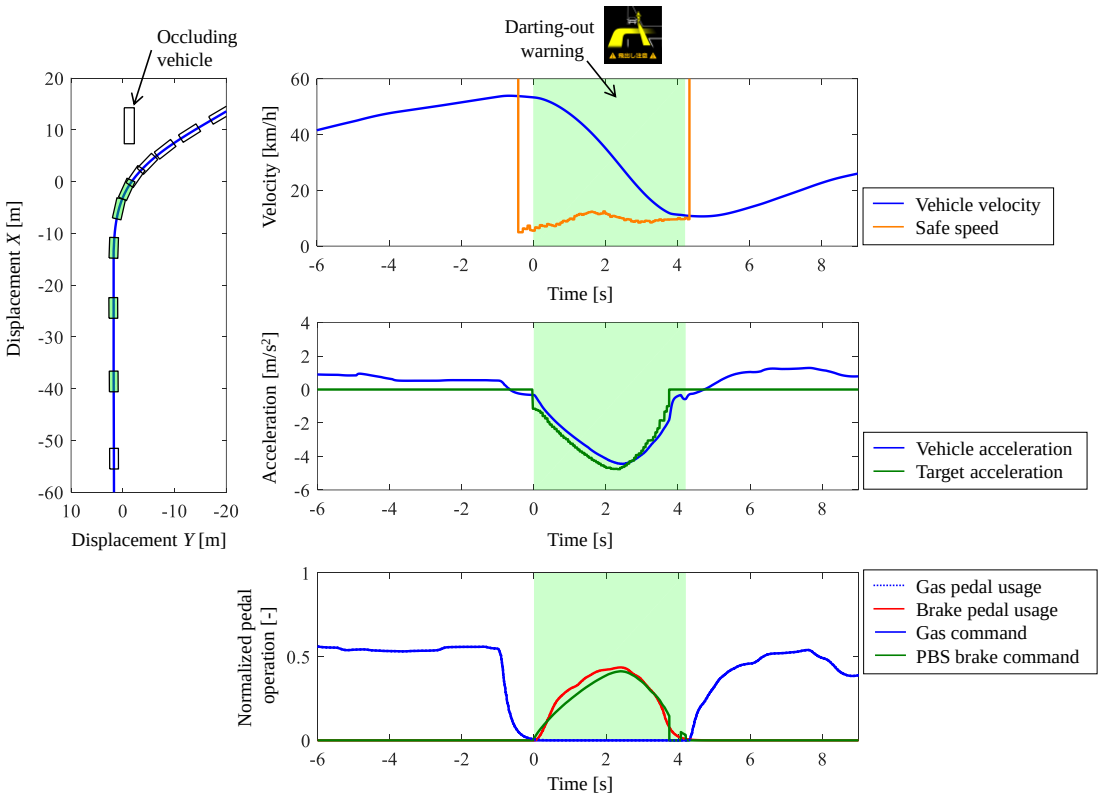
Occluding vehicle
Displacement X [m]
Displacement Y [m]
Darting-out warning
Velocity [km/h]
Vehicle velocity
Safe speed
Time [s]
Acceleration [m/s²]
Vehicle acceleration
Target acceleration
Normalized pedal operation [-]
Gas pedal usage
Brake pedal usage
Gas command
PBS brake command

(16)

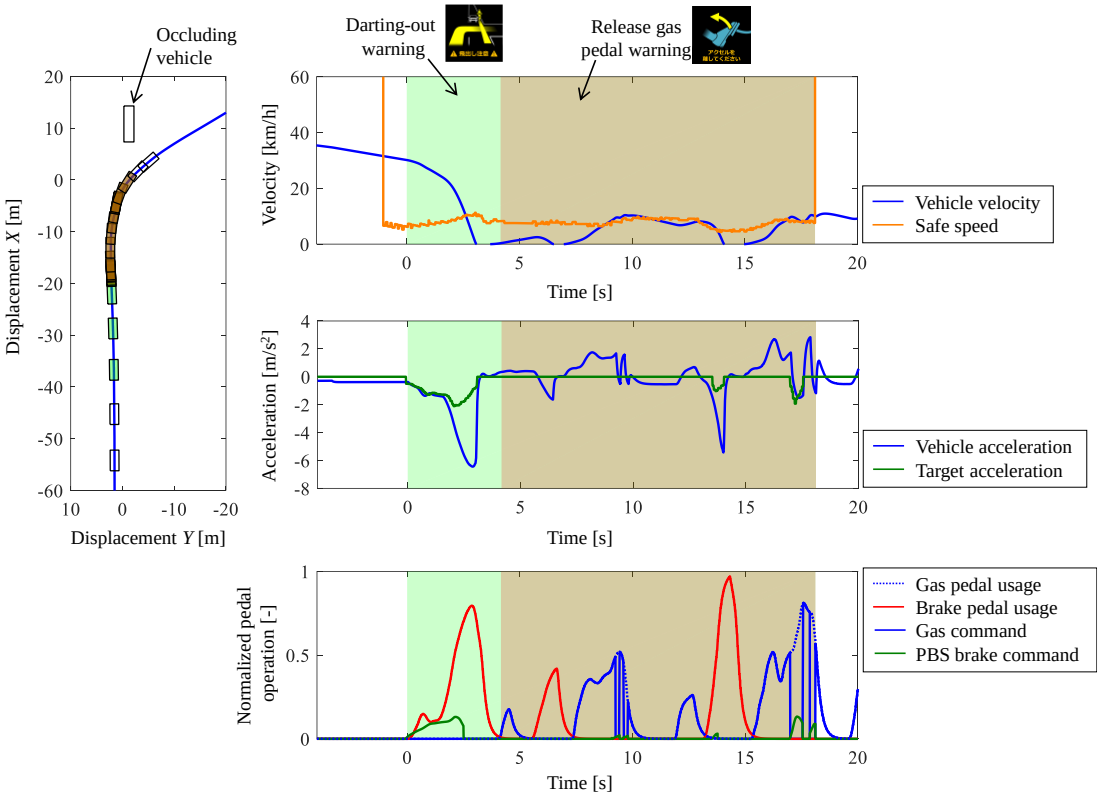
Occluding vehicle
Darting-out warning
Release gas pedal warning
Displacement X [m]
Displacement Y [m]
Velocity [km/h]
Time [s]
Vehicle velocity
Safe speed
Acceleration [m/s²]
Vehicle acceleration
Target acceleration
Normalized pedal operation [-]
Gas pedal usage
Brake pedal usage
Gas command
PBS brake command

(17)

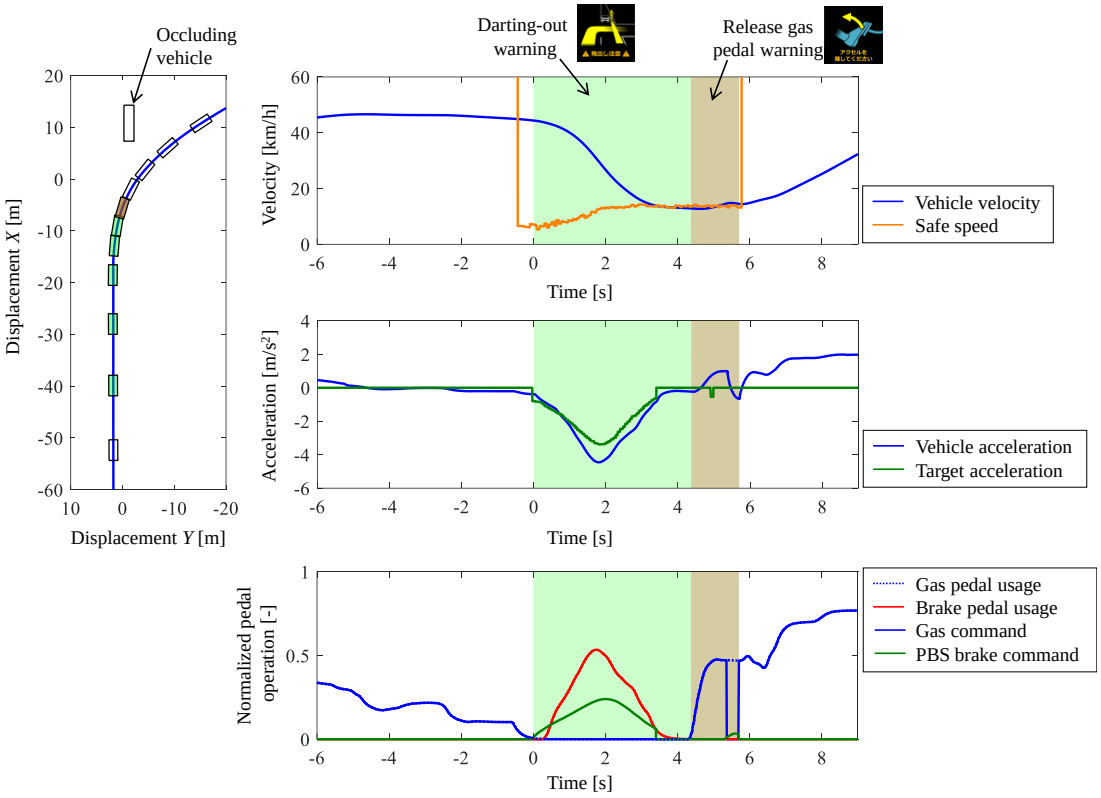
Occluding vehicle
Darting-out warning
Release gas pedal warning
Displacement X [m]
Displacement Y [m]
Velocity [km/h]
Time [s]
Vehicle velocity
Safe speed
Acceleration [m/s²]
Vehicle acceleration
Target acceleration
Normalized pedal operation [-]
Gas pedal usage
Brake pedal usage
Gas command
PBS brake command

(18)

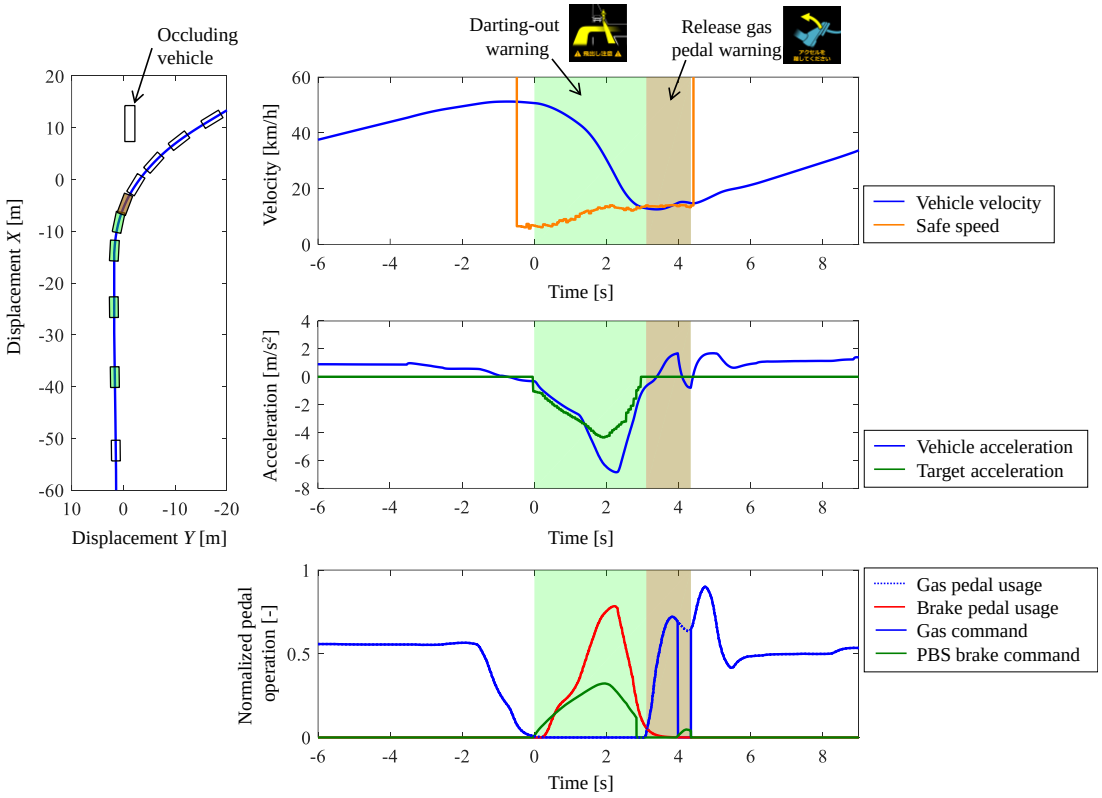
Occluding vehicle
Darting-out warning
Release gas pedal warning
Displacement X [m]
Displacement Y [m]
Velocity [km/h]
Time [s]
Vehicle velocity
Safe speed
Acceleration [m/s²]
Vehicle acceleration
Target acceleration
Normalized pedal operation [-]
Gas pedal usage
Brake pedal usage
Gas command
PBS brake command

(19)

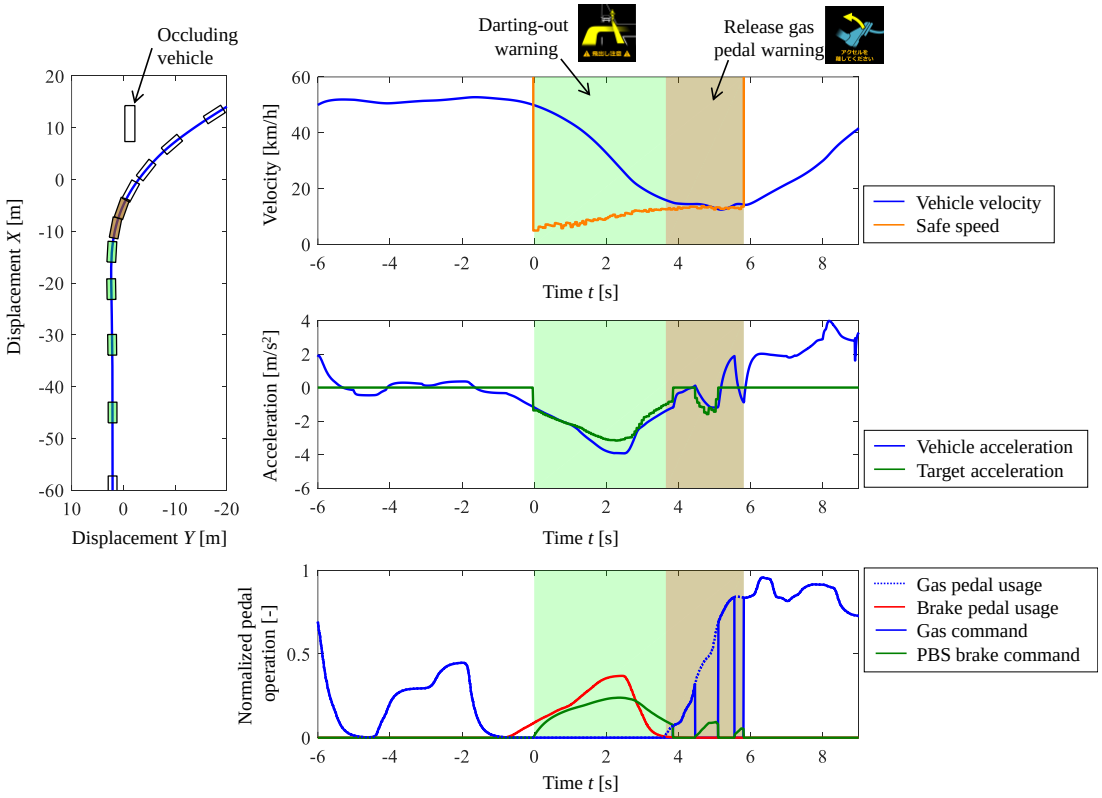
Occluding vehicle
Darting-out warning
Release gas pedal warning
Displacement X [m]
Displacement Y [m]
Velocity [km/h]
Time t [s]
Vehicle velocity
Safe speed
Acceleration [m/s²]
Vehicle acceleration
Target acceleration
Normalized pedal operation [-]
Gas pedal usage
Brake pedal usage
Gas command
PBS brake command

(20)

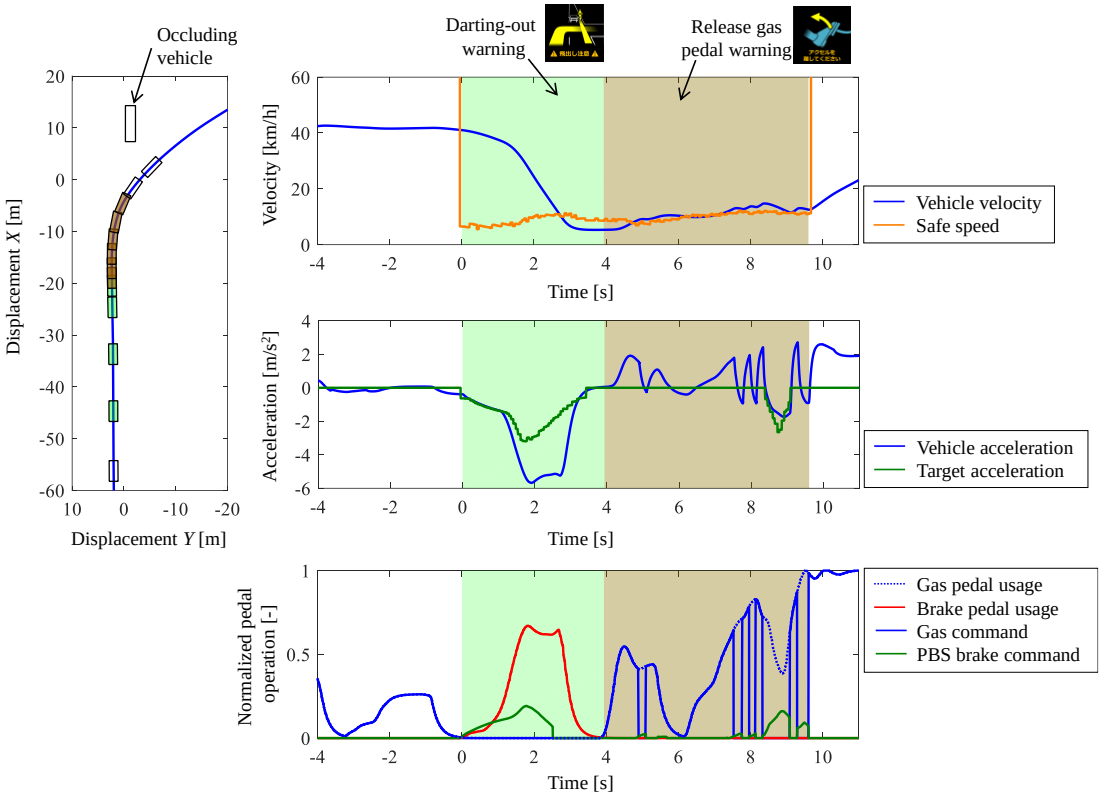
Occluding vehicle
Darting-out warning
Release gas pedal warning
Displacement X [m]
Displacement Y [m]
Velocity [km/h]
Time [s]
Vehicle velocity
Safe speed
Acceleration [m/s²]
Vehicle acceleration
Target acceleration
Normalized pedal operation [-]
Gas pedal usage
Brake pedal usage
Gas command
PBS brake command

(21)

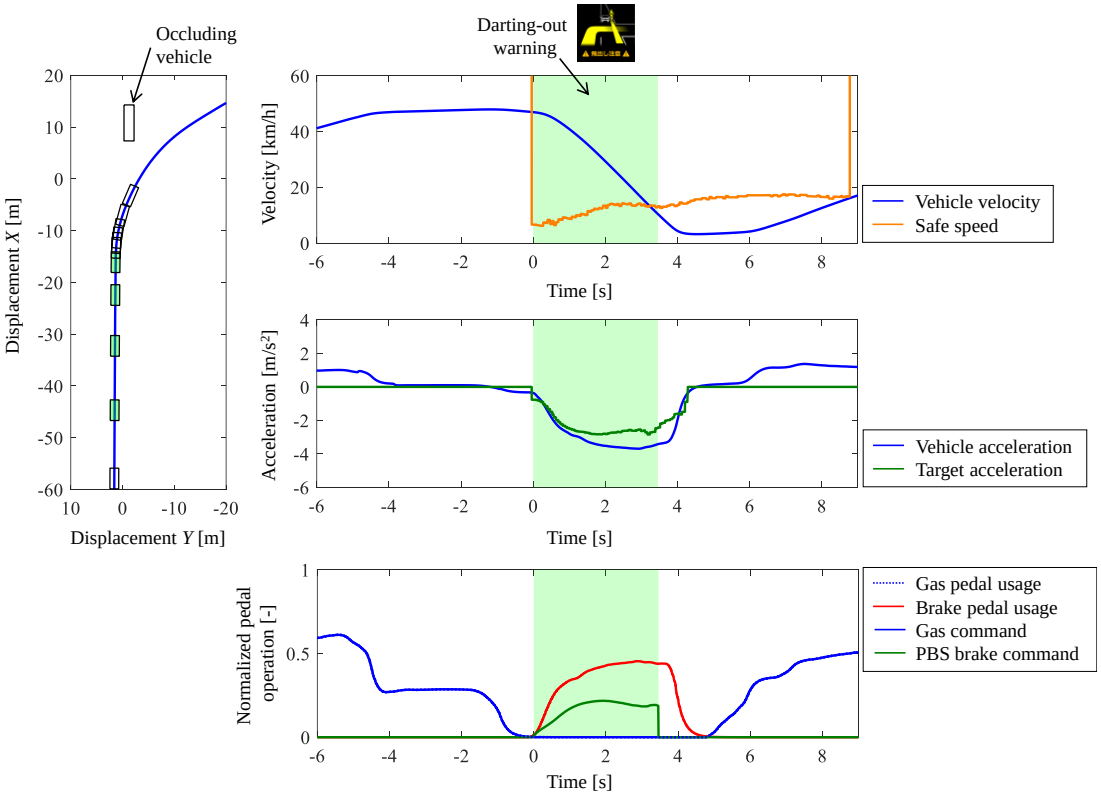
Occluding vehicle
Darting-out warning
Displacement X [m]
Displacement Y [m]
Velocity [km/h]
Time [s]
Vehicle velocity
Safe speed
Acceleration [m/s²]
Vehicle acceleration
Target acceleration
Normalized pedal operation [-]
Gas pedal usage
Brake pedal usage
Gas command
PBS brake command

(22)

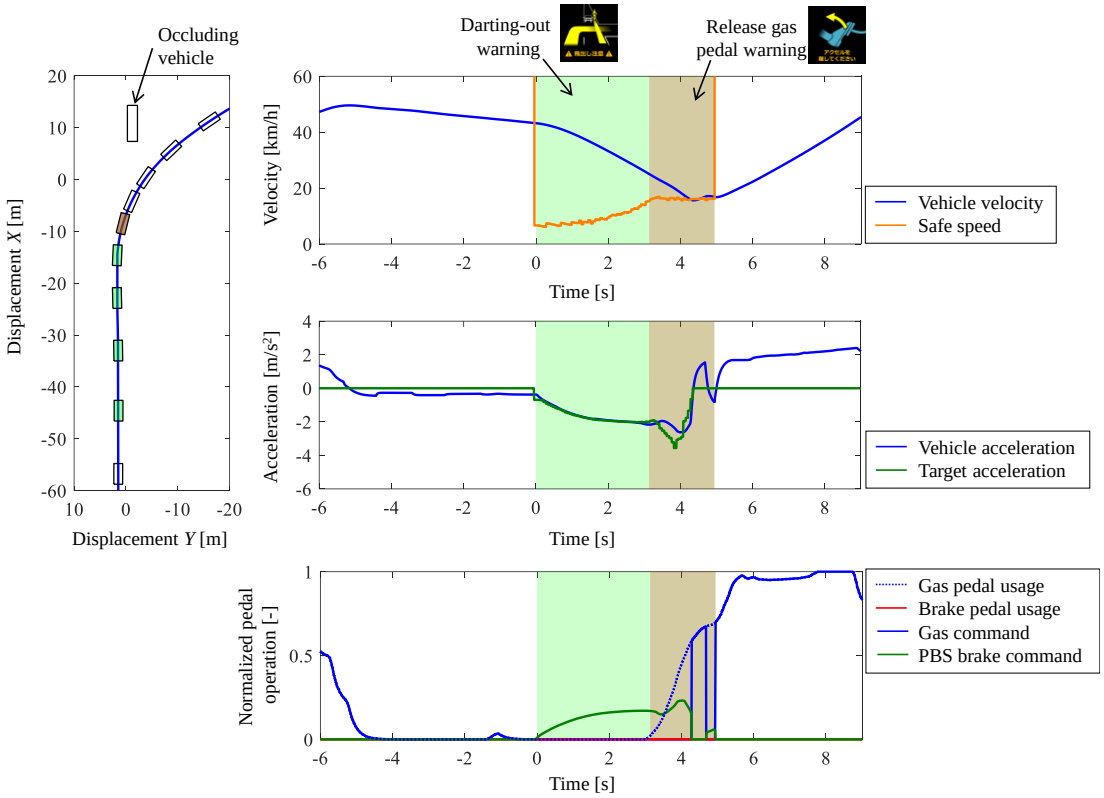
Occluding vehicle
Darting-out warning
Release gas pedal warning
Displacement X [m]
Displacement Y [m]
Velocity [km/h]
Time [s]
Vehicle velocity
Safe speed
Acceleration [m/s²]
Vehicle acceleration
Target acceleration
Normalized pedal operation [-]
Gas pedal usage
Brake pedal usage
Gas command
PBS brake command

(23)

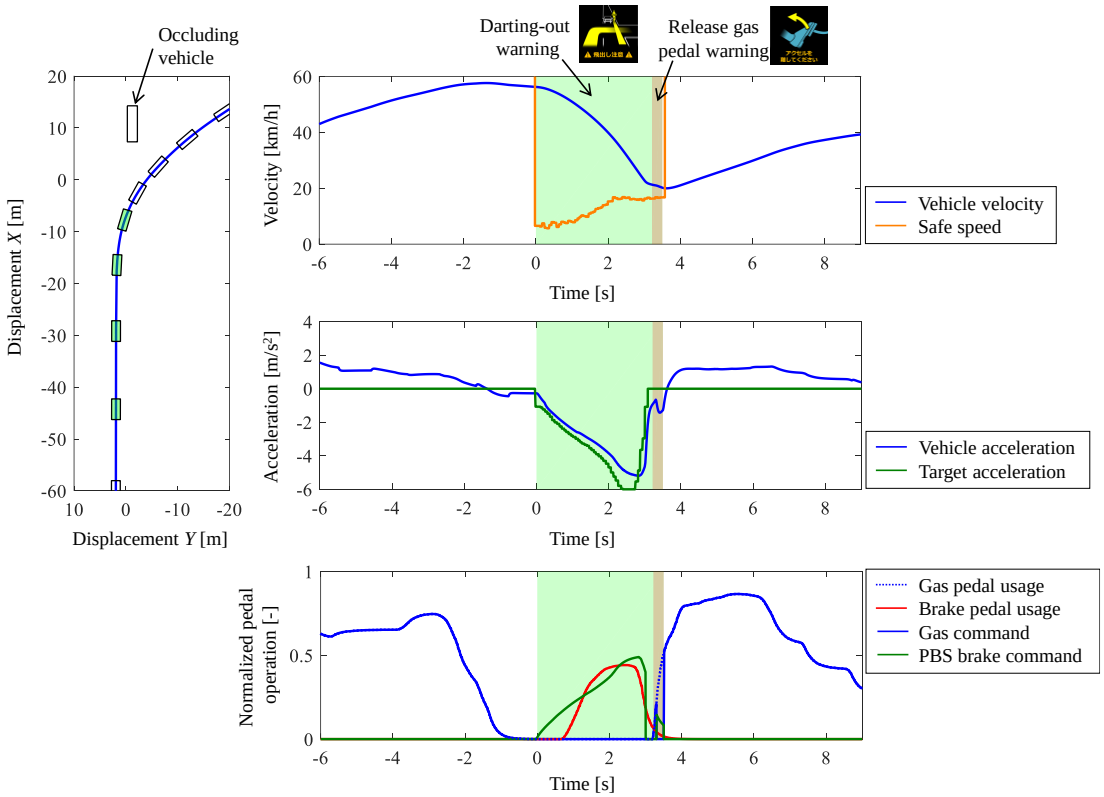
Occluding vehicle
Darting-out warning
Release gas pedal warning
Displacement X [m]
Displacement Y [m]
Velocity [km/h]
Time [s]
Vehicle velocity
Safe speed
Acceleration [m/s²]
Vehicle acceleration
Target acceleration
Normalized pedal operation [-]
Gas pedal usage
Brake pedal usage
Gas command
PBS brake command

(24)

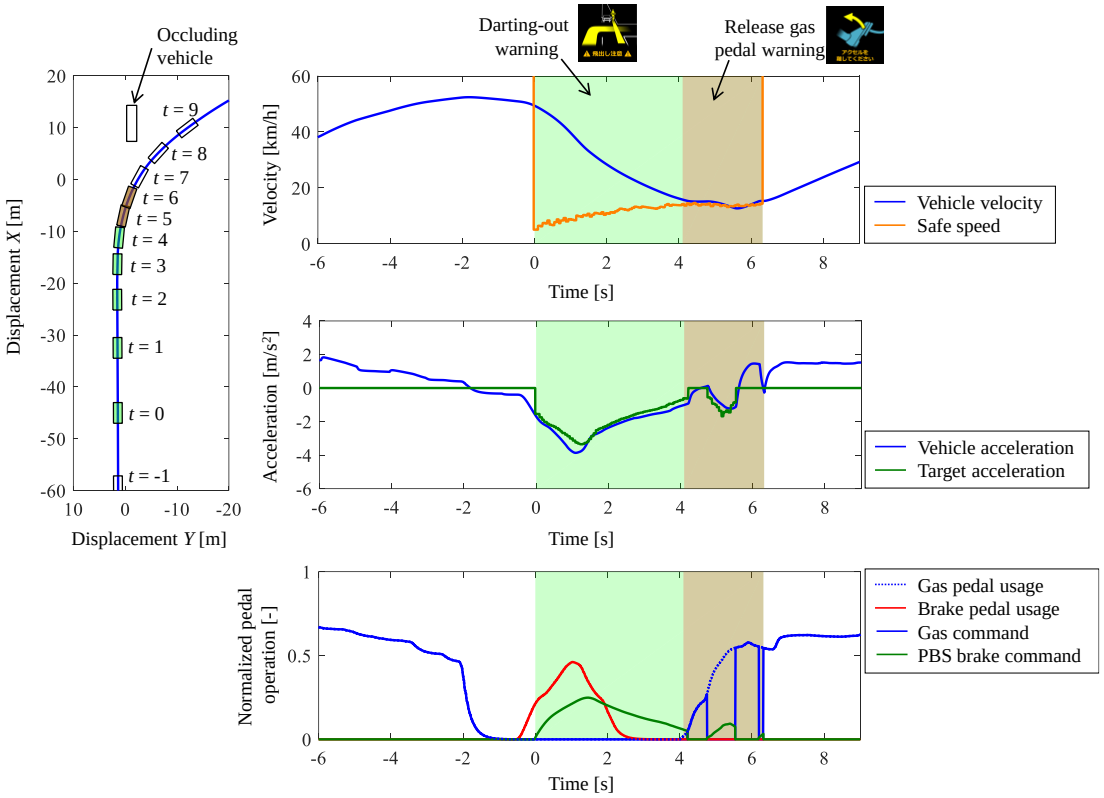
Occluding vehicle
Darting-out warning
Release gas pedal warning
Displacement X [m]
Displacement Y [m]
t = 9
t = 8
t = 7
t = 6
t = 5
t = 4
t = 3
t = 2
t = 1
t = 0
t = -1
Velocity [km/h]
Vehicle velocity
Safe speed
Time [s]
Acceleration [m/s²]
Vehicle acceleration
Target acceleration
Normalized pedal operation [-]
Gas pedal usage
Brake pedal usage
Gas command
PBS brake command

(25)

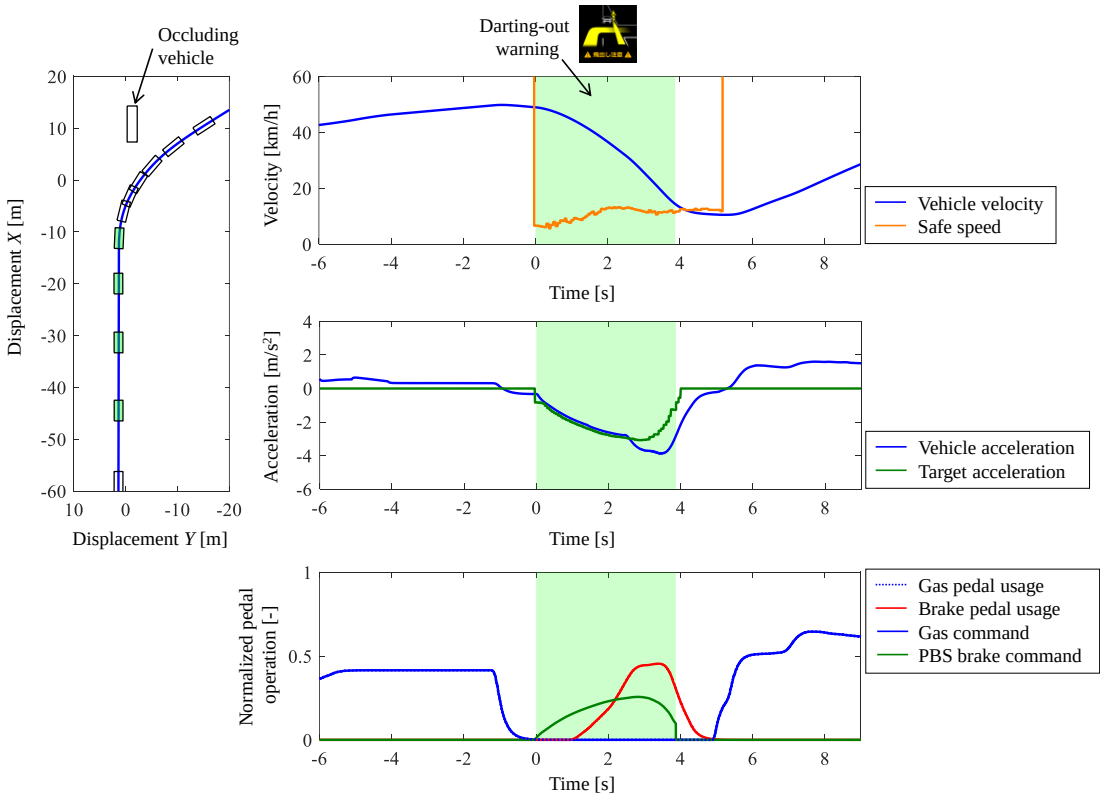
Occluding vehicle
Darting-out warning
Displacement X [m]
Displacement Y [m]
Velocity [km/h]
Vehicle velocity
Safe speed
Time [s]
Acceleration [m/s²]
Vehicle acceleration
Target acceleration
Normalized pedal operation [-]
Gas pedal usage
Brake pedal usage
Gas command
PBS brake command

(26)

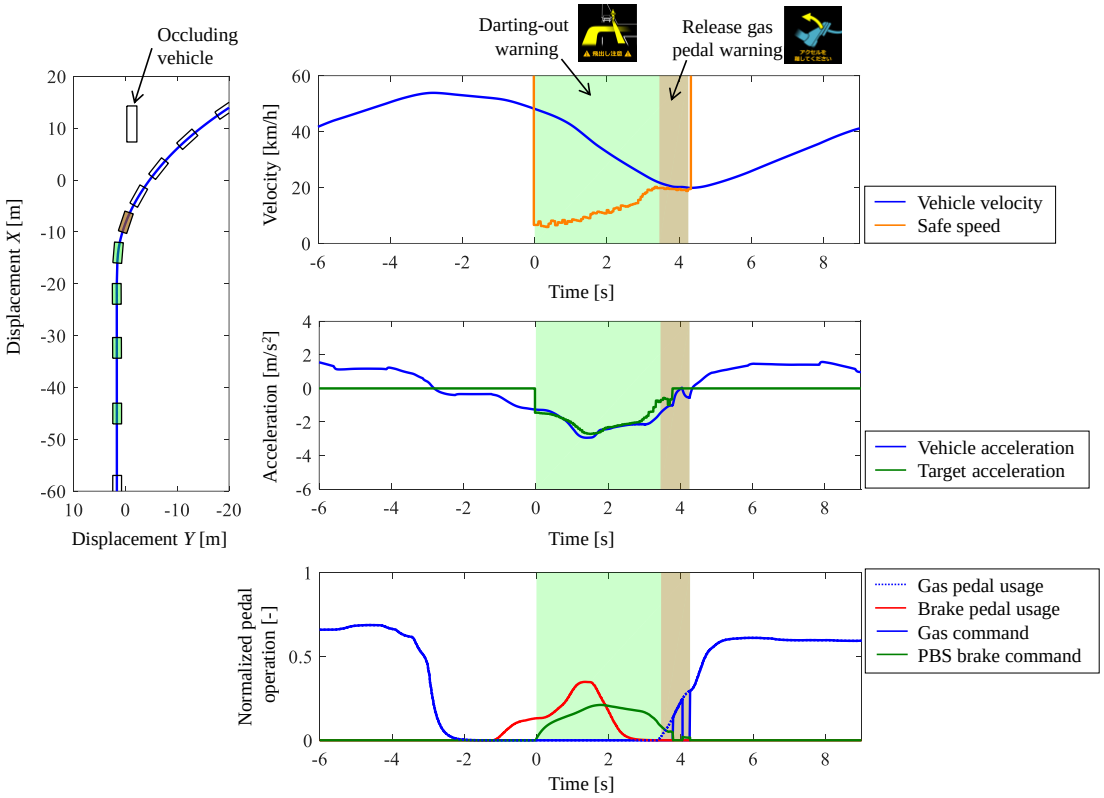
Occluding vehicle
Displacement X [m]
Displacement Y [m]
Darting-out warning
Release gas pedal warning
Velocity [km/h]
Time [s]
Vehicle velocity
Safe speed
Acceleration [m/s²]
Vehicle acceleration
Target acceleration
Normalized pedal operation [-]
Gas pedal usage
Brake pedal usage
Gas command
PBS brake command

(27)

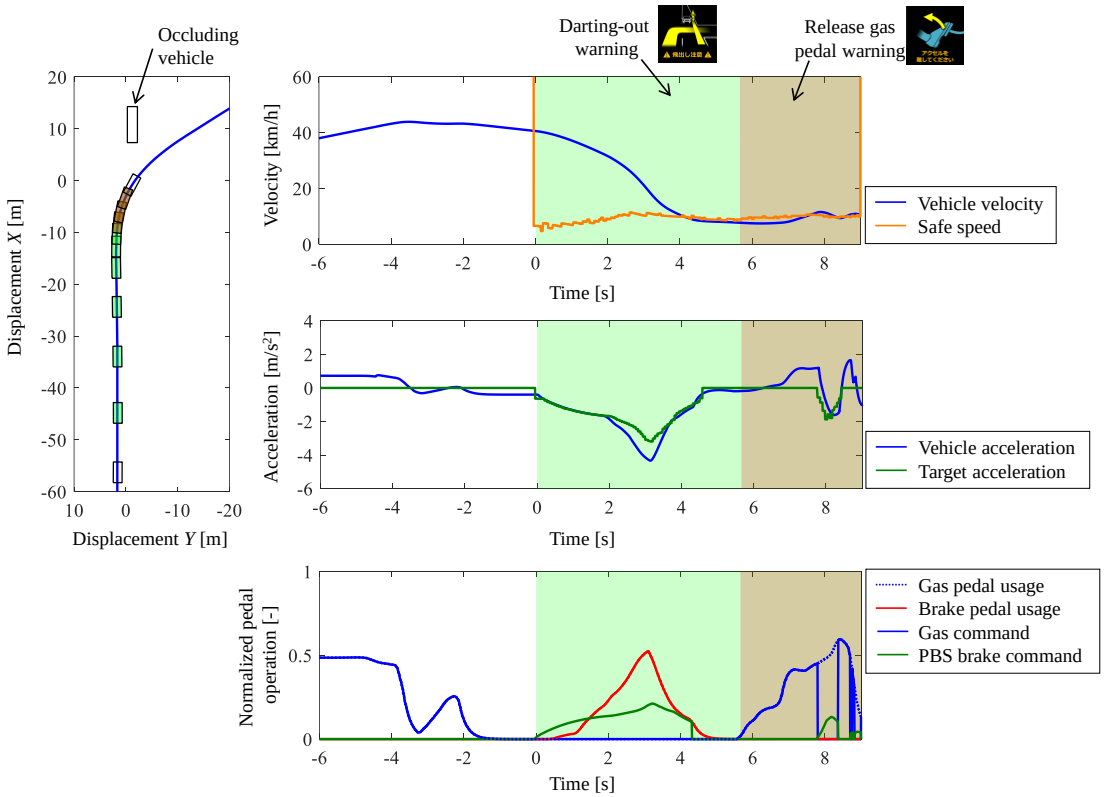
Occluding vehicle
Displacement X [m]
Displacement Y [m]
Darting-out warning
Release gas pedal warning
Velocity [km/h]
Time [s]
Vehicle velocity
Safe speed
Acceleration [m/s²]
Vehicle acceleration
Target acceleration
Normalized pedal operation [-]
Gas pedal usage
Brake pedal usage
Gas command
PBS brake command

(28)

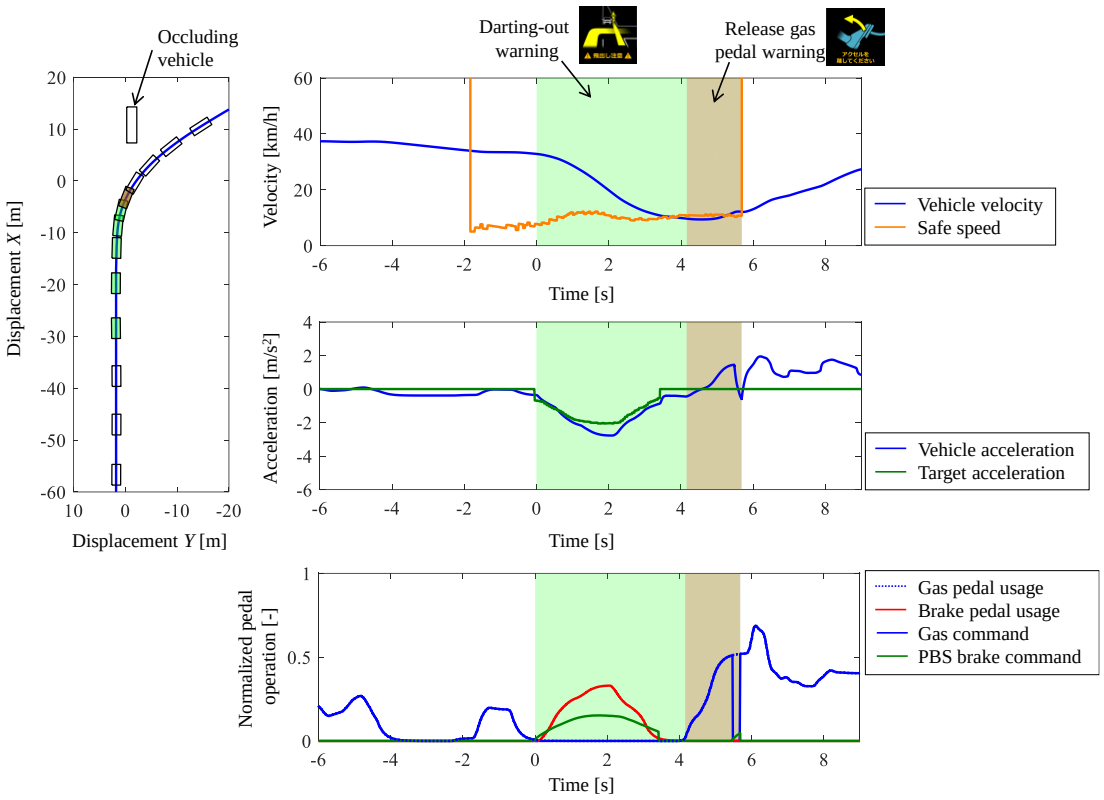
Occluding vehicle
Displacement X [m]
Displacement Y [m]
Darting-out warning
Release gas pedal warning
Velocity [km/h]
Time [s]
Vehicle velocity
Safe speed
Acceleration [m/s²]
Vehicle acceleration
Target acceleration
Normalized pedal operation [-]
Gas pedal usage
Brake pedal usage
Gas command
PBS brake command

(29)

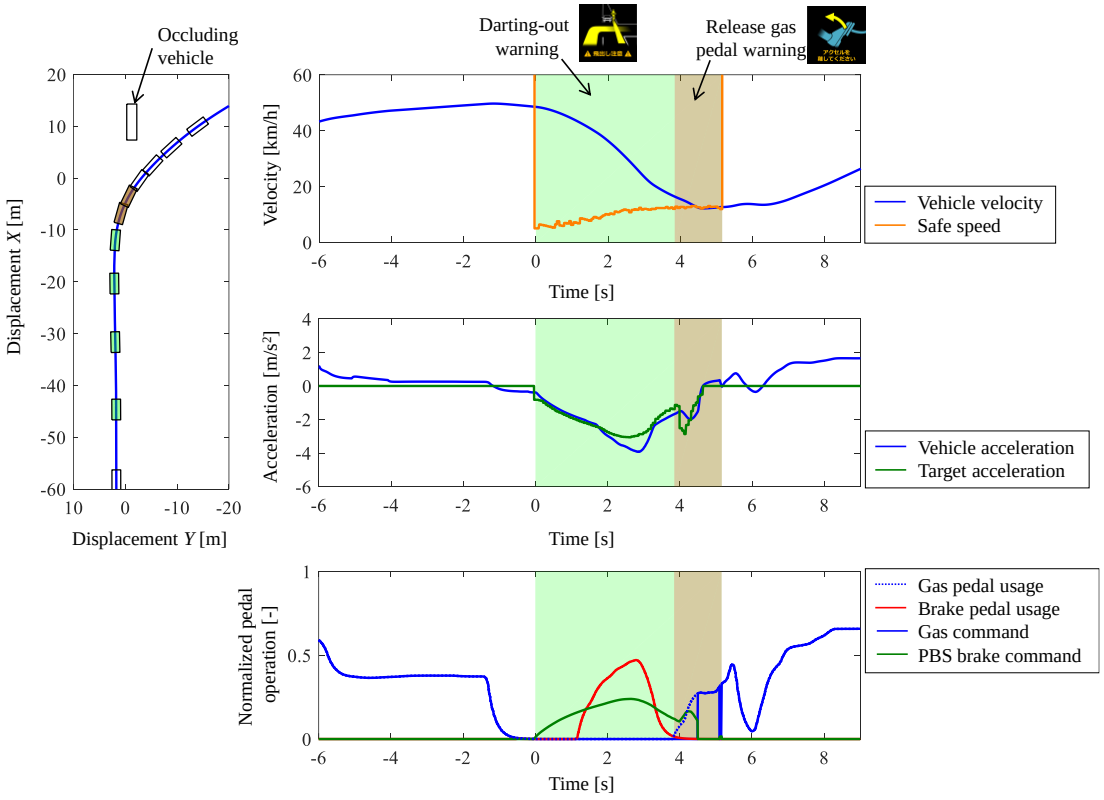
Occluding vehicle
Displacement X [m]
Displacement Y [m]
Darting-out warning
Release gas pedal warning
Velocity [km/h]
Time [s]
Vehicle velocity
Safe speed
Acceleration [m/s²]
Vehicle acceleration
Target acceleration
Normalized pedal operation [-]
Gas pedal usage
Brake pedal usage
Gas command
PBS brake command

(30)

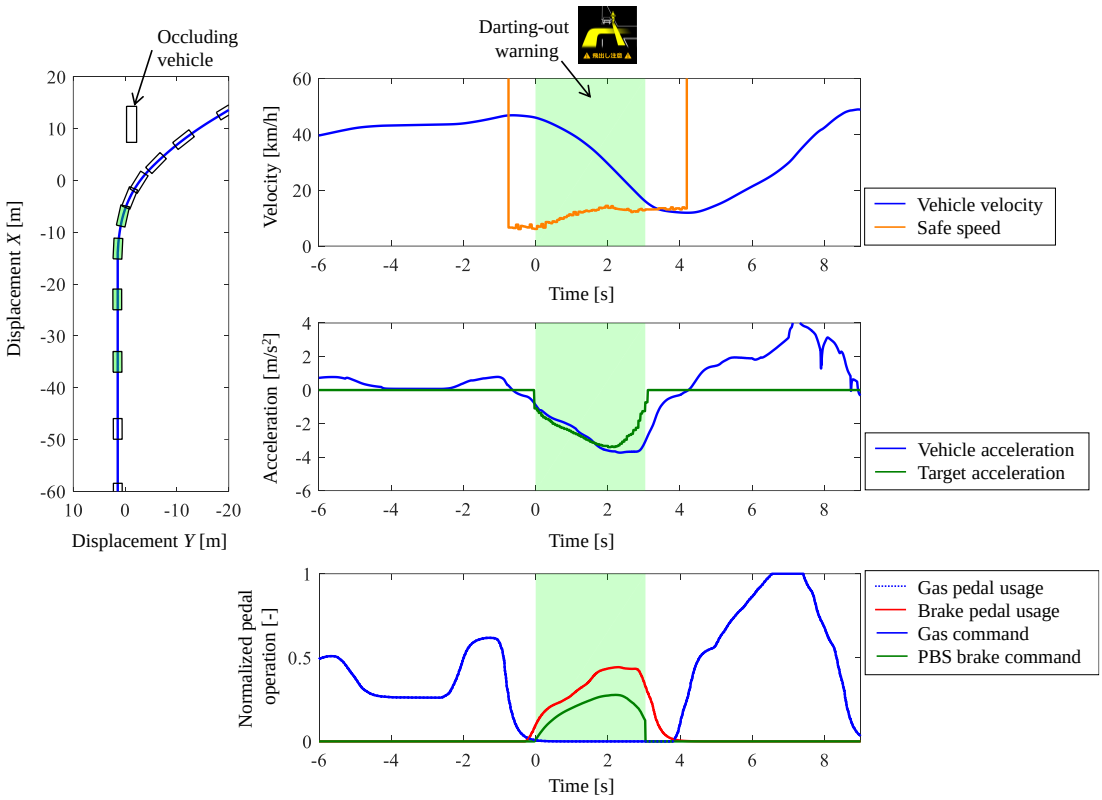
Occluding vehicle
Darting-out warning
Displacement X [m]
Displacement Y [m]
Velocity [km/h]
Time [s]
Vehicle velocity
Safe speed
Acceleration [m/s²]
Vehicle acceleration
Target acceleration
Normalized pedal operation [-]
Gas pedal usage
Brake pedal usage
Gas command
PBS brake command

(31)

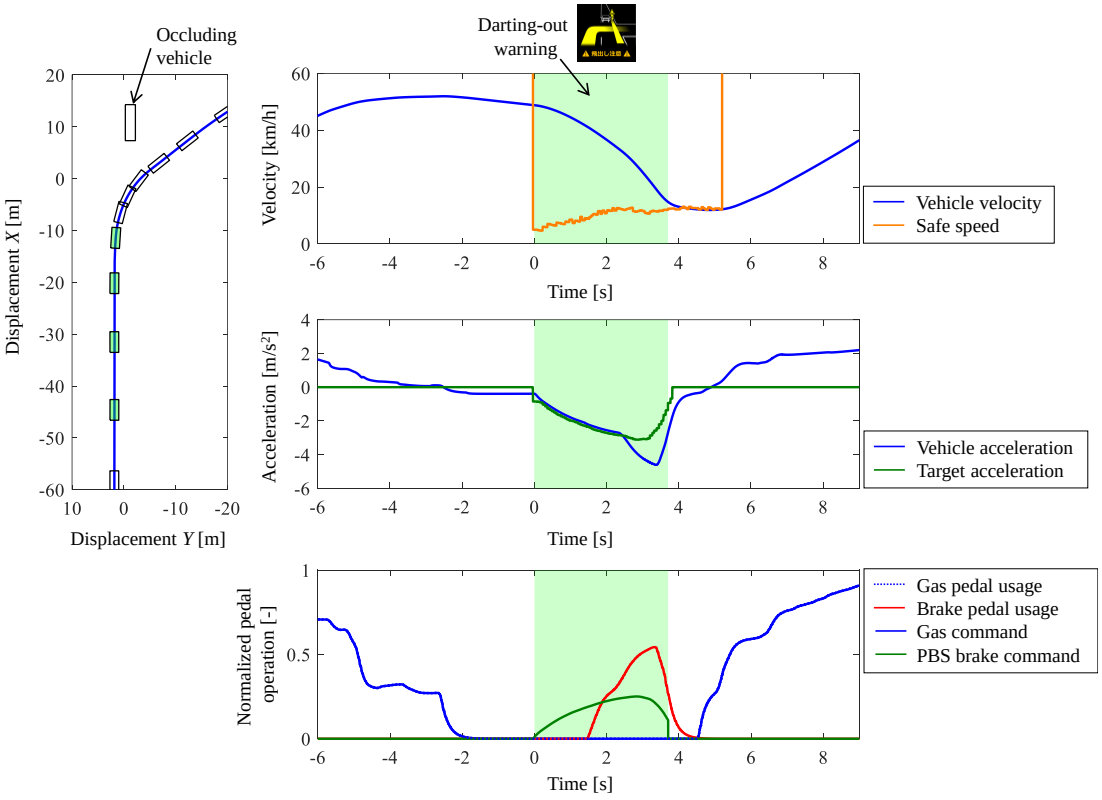
Occluding vehicle
Darting-out warning
Displacement X [m]
Displacement Y [m]
Velocity [km/h]
Time [s]
Vehicle velocity
Safe speed
Acceleration [m/s²]
Vehicle acceleration
Target acceleration
Normalized pedal operation [-]
Gas pedal usage
Brake pedal usage
Gas command
PBS brake command

(32)

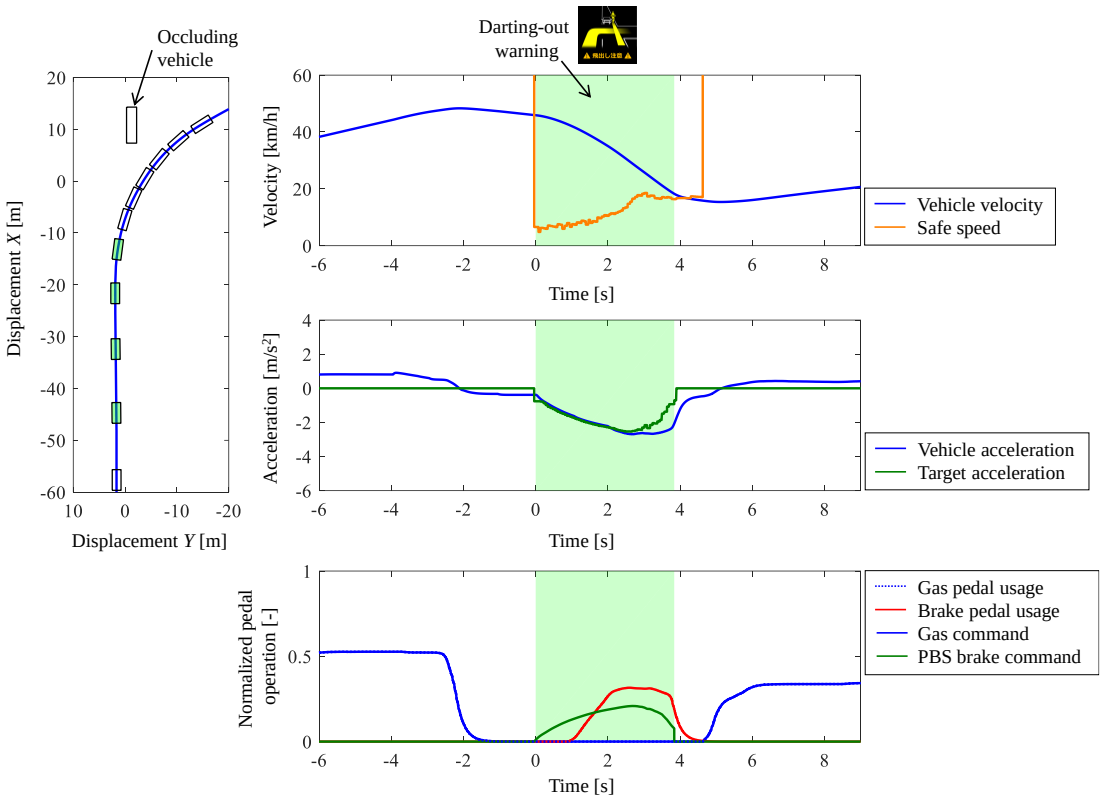
Occluding vehicle
Darting-out warning
Displacement X [m]
Displacement Y [m]
Velocity [km/h]
Time [s]
Vehicle velocity
Safe speed
Acceleration [m/s²]
Vehicle acceleration
Target acceleration
Normalized pedal operation [-]
Gas pedal usage
Brake pedal usage
Gas command
PBS brake command

(33)

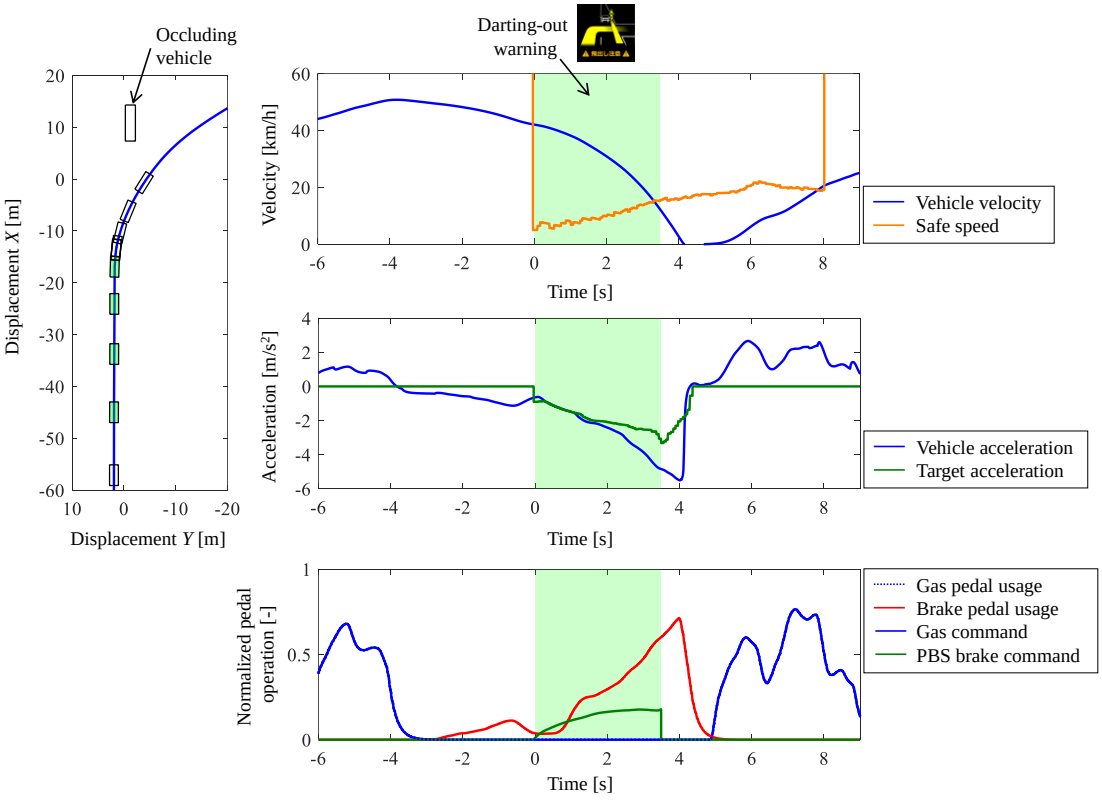
Occluding vehicle
Darting-out warning
Displacement X [m]
Displacement Y [m]
Velocity [km/h]
Time [s]
Vehicle velocity
Safe speed
Acceleration [m/s²]
Vehicle acceleration
Target acceleration
Normalized pedal operation [-]
Gas pedal usage
Brake pedal usage
Gas command
PBS brake command

(34)

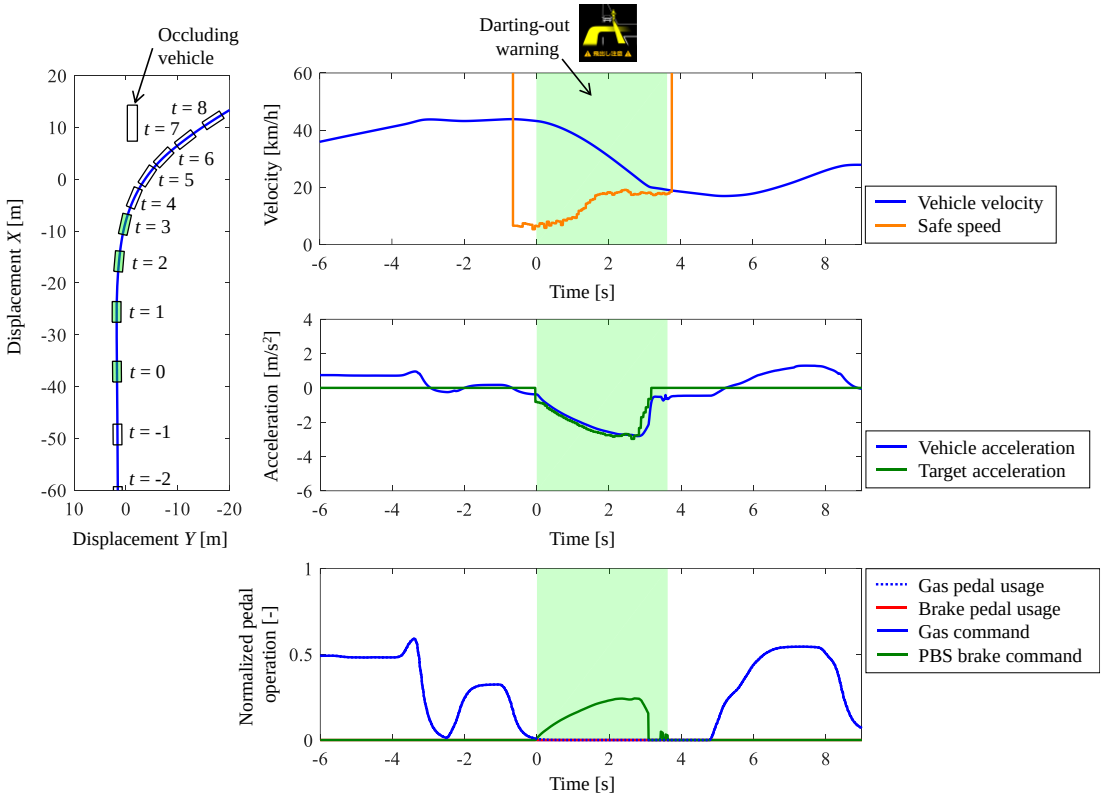
Occluding vehicle
Darting-out warning
t = 8
t = 7
t = 6
t = 5
t = 4
t = 3
t = 2
t = 1
t = 0
t = -1
t = -2
Displacement X [m]
Displacement Y [m]
Velocity [km/h]
Time [s]
Vehicle velocity
Safe speed
Acceleration [m/s²]
Vehicle acceleration
Target acceleration
Normalized pedal operation [-]
Gas pedal usage
Brake pedal usage
Gas command
PBS brake command